

LIBRARY COPY

MORT PAPERS IN—

analytical techniques

conomic geology

engineering geology

geochemical exploration

geochemistry

geomorphology

eophysics

aciology

ound water

ineralogy

re deposits

leontology

trology

uality of water

dimentation

ratigraphy

structural geology

eoretical hydrology

ographic mapping



# GEOLOGICAL SURVEY RESEARCH 1964

## Chapter C

PROPERTY OF:  
U. S. BUREAU OF MINES  
AREA VI MINERAL RESOURCE OFFICE

GEOLOGICAL SURVEY PROFESSIONAL PAPER 501-C

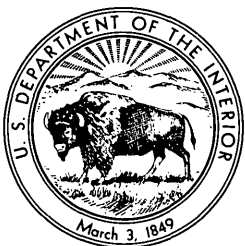
# GEOLOGICAL SURVEY RESEARCH 1964

## Chapter C

---

GEOLOGICAL SURVEY PROFESSIONAL PAPER 501-C

*Scientific notes and summaries of investigations prepared by members of the Geologic and Water Resources Divisions in the fields of geology, hydrology, and related sciences*



---

UNITED STATES GOVERNMENT PRINTING OFFICE, WASHINGTON: 1964

**UNITED STATES DEPARTMENT OF THE INTERIOR**

**STEWART L. UDALL, Secretary**

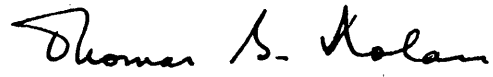
**GEOLOGICAL SURVEY**

**Thomas B. Nolan, Director**

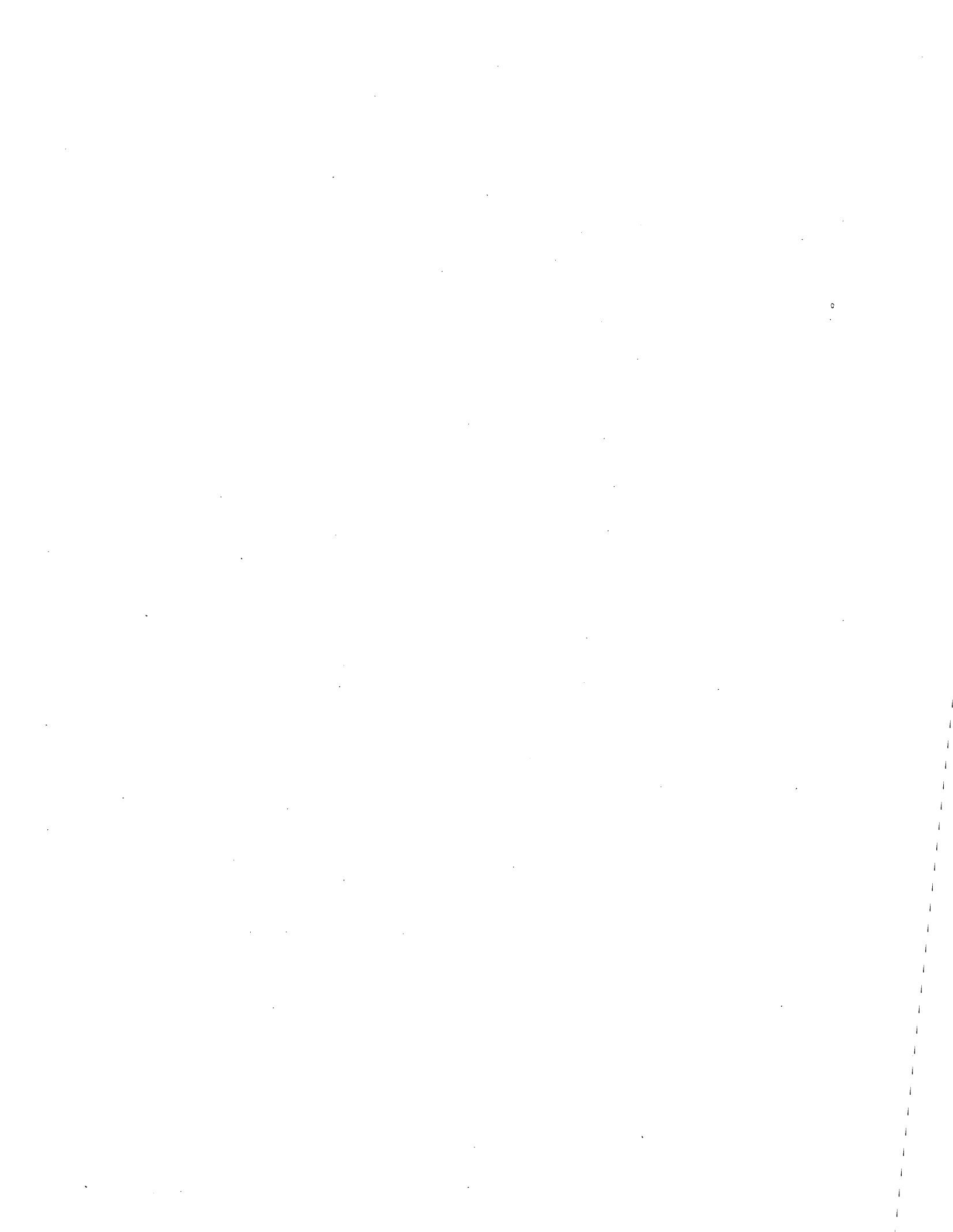
## **FOREWORD**

This collection of 46 short papers is the second of a series to be released as chapters of Geological Survey Research 1964. The papers report on scientific and economic results of current work by members of the Geologic, Conservation, Water Resources, and Topographic Divisions of the U.S. Geological Survey. Some of the papers present results of completed parts of continuing investigations; others announce new discoveries or preliminary results of investigations that will be discussed in greater detail in reports to be published in the future. Still others are scientific notes of limited scope, and short papers on techniques and instrumentation.

Chapter A of this series will be published later in the year, and will present a summary of results of work done during the present fiscal year.



THOMAS B. NOLAN,  
*Director.*



## CONTENTS

	Page
<b>Foreword</b> -----	III
<b>GEOLOGIC STUDIES</b>	
<b>Structural geology</b>	
Late Mesozoic orogenies in the ultramafic belts of northwestern California and southwestern Oregon, by W. P. Irwin-----	C1
Westward tectonic overriding during Mesozoic time in north-central Nevada, by R. E. Wallace and N. J. Silberling-----	10
Strike-slip faulting and broken basin-ranges in east-central Idaho and adjacent Montana, by E. T. Ruppel-----	14
Evidence for a concealed tear fault with large displacement in the central East Tintic Mountains, Utah, by H. T. Morris and W. M. Shepard-----	19
Shape and structure of a gabbro body near Lebanon, Conn., by M. F. Kane and G. L. Snyder-----	22
Outline of the stratigraphic and tectonic features of northeastern Maine, by Louis Pavlides, Ely Mencher, R. S. Naylor, and A. J. Boucot-----	28
<b>Stratigraphy and paleontology</b>	
Stratigraphic importance of corals in the Redwall Limestone, northern Arizona, by W. J. Sando-----	39
Younger Precambrian formations and the Bolsa(?) Quartzite of Cambrian age, Papago Indian Reservation, Ariz., by L. A. Heindl and N. E. McClymonds-----	43
Occurrence and paleogeographic significance of the Maywood Formation of Late Devonian age in the Gallatin Range, southwestern Montana, by C. A. Sandberg and W. J. McMannis-----	50
Petrography of the basement gneiss beneath the Coastal Plain sequence, Island Beach State Park, N.J., by D. L. Southwick-----	55
Offshore extension of the upper Eocene to Recent stratigraphic sequence in southeastern Georgia, by M. J. McCollum and S. M. Herrick-----	61
Upper Eocene smaller Foraminifera from Shell Bluff and Griffin Landings, Burke County, Ga., by S. M. Herrick-----	64
<b>Mineralogy and petrology</b>	
Post-Paleocene West Elk laeoolithic cluster, west-central Colorado, by L. H. Godwin and D. L. Gaskill-----	66
Chemistry of greenstone of the Catoctin Formation in the Blue Ridge of central Virginia, by J. C. Reed, Jr-----	69
Occurrence and origin of laumontite in Cretaceous sedimentary rocks in western Alaska, by J. M. Hoare, W. H. Condon, and W. W. Patton, Jr-----	74
Clay minerals from an area of land subsidence in the Houston-Galveston Bay area, Texas, by J. B. Corliss and R. H. Meade-----	79
Attapulgite from Carlsbad Caverns, N. Mex., by W. E. Davies-----	82
Diagram for determining mineral composition in the system $MnCO_3-CaCO_3-MgCO_3$ , by W. C. Prinz-----	84
<b>Geochemistry</b>	
Lithium associated with beryllium in rhyolitic tuff at Spor Mountain, western Juab County, Utah, by D. R. Shawe, Wayne Mountjoy, and Walter Duke-----	86
A geochemical investigation of the High Rock quadrangle, North Carolina, by A. A. Stromquist, A. M. White, and J. B. McHugh-----	88
Evaluation of weathering in the Chattanooga Shale by Fischer assay, by Andrew Brown and I. A. Breger-----	92
Measurement of relative cationic diffusion and exchange rates of montmorillonite, by T. E. Brown-----	96
<b>Geophysics</b>	
Preliminary structural analysis of explosion-produced fractures, HARDHAT event, Area 15, Nevada Test Site, by F. N. Houser and W. L. Emerick-----	100
Seismicity of the lower east rift zone of Kilauea Volcano, Hawaii, January 1962–March 1963, by R. Y. Koyanagi-----	103
<b>Economic geology</b>	
Paleolatitudinal and paleogeographic distribution of phosphorite, by R. P. Sheldon-----	106
Reconnaissance of zeolite deposits in tuffaceous rocks of the western Mojave Desert and vicinity, California, by R. A. Sheppard and A. J. Gude, 3d-----	114
Ore controls at the Kathleen-Margaret (MacLaren River) copper deposit, Alaska, by E. M. MacKevett, Jr-----	117

**Geomorphology and Pleistocene geology**

	Page
Cavities, or "tafoni", in rock faces of the Atacama Desert, Chile, by Kenneth Segerstrom and Hugo Henrquez-----	C121
Negaunee moraine and the capture of the Yellow Dog River, Marquette County, Mich., by Kenneth Segerstrom-----	126
Ancient lake in western Kentucky and southern Illinois, by W. I. Finch, W. W. Olive, and E. W. Wolfe-----	130
Outline of Pleistocene geology of Martha's Vineyard, Mass., by C. A. Kaye-----	134
Illinoian and Early Wisconsin moraines of Martha's Vineyard, Mass., by C. A. Kaye-----	140
Glacial geology of the Mountain Iron-Virginia-Eveleth area, Mesabi iron range, Minnesota, by R. D. Cotter, and J. E. Rogers-----	144

**Glaciology**

Recent retreat of the Teton Glacier, Grand Teton National Park, Wyo., by J. C. Reed, Jr-----	147
--	-----

**Analytical techniques**

A simple oxygen sheath for flame photometry, by Irving May, J. I. Dinnin, and Fred Rosenbaum-----	152
Determination of iodine in vegetation, by Margaret Cuthbert and F. N. Ward-----	154
Judging the analytical ability of rock analysts by chi-squared, by F. J. Flanagan-----	157
Ultrasonic dispersion of samples of sedimentary deposits, by R. P. Moston and A. I. Johnson-----	159

**HYDROLOGIC STUDIES****Ground water**

Tritium content as an indicator of age and movement of ground water in the Roswell basin, New Mexico, by H. O. Reeder-----	161
Relation of surface-water hydrology to the principal artesian aquifer in Florida and southeastern Georgia, by V. T. Stringfield-----	164

**Quality of water**

Contamination of ground water by detergents in a suburban environment—South Farmingdale area, Long Island, N.Y., by N. M. Perlmutter, Maxim Lieber, and H. L. Frauenthal-----	170
Relation of chemical quality of water to recharge to the Jordan Sandstone in the Minneapolis-St. Paul area, Minnesota, by M. L. Maderak-----	176

**Engineering hydrology**

Geohydrology of storage of radioactive waste in crystalline rocks at the AEC Savannah River Plant, S.C., by G. E. Siple-----	180
--	-----

**Theoretical hydrology**

Stream discharge regressions using precipitation, by H. C. Riggs-----	185
Relation of annual runoff to meteorological factors, by M. W. Busby-----	188

**TOPOGRAPHIC MAPPING****Photogrammetry**

Photogrammetric contouring of areas covered by evergreen forests, by James Halliday-----	190
--	-----

**INDEXES****Subject-----**

195

**Author-----**

197

## LATE MESOZOIC OROGENIES IN THE ULTRAMAFIC BELTS OF NORTHWESTERN CALIFORNIA AND SOUTHWESTERN OREGON

By WILLIAM P. IRWIN, Menlo Park, Calif.

*Work done in cooperation with the California Division of Mines and Geology*

**Abstract.**—The structural style of the pre-Tertiary rocks of northern California and southern Oregon is one of regional thrust faults along which great sheets of ultramafic rocks are emplaced. Ultramafic rocks form a belt along the Klamath Mountains and Sierra Nevada in which they intruded during the Late Jurassic Nevadan orogeny. To the west they form a second belt in which they intruded rocks of the Coast Ranges, probably during the Late Cretaceous. In the Coast Ranges these pre-Tertiary structures have been dislocated and obscured by faults of the San Andreas system.

of use in suggesting areas where critical relations might be examined.

The general concept to be developed is one of westward overriding of great, low-angle thrust plates during the late Mesozoic orogenies, and will rely considerably on the belief that the ultramafic rocks were emplaced primarily as sheets between the thrust plates. This differs from the tectonic style commonly accorded the Pacific coastal terrane, a style dominated by strike-slip movements along high-angle faults such as the San Andreas. The intent is not to minimize the significance of the strike-slip faults, but to point out that low-angle thrust faults may have a role of equal, if not greater, importance in the orogenic history of the Pacific borderland.

The rocks involved in the Nevadan orogeny are distinguished from later rocks by use of the term "subjacent." Subjacent refers to the Paleozoic and Mesozoic rocks involved in the Nevadan orogeny, including the ultramafic and granitic rocks that intruded during that orogeny. The term "superjacent" refers to the late Mesozoic and younger rocks that, in the Klamath Mountains, were deposited unconformably on the subjacent rocks. This article is not greatly concerned with superjacent rocks younger than Late Cretaceous in age, except that they conceal the lateral extensions of the older rocks and thus limit observation. The subjacent rocks predominate in the Klamath Mountains and Sierra Nevada, whereas the superjacent are the principal rocks of the Coast Ranges and Great Valley.

### SUBJACENT (NEVADAN AND OLDER) ROCKS

The subjacent rocks are eugeosynclinal, as they include greenstones, graywacke sandstones, mudstones,

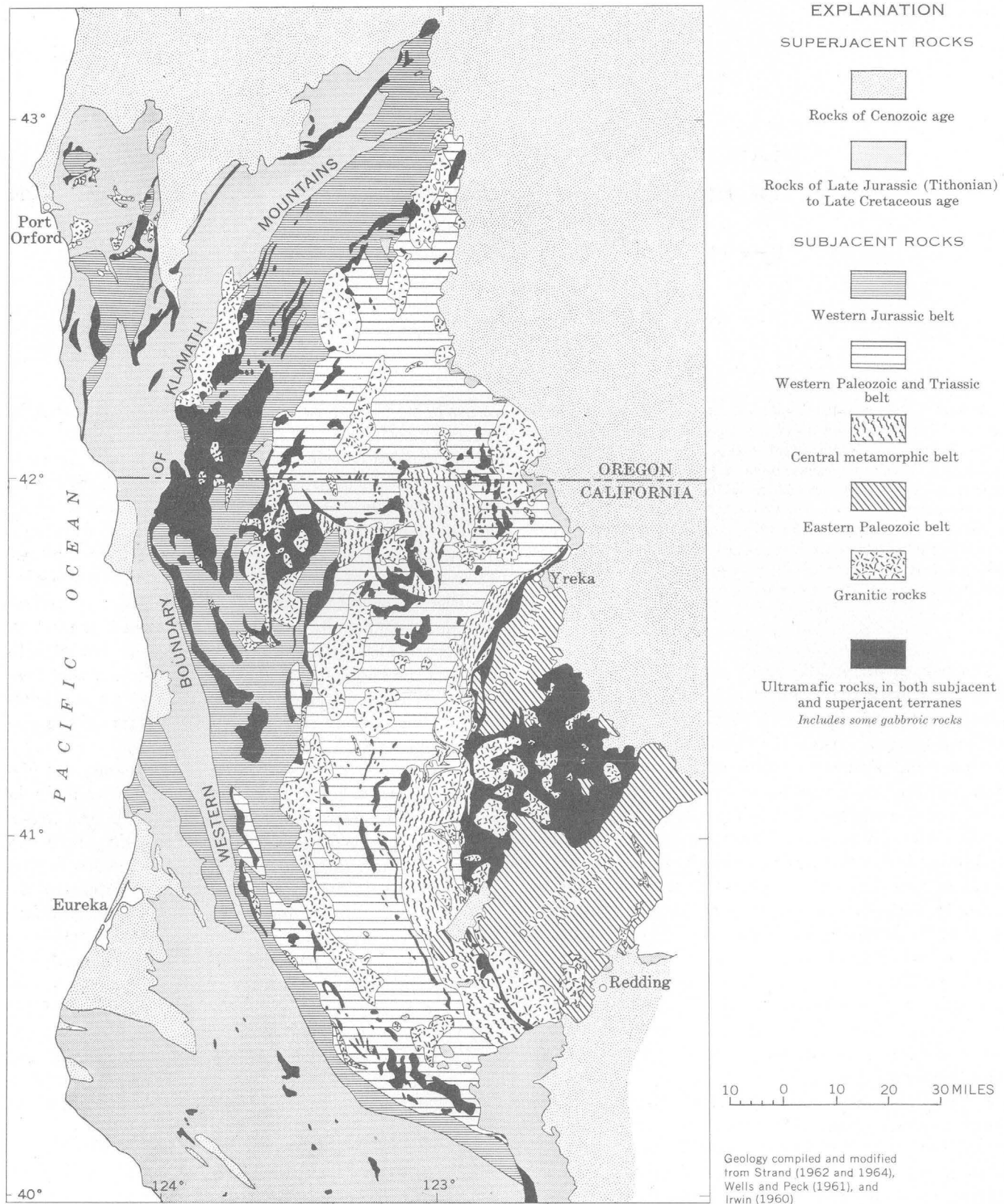


FIGURE 1.—Geologic map of northwestern California and southwestern Oregon.

Geology compiled and modified from Strand (1962 and 1964), Wells and Peck (1961), and Irwin (1960)

thin-bedded chert, and minor limestone. In the Klamath Mountains they occur in several broadly arcuate belts (fig. 1), which from east to west are the eastern Paleozoic, central metamorphic, western Paleozoic and Triassic, and western Jurassic belts (Irwin, 1960). At a few places in all the belts, except the eastern Paleozoic, patches of rocks of adjacent belts are found. Each belt seems to constitute a separate bundle of rocks, as no depositional contacts have been found between the separate bundles, and as the contacts between the belts, or the separate bundles, seem to be either faults or the loci for emplacement of ultramafic or granitic rocks. All the bundles have been intruded by ultramafic and granitic rocks.

The eastern Paleozoic belt is a thick, fairly complete, stratigraphic section that ranges in age from Ordovician(?) upward through the Paleozoic (fig. 2), and

These are the Stuart Fork Formation of Davis and Lipman (1962). They are exposed in windows in the central metamorphic belt, and are considered correlative with rocks of the western Paleozoic and Triassic belt (Davis and Lipman, 1962). The age of the rocks of the central metamorphic belt is not known, except that (1) the rocks are older than ultramafic and granitic rocks emplaced during the Nevadan orogeny; and (2) a  $K^{40}$ - $Ar^{40}$  age of 190 million years, obtained from hornblende of the Salmon Hornblende Schist by M. A. Lanphere (Irwin, 1963), indicates that the metamorphism was earlier than the Nevadan orogeny.

The western Paleozoic and Triassic belt lies west of the central metamorphic belt. It is structurally complex and seems to consist chiefly of Permian and Triassic rocks, although at one locality, fossils suggesting a Silurian and Devonian age were found (Merriam, 1961).

The western Jurassic belt is chiefly slaty mudstones and graywackes of the Galice Formation, which is as young as middle Kimmeridgian in age, and which is an equivalent of the Mariposa Formation of the Sierra Nevada. Along the western boundary of the Klamath Mountains it includes the schist of South Fork Mountain. In both California and Oregon, a few patches of rocks of the western Jurassic belt occur in the Coast Ranges west of the Klamath Mountains boundary.<sup>1</sup> Those in California are schist like that of South Fork Mountain; in Oregon they include the Galice Formation and Colebrooke Schist, a correlative of the schist of South Fork Mountain.

#### SUPERJACENT (POST-NEVADAN) ROCKS

The superjacent, post-Nevadan, rocks are the principal rocks of the Coast Ranges and Great Valley, and include the uppermost Jurassic (Tithonian) and Cretaceous. They occur along the southern, western, and northern perimeter of the Klamath Mountains, and also as a few small patches within the Klamath Mountains (fig. 1). The superjacent deposits are separated into two fundamentally different kinds: eugeosynclinal deposits, and noneugeosynclinal deposits. These two kinds of deposits were laid down penecontemporaneously during the Late Jurassic and Cretaceous and are equivalents, or facies, of one another (Irwin, 1957).

The eugeosynclinal superjacent deposits include the Franciscan Formation in California, and the Dothan Formation<sup>2</sup> and the Franciscan-like part of Diller's

<sup>1</sup> The western boundary of the Klamath Mountains shown on figure 1 more precisely separates the Klamath Mountains and Coast Ranges on the basis of subjacent and superjacent terranes, and structure, than does the boundary as drawn by Diller (1902), who included in the Klamath Mountains all the pre-Tertiary rocks of southwestern Oregon.

<sup>2</sup> The Dothan Formation usually has been regarded as part of the subjacent terrane, rather than superjacent as herein considered. Inclusion of the Dothan with the superjacent formations in no way violates any factual data.

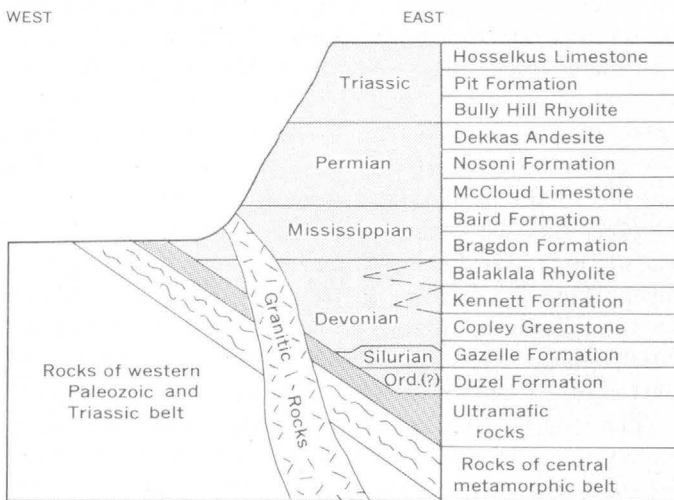


FIGURE 2.—Schematic section across the eastern part of the Klamath Mountains, Calif. Light tone, rocks of eastern Paleozoic belt; dark tone, ultrabasic rocks.

to the east continues on through Triassic into the Middle Jurassic. The strata of Ordovician(?) and Silurian age are known only in the northern part of the belt, whereas Devonian, Mississippian, and Permian strata occupy the remainder. The section is structurally complex in detail, but in general dips to the east. Rhyolitic strata occur at several places in the stratigraphic section, but none are known in the belts to the west.

The central metamorphic belt is separated from the eastern Paleozoic belt by ultramafic rocks. The rocks of the central metamorphic belt are chiefly the Salmon Hornblende Schist and Abrams Mica Schist of Hershey (1901). However, some of the rocks originally described by Hershey as part of the Abrams Mica Schist are now excluded from the central metamorphic belt.

(1898) Myrtle Formation in Oregon. For the most part they are thick assemblages of graywacke, mudstone, pillow lavas, and radiolarian chert. Lentils of distinctive Foraminifera-bearing limestones, the Calera (Lawson, 1914) in California, and the Whitsett (Diller, 1898) in Oregon, are found in the mid-Cretaceous parts of the deposits. The eugeosynclinal terrane is structurally complex and very sparsely fossiliferous, and exotic small blocks of glaucophane schist and ultramafic rock are fairly common features. The eugeosynclinal deposits probably were laid down along the western border of the continental mass, perhaps on the oceanic crust in an offshore environment. No evidence has been found to indicate that these eugeosynclinal rocks were deposited anywhere on the subjacent (continental) rocks.

The noneugeosynclinal superjacent deposits of latest Jurassic and Cretaceous age include the Great Valley sequence (or Sacramento Valley sequence of Irwin, 1957) in California, and the Myrtle Group (Imlay and others, 1959) in Oregon. These deposits were laid down predominantly, if not wholly, on subjacent rocks that formed the continental shelf and slope, and for brevity will hereafter be referred to as shelf deposits, in contrast to the eugeosynclinal deposits. The shelf deposits consist of interlayered beds of graywacke, mudstone, and conglomerate. These rocks more commonly show bedding features such as grading, crossbedding, and sole markings, are more fossiliferous, and generally are less folded and faulted than are the equivalent eugeosynclinal rocks. Other relative differences such as greater K-feldspar content (Bailey and Irwin, 1959) and lower specific gravity (Irwin, 1961) also have been noted.

In California the Lower Cretaceous shelf deposits lap on the subjacent rocks of the Klamath Mountains, including the Shasta Bally batholith ( $K^{40}-Ar^{40}$  age 134 m.y., Curtis and others, 1958). The Upper Jurassic is conformable beneath the Lower Cretaceous along the west side of the Great Valley about 15 miles and more south of Shasta Bally batholith; thus the Upper Jurassic (Knoxville Formation of Tithonian age) also must postdate the intrusion and stripping of the Shasta Bally batholith. At the north end of the Klamath Mountains in Oregon the Upper Jurassic (Riddle Formation of Tithonian age) and Lower Cretaceous (Days Creek Formation), similar to correlative rocks of the Great Valley sequence of California, also lie unconformably on the subjacent rocks. Scattered patches of Lower Cretaceous and Upper Cretaceous shelf deposits lie on the subjacent rocks elsewhere in the Klamath Mountains, and it is clear that these shelf deposits once covered much of the Klamath Mountains. The rela-

tions between the superjacent shelf deposits and subjacent rocks are shown diagrammatically on figure 3. On the left side of the same figure the eugeosynclinal equivalents of the superjacent shelf deposits are shown in thrust-fault contact with the subjacent rocks of the Klamath Mountains province.

### ULTRAMAFIC ROCKS

The ultramafic rocks are an important key in outlining the structural framework of northern California and southern Oregon. They are chiefly peridotite that generally is somewhat serpentined and at many places highly sheared. Some gabbroic rocks occur with the ultramafic rocks, and although of questionable genetic relation, they are included with the ultramafic rocks shown on figures 1 and 4 for cartographic convenience. The ultramafic rocks in the Klamath Mountains intrude subjacent strata as young as Late Jurassic (Kimmeridgian) and are in turn intruded by granite. Thus the ultramafic rocks of the Klamath Mountains belong to the subjacent block, and along with the granitic and other subjacent rocks, are overlain unconformably by the superjacent shelf deposits. In the Coast Ranges the ultramafic rocks intrude superjacent strata as young as early Late Cretaceous (Cenomanian) in age. Thus the ultramafic rocks occur in two belts. Those involved in the Nevadan orogeny lie to the east, and are referred to the Klamath ultramafic belt. Those that intrude Mesozoic superjacent strata lie to the west and are referred to the Coast Range ultramafic belt.

The general trend of the Klamath ultramafic belt is arcuate (fig. 4), parallel to the pattern of the lithic belts of subjacent rocks of the Klamath Mountains. At the south end of the Klamath Mountains the belt presumably extends to the southeast beneath superjacent strata

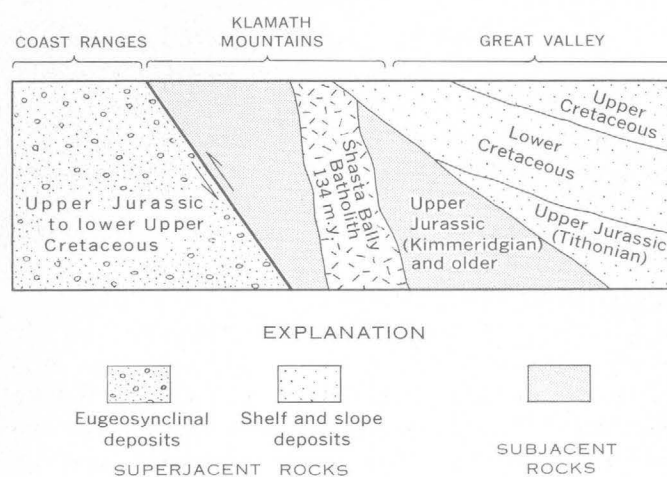


FIGURE 3.—Schematic relations between superjacent and subjacent rocks.

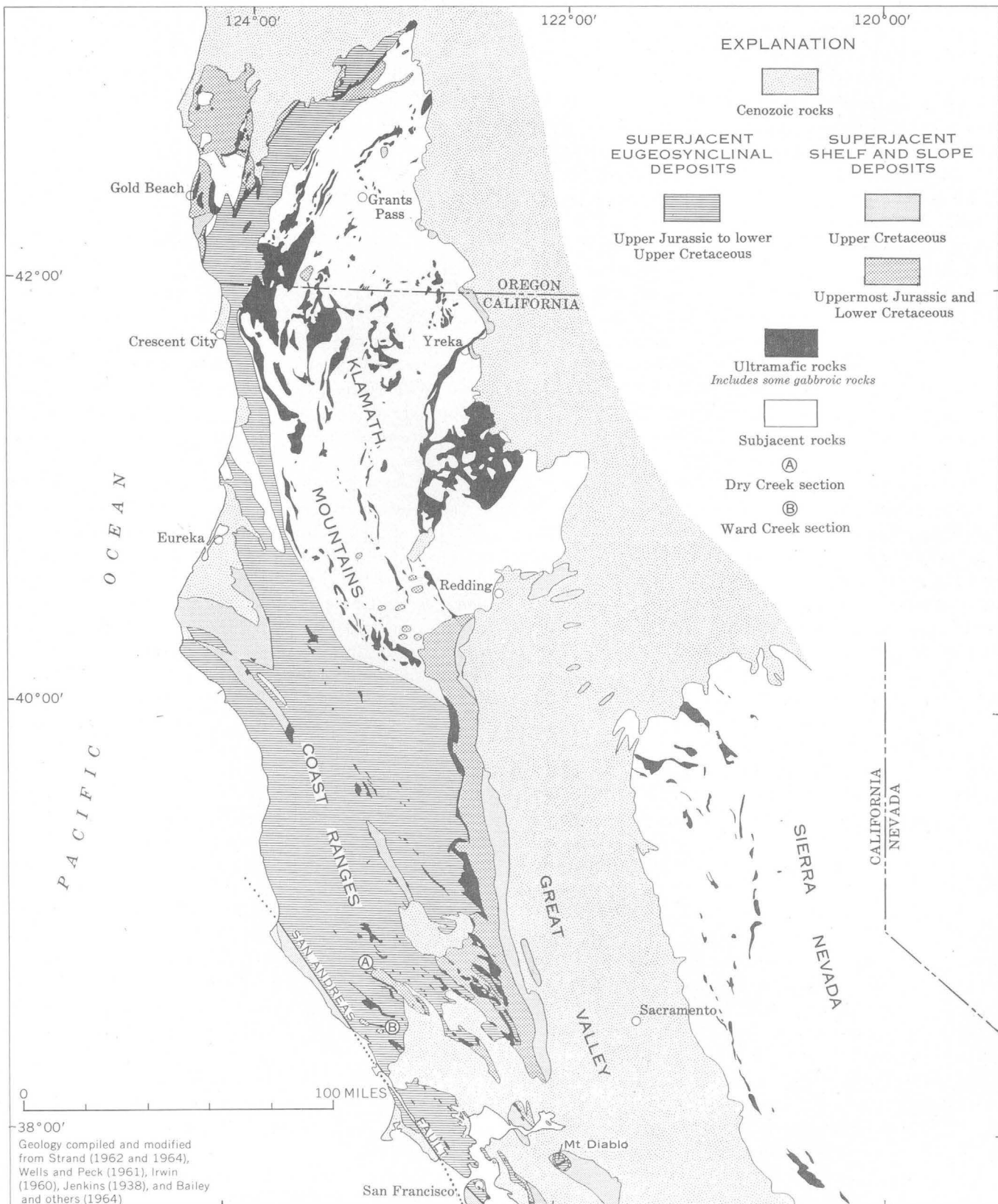


FIGURE 4.—Distribution of ultramafic rocks and two facies of superjacent rocks in northwestern California and southwestern Oregon.

of the Great Valley, and continues southward along the foothills of the western Sierra Nevada. In the eastern Klamath Mountains the ultramafic rocks are regarded as parts of a once-continuous, subhorizontal sheet that separated the rocks of the central metamorphic belt from structurally overlying rocks of the eastern Paleozoic belt (Irwin and Lipman, 1962). The present arcuate outcrop of the ultramafic rocks between the two belts is the eroded lip of the sheet whose roots lie buried beneath the Paleozoic strata to the east. The large area of ultramafic rock that generally separates the Ordovician(?) and Silurian from the younger strata in the eastern Paleozoic belt (fig. 1) is interpreted as a broad arch in the sheet from which the once-overlying Paleozoic strata are largely eroded. In one sense, the area of Ordovician(?) and Silurian strata may even be considered a large outlier, unless it connects with the main body of eastern Paleozoic strata beneath superjacent strata to the northeast. In the southern part of the Klamath Mountains an outlier of Mississippian strata of the eastern Paleozoic belt rests on, but is generally separated from, rocks of the central metamorphic belt by a thin layer of ultramafic rock (Irwin, 1963).

As shown schematically on figure 2, the ultramafic sheet is discordant with the stratigraphic section of the eastern Paleozoic belt. This discordance, in addition to the structural break seemingly required for intrusion of a low-angle sheet of such great magnitude, suggests that the ultramafic sheet intruded along a thrust fault of considerable horizontal translation.

West of the central metamorphic belt, the ultramafic rocks do not as clearly occur as widespread sheets. At many places they are concentrated along boundaries between lithic belts, and within lithic belts as alined, though discontinuous, bodies. Detailed mapping probably will establish an areal sheetlike continuity for many of these now seemingly unrelated bodies. However, at present it is not known whether the ultramafic rocks west of the central metamorphic belt should be considered dislocated portions of several large individual sheets, or whether one might take an extreme view that all the ultramafic rocks of the Klamath Mountains were originally parts of one great sheet that transgressed successively younger strata from the eastern Paleozoic belt to the western Jurassic belt.

The pattern of distribution of ultramafic rocks in the Coast Range belt differs from that of the Klamath belt (fig. 4). Here the arcuate pattern that reflects the structure of the subjacent terrane of the Klamath Mountains is not present. The principal ultramafic body of the Coast Range belt trends north-south along the west side of the Great Valley. At the south end of this large body, approximately at the latitude of Sacramento, the

concentration of ultramafic rock extends to the west as a series of individual, northwesterly oriented bodies. These are thought to be faulted segments of the north-south-trending body. Here, as elsewhere, most of the ultramafic rock of the Coast Ranges occurs along or near contacts between the two facies of superjacent rocks.

#### STRUCTURAL RELATION OF FACIES OF SUPERJACENT ROCKS

The distribution of the two facies of Late Jurassic (Tithonian) and Cretaceous superjacent rocks is shown on figure 4. The eugeosynclinal (Franciscan) facies is confined to the Coast Ranges and is the dominant rock there. Along the west side of the Great Valley the eugeosynclinal facies on the west is separated from the shelf facies (Great Valley sequence) on the east by the major body of ultramafic rock of the Coast Ranges. At the south end of the body, the area of shelf facies swings to the west across the grain of the Coast Ranges, following the concentration of ultramafic rocks. Here the structure seems to have been a broad arch, plunging gently south, in which the rocks of the Great Valley sequence mantled the Franciscan, but which were separated from the Franciscan by an ultramafic sheet. The crest and west limb of the arch have been broken, and its continuity obscured, by numerous steep northwest-trending faults of the San Andreas system, giving a northwest-trending pattern that is typical of the Coast Ranges. Near the San Andreas fault, in the western part of the Coast Ranges at this latitude, patches of rocks of the Great Valley sequence are now outliers completely isolated within large areas of Franciscan rocks, and here, too, the ultramafic rocks are concentrated along the boundaries between the two facies. Two of these outliers of the Great Valley sequence are known (Bailey and others, 1964) as the Ward Creek and Dry Creek sections (fig. 4).

The arch trends along the east side of the Coast Ranges for almost the length of the Great Valley, and is the major structure of the central Coast Ranges east of the San Andreas fault (Bailey and others, 1964). Along the arch are the great piercement structures, such as at Mount Diablo, east of San Francisco, and the Diablo Range. In these piercements the underlying Franciscan rocks have broken through the mantle of Great Valley sequence and younger rocks, and have carried with them some of the intermediate layer of ultramafic rock.

The structural relations between the two facies of late Mesozoic superjacent strata are shown in cross section (fig. 5). In the Coast Ranges, along the line of section, the shelf deposits extend from the Great Valley

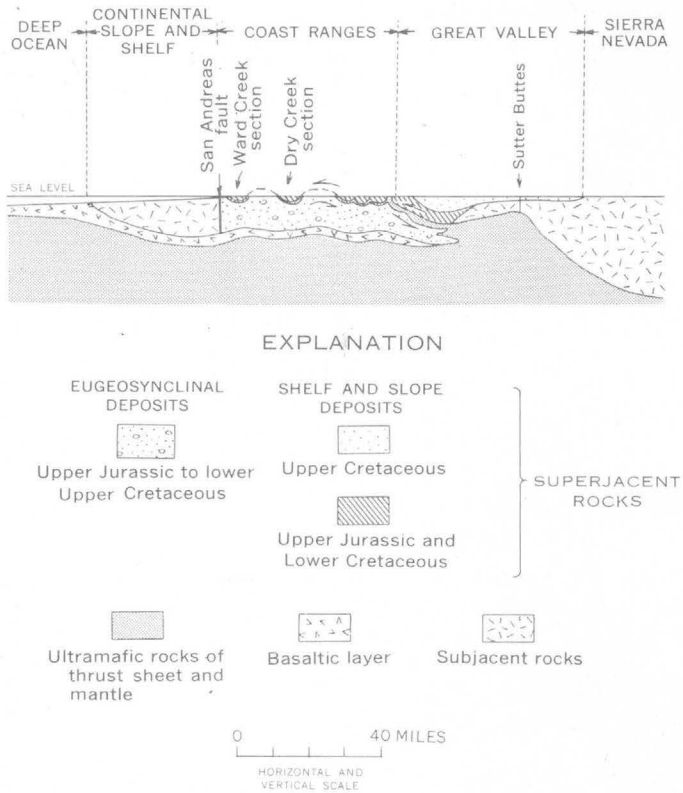


FIGURE 5.—Schematic section showing structural relations between two facies of superjacent rocks.

westward over equivalent eugeosynclinal strata of the Coast Ranges, but are separated by an ultramafic sheet. Note particularly the outlying Ward Creek and Dry Creek sections of shelf deposits, which are mildly deformed in contrast to their surrounding eugeosynclinal equivalents. This juxtaposition of facies seems to demand great relatively westward transport of shelf rocks over eugeosynclinal rocks. As the bulk of the ultramafic rock of the Coast Ranges occurs along boundaries between these juxtaposed facies, most if not all the ultramafic rock may be dislocated parts of a single sheet emplaced along a subhorizontal fault between the two facies. The root zone of the ultramafic sheet lies to the east, presumably connecting with the mantle, and may account for the large positive magnetic anomaly that trends the length of the Great Valley (Irwin and Bath, 1962). As shown on figure 5, the amount of horizontal transport, or relative westward riding of the shelf deposits, is 50 miles or more. The thrusting and intrusion probably were part of the same orogeny that formed the thrust fault along the western boundary of the Klamath Mountains.

#### THRUST-PLATE RELATIONS

The inferred structural relations of the pre-Tertiary strata of the Klamath Mountains and Coast Ranges are

summarized schematically on figure 6. The several lithic belts of the Klamath Mountains are considered thrust plates that successively overlap adjacent plates to the west. Isolated patches of rocks correlative with a specific belt are interpreted to be thrust outliers or windows of the plate to which the correlative rocks have been assigned. For illustrative convenience, the granitic and ultramafic rocks are not outlined, and are included arbitrarily with individual thrust plates. Although ultramafic rock intruded between certain of the thrust plates, its inclusion with individual plates does not in most cases seriously distort the outlines of the thrust plates shown on figure 6. An exception is the outline of the eastern Paleozoic plate. Here, the erosional lip and exposed crest of the broad arch in the ultramafic sheet are included with the eastern Paleozoic plate. Thus the eastern Paleozoic plate as shown on figure 6 is not only the distribution of the rocks of the eastern Paleozoic belt, but includes a reconstruction of the strata of the eastern Paleozoic belt that formerly bridged the broad arch of ultramafic rocks. Because of this, the position of the Gray Rocks outlier, which forms part of this bridge, is shown only by a symbol.

The central metamorphic plate lies below the eastern Paleozoic plate and above the western Paleozoic and Triassic plate. The Oregon Mountains outlier of the eastern Paleozoic plate rests on the central metamorphic plate, and, as suggested by Davis and Lipman (1962), windows at several places along the central metamorphic plate expose portions of the underlying western Paleozoic and Triassic plate. Along its western border the western Paleozoic and Triassic plate lies on the western Jurassic plate, with the Willow Creek, Prospect Hill, and Flint Valley outliers of the western Paleozoic and Triassic plate presumably resting on the western Jurassic plate. Near the boundary between California and Oregon, an area of rocks similar to those of the central metamorphic belt is exposed, presumably in a window, nearly surrounded by abundant ultramafic bodies in the western Paleozoic and Triassic belt.

These thrust plates are depositionally overlapped at the south end of the Klamath Mountains by the superjacent shelf deposits, and thus are older than Late Jurassic (Tithonian) in age. Whether all these thrust plates were developed during a single brief orogenic episode is not clear. However, if all the relevant ultramafic rocks were emplaced during a single brief span of time in the Late Jurassic, between the middle Kimmeridgian and Tithonian Stages, a similar age span seems likely for the major thrusting. The thrusting, the emplacement of the Klamath ultramafic sheets, and the intrusion of granitic batholiths are tentatively

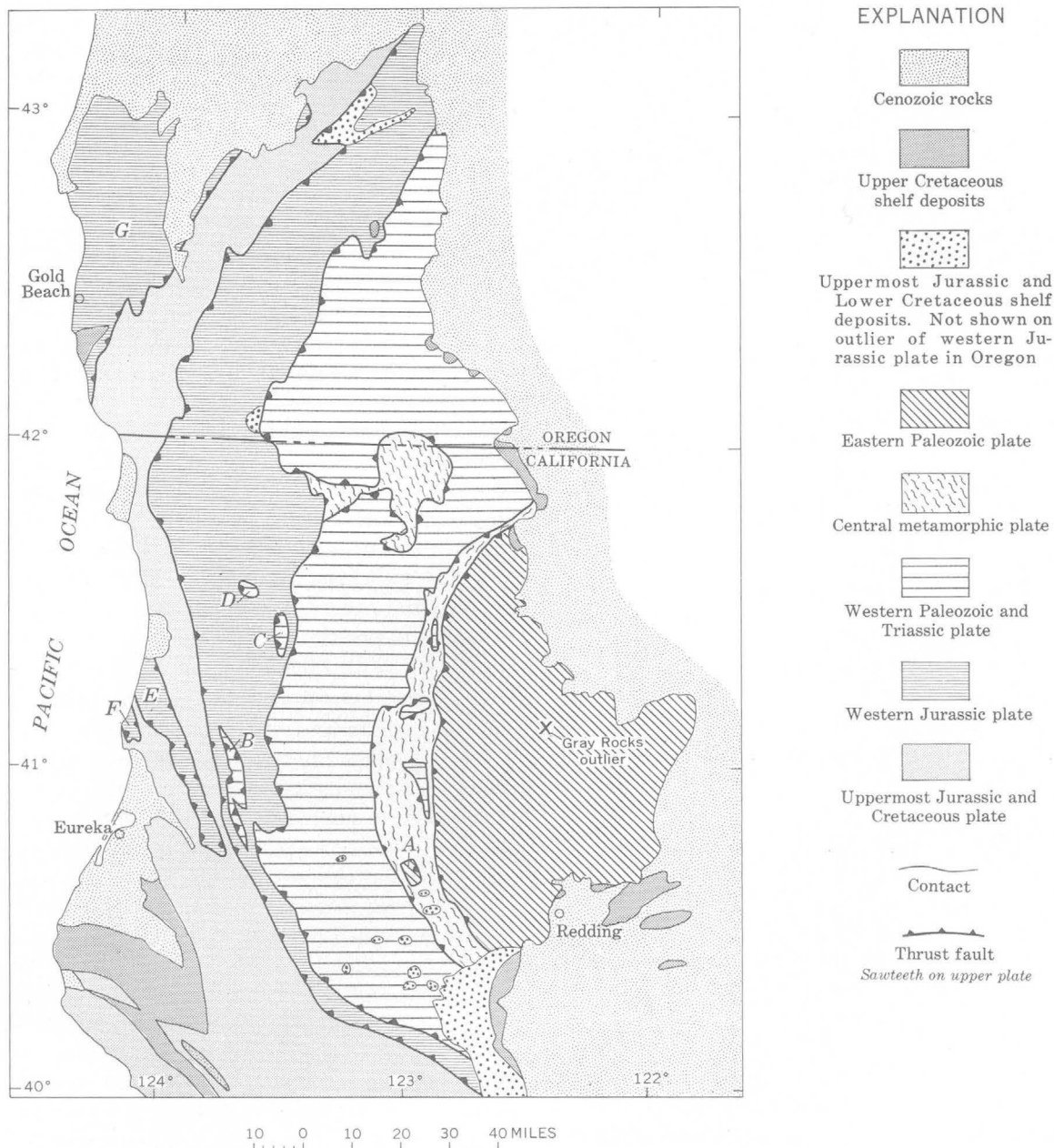


FIGURE 6.—Principal postulated thrust plates of the Klamath Mountains and adjacent Coast Ranges. Thrust outliers are indicated by letter symbol: *A*, Oregon Mountain; *B*, Willow Creek; *C*, Prospect Hill; *D*, Flint Valley; *E*, Redwood Mountain; *F*, Patricks Point; and *G*, southwestern Oregon.

considered closely timed sequential events of the Nevadan orogeny.

The western Jurassic plate is thrust westward over eugeosynclinal superjacent rocks along the western boundary of the Klamath Mountains. The Redwood Mountain and Patrick Point outliers in California, and the outlier formerly considered part of the Klamath Mountains in southwestern Oregon, are postulated to be thrust outliers of the western Jurassic plate resting on eugeosynclinal superjacent rocks.

The eugeosynclinal superjacent rocks along the western boundary of the Klamath Mountains are, at least locally, of Early Cretaceous age and are mildly metamorphosed. It is noteworthy that equivalent shelf deposits, adjacent or only a few miles to the east, are not metamorphosed and lie with depositional contact on thrust plates of subjacent rocks that are structurally higher than the eugeosynclinal superjacent rocks. Hence, the thrusting along the boundary of the Klamath Mountains clearly postdates the Nevadan orogeny,

and is younger than Early Cretaceous. The southwestern Oregon outlier is particularly interesting, as it includes not only subjacent rocks (Galice Formation, Colebrooke Schist, and granitic rocks) of the western Jurassic belt, but also superjacent shelf deposits that were laid down on the subjacent rocks of the plate before the plate was thrust over the superjacent eugeosynclinal rocks.

The thrusting that formed the boundary fault along the west side of the Klamath Mountains presumably was contemporaneous with the thrusting that controlled the emplacement of the ultramafic rocks of the Coast Range belt. The thrusting in both cases is clearly later than Early Cretaceous, and an apparent juxtaposition of superjacent shelf deposits of Late Jurassic and Early Cretaceous age against eugeosynclinal strata of early Late Cretaceous age in the San Francisco Bay area of California and Roseburg area of Oregon suggests that the age of the Coast Range orogeny is post-early Late Cretaceous. An upper limit to the age of the Coast Range orogeny is inferred from the relation of late Late Cretaceous shelf deposits to the older superjacent strata. In the Great Valley, deposition of the superjacent shelf deposits was virtually conformable into the late Late Cretaceous. In the Coast Ranges, however, the relation is one of great unconformity at the few places where the late Late Cretaceous shelf deposits are known to occur on the older shelf and eugeosynclinal rocks.

#### REFERENCES

- Bailey, E. H., and Irwin, W. P., 1959, K-feldspar content of Jurassic and Cretaceous graywackes of northern Coast Ranges and Sacramento Valley, California: Am. Assoc. Petroleum Geologists Bull., v. 43, no. 12, p. 2797-2809.
- Bailey, E. H., Irwin, W. P., and Jones, D. L., 1964, Franciscan and related rocks, and their significance in the geology of western California: California Div. Mines and Geology Bull. 183. [In press]
- Curtis, G. H., Evernden, J. F., and Lipson, J., 1958, Age determination of some granitic rocks in California by the potassium-argon method: California Div. Mines Spec. Rept. 54, 16 p.
- Davis, G. A., and Lipman, P. W., 1962, Revised structural sequence of pre-Cretaceous metamorphic rocks in the southern Klamath Mountains, California: Geol. Soc. America Bull., v. 73, p. 1547-1552.
- Diller, J. S., 1898, Description of the Roseburg quadrangle: U.S. Geol. Survey Geol. Atlas, Folio 49, 4 p.
- 1902, Topographic development of the Klamath Mountains: U.S. Geol. Survey Bull. 196, 69 p.
- Hershey, O. H., 1901, Metamorphic formations of northwestern California: Am. Geologist, v. 27, p. 225-245.
- Imlay, R. W., Dole, H. M., Wells, F. G., and Peck, D. L., 1959, Relations of certain Jurassic and Lower Cretaceous formations in southwestern Oregon: Am. Assoc. Petroleum Geologists Bull., v. 43, no. 12, p. 2770-2785.
- Irwin, W. P., 1957, Franciscan group in Coast Ranges and its equivalents in Sacramento Valley, California: Am. Assoc. Petroleum Geologists Bull., v. 41, no. 10, p. 2284-2297.
- 1960, Geologic reconnaissance of the northern Coast Ranges and Klamath Mountains, California, with a summary of the mineral resources: California Div. Mines Bull. 179, 80 p.
- 1961, Specific gravity of sandstones in the Franciscan and related Upper Mesozoic formations of California: Art. 78 in U.S. Geol. Survey Prof. Paper 424-B, p. B189-B191.
- 1963, Preliminary geologic map of the Weaverville quadrangle, California: U.S. Geol. Survey Mineral Inv. Field Studies Map MF-275.
- Irwin, W. P., and Bath, G. D., 1962, Magnetic anomalies and ultramafic rock in northern California: Art. 25 in U.S. Geol. Survey Prof. Paper 450-B, p. B65-B67.
- Irwin, W. P., and Lipman, P. W., 1962, A regional ultramafic sheet in eastern Klamath Mountains, California: Art. 67 in U.S. Geol. Survey Prof. Paper 450-C, p. C18-C21.
- Jenkins, O. P., 1938, Geologic map of California: California Div. Mines, 6 sheets.
- Lawson, A. C., 1914, Description of the San Francisco district; Tamalpais, San Francisco, Concord, San Mateo, and Hayward quadrangles: U.S. Geol. Survey Geol. Atlas, Folio 193, 24 p.
- Merriam, C. W., 1961, Silurian and Devonian rocks of the Klamath Mountains, California: Art. 216 in U.S. Geol. Survey Prof. Paper 424-C, p. C188-C190.
- Strand, R. G., 1962, Geologic map of California, Olaf P. Jenkins edition, Redding sheet: California Div. Mines and Geology.
- 1964, Geologic map of California, Olaf P. Jenkins edition, Weed sheet: California Div. Mines and Geology.
- Wells, F. G., and Peck, D. L., 1961, Geologic map of Oregon west of the 121st meridian: U.S. Geol. Survey Misc. Geol. Inv. Map I-325.



## WESTWARD TECTONIC OVERRIDING DURING MESOZOIC TIME IN NORTH-CENTRAL NEVADA

By ROBERT E. WALLACE and NORMAN J. SILBERLING, Menlo Park, Calif.

*Work done in cooperation with the Nevada Bureau of Mines*

**Abstract.**—Large-scale overturned folds indicate that higher structural units rode westward over lower units during Jurassic-Cretaceous orogeny. The examples discussed are in a belt extending from the vicinity of Lovelock, Nev., to the Hot Springs Range northeast of Winnemucca, Nev., a distance of more than 100 miles.

The purpose of this article is to reemphasize the presence of a westward-directed movement pattern of Mesozoic age in the tectonics of north-central Nevada, a fact which may be lost sight of in the discussions of more predominant eastward-directed movement patterns of Paleozoic age of the Roberts Mountains thrust (Roberts and others, 1958, p. 2850-2854), and other large thrusts of Late Cretaceous and early Tertiary age in the central and eastern Great Basin.

The chief evidence presented here that higher structural units have ridden westward over lower units is the geometry of large-scale overturned folds. Although thrust faults are involved in this movement pattern, the direction of movement of upper-plate rocks commonly cannot be determined from thrust relations alone; neither is the relation of folding and thrust faulting clear in every case. The term "tectonic overriding" is used as a general descriptive term to include any type of strain, either folding or faulting, in which higher tectonic reference points move over lower reference points. By use of this term, genetic implications, such as the nature of coupling between folds and faults or origin of stresses, are avoided.

Muller (1949, p. 54) first postulated westward overthrusting of Jurassic age in the region, and Willden (1961, p. C116) describes paleogeographic evidence for a westward-directed thrust of post-Middle Triassic age in the Kings River Range, Nev. Silberling and Rob-

erts (1962, p. 50-52) discuss possible movement directions of post-Triassic thrust plates as based on paleogeographic relations of Triassic rocks, and prefer the interpretation of westward overriding along the Tobin, Willow Creek, and other faults of known Mesozoic age in the East, Tobin, and Sonoma Ranges.

The examples of overturned folds discussed below and illustrated on figure 2 are in a northeast-trending belt extending from the vicinity of Lovelock, Nev., to the Hot Springs Range northeast of Winnemucca, Nev. (fig. 1). Although the belt is only crudely defined, there seems to be enough regional data now available to establish its reality as a more or less continuous movement field. The entire extent of the westward-movement field is as yet unknown, but the small remnant of a westward-directed thrust plate described by Willden in the Kings River Range is about 40 miles northwest of the Hot Springs Range.

Westward tectonic overriding represented in all examples cited except in the Hot Springs Range probably is related to Jurassic-Cretaceous orogeny. Within the belt, intrusive rocks believed to be of Late Jurassic or Early Cretaceous age seem to be unaffected by the folding. However, ages of all critical intrusive bodies are not known with certainty. In the Hot Springs Range, only rocks of Cambrian age are involved, and Roberts and others (1958, p. 2829) believe that these rocks are in approximately normal position on the west flank of a major anticline. In the Edna Mountains, strata of the Preble Formation, also part of the anticline, are overlain unconformably by the Antler sequence which ranges in age from Middle Pennsylvanian to Permian. The implication, although indirect, is that the overturned folds in Cambrian rocks of the Hot Springs Range were produced in pre-Middle Pennsylvanian time. We

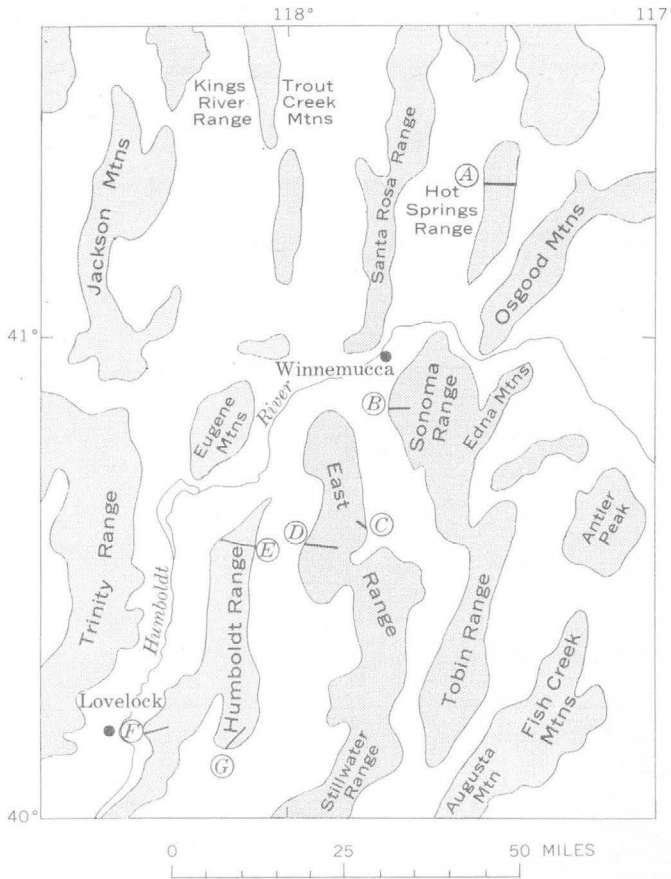


FIGURE 1.—Map showing location of examples of westward overriding of probable Jurassic-Cretaceous age. Letters and accompanying lines indicate location of sections shown on figure 2.

believe that this indirect implication is not sufficiently strong to rule out the possibility that the asymmetry of the folds in the Hot Springs Range is indeed related to Jurassic-Cretaceous orogeny, even though some type of deformation prior to Middle Pennsylvanian time is clearly represented.

In contrast to the movement pattern in this belt, Roberts (1951) found that in the Antler Peak area to the east, overturning is predominantly toward the east and is of Paleozoic age. James Gilluly and Olcott Gates (report in preparation) show similar relations in the northern Shoshone Range. To the west, in the Jackson Mountains, overturning and thrusting of probable Late Cretaceous and early Tertiary age is directed eastward (Willden, 1958, p. 2397).

The belt of westward overriding may represent secondary structures complimentary to a more general eastward-directed movement pattern, forming where eastward movement of upper-plate rocks was locally impeded. Or, more likely, it may represent a period of

movement reversal, possibly more widespread than now recognized.

#### EXAMPLES OF OVERTURNED FOLDS

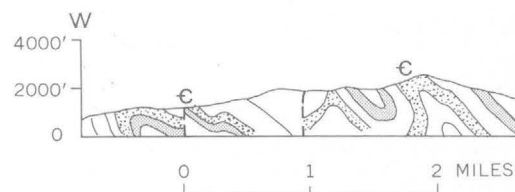
*Hot Springs Range (fig. 2A)* (Hotz and Willden, 1960).—Rocks of the Harmony Formation of Late Cambrian age underlie most of the Hot Springs Range and have been thrown into a series of overturned folds, the axial planes of which strike about N. 20° E., and have dips ranging from 45° to 55° E.

*Western Sonoma Range (fig. 2B)* (Ferguson and others, 1951).—A series of large faulted overturned folds, involving rocks of the Prida, Natchez Pass, Grass Valley, Dun Glen, and Winnemucca Formations of Middle and Late Triassic age are overridden by rocks of the Harmony and Sonoma Range Formations of Late Cambrian and Ordovician(?) ages respectively. The axial planes of the folds strike almost north and dip about 50° E. Some of these folds may be collinear with folds in the northeastern East Range.

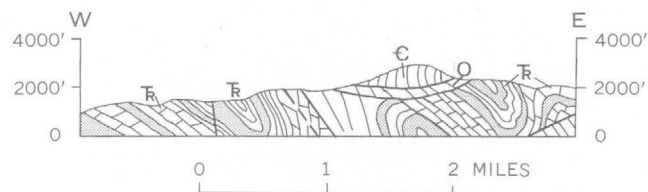
*Northeastern East Range (fig. 2C)* (Ferguson and others, 1951).—An overturned syncline and anticline involve rocks of the Prida, Natchez Pass, Grass Valley, Dun Glen, and Winnemucca Formations of Middle and Late Triassic age as well as the underlying Koipato Group of Permian and Early Triassic age. Axial planes strike about N. 30° E. and dip about 55°. Silberling and Roberts (1962, pl. 2) regard these rocks, as well as the underlying Havallah Formation, as having been overridden from the southeast by the Paleozoic rocks that form the upper plate of the Willow Creek thrust.

*Western East Range (fig. 2D)*.—An overturned anticline extends for about 10 miles along the western flank of the East Range. The strike of its axial plane ranges from north to N. 35° E., and its dip from 40° to 60° E. Rocks of the Leach and Inskip Formations are involved in the fold, and the entire block is thrust over rocks of the Winnemucca sequence. Silberling and Roberts (1962, p. 46) suggest that the Leach is of Ordovician age and that the Inskip may be of Mississippian age, but age assignments are still uncertain.

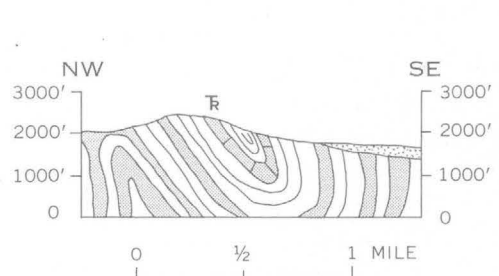
*Northern Humboldt Range (fig. 2E)*.—The overturned flank of a major fold represents westward overriding. This movement pattern appears to be superimposed upon a smaller scale and possibly older pattern of eastward overriding, including overturned folds and thrust faults. At the extreme north end of the range and in low hills northeast of the main Humboldt Range, the overturned flank approaches a recumbent attitude. Strata of the Koipato Group of Permian and Early Triassic age and of the Prida, Natchez Pass, and Grass Valley Formations of Middle and Late Triassic age are involved in the deformation.



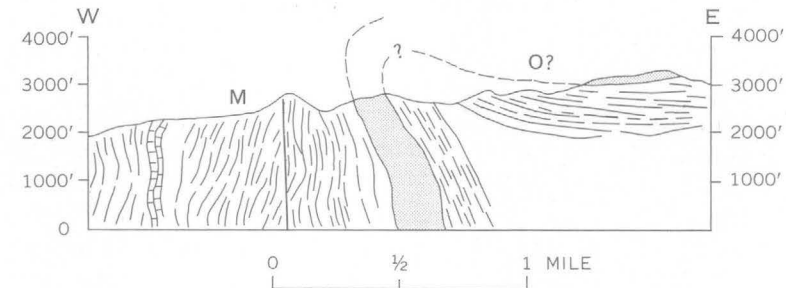
A. Hot Springs Range



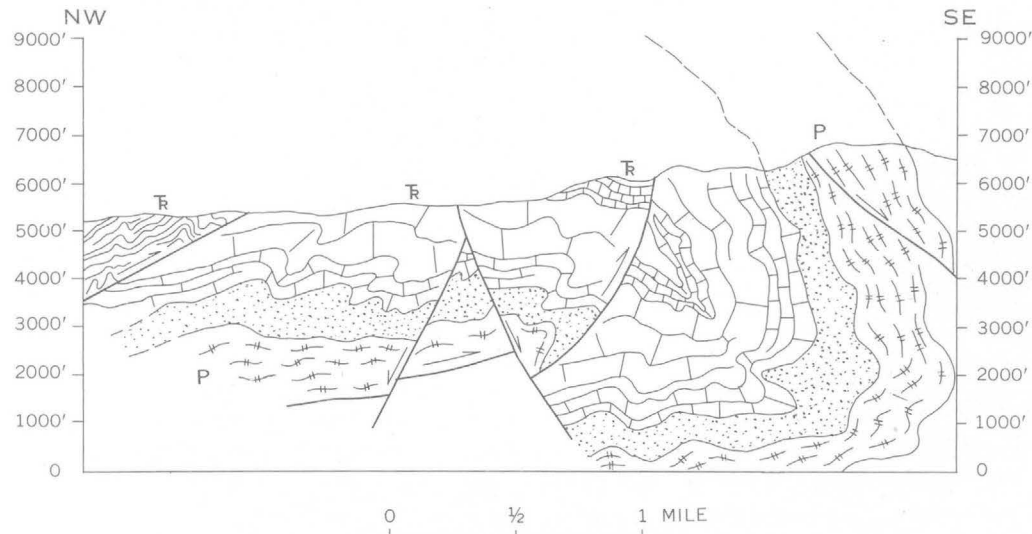
B. Western Sonoma Range, Mullen Canyon



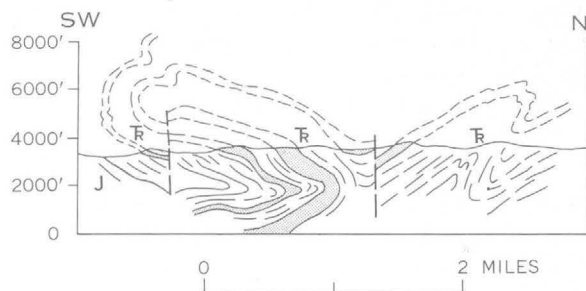
C. Northeastern East Range



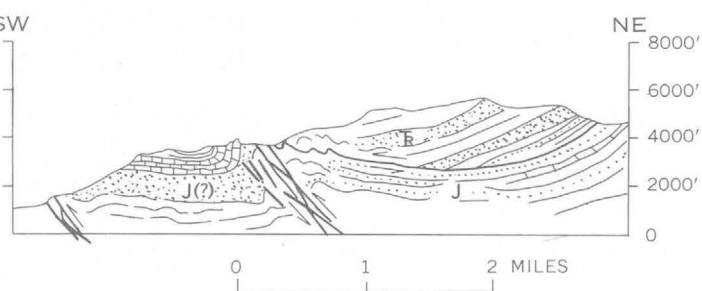
D. Western East Range



E. Northern Humboldt Range



F. Southern Humboldt Range



G. West Humboldt Range, Gypsum Peak

FIGURE 2.—Diagrammatic sections illustrating overturned folds described in text. Location of sections shown on figure 1. Symbols: C, Cambrian; O, Ordovician; M, Mississippian; P, Permian; R, Triassic; J, Jurassic. Patterns show structure of the folded beds but do not necessarily indicate the lithology.

*Southern Humboldt Range (fig. 2F).*—A large fan fold is interpreted as representing an overall movement direction to the southwest. The southwest limb is the larger, far more complex limb of the two and is recumbently overturned. Rocks of Late Triassic and Early Jurassic age are involved.

*West Humboldt Range (fig. 2G).*—Due east of Lovelock, Nev., a thrust plate composed of rocks of Late Triassic age rests on rocks of Early Jurassic age. Along the western margin of the thrust plate as exposed, gypsumiferous beds and their enclosing strata have been thrown into an asymmetric syncline. The age of the gypsumiferous beds is not certain but is believed to be Early Jurassic. The asymmetry of the fold, the axial plane of which dips about 50° E., implies overriding from east to west.

#### REFERENCES

Ferguson, H. G., Muller, S. W., and Roberts, R. J., 1951, Geology of the Winnemucca quadrangle, Nevada: U.S. Geol. Survey Geol. Quad. Map GQ-11.

- Hotz, P. E., and Willden, Ronald, 1960, Preliminary geologic map and sections of the Osgood Mountains quadrangle, Humboldt County, Nevada: U.S. Geol. Survey Mineral Inv. Field Studies Map MF-161. [1961]
- Muller, S. W., 1949, Sedimentary facies and geologic structures in the Basin and Range province, in Longwell, C. R., chm., Sedimentary facies in geologic history [symposium]: Geol. Soc. America Mem. 39, p. 49-54.
- Roberts, R. J., 1951, Geology of the Antler Peak quadrangle, Nevada: U.S. Geol. Survey Geol. Quad. Map GQ-10.
- Roberts, R. J., Hotz, P. E., Gilluly, James, and Ferguson, H. G., 1958, Paleozoic rocks of north-central Nevada: Am. Assoc. Petroleum Geologists Bull., v. 42, no. 12, p. 2813-2857.
- Silberling, N. J., and Roberts, R. J., 1962, Pre-Tertiary stratigraphy and structure of northwestern Nevada: Geol. Soc. America Spec. Paper 72, 53 p.
- Willden, C. R., 1958, Cretaceous and Tertiary orogeny in Jackson Mountain, Humboldt County, Nevada: Am. Assoc. Petroleum Geologists Bull., v. 42, no. 10, p. 2378-2398.
- , 1961, Major westward thrusting of post-Middle Triassic age in northwestern Nevada: Art. 192 in U.S. Geol. Survey Prof. Paper 424-C, p. C116-C118.



## STRIKE-SLIP FAULTING AND BROKEN BASIN-RANGES IN EAST-CENTRAL IDAHO AND ADJACENT MONTANA

By EDWARD T. RUPPEL, Denver, Colo.

*Abstract.*—The Lost River Range, Lemhi Range, and Beaverhead Mountains, basin-ranges in east-central Idaho and adjacent Montana, were broken in Pleistocene time by north-trending, dominantly right-lateral strike-slip faults. These faults, which control a peculiar pattern of mountain spurs and reentrant valleys, are in a zone about 50 miles wide that extends northward about 150 miles from Arco, Idaho, into the Big Hole Basin, Mont.

The Lost River and Lemhi Ranges, and the Beaverhead Mountains of east-central Idaho and adjacent Montana are remarkably long mountain ranges that trend N. 30° W., are separated by broad valleys, and have long been recognized as basin-ranges (fig. 1) (Meinzer, 1924, p. 5, 15–16; Shenon, 1928, p. 5; Anderson, 1947, p. 67–68). Only a few range-front faults have been mapped, however, and the ranges and valleys have at times been attributed to erosion (Umpleby, 1913, p. 30), thrust faulting (Kirkham, 1927, p. 24), or down-warping (Ross, 1961, p. 236; 1947, p. 1137–1139; 1938, p. 85–87). Range-front faults were first recognized by Shenon (1928, p. 5) along the southwest side of the Beaverhead Mountains near Nicholia, and the fault on the southwest side of the Lemhi Range near Patterson was later recognized and mapped by Ross (1947, p. 1137–1139). Baldwin (1951, p. 892) discussed frontal faults bounding the southwest sides of both the Lemhi and Lost River Ranges. The physical characteristics of the basins and ranges have been described by Anderson (1947, p. 63–67).

Most of these writers have commented, too, on the offset or broken pattern of the basin-ranges. Umpleby (1917, p. 16, 19), Kirkham (1927, p. 10), and Anderson (1947, p. 70) described the reentrant valleys in the Arco Hills (12<sup>1</sup> fig. 1) and at Wet Creek (8) and considered them to be old erosion valleys flooded with lava. Baldwin (1951, p. 892, 899) mentioned the ". . . offset pat-

tern of the ranges," and ascribed the offsets to range-front normal faults. The examples cited by these writers are mostly in the Lost River Range, but similar topographic features are also characteristic of both the Lemhi Range and Beaverhead Mountains (see accompanying table).

The striking similarities among the broken basin-ranges suggest a common cause. In the Lemhi Range and Beaverhead Mountains, near the town of Leadore, detailed mapping has shown that the broken pattern is controlled by north-trending strike-slip faults; in the other areas, reconnaissance mapping suggests that the broken pattern is invariably controlled by strike-slip faults similar in nearly all respects to those near Leadore. The broken basin-ranges of east-central Idaho and adjacent Montana therefore reflect a major zone of strike-slip faulting as much as 50 miles wide that extends northward from the Snake River Plain near Arco, Idaho, to the Big Hole Basin in western Montana, a distance of nearly 150 miles. The zone may extend into the Bitterroot Valley in western Montana.

### CENOZOIC STRUCTURAL EVENTS NEAR LEADORE, IDAHO

#### Early faulting<sup>2</sup>

The history of faulting is best known in the area of detailed mapping near Leadore, Idaho. The earliest faults recognized there are flat thrusts that break the pre-Tertiary rocks in the Lemhi Range and in the Beaverhead Mountains. The thrusting occurred before the eruption of the Challis Volcanics, which probably are mainly of Oligocene age but may extend into the Eocene and the lower Miocene (Ross, 1961, p. 179). The flat thrust faults north of Leadore were broken by west-trending high-angle faults of uncertain age, and subsequently both of these early sets of faults were moderately folded. Following the folding, movement on the

<sup>1</sup> Numbers shown in parentheses in text refer to localities shown on figure 1 and in the table.

<sup>2</sup> Early Cenozoic faults are not shown on figure 1.

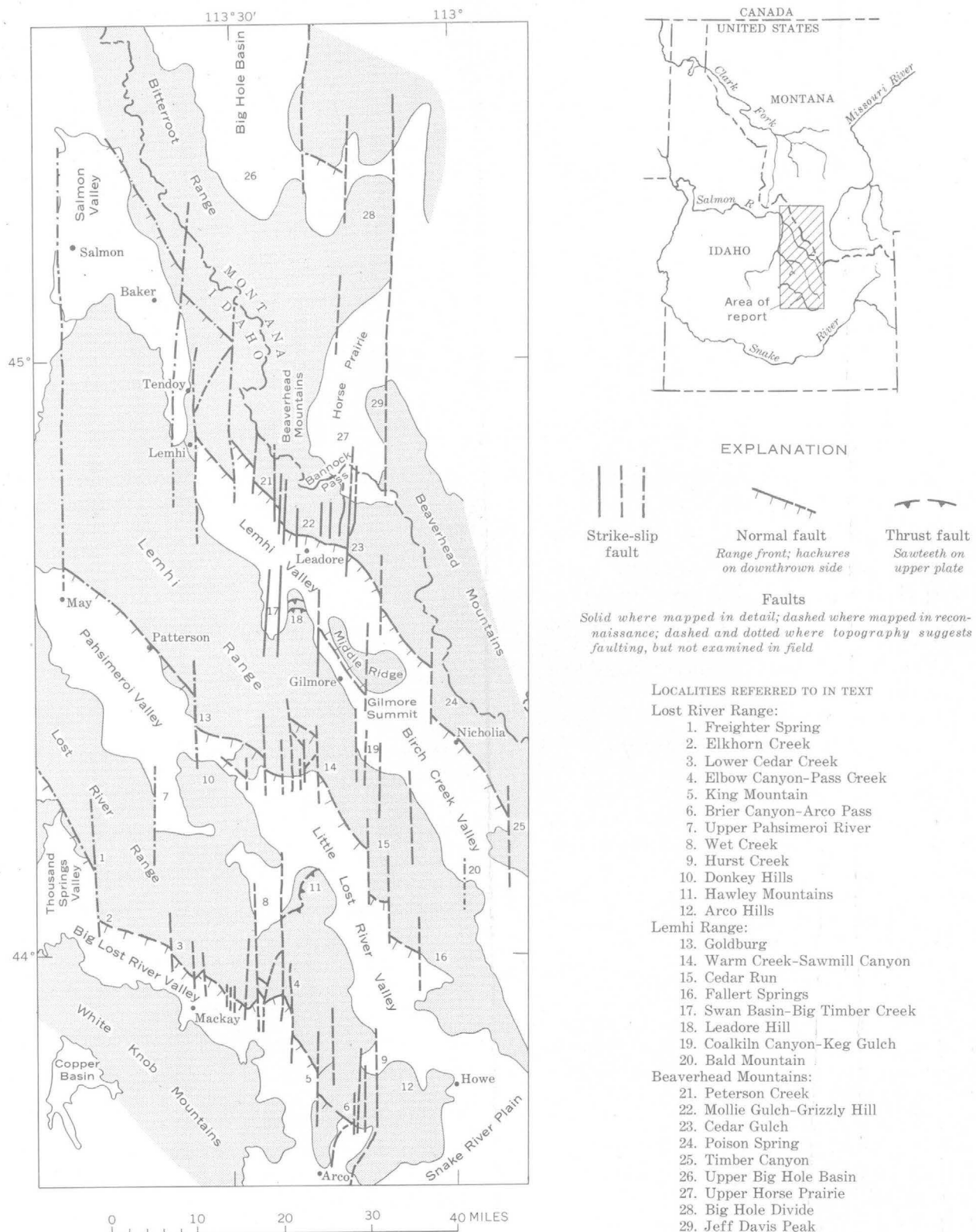


FIGURE 1.—Late Cenozoic faults in east-central Idaho and adjacent Montana. Mountains shown by pattern.

*Topographic features related to strike-slip faulting at various localities in the basin-ranges of east-central Idaho and adjacent Montana*  
 [Numbers in parentheses refer to localities shown on figure 1]

Major topographic feature	Idaho		Idaho and Montana Beaverhead Mountains-Bitterroot Range
	Lost River Range	Lemhi Range	
Sharply angled or offset range front.	(1) Freighter Spring <sup>1</sup> (2) Elkhorn Creek <sup>1</sup> (3) Lower Cedar Creek <sup>1</sup> (4) Elbow Canyon <sup>2</sup> (5) King Mountain <sup>2</sup> (6) Brier Canyon, Arco Pass <sup>2</sup>	(13) Goldburg <sup>2</sup> (14) Warm Creek <sup>2</sup> (15) Cedar Run <sup>2</sup> (16) Fallert Springs <sup>2</sup>	(21) Peterson Creek <sup>2</sup> (22) Mollie Gulch <sup>3</sup> (23) Cedar Gulch <sup>3</sup> (24) Poison Spring <sup>1</sup> (25) Timber Canyon <sup>1</sup>
Reentrant valleys-----	(7) Pahsimeroi River <sup>1</sup> (8) Wet Creek <sup>2</sup> (9) Hurst Creek <sup>2</sup>	(17) Swan Basin <sup>3</sup>	(26) Upper Big Hole Basin <sup>2</sup> (27) Upper Horse Prairie <sup>2</sup>
Mountain spurs-----	(10) Donkey Hills <sup>1</sup> (11) Hawley Mountains <sup>2</sup> (12) Arco Hills <sup>2</sup>	(18) Leadore Hill <sup>3</sup> (19) Coalkin Canyon and Keg Gulch <sup>1</sup> (20) Bald Mountain <sup>1</sup>	(28) Big Hole Divide <sup>2</sup> (29) Jeff Davis Peak <sup>2</sup>

<sup>1</sup> Not studied in field; fault origin not proved.

<sup>2</sup> Area of reconnaissance mapping.

<sup>3</sup> Area of detailed mapping.

normal faults of the range-front system started to block out the mountains in their present form.

#### Range-front faults

The time of movement on the range-front faults cannot yet be dated very closely, but the relation of range-front faults and valley fill in the Lemhi Valley suggests that most of the movement was in Miocene and Pliocene time. The valley fill seems to consist largely of tuff and tuffaceous clastic rocks, and gravity data suggest that it is at least 9,000 feet thick (W. T. Kinoshita, written communication, 1962). In the southern part of the Lemhi Valley the valley-fill deposits are everywhere bounded by range-front faults or by the younger strike-slip faults; but equivalent rocks farther north in the valley unconformably overlie the Challis Volcanics (Anderson, 1961, p. 32).

The oldest valley-fill rocks are along the range front north of Leadore; vertebrate fossils from these tuffaceous rocks have not been studied in any detail, but in general a Miocene age seems likely, perhaps middle Miocene (Wilson, 1946; Schulz and Falkenbach, 1947, p. 186-187; Anderson, 1961, p. 34; L. P. Richards, written communication, 1962). About a third of these rocks are tuffaceous conglomerate mainly composed of subangular to subrounded pebbles, cobbles, and boulders from the Precambrian and Paleozoic rocks in the adjacent Beaverhead Mountains, which suggests that movement on the frontal fault system was about contemporaneous with deposition.

Clean, fine-grained tuff and tuffaceous rocks on Middle Ridge, east of Gilmore, are at the present top of the valley fill. Knowles <sup>3</sup> considered these rocks to be

no older than Pliocene, on the basis of fresh-water diatoms contained in them, and it seems unlikely that their deposition could have continued long into the Pleistocene, for the deposits are beveled by a pediment that is capped by moraine of probable early Wisconsin age and that must have been cut largely in late Pliocene and early Pleistocene time. The pediment also cuts across the range-front fault on the west side of Middle Ridge and bevels the pre-Tertiary rocks between the fault and the present mountain front, which lies more than a mile to the west. After the moraine was deposited, the pediment east of the fault was raised by about 400 feet of reverse movement on the range-front fault; except for this reverse movement, the range-front fault near Gilmore must have been inactive during the time of pediment cutting, and consequently since late Pliocene or early Pleistocene time.

The range-front fault system on the east side of the Lemhi Valley must have had periodic normal movement to very recent time, even though the main movement was earlier. No pediment cuts across this fault system, the drainage pattern is disrupted at the range front, young alluvial fans are beheaded at the range front, and the steep westward-facing slope of the Beaverhead Mountains clearly is a but slightly modified fault scarp. Reconstruction of drainage profiles in some of the canyons north of Leadore suggests that the latest movement on this fault system relatively lowered the valley block about 200 feet. However, the very late movements on the range-front system may represent local readjustments related to movement on the north-trending faults.

The history of range-front faulting in the Big Lost River Valley, the Pahsimeroi-Little Lost River Valleys,

<sup>3</sup> R. R. Knowles, 1960, Geology of the southern part of the Leadore quadrangle, east-central Idaho: Pennsylvania State Univ., M.S. thesis, p. 71.

and the Birch Creek Valley has been similar to that in the Lemhi Valley.

#### North-trending strike-slip faults

The north-trending faults in the vicinity of Leadore cut all of the other faults. This faulting probably could not have begun much before the culmination of major movement on the range-front faults in late Pliocene or early Pleistocene time. The major displacements probably were completed by late Pleistocene time, for some faults are partly obscured by late Pleistocene surficial deposits, most drainage interrupted by the faults has been reintegrated, and many large canyons are partly cut along north-trending faults. Nevertheless, some movement is more recent—the lower parts of some glaciated valleys south of the Swan Basin (17) in the Lemhi Range appear to have been cut off, some of the younger glacial deposits west of Leadore are displaced, and some of the faults cut very young surficial deposits, behead young alluvial fans, and disrupt present drainage patterns.

Despite their youth, most of the north-trending faults are not particularly obvious. But the faults near Leadore and those in the other areas share many common characteristics, and exhibit most of the features said to be typical of strike-slip faults (DeSitter, 1959, p. 173-174). The faults are exceptionally straight, and many of them maintain their northward strike for many miles; their dips are vertical or nearly so. Brecciated zones as much as 500 feet wide are present at many places along the faults, commonly with correspondingly wide depressions cut into them; at as many other places, the faults are clean breaks without recognizable breccias. At Brier Canyon (6) and west of Sawmill Canyon (14), beds of sedimentary rocks have been dragged parallel to the faults. Landslides and slumps that are covered with thin soil and sparse vegetation, but that retain their initial hummocky form, are common along the faults and clearly were triggered by movements on them.

The larger strike-slip faults are accompanied by many parallel small faults, and some are linked together by curving northwest- and northeast-trending faults that transferred the major movement from one north-trending fault to another. At the north end of Leadore Hill (18), the strike-slip faults appear to merge with flat, south-dipping thrust faults. Similar thrusts probably are present at the north end of the Hawley Mountain spur (11) and north of Arco Pass (9), but they have not yet been recognized in the Arco Hills (12)<sup>4</sup> or in the Donkey Hills (10) (Ross, 1947); the geology

of the mountain spurs in Montana, the Jeff Davis Peak area (29) and the Big Hole Divide (28), is virtually unknown.

North of Leadore, on Grizzly Hill (22), the horizontal displacement on individual north-trending faults is as much as 1½ miles, and the aggregate displacement on groups of closely spaced faults is as much as 4 miles. The north-trending segment of the Lemhi Valley between Lemhi and Tendoy, northwest of Leadore, may be controlled by faults with an aggregate horizontal displacement of about 8 miles. In the Swan Basin (17), south of Leadore, horizontal displacement on the faults is more difficult to determine, but possibly the aggregate movement has been about 8 miles. In the Lost River Range and Beaverhead Mountains, the horizontal movements seem to be of the same order of magnitude. Geologic evidence indicates that the displacement is right lateral on most of the strike slip faults, although the offset pattern of the ranges suggests left-lateral displacement; the reason for this anomalous relation is not yet clear.

The amount of vertical displacement on the faults appears to be small, but it can be satisfactorily determined in only a few places. Some of the smaller strike-slip faults on Grizzly Hill, faults that have several hundred feet of horizontal displacement, have no appreciable component of vertical movement, for they do not break the smoothness of stripped thrust surfaces that control much of the rolling upland topography here. The Cedar Gulch fault (23) east of Leadore, offsets the range-front fault system about 6,000 feet horizontally, beheads very young alluvial fans, and is responsible for offsets in the distribution of Tertiary tuffaceous rocks and in drainage mentioned by Alden (1953, p. 41). This fault together with other parallel faults has triggered large landslides in the basin south of Bannock Pass. Closely comparable faults in the other areas (fig. 1) include the fault on the east side of Sawmill Canyon (14) in the Lemhi Range and the Elbow Canyon fault (4) in the Lost River Range east of Mackay. The calculated vertical displacement necessary to give the apparent horizontal displacement on the Cedar Gulch fault is about 4,000 feet—and yet this young fault, with all its effects on upper Tertiary and Quaternary deposits, is without any well-defined scarp. By way of contrast, the older range-front faults are marked by the looming scarp front of the Beaverhead Mountains, almost 2,000 feet high. The same sort of calculation can be made for most of the other north-trending faults in the Beaverhead Mountains near Leadore, and the conclusion that movement on the faults was dominantly horizontal seems inescapable. The widely distributed north-trending faults in east-central

<sup>4</sup> J. P. Shannon, Jr., 1959, Geology of the Howe Peak area, Lost River Range, Butte County, Idaho: Northwestern Univ., M.S. thesis.

Idaho and adjacent Montana clearly are part of a single strike-slip system on which there has been much horizontal displacement in relatively recent times.

The forces responsible for the strike-slip faulting are not yet understood, but a genetic relation is suggested by the coincidence in time of strike-slip faulting, eruptions of most of the basaltic lavas in the Snake River Plain, development of the Snake River depression in the eastern, northeast-trending part of the Snake River Plain, and the arching north of this part of the Plain (Kirkham, 1927, p. 11, 13, 24-26). Also, the apparent western boundary of the strike-slip zone intersects the area where the Snake River Plain bends to the northeast, which is also where the Plain changes from a fault-bounded graben in its western part (Malde, 1959, p. 272; Malde and Powers, 1962, p. 1203), to a depression of uncertain origin in its eastern part. Kirkham (1927, p. 11, 13, 24-26) early believed that the eastern part of the Snake River depression was downwarped, and that accompanying isostatic uplift arched the region to the north. Hamilton (1963, p. 785), following Carey (1958, fig. 56), suggested that the eastern part of the depression is a product of tensional rifting or thinning of the crust resulting from northwestward drifting of the Idaho batholith. The forces required for tensional rifting parallel to this part of the plain trending N. 30-40° E. can be resolved into those required to form north-trending right-lateral strike-slip faults.

#### REFERENCES

- Alden, W. C., 1953, Physiography and glacial geology of western Montana and adjacent areas: U.S. Geol. Survey Prof. Paper 231, 200 p. [1954]
- Anderson, A. L., 1947, Drainage diversion in the northern Rocky Mountains of east-central Idaho: Jour. Geology, v. 55, no. 2, p. 61-75.
- Anderson, A. L., 1961, Geology and mineral resources of the Lemhi quadrangle, Idaho: Idaho Bur. Mines and Geology Pamph. 124, 111p.
- Baldwin, E. M., 1951, Faulting in the Lost River Range area of Idaho: Am. Jour. Sci., v. 249, p. 884-902.
- Carey, S. W., 1958, The tectonic approach to continental drift, in Carey, S. W. ed., Continental drift, a symposium: Australia, Univ. Tasmania, p. 177-355.
- DeSitter, L. U., 1959, Structural geology: New York, McGraw-Hill Book Co., Inc., P. 173-174.
- Hamilton, Warren, 1963, Overlapping of late Mesozoic orogens in western Idaho: Geol. Soc. America Bull., v. 74, p. 779-788.
- Kirkham, V. R. D., 1927, A geologic reconnaissance of Clark and Jefferson and parts of Butte, Custer, Fremont, Lemhi, and Madison Counties, Idaho: Idaho Bur. Mines and Geology Pamph. 19, 47 p.
- Malde, H. E., 1959, Fault zone along northern boundary of western Snake River Plain, Idaho: Science, v. 130, no. 3370, p. 272.
- Malde, H. E., and Powers, H. A., 1962, Upper Cenozoic stratigraphy of western Snake River Plain, Idaho: Geol. Soc. America Bull., v. 73, p. 1197-1220.
- Meinzer, O. E., 1924, Ground water in Payshimeroi Valley, Idaho: Idaho Bur. Mines and Geology Pamph. 9, 35 p.
- Ross, C. P., 1938, Geology and ore deposits of the Bayhorse region, Custer County, Idaho: U.S. Geol. Survey Bull. 877, 161 p.
- 1947, Geology of the Borah Peak quadrangle, Idaho: Geol. Soc. America Bull., v. 58, p. 1085-1160.
- 1961, Geology of the southern part of the Lemhi Range, Idaho: U.S. Geol. Survey Bull. 1081-F, p. 189-260.
- Schulz, C. B., and Falkenbach, C. H., 1947, Merychyinae, a new subfamily of oreodonts: Am. Mus. Nat. History Bull., v. 88, art. 4, p. 157-286.
- Shenon, P. J., 1928, Geology and ore deposits of the Birch Creek district, Idaho: Idaho Bur. Mines and Geology Pamph. 27, 25 p.
- Umpleby, J. B., 1913, Geology and ore deposits of Lemhi County, Idaho: U.S. Geol. Survey Bull. 528, 182 p.
- 1917, Geology and ore deposits of the Mackay region, Idaho: U.S. Geol. Survey Prof. Paper 97, 129 p.
- Wilson, J. A., 1946, Preliminary notice of a new Miocene vertebrate locality in Idaho [abs.]: Geol. Soc. America Bull., v. 57, no. 12, p. 1262.



## EVIDENCE FOR A CONCEALED TEAR FAULT WITH LARGE DISPLACEMENT IN THE CENTRAL EAST TINTIC MOUNTAINS, UTAH

By H. T. MORRIS and W. M. SHEPARD,<sup>1</sup>  
Menlo Park, Calif., Denver, Colo.

*Abstract.*—The apparent termination of the Oquirrh-East Tintic fold system and the East Tintic thrust fault in the lava-covered central part of the East Tintic Mountains, Utah, suggests the presence of a heretofore unsuspected northeast-trending tear fault of regional significance. This fault may be the localizing feature of yet undiscovered base-metal and silver ore deposits.

The apparent termination of the Oquirrh-East Tintic system of folds in the lava-covered central part of the East Tintic Mountains of west-central Utah suggests the presence of a heretofore unsuspected northeast-trending tear fault of regional significance (fig. 1). Contributory evidence for the existence of such a structure is furnished by deep drill holes that have disclosed the probable termination of the concealed East Tintic thrust fault 4 miles southeast of Eureka, and by the exposure of a northeast-trending tear fault with large displacement in the southern part of West Mountain, 15 miles northeast of the central East Tintic Mountains. The inferred tear fault in the East Tintic Mountains is believed to be similar to strong tear faults exposed elsewhere in the range and in the adjacent Gilson Mountains. Like some of these transverse faults, it may be the localizing feature of concealed ore deposits.

The folds of the Oquirrh-East Tintic system were formed concomitantly with thrust faulting during the early Laramide orogeny and involve rocks of late Precambrian to Permian age. They occur in an arcuate belt, convex eastward, that extends from the central Oquirrh Mountains near Bingham, 11 miles north of the north boundary of figure 1, to the central East Tintic Mountains, a distance of about 50 miles. The axes of adjacent synclines and anticlines are 3 to 5 miles apart and are approximately parallel; the minimum amplitudes of the folds range from 6,500 to 13,000 feet. In

the northern East Tintic Mountains the fold axes strike southeasterly, but the strike changes progressively southward until at the edge of the lava field the strike is nearly due south. The degree of asymmetry of the folds also increases southward from the Oquirrh Mountains, and the westernmost anticline and syncline are overturned locally near the edge of the lava field.

In the East Tintic Mountains, the amplitudes of the folds increase steadily southward to the point where the folds are covered by the postorogenic volcanic rocks. South of the central part of the range, however, scattered erosional windows in the lavas south of the area of Tertiary intrusions show that the sedimentary rocks are not appreciably folded. The beds in general strike eastward or northeastward and dip south, forming a broad, faulted homocline that extends southward to the southernmost part of the East Tintic Mountains and eastward to the Wasatch Mountains and beyond. The abruptness of the apparent termination of the folds thus suggests the presence of a transverse fault of sufficient displacement to delimit flexures of large amplitude and regional extent. The total concealment of a fault of such large magnitude is possibly explained by the erosional development of an east- or northeast-trending valley along the fault zone and the filling of this valley with pyroclastic and flow rocks during the earliest phases of the volcanic eruptions. This valley has not since been reexposed.

The structure of the sublava sedimentary rocks in the central East Tintic Mountains is reasonably well known from surface exposures, mine workings, and drill holes. Of particular interest is the East Tintic thrust fault (Bush and others, 1960, p. 1127-1129, 1532) that cuts the east limb of the East Tintic anticline below the lavas east of Eureka. This low-angle fault strikes northward and dips to the west; it cuts Paleozoic carbonate rocks and quartzite and displaces them about

<sup>1</sup> Bear Creek Mining Co.

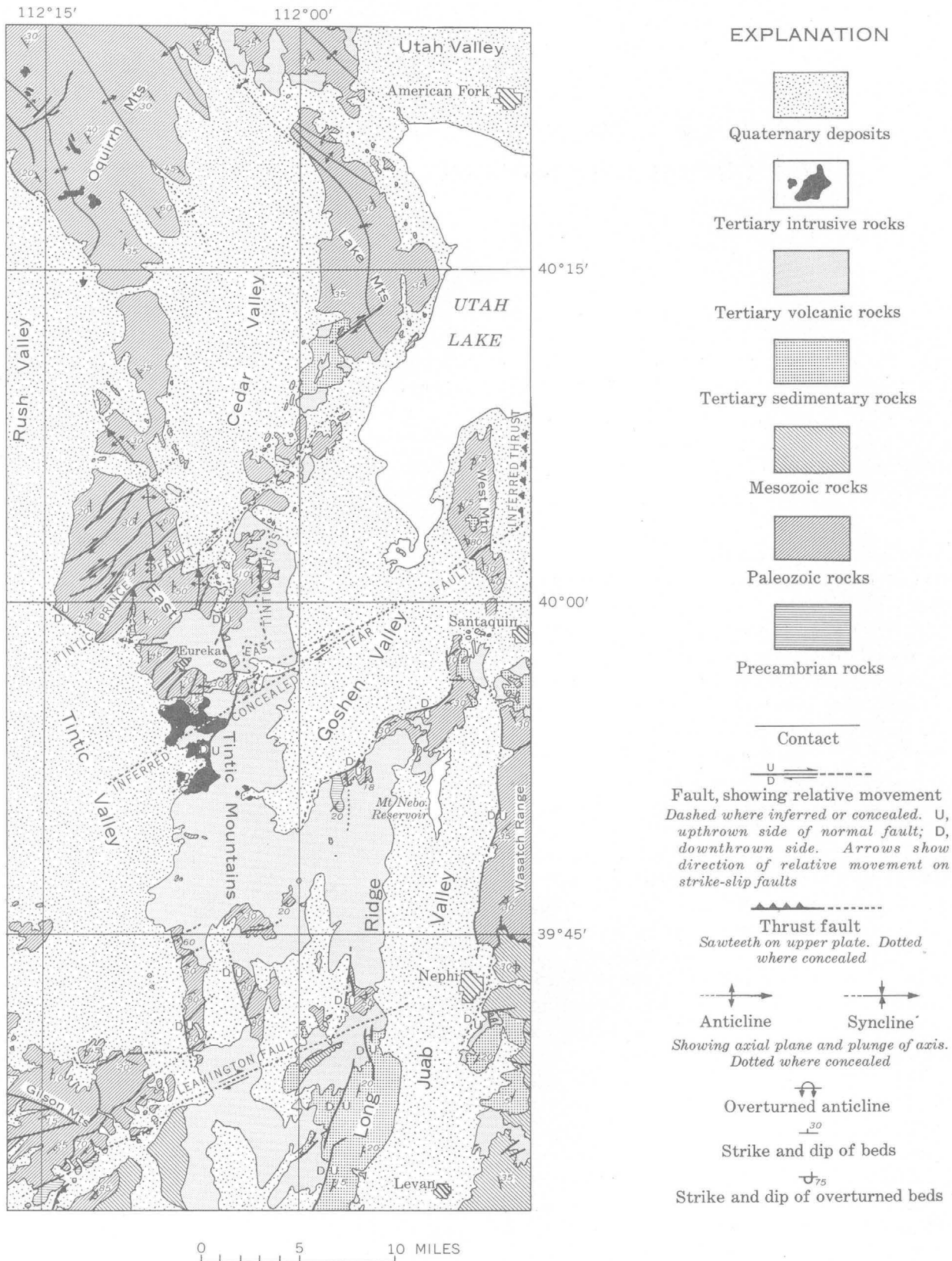


FIGURE 1.—Generalized geologic map of the East Tintic Mountains and adjacent areas, west-central Utah. Geology from original and published sources.

5,000 feet relatively to the east. The sublava position of the thrust trace has been established by drill holes to a point 4 miles east-southeast of Eureka, where the thrust apparently ends against a concealed fault that is indicated by the pattern of drill holes to have a northeast strike and a near vertical dip. The drill holes on the northwest side of this inferred fault enter carbonate rocks of the upper and lower plates of the East Tintic thrust. On the southeast side, however, six drill holes enter rocks that structurally are best correlated with rocks deep in the lower plate of the thrust. Inasmuch as it seems to terminate the thrust, this steep, concealed fault probably has large displacement and thus may be the inferred tear fault that delimits the major folds. The indicated strike of the concealed fault is somewhat more northeasterly than the average strike of the inferred regional fault as shown on figure 1, but this may be the result of a local bend similar to that shown on the exposed part of the Tintic Prince fault 4½ miles northwest of Eureka. Alternatively, the fault indicated by the drill holes may be one of several faults that together may form the concealed transcurrent structure.

A fault that is the possible continuation of the inferred tear is exposed in the southern part of West Mountain, where it brings the upper, Permian, part of the Oquirrh Formation against rocks 25,000 or more feet lower in the section. Hintze (1962, p. 75) and others have described this fault as a thrust that displaced rocks of Permian age relatively southward over rocks of Cambrian to Mississippian age. An alternative interpretation, which is more in keeping with the regional pattern of north-trending thrust faults and northeast-trending tear faults, is suggested from the geologic relations of the exposed rocks. The trace of the fault across the ridgelike mountain is nearly straight, indicating a steep, if not vertical, fault plane. The Permian rocks strike north-northeast and are overturned to the east, suggesting that the rocks northwest of the fault did not move southward, but relatively eastward, horizontally past the rocks southeast of the fault, in the manner of a tear. The projected strike, dip, and displacement of this tear are comparable with the indicated strike, dip, and displacement of the inferred concealed fault in the central East Tintic Mountains.

Thus, this fault may be the eastward continuation of the concealed fault. If one assumes that both faults are part of a single zone of transverse tears of regional proportions, the strike of this zone is approximately N. 55°–60° E., which is close to the N. 60°–65° E. strike of the conspicuous Leamington fault that separates upper Paleozoic carbonate rocks and sandstone from upper Precambrian quartzite and argillite in the southern part of the Gilson Mountains. The Leamington fault is here interpreted also to be a tear fault, forming the south edge of the upper plate of the Nebo-Charleston thrust fault, which is best exposed a short distance northeast of Nephi.

The absence of a comparable tear fault in the Wasatch Range on strike with the strong fault in the southern part of West Mountain suggests the possibility that the tear fault terminates at a thrust fault whose trace is concealed beneath the alluvium in Utah Valley. A possible remnant of such a thrust fault may be the small thrust plate shown by Baker and Crittenden (1961) on the west slope of Mt. Timpanogos east of Pleasant Grove, Utah.

Conclusive evidence for the existence of a major tear fault in the central East Tintic Mountains will be furnished only by the actual interception of such a structure in mine workings. Continued exploration for blind ore bodies in the Tintic and East Tintic mining districts conceivably could test this hypothesis in the foreseeable future, especially since a transverse fault of this magnitude may possibly be the site of undiscovered base-metal and silver ore bodies.

#### REFERENCES

- Baker, A. A., and Crittenden, M. D., Jr., 1961, Geologic map of the Timpanogos Cave quadrangle, Utah: U.S. Geol. Survey Geol. Quad. Map GQ-132.
- Bush, J. B., Cook, D. R., Lovering, T. S., and Morris, H. T., 1960, The Chief Oxide-Burgin area discoveries, East Tintic district, Utah; a case history, pts. 1 and 2: Econ. Geology, v. 55, no. 6, p. 1116–1147, and no. 7, p. 1507–1539.
- Hintze, L. F., 1962, Structure of the southern Wasatch Mountains and vicinity, Utah, in Hintze, L. F., ed., Geology of the southern Wasatch Mountains and vicinity, Utah: Brigham Young Univ. Geology Studies, Provo, Utah, v. 9, pt. 1, p. 70–79.



## SHAPE AND STRUCTURE OF A GABBRO BODY NEAR LEBANON, CONNECTICUT

By MARTIN F. KANE and GEORGE L. SNYDER, Houston, Tex., and Denver, Colo.

*Work done in cooperation with the  
State of Connecticut Geological and Natural History Survey*

**Abstract.**—Geologic and gravity evidence indicates that the discordant gabbroic intrusive body near Lebanon, Conn., is a northeast-trending boat-shaped mass 10 miles long, 2 miles wide, and 3,000 feet deep, attached by its stern to a dominantly northwest-trending curved sheet 15 miles long by as much as half a mile wide.

An intrusive gabbro body near the village of Lebanon, Conn., (fig. 1) was first studied in detail by Dow,<sup>1</sup> and the name Lebanon Gabbro was first applied to it in published print by Foye (1949, p. 49). These and other maps have generally shown the gabbro as an elliptical mass 4 miles long by 1 mile wide within the Willimantic quadrangle north of Lebanon, although Percival (1842, geologic map) originally indicated that the gabbro might extend outside this small ellipse. More recent mapping (fig. 1) indicates that the gabbro extends as a three-pronged pinwheel into the adjoining Columbia, Colchester, and Fitchville quadrangles, and that its surface area is more than 300 percent greater than that previously mapped. A synformal roof pendant of metasediments, the Kick Hill roof pendant, caps part of the gabbro north of Lebanon. The otherwise sinuously continuous gabbro body is offset by three parallel normal faults in the central part of the mass.

The geologic data indicate crudely that the shape of the gabbro body might be likened to that of an elliptical pod attached by one end to a gently to steeply dipping curved tabular sheet. Foliation within the southeastern and northwestern arms of the gabbro, the curved tabular sheet, is uniformly parallel to the walls of the gabbro and generally is parallel to the schistosity and bedding of the surrounding wallrocks. Geologic evidence sug-

gests strongly that this part of the body is tabular and probably largely sill like. Locally, however, the gabbro cuts across contacts or the strike of schistosity of the surrounding metasediments, and near the place where the three parts of the body join, the gabbro appears to dip southward much more steeply than the nearby wallrocks. In the northeast arm of the elliptical podlike part of the gabbro, foliation is much less uniform in strike but appears to dip inward along the northwest and southeast contacts of this part of the gabbro. Lineation in the northeast arm trends much more uniformly; generally it is parallel to the direction of elongation of the mass, plunges inward at a low angle from both ends, and is generally horizontal near the center. It would appear from the internal structures that this part of the gabbro may bottom at depth and be shaped like a boat attached at its stern end to the more tabular part of the gabbro. A keel for this boat can be projected from its prow end using the available lineation data, and this would indicate that the gabbro in the northeast arm should bottom at a maximum depth of 1 mile.

Gravity measurements were made in 1961 along four profiles across the gabbro (fig. 1) in order to check the geologic interpretation of its shape (Bean, 1953; Bott, 1956; Kane, 1961), especially in the northeastern part of the body, and also to check on the presence or absence of the gabbro in some areas where surface outcrops are absent and the mapping was based on indirect evidence. The gravity studies in general substantiate the geologic mapping and geologic indications of structural shape and have made them more precise. A reconnaissance gravity survey of the surrounding region (unpublished data) shows a positive anomaly over the gabbro near Lebanon, superimposed on the south flank of a larger, broader gravity low centered on the Willimantic dome.

<sup>1</sup>D. W. Dow, 1942, The Lebanon gabbro of Connecticut: Northwestern Univ., unpub. M.S. thesis.

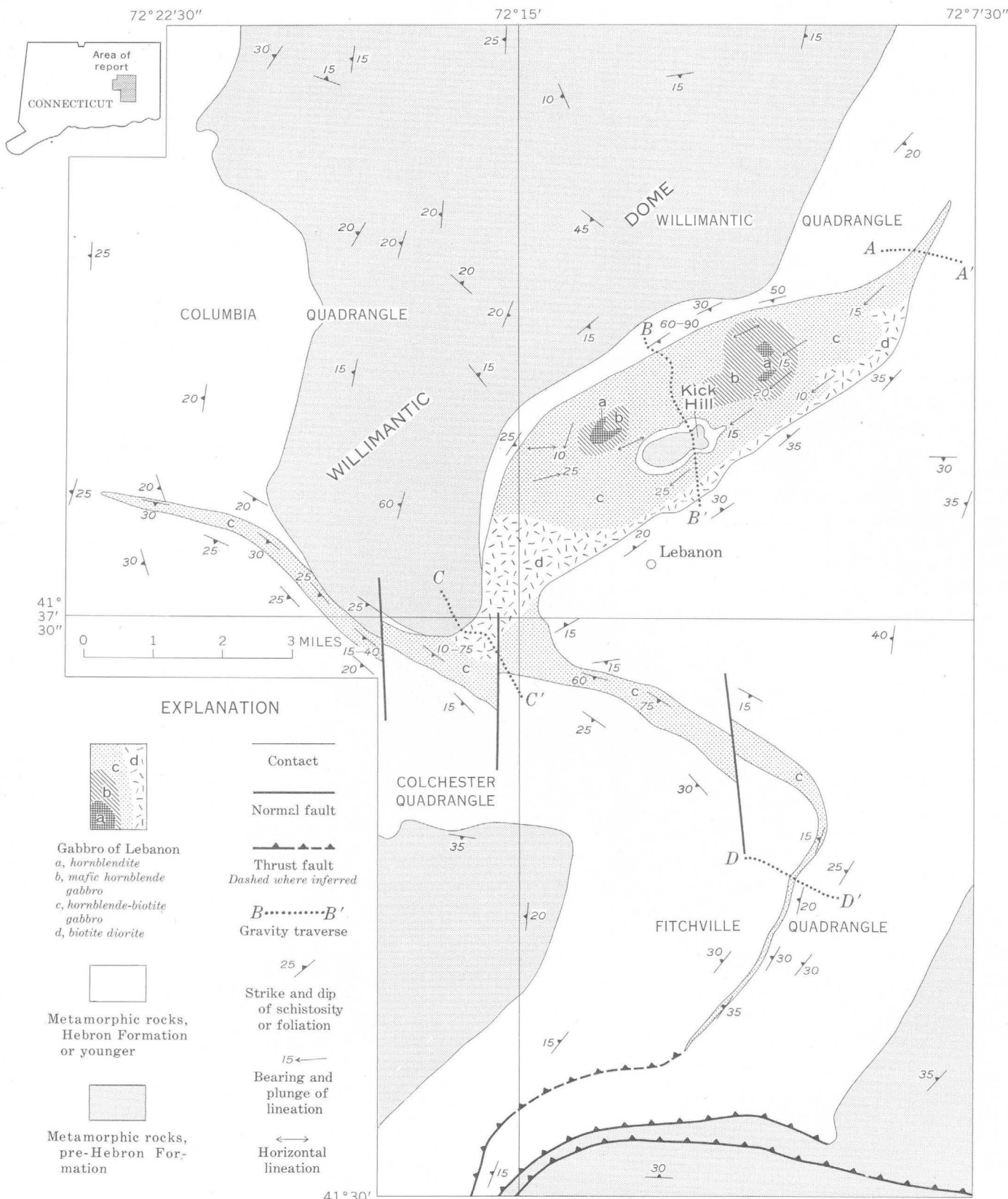


FIGURE 1.—Generalized geologic map of pre-Pennsylvanian rocks in part of eastern Connecticut. Geology by George L. Snyder, 1956-61.

In order to interpret the gravity data, specific gravities of the rocks in this part of Connecticut were measured on a Jolly balance; the averages of the measurements for certain groups of these rocks are given in the accompanying table. These data show that the average density contrast between gabbro and metamorphic country rock is +0.2 grams per cubic centimeter.

The Bouguer anomalies for four profiles over the gabbro are shown on figures 2 and 3. Profile A-A' crosses the inferred extension of gabbro northeast of all known outcrops in an area underlain by unconsolidated sand and gravel. If the two central measurements of relatively low gravity are caused by a local thickening of the unconsolidated rocks, the anomaly (as generalized) indicates that gabbro is present, and probably bottoms within a few hundred feet. The overall regional gradient in this area probably reflects a west-dipping contact with dense basement rocks at depth.

Profile B-B' (fig. 3) crosses the gabbro and its synformal roof pendant near the center of the northeastern arm. Because the anomaly is contained entirely within the boundaries of the gabbro, the mass of the gabbro must be concentrated inside its mapped contacts, that is, the outer boundaries dip generally inward. A simple triangular cross section, with its apex 3,000 feet below its base has a computed gravity anomaly very similar

#### Densities of some rocks of eastern Connecticut

Rock type	Individual specific gravity measurements on small rock specimens	Unweighted average density (g per cm <sup>3</sup> )	Roundey density (g per cm <sup>3</sup> )
<b>Gabbroic rocks</b>			
Biotite diorite-----	2. 88, 2. 89	2. 89	
Hornblende-biotite gabbro-----	2. 91, 2. 93	2. 92	
Mafic hornblende gabbro-----	3. 04, 3. 04	3. 04	
Hornblendite-----	3. 10, 3. 11	3. 11	3. 0
<b>Metasedimentary country rocks</b>			
Scotland Schist, muscovite schist-----	2. 97, 2. 97	2. 97	
Scotland Schist, biotite schist-----	2. 73, 2. 73	2. 73	
Hebron Formation, calc-silicate rock-----	2. 80, 2. 81	2. 81	
Hebron Formation, carbonaceous biotite schist-----	2. 73, 2. 74	2. 74	
Tatnic Hill Formation, sillimanite-garnet gneiss-----	2. 95, 2. 98, 3. 00	2. 98	
Tatnic Hill Formation, biotite-muscovite schist-----	2. 71, 2. 72	2. 72	2. 81
Fly Pond Member of Tatnic Hill Formation, calc-silicate rock-----	2. 87, 2. 89	2. 88	
Brimfield Schist, muscovite-biotite-garnet schist-----	2. 73, 2. 76, 2. 82, 2. 83, 2. 89	2. 81	
Quinebaug Formation, hornblende gneiss-----	2. 74, 2. 76	2. 75	
Quinebaug Formation, biotite gneiss-----	2. 68, 2. 69	2. 69	

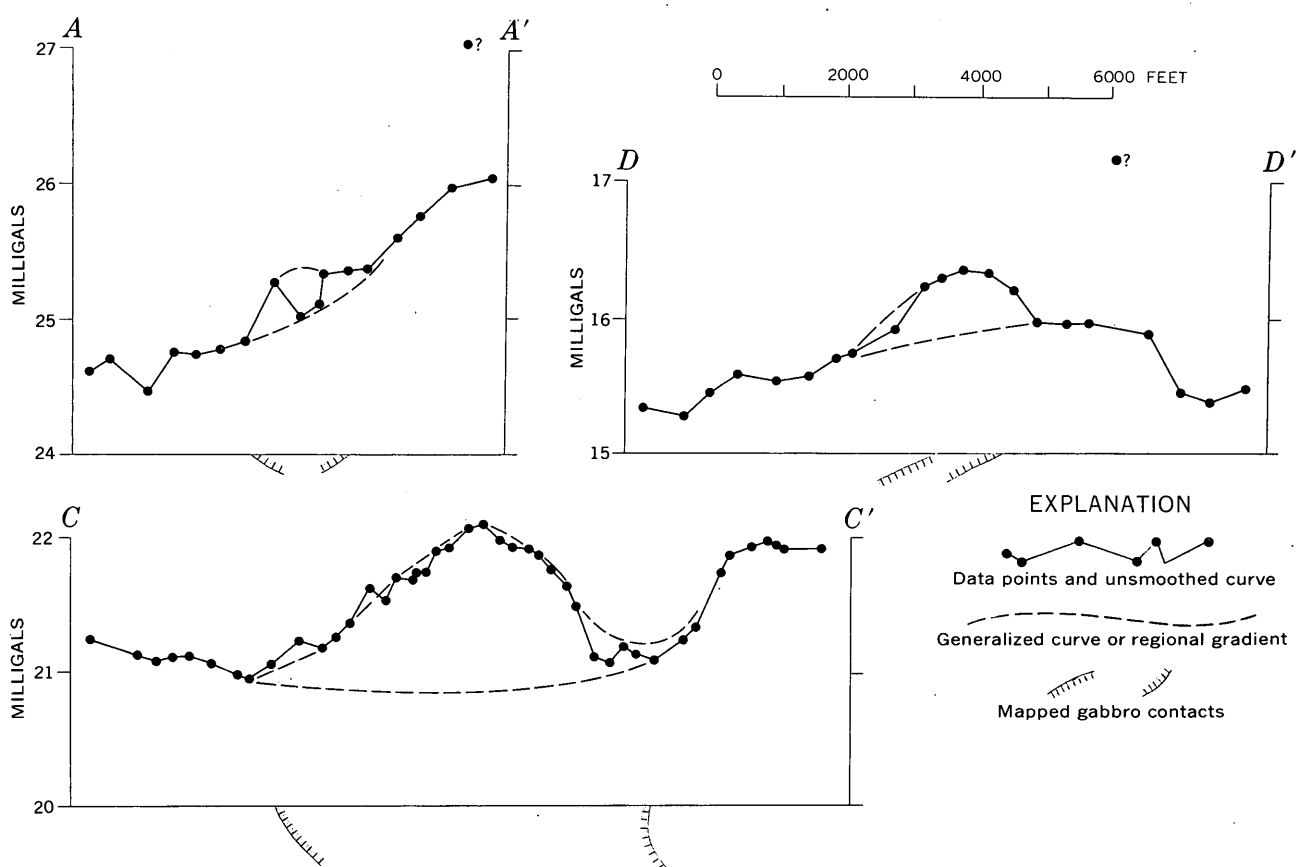


FIGURE 2.—Bouguer gravity anomalies and mapped geologic contacts along profiles A-A', C-C', and D-D' across gabbro.

to the residual Bouguer anomaly (fig. 3). The depth of bottoming would be somewhat less if the more dense mafic phases of the gabbro thicken with depth as assumed on figure 4; the depth would be somewhat more if the density contrast between gabbro and the metamorphic country rock is less. The anomaly along profile  $B-B'$  has a slight asymmetry to the south, the nature of which suggests that the effective center of mass is

south of the profile center. Because the density of the gabbro at the surface is greater to the north of the profile center, the anomaly asymmetry is probably caused by a shape that is asymmetric to the south, in the manner shown in the preferred cross sectional shape on figure 3. The two mapped units of the synformal roof pendant are reflected by the double-stepped, flattened peak of anomaly  $B-B'$  (fig. 3); the estimated depth of

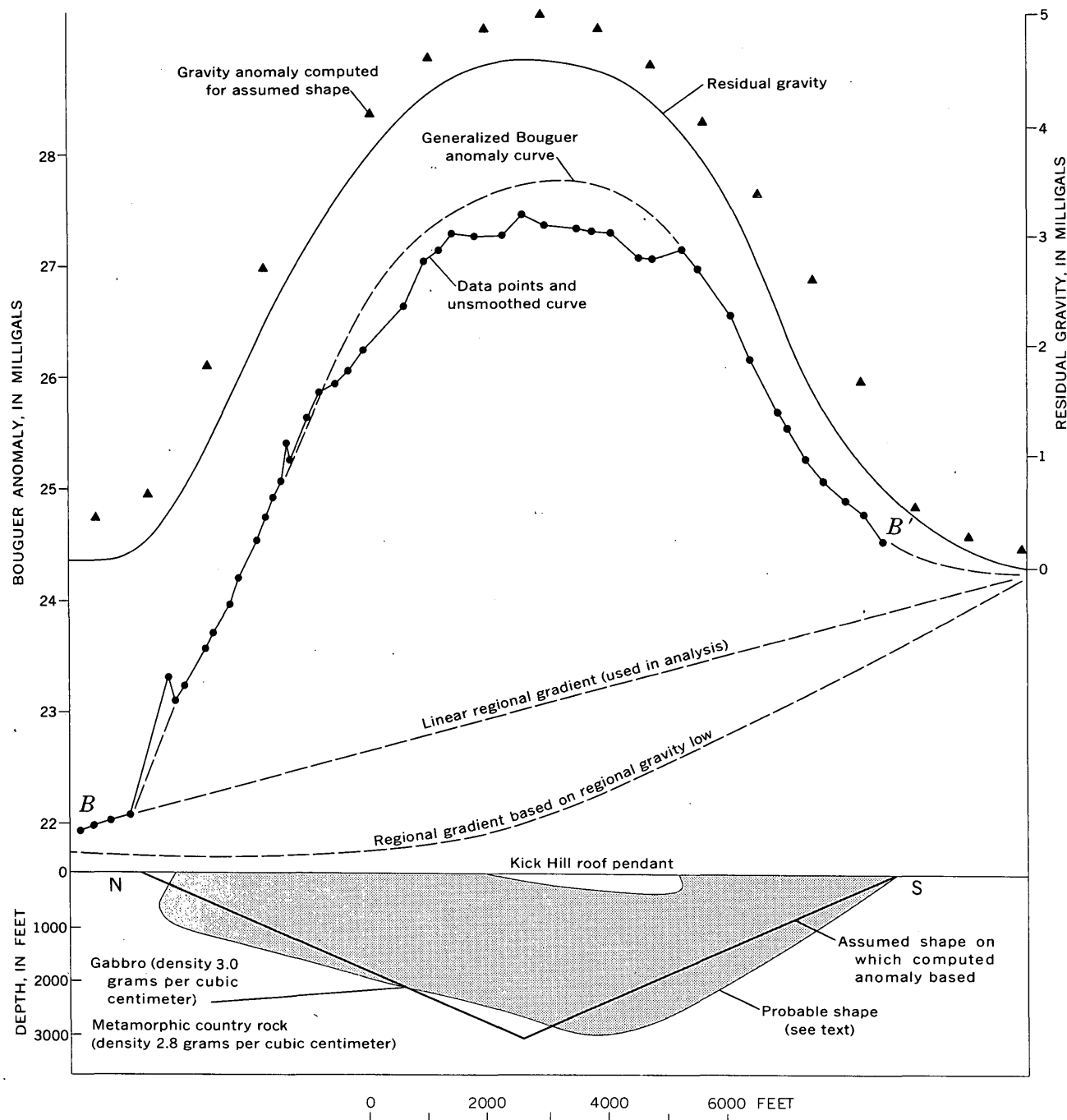


FIGURE 3.—Bouguer anomaly, residual gravity, and probable cross-sectional shape of northeast arm of gabbro at gravity profile  $B-B'$ .

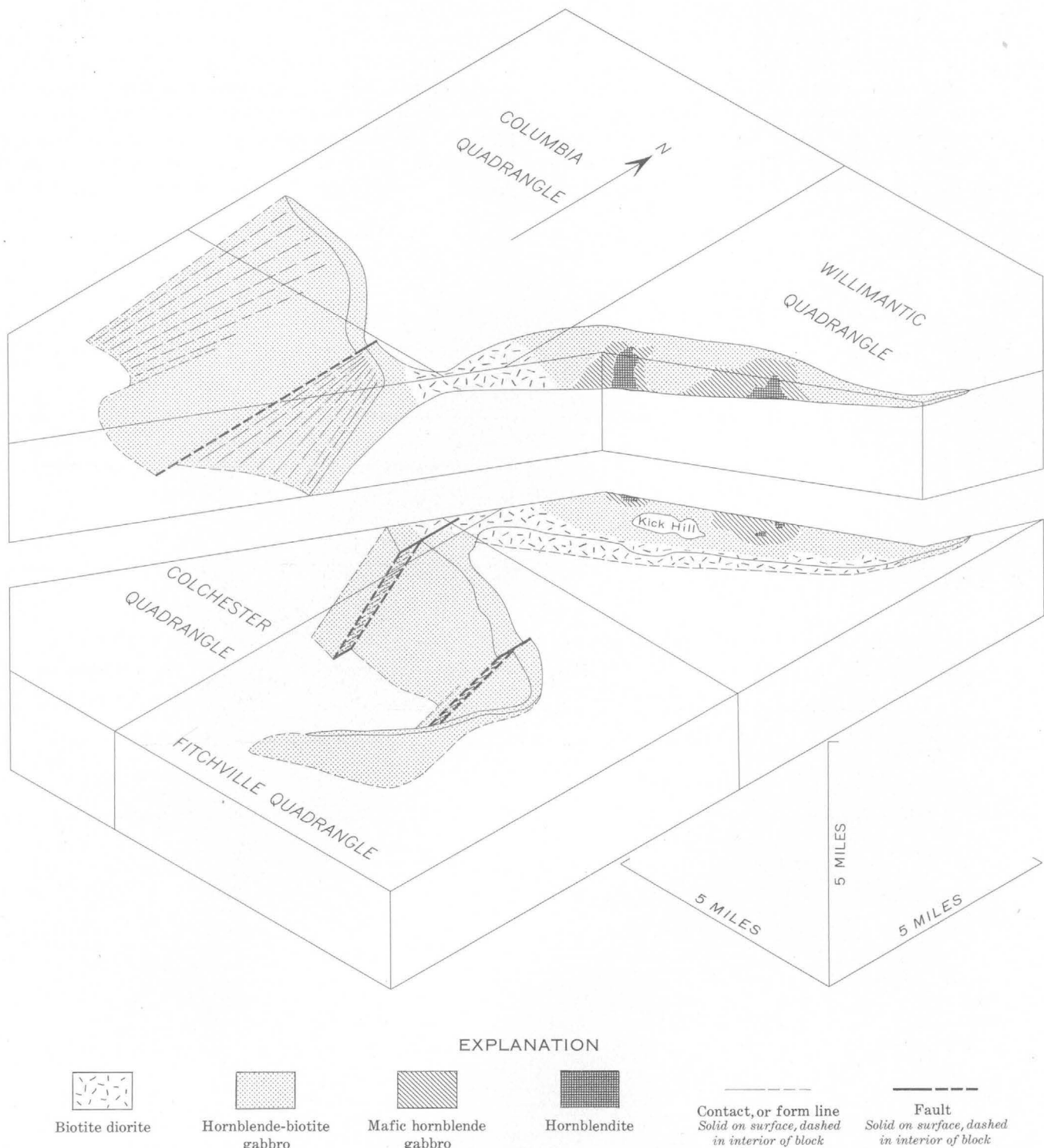


FIGURE 4.—Block diagram and longitudinal section of gabbro body at Lebanon, Conn.

the bottom of the pendant is 300 to 500 feet. Details of the dipping contacts shown on figure 3 are based partly on field observations and partly on the limits imposed by gravity profile  $B-B'$ .

Profile  $C-C'$  (fig. 2) confirms the existence of gabbro in an area where the bedrock is buried beneath unconsolidated surficial deposits. Amplitude of the anomaly indicates that the mass narrows sharply with depth if it continues below 2,000 feet.

The high in profile  $D-D'$  (fig. 2) reaches a maximum over the central area of gabbro, but extends for a considerable distance into the areas of metasediments on both sides, an overlap possibly reflecting repetition of the gabbro at depth by a branch of the fault mapped to the northwest. However, the asymmetry of the curve does seem to reflect the gentle westward dip at the surface.

The structural configuration of the entire body of gabbro near Lebanon, Conn., inferred from gravity and

geologic data is shown on figure 4. Further work is necessary to determine the absolute limits of the extremities of the body, the nature of the structure where the three arms join, and the possible thickening with depth of the mafic gabbro phases, as postulated in the longitudinal section of figure 4.

#### REFERENCES

- Bean, R. J., 1953, The relation of gravity anomalies to the geology of central Vermont and New Hampshire: Geol. Soc. America Bull., v. 64, p. 509-538.  
Bott, M. H. P., 1956, A geophysical study of the granite problem: Quart. Jour. Geol. Soc. London, v. 112, p. 45-67.  
Foye, W. G., 1949, The geology of eastern Connecticut: Connecticut Geol. Nat. History Survey Bull. 74, 95 p.  
Kane, M. F., 1961, Structure of plutons from gravity measurements: Art. 242 in U.S. Geol. Survey Prof. Paper 424-C, p. C258-C259.  
Percival, J. G., 1842, Report on the geology of the State of Connecticut: New Haven, Conn., Osborn and Baldwin, 495 p.



## OUTLINE OF THE STRATIGRAPHIC AND TECTONIC FEATURES OF NORTHEASTERN MAINE

By LOUIS PAVLIDES, ELY MENCHER,<sup>1</sup> R. S. NAYLOR,<sup>2</sup> and A. J. BOUCOT,<sup>2</sup>  
Beltsville, Md.; Cambridge, Mass.; Pasadena, Calif.

**Abstract.**—Northeastern Maine is underlain by Cambrian(?) to Middle Devonian sedimentary and volcanic rocks that locally have been regionally metamorphosed within the greenschist facies. These rocks are generally highly folded and faulted. Markedly contrasting lithofacies are present between rocks of the same age in the Ordovician and Silurian; the Silurian also has contrasting biofacies relations. Vulcanism occurred from Cambrian(?) through Early Devonian time; its intensity, however, was greatest in the Ordovician and Early Devonian. Some of the Ordovician volcanic terrane emerged as land near the close of the Ordovician and in Early Silurian time. Such terrane contains peripheral deposits of Lower Silurian rocks with faunas that are older in the south and younger in the north, suggesting a southeast to northwest marine transgression in Silurian time.

At least four tectonic episodes (recognized by 3 unconformities and 1 nonsequence) have affected the area: the youngest, or Acadian, is the most widespread and clearly imprinted orogeny of the region. The initial severe folding of this orogeny was followed by the emplacement of felsic plutons and a later pulse of broad warping.

Detailed and reconnaissance geologic mapping in recent years by geologists of the U.S. Geological Survey, the Massachusetts and California Institutes of Technology, and others (see fig. 1) have considerably revised earlier concepts of the geology of northeastern Maine (Keith, 1933). This article summarizes some of the stratigraphic and tectonic features of the region as now known. Undoubtedly, future geologic work will revise many of these concepts. The Maine Geological Survey and the National Science Foundation financially supported, in part, some of the mapping carried out by the university geologists.

In general, the nomenclature used for the ages determined by fossils, especially in the Silurian, and consequently the names of the stratigraphic sections described in this article are those of the European Stand-

ard section. Although the American section is accepted for the Devonian, European terminology is also used for the Devonian in this article. The American and European Standard sections are compared in the accompanying table. Some of the rocks in the region are not closely dated and are shown as possibly including rocks of 2 or 3 systemic subdivisions. Such lithologic units will not be discussed in this article, except as they may relate to the broad regional problems.

### STRATIGRAPHY

#### Cambrian

Closely folded early and middle Paleozoic rocks underlie northeastern Maine. Although the rocks of this region at many places are weakly metamorphosed (chlorite grade), the original character of many is still well preserved. For convenience, the nomenclature of sedimentary and volcanic rocks is generally used in this article rather than metamorphic names or prefixes. The oldest rocks of the region are exposed in the Weeksboro-Lunksoos Lake anticline (fig. 1). Neuman (1962, p. 794) reported that these rocks from the southern part of the anticline consist of "quartzite and slate, interbedded in varying proportions, and contain red slate with *Oldhamia smithi* Ruedemann." In assigning a Cambrian(?) age to the Grand Pitch Formation, Neuman (1962, p. 796) indicated that the formation is probably of Early Cambrian age but may be as old as late Precambrian or as young as Early Ordovician. In the northern part of the anticline, near Weeksboro, the core rocks are somewhat different from typical Grand Pitch; here they consist mostly of phyllite with thin (1 inch to 1 foot) quartzite layers but locally are made up of massive, thick-bedded (1 to 5 feet) quartzite with thin phyllite interbeds. Volcanic rocks occur locally with the phyllite and thin quartzite facies (Pavlides, unpublished data).

<sup>1</sup> Massachusetts Institute of Technology.

<sup>2</sup> California Institute of Technology.

Correlation of the Standard and American sections for the Ordovician through Middle Devonian<sup>1</sup>

	Standard section				American section		Graptolite zones					
		Series			Series	Stages						
Devonian	Middle	Givetian		Middle	Erian	Hamilton						
		Eifelian				Onondaga						
		Upper	Lower			Disconformity						
	Lower			Lower	Ulsterian	Schoharie <sup>2</sup>						
	Emsian					Esopus						
	Siegenian					Oriskany						
	Upper	Lower				Becraft	Helderbergian					
						New Scotland						
	Gedinnian					Manlius-Coeymans						
Silurian	Upper	Ludlovian	Upper ?—? Lower	Upper	Cayugan	Cobleskill-Rondout	?—? 36					
						Bertie						
						Salina						
	Lower	Wenlockian		Middle	Niagaran	Lockport	32 31 26 25					
		Llandoveryan	Upper C <sub>6</sub> C <sub>1</sub> B <sub>3</sub> B <sub>1</sub> A <sub>4</sub> A <sub>1</sub>			Rochester						
						Clinton						
						Medina						
						Albion						
Ordovician		Ashgillian			Upper	Cincinnatian	Richmond	15				
		Caradocian					Maysville	14				
		Llandeilian					Eden					
		Llanvirnian			Middle	Champlainian	Trenton	13				
		Arenigian					Wilderness (Black River)					
		Tremadocian					Porterfield					
							Ashby					
							Marmor	9				
							Whiterock					
					Lower	Canadian	Canadian Series	6 1				

<sup>1</sup> Compiled from the following sources: Ordovician W. B. N. Berry (1960, table 1); Silurian and Devonian (exclusive of the Silurian graptolite zones) Boucot and others (1964); Silurian graptolite zones, Elles and Wood (1901-18, p. 526) and Davis (1961, p. 302).<sup>2</sup> Equivalent to zone B of Oliver (1960).

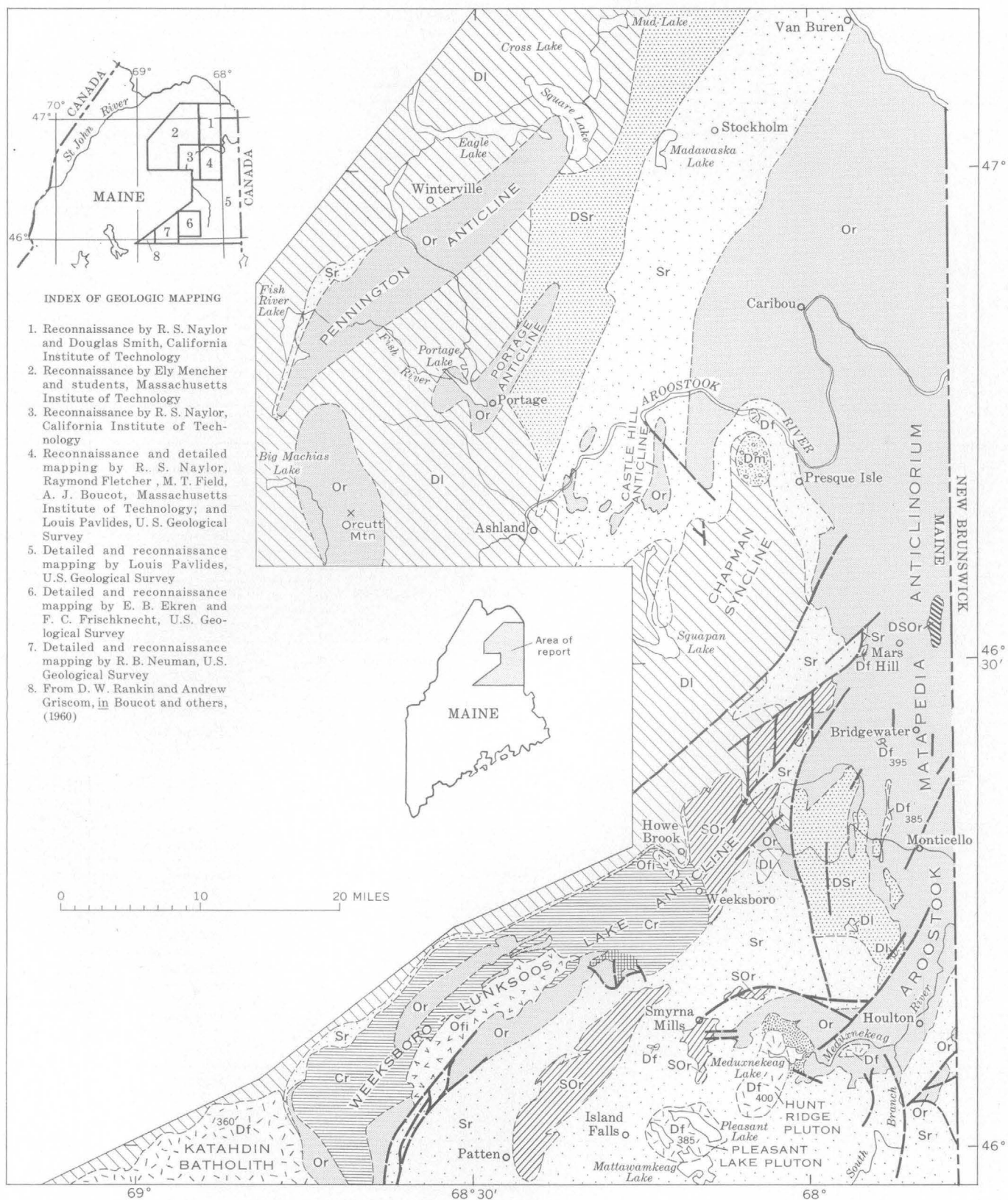
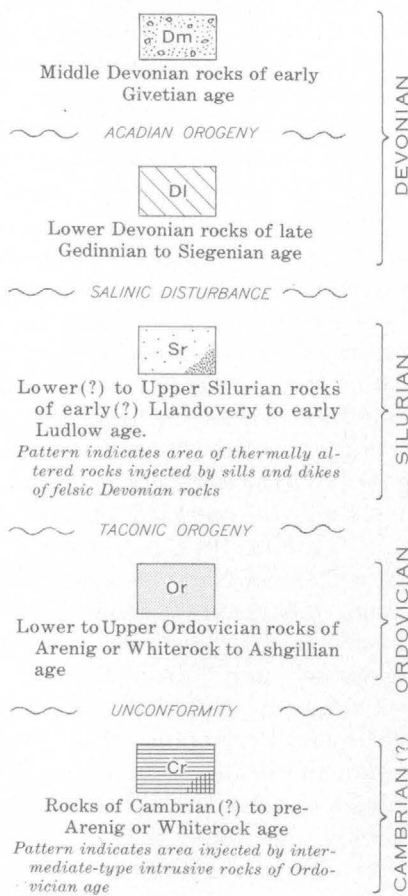


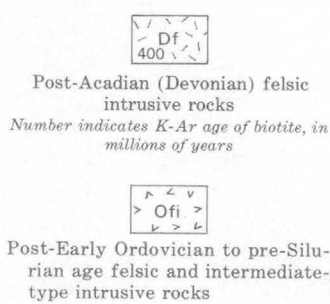
FIGURE 1

## EXPLANATION

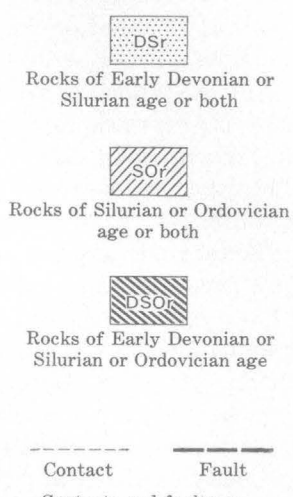
## SEDIMENTARY AND VOLCANIC ROCKS



## INTRUSIVE ROCKS



## SEDIMENTARY AND VOLCANIC ROCKS NOT CLOSELY DATED



— — — Contact  
— — — Fault  
Contacts and faults are approximate or inferred

FIGURE 1.—Generalized preliminary geologic map of northeast Maine.

quartzose limy layers have convolute layering and subtle graded bedding. To some degree the limy rocks of the Aroostook-Matapedia anticlinorium resemble calcareous flysch as described by Dzulynski and others (1959, p. 1095-1096).

West of the limy rocks of the Aroostook-Matapedia anticlinorium are anticlines with volcanic rocks, chert, argillite, and graywacke and slate of Ordovician age (Boucot and others, 1964; Ely Mencher, unpublished data).

Graptolites of zone 13 (*Orthograptus truncatus* var. *intermedius* zone) of Trenton age have been found in the ribbon rock member (Pavlides and others, 1961, p. B65-B66) of the Meduxnekeag Formation in the Aroostook-Matapedia anticlinorium and also in the Castle Hill anticline (Boucot and others, 1964; W. B. N. Berry, written communication, 1961). It is possible that the Pyle Mountain Argillite of Ashgillian (Richmond) age at Castle Hill (Boucot and others, 1964) has an equivalent in the limy rocks of the Aroostook-Matapedia anticlinorium in Maine, although Ashgillian fossils have not as yet been found in the latter.

The only Ordovician graptolite zone definitely determined from either the Portage or Pennington anticlines is zone 12 (*Climacograptus bicornis* zone) of Wilderness age of Cooper (1956), but possibly zone 11 (*Nemagraptus gracilis*; Porterfield age) is also present (W. B. N. Berry, written communications, 1962 and 1963).

## Ordovician

Most of the other major anticlinal folds of the area have Ordovician rocks in their cores (fig. 1). There is a marked contrast in facies between chiefly calcareous rocks in the eastern part of the area and sedimentary and volcanic rocks of the same age to the west. The Meduxnekeag Formation of Middle to Late(?) Ordovician age (Pavlides, 1962) forms the core of a large regional fold herein named the Aroostook-Matapedia anticlinorium. Rocks similar to the ribbon rock member of the Meduxnekeag Formation extend from northeastern Maine across part of northern New Brunswick to the Matapedia Valley region of Gaspé in Quebec, and thence across the Gaspé Peninsula to about Percé (Pavlides, and others, 1961, p. B66-B67; see also Neale and others, 1961, fig. 1). In northeastern Maine the Meduxnekeag Formation consists chiefly of impure ankeritic and calcitic layers interlayered with each other and with slate and locally with graywacke. Lenticular units of slate or slate and graywacke also are present. Locally,

Similar facies relations are present in the southern part of the described area. Here two areas of Ordovician rocks that contrast in lithology but appear to be of the same age as the ribbon rock member of the Meduxnekeag Formation are present outside of, but on both sides of, the Aroostook-Matapedia anticlinorium. The rocks about 9 miles west of Monticello (fig. 1) consist of graywacke, slate, volcanic rocks, and interbedded carbonaceous chert (radiolarian) and argillite. The carbonaceous chert and argillite contain zone-12 graptolites (W. B. N. Berry, written communication, 1961). To the south and east of Houlton the Ordovician rocks are green phyllite and black carbonaceous slate which have yielded poorly preserved graptolites, datable nonetheless as of zones 11 or 12 and late Middle Ordovician (W. B. N. Berry, written communication, 1961). Brachiopods occur within the Aroostook-Matapedia anticlinorium in ribbon rock at Houlton and are not incompatible with a Middle to Late Ordovician age (R. B. Neuman, 1961, written communication).

The Ordovician rocks along the central part and at the south end of the Weeksboro-Lunksoos Lake anticline are chiefly volcanic rocks; they consist of greenstone, volcanic conglomerate, graywacke, and tuffaceous sandstone (Neuman, 1960). A rich brachiopod fauna from the Shin Brook Formation, which occurs in a local syncline along the central part of the Weeksboro-Lunksoos Lake anticline, dates these rocks as of Arenig or Whiterock age of Cooper (1956) (Newman, 1964). Another somewhat different suite of volcanic rocks occurs along the southeast side of the anticline (Ekren, 1961). Here the rocks are chiefly spilite, keratophyre, tuffaceous conglomerate, and sandstone overlain by chert of Middle Ordovician age (Neuman, 1960, p. 166). At the north end of the Weeksboro-Lunksoos Lake anticline the thick sequence of volcanic rocks of the Dunn Brook Formation (Pavlides, 1964) consists chiefly of keratophyre, tuff, volcanic breccia, and conglomerate and metaperlite with local sandstone and slate interbeds. The Dunn Brook, in part, may be equivalent to the volcanic rocks to the south along the anticline; however, it cannot be dated any closer than of Ordovician or Silurian age or both (Pavlides, 1964).

### Silurian

Markedly contrasting depositional environments are also shown by the Silurian strata of northeastern Maine, although in the southern part of the region the contrast is more strikingly one of biofacies than lithofacies. West of the Aroostook-Matapedia anticlinorium in the northern part of the area the Silurian consists of the Perham and Frenchville Formations (Boucot and others, 1964). The Frenchville, the low-

est Silurian unit recognized in this particular belt, consists of lithic arkose, graywacke, conglomerate, and minor amounts of shale. Brachiopods from this unit are of late Llandovery ( $C_4-C_5$ ) age (Boucot and others, 1964). The Perham Formation consists mostly of shale and siltstone, minor amounts of limestone, and limestone breccia and lenticular ferruginous manganese deposits of sedimentary origin. Its lower member is of Wenlock age, whereas its upper member is of early Ludlow age (Boucot and others, 1964). North of the Castle Hill anticline, the Frenchville Formation crops out in the cores of smaller anticlines. It also encloses the north end of the Castle Hill anticline north of the fault that diagonally cuts the anticline (fig. 1). South of the fault, the formation is present only on the west limb of the anticline but appears to thicken to the west and encloses the volcanic rocks of Ordovician age that make up the core of most of the smaller unnamed anticlines there (fig. 1). To the east the stratigraphic position of the Frenchville is occupied by the so-called "nubbly limestone" (White, 1943, p. 129), which overlies the limy Ordovician rocks of the Aroostook-Matapedia anticlinorium. Ostracods of about early Clinton age (late Llandovery,  $C_3-C_4$ ) have been identified from the "nubbly limestone" unit (Jean Berdan, written communication, 1963) indicating that it is of the same age as the Frenchville Formation. The Frenchville may be a near-shore or possibly even a strand-line deposit of a mainland or islands that lay to the west, whereas the "nubbly limestone" may be the eastern lithofacies developed farther offshore.

The Silurian on the west flank of the Pennington anticline consists of conglomerate, limestone, and calcareous siltstone. Clasts of the subjacent Ordovician volcanic rocks occur in conglomerate. Paleontologic data indicate that these clastic basal Silurian rocks are of early Ludlow age and hence younger than those immediately west of the Aroostook-Matapedia anticlinorium.

Less extreme differences in lithofacies, but marked differences in biofacies, characterize the Silurian in the southern part of the area. Here the Silurian near Smyrna Mills and Houlton (fig. 1) consists chiefly of micaceous siltstone and quartzite commonly interlayered with slate; conglomerate and graywacke are locally abundant, and lenticular, sedimentary, ferruginous manganese deposits occur at several horizons. This Silurian terrane has yielded many graptolite localities (Louis Pavlides and W. B. N. Berry, unpublished data) ranging in age from early(?) Llandovery to early Ludlow. The presence of early(?) and middle Llandovery age rocks here contrasts with conditions in the northern part of the region where the earliest

dated rocks of Silurian age are of late Llandovery ( $C_3-C_5$ ) age. The rather thick section of graptolitic Silurian rocks of the eastern part of the southern region differs markedly from the thinner belt of Silurian rocks along the northwest flank of the Weeksboro-Lunksoos Lake anticline. The latter rocks are chiefly sandstone, conglomerate, and siltstone. The oldest rocks in this belt have brachiopods of late Llandovery ( $C_3-C_6$ ) age, especially in the Shin Pond and Island Falls quadrangles (Boucot and others, 1964). These ages correspond to the basal Silurian Frenchville Formation and "nubbly limestone" of the northern region, and like the Frenchville appear to be near-shore deposits. The available paleontologic evidence on the west side of the Weeksboro-Lunksoos Lake anticline also suggests that Silurian seas did not reach this region prior to late Llandovery time.

The Maple Mountain Formation of the Hovey Group at the north end of the Weeksboro-Lunksoos Lake anticline cannot be more closely dated than Silurian (Pavlides, 1964). Lenticular graywacke and conglomerate are present at the base of the formation. Above these basal rocks is a thick sequence of slate with sparser thin interbeds of graywacke and micaceous quartzite. Near the top of the Maple Mountain Formation are lenticular ferruginous manganese deposits (Pavlides, 1962). Brachiopods from the basal layers are of Silurian age, but beyond that they cannot be further subdivided. A Silurian monograptid has been found within one of the manganese deposits (Pavlides, 1962, p. 23); poor preservation prevents a closer dating.

#### Devonian

The oldest Devonian rocks of northeast Maine are of Late Gedinnian (New Scotland) age. Within the Chapman syncline they occur in the Dockendorff Group (Boucot and others, 1964). The Hedgehog Formation is the basal unit of the Dockendorff Group and is composed of lenses of volcanic rocks interlayered with minor amounts of lenticular sedimentary rocks. Above the Hedgehog are three formations that appear to be lithofacies of similar age. At the north end of the Chapman syncline is the Edmunds Hill Andesite that to the south interfingers with the Chapman Sandstone, which in turn grades southward into the Swanback Formation (argillite, shale, and quartzite). Brachiopod faunas that occur in the Hedgehog Formation, the Chapman Sandstone, and the Swanback Formation are of late Gedinnian age. Late Gedinnian age rocks also occur on the north and south sides of the Pennington anticline (Ely Mencher, unpublished data), where they consist of fossiliferous limestone, calcareous mudstone, and conglomerate. In the southern part of the area (fig. 1),

rocks of late Gedinnian age consist of calcareous slate and limestone containing a shelly fauna. They occur in a few areas northwest of Houlton within terrane mapped as undifferentiated Silurian and Devonian rocks (fig. 1). Rocks younger than late Gedinnian are not known from the southern part of the region. However, on the north and south side of the Pennington anticline (fig. 1), the upper Gedinnian rocks are conformably overlain by micaceous and carbonaceous mudstone and sandstone. At one locality, brachiopods from these rocks are of Becroft to Oriskany (Siegenian) age (A. J. Boucot, written communication, 1963), whereas spores from well-preserved flora are thought to range into the Middle Devonian (D. C. McGregor, written communications, 1962 and 1963). For purposes of this report a Siegenian age is accepted for these rocks.

These Gedinnian-Siegenian rocks appear to grade both upward and laterally into slates typical of the Seboomook Formation. At the south end of the Pennington anticline, rocks of Seboomook lithology lie in direct contact with the Silurian, and fossils close to the Seboomook base are of late Gedinnian age (Ely Mencher, unpublished data; A. J. Boucot, written communication, 1963). Blue-gray slate with minor interbeds of hard sandstone characterizes the Seboomook Formation throughout the northwestern part of the region. At the south end of the Chapman syncline and extending as far south as Howe Brook, the Seboomook consists of slate and quartzite interbedded in different proportions and is cyclically layered with quartzite grading upward into slate. At one place near Howe Brook, the Seboomook contains reworked brachiopods and corals of late Llandovery ( $C_3-C_5$ ) age near its base as well as clasts of igneous rocks probably derived from the Weeksboro-Lunksoos Lake anticline to the south. The age of the Seboomook here may be as old as Silurian (post-Llandovery) or as young as Devonian; it is provisionally considered to be New Scotland (?). In most of northern Maine, however, the age of the Seboomook is Siegenian (Becraft to Oriskany).

The Mapleton Sandstone west of Presque Isle (fig. 1) consists of coarse conglomerate at the base that grades upward into conglomerate and coarse sandstone; the upper part of the formation consists of sandstone and siltstone with thin beds of fine-grained conglomerate (Boucot and others, 1964). The Mapleton rests with angular unconformity on Silurian and Lower Devonian rocks (fig. 1). Spiny psilophytes and spores from the Mapleton suggest that it is Givetian (Upper Middle Devonian—J. M. Schopf, appendix I in Boucot and others, 1964). Two clasts from the Mapleton have been found that contain brachiopods of New Scotland age, also indicating that this formation is younger than late Gedinnian.

## TECTONICS

### **Structural features**

The Paleozoic rocks of northeastern Maine, are mostly incompetent pelites, limestones, and tuffs. Such rocks are thrown into tightly compressed steep-limbed folds and are almost everywhere cut by steeply dipping slaty cleavage. Fold plunges range from moderate to steep, and some folds may even have inverted plunges (Pavlides, 1962, pl. 5; and unpublished data). Thick sequences of competent rocks such as those in the Chapman syncline are more gently folded, and they have moderate to gentle dips. In general, sandstones, conglomerates, greenstones, and some felsites constitute the competent rocks of the region. The folding described above is mostly of a rather short wave length, and such folds are second-order crenulations on the anticlinal and synclinal folds of regional extent within the area, some of which are named in figure 1. However, because of the generalization introduced into figure 1, and the scale of the map, the contacts shown, especially at the noses of folds, are of necessity smooth.

The overall fold pattern of at least the northwestern part of the described area and the surface distribution of the Ordovician rocks there are thought to reflect the difference in competency between the Devonian sediments and the more rigid basement of Ordovician rocks upon which they rested. The surface of this basement had considerable topographic relief and stood above the level of the Early Devonian sea in many places (Ely Mencher, unpublished data).

Transverse cleavage, with a north to northeast trend, is in many places parallel with fold axes, especially in the northern part of the area. In the southern part of the region, cleavage with a north or northeast trend locally lies athwart fold axes that trend northwest (Louis Pavlides, unpublished data). Between Houlton and Smyrna Mills, fold axes and nearly parallel cleavage trend east; at one place the cleavage trends northwest and reflects the drag of the nearby postkinematic Hunt Ridge and Pleasant Lake plutons (fig. 1).

Faults are difficult to recognize, and movement direction is generally not known. Strike-slip movement is probably important on some faults, especially those with a northeast strike (Pavlides, 1962, p. 47). Most of the faults probably dip steeply; low-angle thrusts have not been recognized. There is a possibility that the large, arcuate fault, extending from about 6 miles west of Bridgewater, southward towards Houlton, may, in part, be a thrust; but this interpretation awaits firmer documentation from a closer dating of some of the rocks on the east and west sides of the fault.

A general curved pattern displayed by many of the large folds, as well as the second-order folds of the region, is believed to be a regional feature of the tectonic

grain of northeast Maine. Locally, however, the trends of fold axes have been modified by the drag of postkinematic plutons. Such modification and rotation of trends of fold axes occurred at the south end of the Aroostook-Matapedia anticlinorium where fold axes within the anticlinorium, as well as on either side of it, strike nearly east-west in contrast to north and northeast trends to the east and north of this area. This rotation seems clearly related to the emplacement of the Hunt Ridge and Pleasant Lake plutons (fig. 1).

The south end of the Weeksboro-Lunksoos Lake anticline also appears to have been rotated from a northeast-trending fold to a southeast-trending fold because of the drag of the Katahdin batholith (fig. 1) (Boucot and others, 1960). Near the northeast end of this anticline the trend of the anticline is nearly north rather than northeast. Here, also, the north trend may be related to rotation by a pluton that exists at depth. A gravity low centered over the Hunt Ridge pluton (Kane and others, report in preparation) extends northward from this pluton and strikes towards the northeast end of the Weeksboro-Lunksoos Lake anticline (Andrew Griscom and M. F. Kane, unpublished data). It may reflect a buried intrusive of large size, and such an intrusive, if indeed present, could have rotated the north end of the Weeksboro-Lunksoos Lake anticline during its emplacement after regional folding.

### **Unconformities and intrusive rocks**

Unconformities of both a regional and local nature occur at many places in northeast Maine. The oldest of these separates rocks of the Grand Pitch Formation of Cambrian(?) age, presumably by angular discordance, from the overlying Early or Middle Ordovician Shin Brook Formation (Neuman, 1960; 1964). However, Silurian rocks overlie much of the Grand Pitch Formation, especially along the northwest side of the Weeksboro-Lunksoos Lake anticline (fig. 1). The Grand Pitch Formation is complexly folded and characterized by well-developed shear cleavage that has disrupted and offset complexly folded layers. This style of deformation contrasts with that in the less complexly deformed overlying younger rocks. It seems reasonable, therefore, that the Grand Pitch Formation was affected by folding in Late Cambrian or Early Ordovician time, although the angular unconformity between the Grand Pitch Formation and the volcanic rocks is not clearly exposed. A pre-Taconic unconformity has been reported in the Eastern Townships of Quebec (Cooke, 1955; Riordon, 1957), but the nature and extent of the tectonic event that accompanied it have not yet been explored.

Along the southeast flank of the Weeksboro-Lunksoos Lake anticline, dioritic rocks complexly inject the Mid-

dle Ordovician greenstones (Neuman, 1960, p. 166) and the Grand Pitch Formation of Cambrian(?) age, indicating that this pluton and possibly the one near the north end of the anticline were emplaced at some time after the Middle Ordovician. Clasts of this pluton have been found in adjacent Silurian conglomerate of probable late Llandovery age along the southeast side of the anticline (Neuman, 1960; oral communication, 1964), indicating that the pluton is at least of pre-late Llandovery age. This and the related plutons are considered to be of Ordovician(?) age. It is not clear, however, what the time relationship of these Ordovician(?) intrusive rocks is to the Taconic orogeny (described below).

The Taconic, is a rather widespread tectonic event in parts of the northern Appalachians. It probably occurred at somewhat different times and with contrasting types of tectonism at different places from Middle Ordovician through Early Silurian times (Boucot and others, 1964). At many places it is an angular break, but it is also commonly a disconformity, as in most parts of northeast Maine. For example, along the west side of the Aroostook-Matapedia anticlinorium, bedding is parallel between Silurian and Ordovician rocks along or near their contact. Also, the Caradocian and Ashgillian age rocks of the Castle anticline appear to be conformably overlain by late Llandovery ( $C_4-C_5$ ) age rocks of the Frenchville Formation. Here the stratigraphic gap may represent local uplift and non-deposition from the close of the Ordovician through pre-Frenchville Formation time. To the south, in the Smyrna Mills area (fig. 1), early (?) and middle Llandovery graptolites have been identified (W. B. N. Berry, written communication, 1962) from within the Silurian rocks (Louis Pavlides, unpublished data), and there may be even less of a stratigraphic break here, if indeed any at all is present, between the Silurian and Ordovician rocks.

A nonsequence, named the Salinic disturbance by Boucot (1962), is also present in northern Maine, as well as in northern New Brunswick and adjacent Quebec (Boucot and others, 1964). This faunal break occurs between the Silurian and the Devonian and is characterized by the absence of rocks containing fossils of late Ludlow (Cobleskill and Rondout) age and early Gedinnian (Manlius and Coeymans) age. West of Presque Isle, for example, the Hedgehog Formation of late Gedinnian age rests on the upper part of the Perham Formation of early Ludlow age (Boucot and others, 1964). The Salinic disturbance may have been accompanied by local uplift. The presence of re-worked late Llandovery ( $C_3-C_5$ ) age brachiopods and corals in Seboomook (New Scotland age (?)) lithology

near Howe Brook may represent this event, if indeed the Seboomook here is of late Gedinnian age.

The Acadian orogeny is the most important and widespread orogeny of the northern Appalachians. It is dated west of Presque Isle (fig. 1) by the position of the Mapleton Sandstone of early Givetian (Hamilton) age, which lies with angular unconformity on both the Hedgehog Formation of late Gedinnian age and rocks of Silurian age. The Hedgehog Formation is of the same age as part of the Seboomook Formation, other parts of which may range in age up to Siegenian (Oriskany). Because the sequence of rocks from the Hedgehog Formation upward through the Seboomook Formation is conformable and appears to have been deformed by the same orogenic event, it seems probable that the Acadian orogeny in this area took place during Emsian or Eifelian time; namely, after the Siegenian (Oriskany) but prior to Givetian (Hamilton) time, the age of the Mapleton Sandstone. The broad open fold that the Mapleton Sandstone occupies reflects a later less severe period of folding, probably a later pulse of the Acadian orogeny.

Other rocks in northern Maine that may date the Acadian orogeny are in the southwest part of the map area on the north side of the Katahdin batholith. Here the Trout Valley Formation of Dorf and Rankin, 1962, unconformably overlies the Traveler Rhyolite of Toppan, 1932, which in turn rests conformably on rocks of Becroft and Oriskany age (Dorf and Rankin, 1962, p. 1001). Plant fossils from the basal parts of the Trout Valley have been dated as of late Early Devonian age (Dorf and Rankin, 1962, p. 1003). This age differs somewhat from the late Middle Devonian age of the flora from the Mapleton Sandstone described earlier. This difference in age between the two formations, however, may be more apparent than real. It may stem from the different stratigraphic positions the Onondaga is assigned by the different paleobotanists who have dated the flora from these two formations (Boucot and others, 1964).

Felsic intrusive rocks were emplaced in northeast Maine following the initial severe folding of the Acadian orogeny. The Katahdin batholith (fig. 1) intrudes rocks of Becroft and Oriskany age and also the Traveler Rhyolite (Rankin, 1960, p. 30). It has thermally altered the country rock it intrudes and has brecciated and locally injected some of it. The other felsic intrusives to the northeast differ from the Katahdin batholith in that they are emplaced in folded rocks no younger than early Ludlow in age; generally, they have well-developed thermal aureoles, as in the case of the Hunt Ridge and Pleasant Lake plutons (Pavlides and Canney, 1964). The Hunt Ridge pluton is unique

among this northeast group of intrusive rocks, in that it has a wide injected border zone on its north and east sides consisting mostly of felsic sills and dikes emplaced in thermally altered Silurian rocks.

The potassium-argon age of biotite from the felsic intrusives northeast of the Katahdin batholith (fig. 1) ranges from 385 to 400 million years, compared to 360 m.y. for the age of biotite from the Katahdin batholith (Faul and others, 1963, p. 4-14).

### GEOLOGIC HISTORY

Northeast Maine is part of a geosynclinal belt in which sediments and volcanic rocks accumulated intermittently from Cambrian(?) to Middle Devonian time. During Cambrian(?) time, quartzose sands and pelites of various kinds were the dominant sediments deposited (Grand Pitch Formation). Some vulcanism characterized the Cambrian(?) in this region, as minor amounts of volcanic rocks occur within the Grand Pitch Formation. At some time after the sedimentation and vulcanism but before the early Middle and Early Ordovician Shin Brook Formation was deposited, the Grand Pitch Formation was folded. Following this folding and a period of erosion or nondeposition or both, a time of widespread vulcanism set in along the western part of the region. Apparently, it started and lasted through Arenig to, in part, Llanvirnian (Whiterock) times in the central and southern region of the Weeksboro-Lunksoos Lake anticline where the rocks of the Shin Brook Formation were laid down. To the north, the oldest vulcanism recognized is of Caradocian age, as older volcanic rocks have not been recognized in the Ordovician terrane of the Pennington and Castle Hill anticlines. The younger Ordovician strata that overlie the Caradocian volcanic rocks of the Castle Hill anticline are the Pyle Mountain Argillite of Ashgillian age, so that vulcanism in this part of northern Maine did not extend into uppermost Ordovician (Richmond) time. The limy Ordovician (Caradocian, in part) rocks of the Aroostook-Matapedia anticlinorium in the eastern part of northeast Maine have no associated volcanic rocks. Little if any volcanic detritus was deposited from the western volcanic terrane into the area where the contemporaneous impure limestones of the Meduxnekeag Formation were being deposited. Here graywacke containing volcanic clasts occurs in the Meduxnekeag Formation, mostly in a unit below the limestone sequence or the ribbon rock member of the formation (Pavlides, 1962, p. 10). Volcanic clasts are less common or absent in the sparse graywacke interbeds of the ribbon rock member (Louis Pavlides, unpublished data).

Hence, only the western part of the region (fig. 1) was a terrane volcanically active at different times from

Early through Middle Ordovician time. Possibly it was a volcanic mainland or even a chain of volcanic islands. At any event, it appears to have been an area that permitted migration of marine faunas between northern Europe and this part of North America, as Ordovician volcanic and sedimentary rocks about 5½ miles east of Ashland contain brachiopods more common to Great Britain and Europe than to other parts of the United States (Neuman, 1963). In contrast, the eastern part of the region was one in which impure limestones were the chief sediments that formed, and they may, in part, have been deposited by turbidity currents, if some of their flyschlike features are actually reliable and are diagnostic features of turbidites. The small areas of Ordovician rocks on the southeast side of the Aroostook-Matapedia anticlinorium may also represent still another environment of deposition, in that they are graptoitic carbonaceous pelites without associated volcanic rocks.

The Taconic orogeny was a period of nondeposition and local uplift. The dioritic pluton along the Lunksoos Lake-Weeksboro anticline may have been emplaced during the Taconic. It was probably during the Taconic disturbance that the Weeksboro-Lunksoos Lake anticline and much of the other Ordovician terrane of the northern part of the region (fig. 1) emerged into land. The Silurian seas transgressed progressively northwestward from early(?) or middle Llandovery to Ludlow time. By late Llandovery time they had covered most of northern Maine, except that they may not have transgressed westward as rapidly, and therefore, did not reach the Pennington anticline area until early Ludlow time. Vulcanism in northeast Maine was not as pronounced during the Silurian as it was during the Ordovician. The only volcanic rocks that may have accumulated here during the Silurian are in the Dunn Brook Formation, if indeed any part of this formation is of Silurian age. Nevertheless, some volcanic activity did take place at this time as ash layers a few inches thick are interlayered with the sedimentary manganese deposits of the region (Pavlides, 1962, p. 36; White, 1943, p. 134). The source of these ash layers is not known; the ash may have been erupted from distant volcanoes.

The Salinic disturbance, which separates the youngest Silurian from the oldest Devonian rocks of northeast Maine, locally may have been a period of temporary withdrawal of the seas from northern Maine or a period of nondeposition. There is no evidence of any widespread erosional break associated with this event, except perhaps locally as near Howe Brook (already described). With the resumption of widespread sedimentation in northern Maine during late Gedinnian time,

certain changes in the conditions that prevailed on the nearby land areas are reflected in the biostratigraphic record. Formations of New Scotland age, such as the Chapman Sandstone and the Swanback Formation, contain layers with marine invertebrate faunas as well as beds with fragments of psilophyton-type plants (Boucot and others, 1964; Louis Pavlides, unpublished data); these represent the first record of terrestrial plants in the nearby land areas of northeast Maine. Also during late Gedinnian time, northeast Maine again experienced an era of pronounced vulcanism. There are volcanic rocks interbedded in the Devonian slates on the southwest side of the Pennington anticline. The volcanic rocks of the Hedgehog Formation west of Presque Isle are part of a broad but discontinuous belt of volcanic activity that extended to the southwest of Presque Isle for about 150 miles and northeast to Chaleur Bay for about 130 miles during New Scotland time (Boucot and others, 1964, fig. 2). Some of the sedimentary rocks laid down during the Siegenian may have been deposited as turbidites, judging by such features as the cyclical layering and graded bedding that occur in much of the Seboomook Formation. These rocks are part of the Connecticut Valley-Gaspé synclinorium described by Cady (1960). Following the deposition of the Tomhegan Formation (Boucot, 1961, p. 161-163), now dated as of lower Emsian (Schoharie) age (Boucot, unpublished data), the seaways that covered northern Maine were destroyed as the Acadian orogeny began. Most of the structural features of the pre-Middle Devonian rocks of northern Maine and, indeed, of most of the northern Appalachians were imprinted by this orogeny. The rocks were closely folded and probably faulted during the Acadian, although the faults of northeast Maine are not closely dated. Slaty cleavage that parallels fold axes, as well as locally cuts across them, probably developed as a late phase of the folding or soon thereafter.

The last major event during the Acadian orogenic episode was the emplacement of postkinematic felsic plutons that locally have modified the trends of fold axes (Smyrna Mills area, fig. 1). These plutons are characterized by well-developed thermal aureoles within which cleavage is mostly obliterated or obscured. They probably were emplaced near the surface rather than at great depths within the crust and belong to the epizone, or possibly are transitional with the mesozone plutons, as defined by Buddington (1959).

Regional metamorphism that affected the area probably occurred nearly contemporaneously with the emplacement of the plutons. It is noteworthy that the rocks in the northern part of the region are relatively unmetamorphosed, whereas those to the south, near the

areas of Devonian plutonic activity, have undergone low-rank (greenschist facies) regional metamorphism. The rank of this metamorphism corresponds to the epizonal nature of the plutonism.

A second pulse of the Acadian orogeny or possibly a separate, later orogeny is indicated in northeast Maine by the relations of the terrestrial plant-bearing Mapleton Sandstone. This unit lies unconformably on the steeply dipping, folded rocks deformed by the Acadian orogeny and is itself folded into an open syncline with moderate to gentle dips. With the close of the episode of post-Mapleton folding, the record of the tectonic history of northern Maine apparently ends. Presumably, northern Maine remained an emerged area through the rest of geologic time and possibly supplied sediment for the later Devonian and Carboniferous rocks that accumulated in southeastern Maine and in the Maritime Provinces of Canada.

## REFERENCES

- Berry, W. B. N., 1960, Correlation of Ordovician graptolite-bearing sequences: *Internat. Geol. Cong.*, 21st, pt. 7, p. 97-108.
- Boucot, A. J., 1961, Stratigraphy of the Moose River synclinorium, Maine: *U.S. Geol. Survey Bull.* 1111-E, p. 153-188.
- 1962, Appalachian Siluro-Devonian, in Coe, Kenneth, ed., *Some aspects of the Variscan fold belt: Inter-university Geol. Cong.*, 9th, Exeter, Manchester Univ. Press, p. 155-163.
- Boucot, A. J., Field, M. T., Fletcher, Raymond, Forbes, W. H., Naylor, R. S., and Pavlides, Louis, 1964, Reconnaissance bedrock geology of the Presque Isle quadrangle, Maine: *Maine Geol. Survey Quad. Mapping Ser.*, no 2, 123 p.
- Boucot, A. J., Griscom, Andrew, Allingham, J. W., and Dempsey, W. J., 1960, Geologic and aeromagnetic map of Maine: *U.S. Geol. Survey open-file report*.
- Buddington, A. F., 1959, Granite emplacement with special reference to North America: *Geol. Soc. America Bull.*, v. 70, no. 6, p. 671-747.
- Cady, W. H., 1960, Stratigraphic and geotectonic relationships in northern Vermont and southern Quebec: *Geol. Soc. America Bull.*, v. 71, p. 531-576.
- Cooke, H. C., 1955, An early Paleozoic orogeny in the Eastern Townships of Quebec: *Geol. Assoc. Canada Proc.* 1955, v. 7, pt. 1, p. 113-121.
- Cooper, G. N., 1956, Chazyan and related brachiopods [U.S.-Canada]: *Smithsonian Misc. Colln.*, v. 127, pt. 1, p. 1-1, 024.
- Davis, A. M. (Stubblefield, C. J.), 1961, An introduction to paleontology, 3d ed.: London, Thomas Murby and Co., 322 p.
- Dorf, Erling, and Rankin, D. W., 1962, Early Devonian plants from the Traveler Mountain area, Maine: *Jour. Paleontology*, v. 36, p. 999-1,004.
- Dzulynski, Stanislaw, Ksaizkiewicz, Marion, and Kuenen, Ph. H., 1959, Turbidites in flysch of the Polish Carpathian Mountains: *Geol. Soc. America Bull.*, v. 70, p. 1,089-1,118.
- Ekren, E. B., 1961, Volcanic rocks of Ordovician age in the Mount Chase Ridge, Island Falls quadrangle, Maine: Art. 309 in *U.S. Geol. Survey Prof. Paper* 424-D, p. D43-D46.

- Elles, G. L., and Wood, E. M. B., 1901-18, Monograph of British graptolites: Palaeontograph Soc. London, pt. I-XI, p. c-lxxi and 539.
- Faul, Henry, Stern, T. W., Thomas, H. H., and Elmore, P. L. D., 1963, Age of intrusion and metamorphism in the northern Appalachians: Am. Jour. Sci., v. 261, p. 1-19.
- Keith, Arthur, 1933, Preliminary geologic map of Maine: Maine Geol. Survey.
- Neale, E. R. W., Béland, J. R., Potter, R. R., and Poole, W. H., 1961, A preliminary tectonic map of the Canadian Appalachian region based on age of folding: Canadian Mining Metall. Bull., v. 54, p. 687-694.
- Neuman, R. B., 1960, Pre-Silurian stratigraphy in the Shin Pond and Stacyville quadrangles, Maine: Art. 74 in U.S. Geol. Survey Prof. Paper 400-B, p. B166-B168.
- 1962, The Grand Pitch Formation: new name for the Grand Falls Formation (Cambrian?) in northeastern Maine: Am. Jour. Sci., v. 260, p. 794-797.
- 1963, Caradocian (Middle Ordovician) fossiliferous rocks near Ashland, Maine: Art. 30 in U.S. Geol. Survey Prof. Paper 475-B, p. B117-B119.
- 1964, Fossils in Ordovician tuffs, northeast Maine: U.S. Geol. Survey Bull. 1181-E. [In press]
- Oliver, W. A., 1960, Coral faunas in the Onondaga limestone of New York: U.S. Geol. Survey Prof. Paper 400-B, p. B171-B174.
- Pavlides, Louis, 1962, Geology and manganese deposits of the Maple and Hovey Mountains area, Aroostook County, Maine: U.S. Geol. Survey Prof. Paper 362, 116 p.
- 1964, The Hovey Group in northeastern Maine: U.S. Geol. Survey Bull. 1194-B. [In press]
- Pavlides, Louis, and Canney, F. C., 1964, Geological and geochemical reconnaissance, southern part of the Smyrna Mills quadrangle, Aroostook County, Maine: Art. 140 in U.S. Geol. Survey Prof. Paper 475-D, p. D96-D99.
- Pavlides, Louis, Neuman, R. B., and Berry, W. B. N., 1961, Age of the "ribbon rock" of Aroostook County, Maine: Art. 30 in U.S. Geol. Survey Prof. Paper 424-B, p. B65-B67.
- Rankin, D. W., 1960, Paleogeographic implication of deposits of hot ash flows: Internat. Geol. Cong., 21st, Copenhagen, pt. 12, p. 19-34.
- Riordon, P. H., 1957, Evidence of a pre-Taconic orogeny in southeastern Quebec: Geol. Soc. America Bull., v. 78, p. 389-394.
- Toppin, F. W., 1932, The geology of Maine: Schenectady, N. Y., Union College, Dept. Geology, 141 p.
- White, W. S., 1943, Occurrence of manganese in eastern Aroostook County, Maine: U.S. Geol. Survey Bull. 940-E, p. 125-161.



## STRATIGRAPHIC IMPORTANCE OF CORALS IN THE REDWALL LIMESTONE, NORTHERN ARIZONA

By WILLIAM J. SANDO, Washington, D.C.

**Abstract.**—Analysis of coral distribution in the Redwall Limestone of northern Arizona indicates that the Horseshoe Mesa Member, highest unit of the formation in Grand Canyon, has been removed by post-Redwall, pre-Pennsylvanian erosion in most of the area south of the Canyon. The Redwall coral faunas suggest an age range from late Kinderhook to early Meramec for the formation. The Redwall is correlated with all but the lowermost part of the Madison Group and with post-Madison Mississippian strata.

Recent intensive study of the Redwall Limestone of northern Arizona by a team of investigators lead by E. D. McKee and R. C. Gutschick (report in preparation) has contributed a wealth of information on the stratigraphy and paleontology of this familiar but poorly understood formation. McKee (1958, 1960a, 1960b, 1960c, 1963) has published several preliminary papers on lithologic subdivisions and sedimentation of the Redwall, and Yochelson (1962) and Sando (1963) have published papers on descriptive paleontology. However, none of the published work deals with recent revisions in the stratigraphy of the formation. The purpose of this report is to present some of the more important biostratigraphic conclusions gained from a study of the Redwall coral faunas.

Rugose and tabulate corals, among the more common of the Redwall fossils, have proved to be very helpful in interpreting the stratigraphy of the formation, determining its age, and establishing correlations with other stratigraphic units. Many of the stratigraphic interpretations of an earlier paper on the Redwall corals (Easton and Gutschick, 1953) have been revised on the basis of more extensive collections. Approximately a thousand specimens collected from 34 stratigraphic sections measured by McKee and Gutschick (figs. 1 and 2) provided the evidence for new stratigraphic interpretations.

McKee (1963) has recently given formal member designations to the four lithologic subdivisions of the

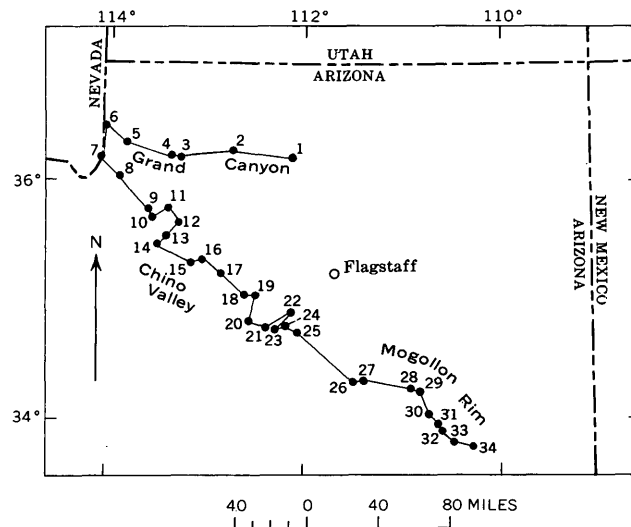


FIGURE 1.—Index map of northern Arizona, showing location of coralliferous sections of Redwall Limestone. 1, North Kaibab; 2, Havasu Canyon; 3, Whitmore Wash; 4, Parashant Canyon; 5, Grand Wash; 6, Pakoon; 7, Iceberg Canyon; 8, Quartermaster Canyon; 9, Bridge Canyon; 10, Hindu Canyon; 11, Diamond Creek; 12, Metuck Canyon; 13, Peach Springs-Nelson; 14, Ring Cone; 15, Seligman Field; 16, Chino Point; 17, Picacho Butte; 18, Black Mesa; 19, Drake quarry; 20, Simmons; 21, Lonesome Valley; 22, Sycamore Canyon; 23, Mingus Pass; 24, Jerome; 25, Clemenceau quarry; 26, Natural Bridge; 27, Pine; 28, Colcord Canyon; 29, O. W. Ranch; 30, Brush Mountain; 31, Salt River Draw 1; 32, Salt River Draw 2; 33, Salt River U.S. 60; 34, Black River Crossing.

Redwall that were previously recognized by various geologists. The lowermost unit, the Whitmore Wash Member, rests unconformably on various formations of Devonian age and, locally, on Cambrian strata. It consists of thick-bedded limestone or dolomite or a combination of limestone and dolomite. Overlying the Whitmore Wash is the Thunder Springs Member, which consists of a resistant series of alternating limestone or dolomite and chert beds which form a conspicuous banded cliff. The Thunder Springs is succeeded by the Mooney Falls Member, predominantly

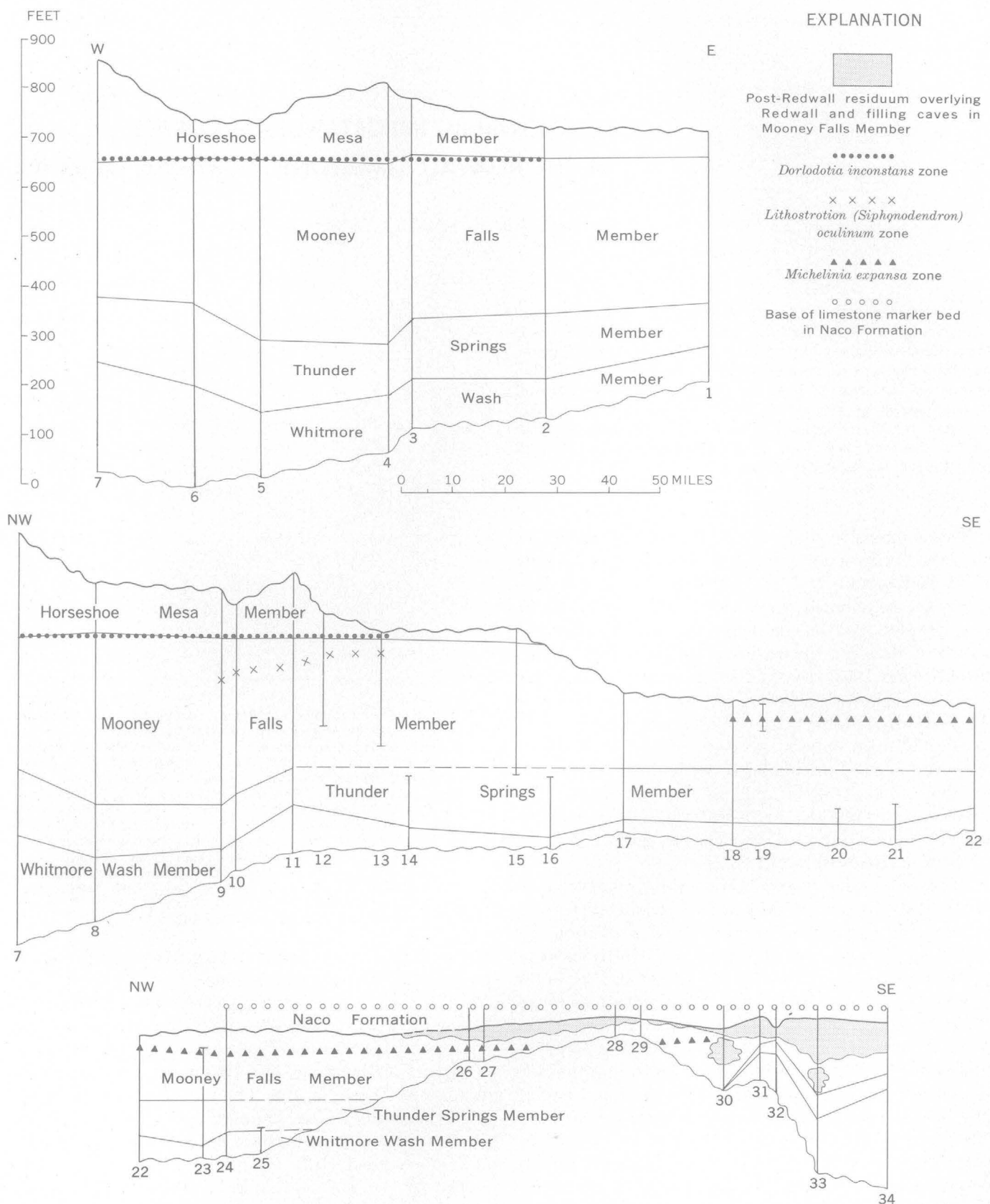


FIGURE 2.—Stratigraphic sections of the Redwall Limestone, northern Arizona. Numbers refer to locations shown on figure 1. Overlying rocks are of Pennsylvanian age, and underlying rocks are Devonian. Measured sections by E. D. McKee and R. C. Gutschick.

fine- to coarse-grained, largely crinoidal limestone in thick beds which crop out in a massive cliff. The highest subdivision is the Horseshoe Mesa Member, predominantly thin-bedded, fine-grained limestone, which forms receding ledges overlying the massive Mooney Falls cliff. The top of the Horseshoe Mesa is an ancient karst surface overlain unconformably by beds of Pennsylvanian age in the Supai and Naco Formations.

Biostratigraphic analysis of the coral faunas has a significant bearing on four key stratigraphic problems of the Redwall: (1) recognition of the Mooney Falls-Horseshoe Mesa boundary in the Grand Canyon region, (2) identification of the Redwall members in the various sections studied in northern Arizona, (3) interpretation of the significance of the residuum that overlies and fills caves in the formation in the Mogollon Rim region, and (4) correlation of the Redwall with other formations in the Cordilleran region.

The boundary between the Mooney Falls Member and Horseshoe Mesa Member is generally marked by a change from thick-bedded, medium- to coarse-grained limestone below to thin-bedded, fine-grained limestone above. However, these relationships are not everywhere consistent because characteristic Horseshoe Mesa rock types commonly occur in the Mooney Falls Member, and Mooney Falls types are known in the Horseshoe Mesa Member at some localities. Consequently, other criteria have been used in some sections to supplement the gross lithologic criteria for placement of the contact. Among the more useful supplementary criteria is the position of the *Dorlodotia inconstans* zone, characterized by the occurrence of large dendroid lithostrotionoid corals in cherty limestone within a few feet above or below the contact established on bedding criteria. This zone has been recognized in most of the sections studied in central and western Grand Canyon and has been used as a datum of contemporaneity in erecting the stratigraphic framework in that area (figs. 2, 3). *Dorlodotia inconstans* is absent in the Chino Valley and Mogollon Rim region, except for its occurrence in residual products overlying the post-Redwall karst surface and in solution cavities within the Mooney Falls Member in the Chino Valley area. This observation is one of the key factors in the recognition that post-Redwall erosion removed all the Horseshoe Mesa Member in most of the area south of the Grand Canyon.

The stratigraphic distribution of several coral taxa (fig. 3) has been used to establish relations between the various members of the Redwall in the Grand Canyon and their counterparts in the Chino Valley and Mogollon Rim regions south of Grand Canyon. The absence of species of *Ektasophyllum* and *Lithostrotion* (*Siphonodendron*), as well as the occurrence of *Dorlodotia* only in residual deposits, south of Grand Canyon sup-

ports the conclusion that the Horseshoe Mesa Member and part of the Mooney Falls Member are not now present in the Chino Valley and Mogollon Rim. Species of *Homalophyllites* and *Zaphrentites* are common in the Redwall below the upper part of the Mooney Falls Member throughout the area studied. *Vesiculophyllum incrassatum*, which ranges from the base of the Redwall into the Horseshoe Mesa Member in Grand Canyon, is found in pre-Horseshoe Mesa beds in the Chino Valley and Mogollon Rim.

The *Michelinia expansa* zone, characterized by *Michelinia expansa* and *Lithostrotionella circinatus*, provides a convenient marker for linking many of the sections in the Chino Valley. This zone has been traced onto both flanks of the Pine arch, where overlap of the Thunder Springs and Whitmore Wash Members by the Mooney Falls Member has been established on lithic and faunal evidence (sections 26–30, fig. 2).

Residual deposits similar in lithology and stratigraphic position to the Molas Formation of Colorado were formed during the karst event that immediately followed Redwall deposition. These deposits overlie the formation and fill caves within it in the Mogollon Rim region. The residuum contains corals representative of Mooney Falls levels younger than those now present in the bedrock in a given section. The significance of species of *Aulina*, also found in the residuum, is difficult to evaluate because the Aulinas are not known from the bedrock and have not been found elsewhere on the North American continent. Inasmuch as the known range of *Aulina* in Europe and Asia is upper Viséan through lower Namurian, these corals probably represent an interval of Meramec or, possibly, Chester age.

With respect to regional correlation, the most important faunal change relating to corals occurs at the base of the *Lithostrotion* (*Siphonodendron*) *oculatum* zone in the upper third of the Mooney Falls Member (fig. 3). The coral fauna above this datum includes *Siphonodendron*, *Dorlodotia*, and *Ektasophyllum*, which are characteristic of Upper Mississippian (early Meramec) strata in the northern Cordilleran region. *Siphonodendron* occurs in the uppermost part of the Madison Group (zone D of Sando and Dutro, 1960) in Montana and Wyoming, whereas *Dorlodotia* and *Ektasophyllum* are found in post-Madison Mississippian limestones in Utah and Idaho. The Redwall Limestone below the zone of *Siphonodendron* contains an Early Mississippian coral fauna characterized by species of *Homalophyllites*, *Zaphrentites*, *Michelinia*, and *Lithostrotionella*. These forms appear to represent uppermost Kinderhook and Osage equivalents and compare with faunas found in zones C<sub>1</sub> and C<sub>2</sub> of the Madison Group (Sando and Dutro, 1960).

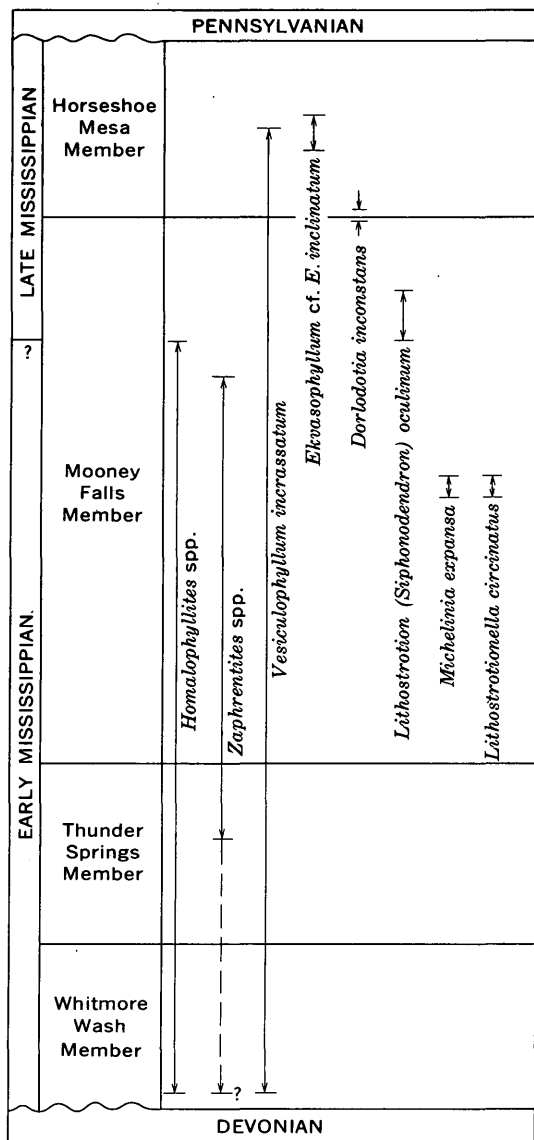


FIGURE 3.—Generalized columnar section of Redwall Limestone, showing composite stratigraphic ranges of important coral taxa in northern Arizona.

The interpretations expressed in this article differ significantly from those of Easton and Gutschick (1953). The new interpretations are based mainly on a regional synthesis of many coralliferous sections, information that was largely not available at the time of Easton and Gutschick's study. The new studies indicate that the stratigraphic unit designated as Member IV by Easton and Gutschick (1953, p. 4, text fig. II) in the area south of Grand Canyon is not the same as the highest unit of the Grand Canyon (now called Horseshoe Mesa Member). On the contrary, the Horseshoe Mesa Member was removed from most of the area

south of Grand Canyon by post-Redwall, pre-Pennsylvanian erosion which produced residual products that filtered down into the Mooney Falls Member via solution cavities and, locally, resulted in mixing of rocks and faunas from several stratigraphic levels. The recognition of mixed faunas, along with revised correlation of coralliferous intervals at some localities and discovery of some forms at levels where they were previously unrecognized has resulted in a somewhat different picture of stratigraphic ranges for many of the species described by Easton and Gutschick.

Although the previous authors specifically confined their remarks on regional correlation to the Jerome region south of Grand Canyon where the uppermost part of the formation is missing (Easton and Gutschick, 1953, p. 8), their study is the principal reference on faunal correlation of the formation and has at least an implied significance as a Redwall standard. For this reason, it is important to point out that the new studies disagree with Easton and Gutschick's (1953, p. 8) statement that "the Redwall is almost all referable to the Kinderhookian Series". The new evidence suggests that most of the formation is of Osage age (an interpretation actually anticipated by Easton and Gutschick in the footnote on page 7 of their paper) and that the age range of the Redwall is from late Kinderhook to early Meramec.

#### REFERENCES

- Easton, W. H., and Gutschick, R. C., 1953, Corals from the Redwall Limestone (Mississippian) of Arizona: Southern California Acad. Sci. Bull., v. 52, pt. 1, p. 1-11, 2 figs., 3 pls.
- McKee, E. D., 1958, The Redwall Limestone, in New Mexico Geol. Soc. Guidebook 9th Ann. Field Conf.: p. 74-77, 2 figs.
- 1960a, Cycles in carbonate rocks: Am. Jour. Sci., v. 258-A, p. 230-233, 1 fig.
- 1960b, Lithologic subdivisions of the Redwall Limestone in northern Arizona—their paleogeographic and economic significance: Art. 110 in U.S. Geol. Survey Prof. Paper 400-B, p. B243-B245.
- 1960c, Spatial relations of fossils and bedded cherts in the Redwall Limestone, Arizona: Art. 210 in U.S. Geol. Survey Prof. Paper 400-B, p. B461-B463.
- 1963, Nomenclature for lithologic subdivisions of the Mississippian Redwall Limestone, Arizona: Art 65 in U.S. Geol. Survey Prof. Paper 475-C, p. C21-C22.
- Sando, W. J., 1963, New species of colonial rugose corals from the Mississippian of northern Arizona: Jour. Paleontology, v. 37, no. 5, p. 1074-1079, pls. 145-146, 1 text fig.
- Sando, W. J., and Dutro, J. T., Jr., 1960, Stratigraphy and coral zonation of the Madison Group and Brazer dolomite in northeastern Utah, western Wyoming, and southwestern Montana, in Wyoming Geol. Assoc. Guidebook 15th Ann. Field Conf.: p. 117-126, 3 figs., 1 pl.
- Yochelson, E. L., 1962, Gastropods from the Redwall Limestone (Mississippian) in Arizona: Jour. Paleontology, v. 36, no. 1, p. 74-80, pl. 17.



## YOUNGER PRECAMBRIAN FORMATIONS AND THE BOLSA(?) QUARTZITE OF CAMBRIAN AGE, PAPAGO INDIAN RESERVATION, ARIZONA

By L. A. HEINDL and NEAL E. McCLYMONDS,  
Arlington, Va., San Juan, P.R.

*Work done in cooperation with the U.S. Bureau of Indian Affairs*

**Abstract.**—The Apache Group of younger Precambrian age crops out in 1,500-foot sequences in the Vekol and Slate Mountains. An overlying clastic unit, heretofore referred to as the Troy Quartzite, is correlated tentatively with the recently redefined Bolsa Quartzite of Cambrian age. This clastic unit is here designated the Bolsa(?) Quartzite. It is also exposed in the Waterman Mountains where, however, it rests on granitic rocks. It is overlain conformably by the Abrigo Formation of Cambrian age in the three mountain ranges.

Younger Precambrian and Paleozoic sedimentary rocks crop out in the Vekol, Slate, and Waterman Mountains in the northeastern part of the Papago Indian Reservation of south-central Arizona (figs. 1 and 2). These outcrops include the westernmost known exposures of the Apache Group of Younger Precambrian age. Also included is a clastic unit between the Apache Group and the Abrigo Formation of Cambrian age which could be correlated with either the Troy Quartzite of Precambrian age or the Bolsa Quartzite of Cambrian age. Evidence presented herein (p. C48) indicates strongly, though not conclusively, that the clastic unit is of Cambrian age; here the unit is correlated tentatively with the Bolsa and is thus designated Bolsa(?) Quartzite.

The areas where these rocks crop out are shown on geologic maps prepared by Darton and others (1924), Wilson and Moore (1959), and Wilson and others (1960), and partial sections have been described briefly by Darton (1925) and Hadley (1944). These rocks are described in detail in unpublished theses by W. G. Hogue; R. H. Carpenter, A. W. Ruff, N. E. McClymonds, and D. F. Hammer.<sup>1</sup> Brief descriptions of the

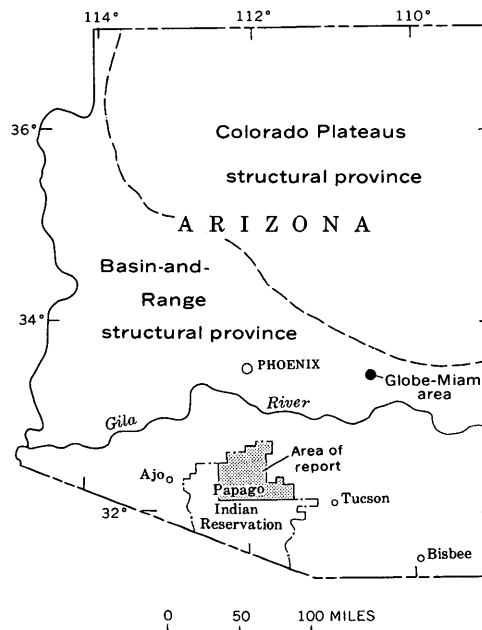


FIGURE 1.—Map showing area of report in relation to the structural provinces and larger population centers in Arizona.

Precambrian and Paleozoic sedimentary rocks by McClymonds (1959a, 1959b) were concerned mainly with correlation of the Paleozoic sequences.

<sup>1</sup> W. G. Hogue, 1940, Geology of the northern part of the Slate Mountains, Pinal County, Ariz.: Arizona Univ., M.A. thesis.

R. H. Carpenter, 1947, The geology and ore deposits of the Vekol Mountains, Pinal County, Ariz.: Stanford Univ., Ph. D. thesis.

A. W. Ruff, 1951, The geology and ore deposits of the Indiana mine area, Pima County, Ariz.: Arizona Univ., M.A. thesis.

N. E. McClymonds, 1957, Stratigraphy and structure of the Waterman Mountains, Pima County, Ariz.: Arizona Univ., M.A. thesis.

D. F. Hammer, 1961, Geology and ore deposits of the Jackrabbit area, Pinal County, Ariz.: Arizona Univ., M.A. thesis.

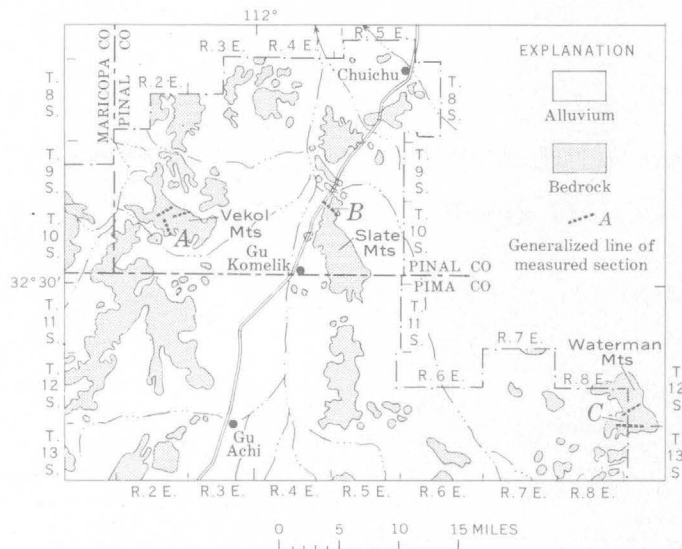


FIGURE 2.—Map showing location of the measured sections of the Apache Group and Bolsa(?) Quartzite in the Vekol (*A*), Slate (*B*), and Waterman (*C*) Mountains, Papago Indian Reservation, Ariz.

A review of the literature on Precambrian and Cambrian rocks in southern Arizona reveals considerable uncertainty about the age and correlation of the clastic rocks older than the Abrigo Formation and younger than the Mescal Limestone of the Apache Group. As originally described by Ransome (1903), the Apache Group in the Globe-Miami area consisted, in ascending order, of the Scanlan Conglomerate, Pioneer Shale, Barnes Conglomerate, and Dripping Spring Quartzite, and was tentatively considered to be of Cambrian age. On the basis of later work, Ransome (1915) added the Mescal Limestone, local basalt flows immediately overlying the Mescal, and the Troy Quartzite to the upper part of the Apache Group. Previously, Ransome (1904) also had described the Bolsa Quartzite and Abrigo Limestone, both of Cambrian age, but could not determine whether they were younger than or partly of the same age as the Apache Group. Darton (1932) concluded that the Troy Quartzite should be excluded from the Apache Group, and he assigned the Troy to the Cambrian.

Thus, the clastic rocks underlying the Abrigo Formation in southern Arizona were assigned to either the Troy Quartzite or the Bolsa Quartzite—two stratigraphic units whose relations and definition were not clear. For many years, general practice has been to apply the term Troy to quartzite that overlaps the Apache Group, and the term Bolsa to quartzite that overlaps older Precambrian schist and granitic rocks (Dickinson, 1959). This usage, however, was not consistent. All previous reports on the Papago Indian

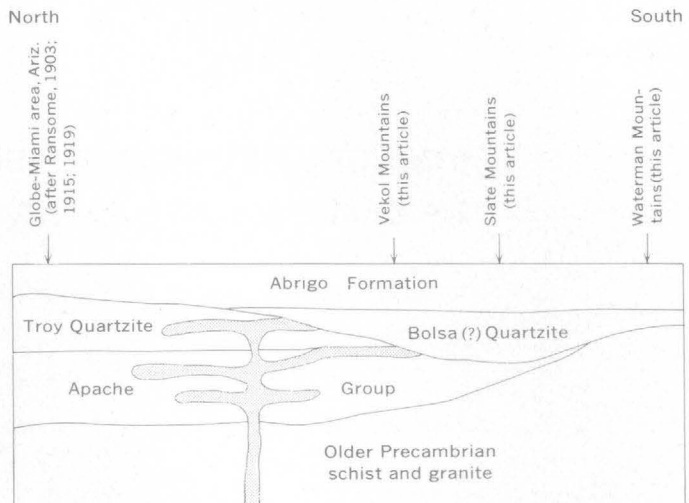


FIGURE 3.—Synoptic diagram showing relations of the Apache Group, Troy Quartzite, and diabase sills and intrusions (shaded) of younger Precambrian age and Bolsa(?) Quartzite and Abrigo Formation of Cambrian age. Not to scale.

Reservation referred the clastic unit immediately beneath the Abrigo to the Troy Quartzite of Cambrian age, regardless of whether the underlying rocks were sedimentary rocks of the Apache Group or Precambrian granite.

Work by Shride (1958) indicated that the Troy should be reincluded in the Apache Group and reassigned to the Precambrian. Krieger (1961) reported the Troy and Bolsa Quartzites in contact, and distinguished the Troy and Bolsa on (a) the basis of color, composition, and bedding, (b) the presence of diabase sills in the Troy, and (c) the fact that the Bolsa locally rests on an eroded surface cut on diabase that intrudes the Troy (fig. 3). Although the Troy and Bolsa are virtually concordant, they are separated by a considerable hiatus. Peterson (1962) accepted the Precambrian age for the Troy but did not consider it a part of the Apache Group; his conclusion is the currently accepted status of the Troy.

The original formations of the Apache Group have also been redefined. H. C. Granger and R. B. Raup (written communication, April 16, 1962) consider the Barnes Conglomerate to be a basal member of the Dripping Spring Quartzite, and C. R. Willden (written communication, May 22, 1962) considers the Scanlan Conglomerate to be a bed within the Pioneer Formation. As the beds of conglomerate within the Apache Group, where exposed on the Papago Indian Reservation, are thin and discontinuous, and lenses of conglomerate similar to the Barnes occur at several horizons near the base of the Dripping Spring Quartzite, the proposed reduction of the Barnes and Scanlan from formation rank seems reasonable, and the Apache

Group consists, therefore, of the Pioneer Formation, Dripping Spring Quartzite, and Mescal Limestone.

On the Papago Indian Reservation, the Apache Group, the Bolsa(?) Quartzite, and the Abrigo Formation are well exposed in the Vekol and Slate Mountains. The Apache Group rocks are similar to the type sequence in the Globe-Miami area; although the formations composing the Apache Group differ in thickness, their combined thickness and the sequence of rock types are nearly the same as in the type area (see accompanying table). The Apache Group is missing in the Waterman Mountains, but the Bolsa(?) and Abrigo are exposed; here the Bolsa(?) rests unconformably on Precambrian granite. The following measured sections are representative of the Apache Group and Bolsa(?) Quartzite on the reservation.

*Thicknesses, in feet, of the Pioneer Formation, Dripping Spring Quartzite, and Mescal Limestone of the Apache Group in the Vekol and Slate Mountains and in the Globe-Miami area, Arizona*

Unit	Vekol Mountains		Slate Mountains			Globe-Miami area
	Carpenter <sup>1</sup>	McClymonds (this article)	Hogue <sup>1</sup>	Hammer <sup>1</sup>	McClymonds (this article)	After Peterson (1962)
Mescal Limestone--	291	345	240	193	235	360
Dripping Spring Quartzite-----	<sup>2</sup> 700	825	850	1, 179	975	840
Pioneer Formation-----	<sup>2</sup> 400	350	450	374	440	300
Total (Apache Group)-----	<sup>2</sup> 1, 390	1, 520	1, 540	<sup>2</sup> 1, 750	1, 650	1, 500

<sup>1</sup> See footnote, p. C43.

<sup>2</sup> Estimated or rounded thickness.

### Vekol Mountain Section

*Generalized stratigraphic section of the Pioneer Formation, Dripping Spring Quartzite, and Mescal Limestone of the Apache Group of younger Precambrian age, and the Bolsa(?) Quartzite of Cambrian age in the Vekol Mountains, Pinal County, Ariz. (Based on composite sections: Pioneer Formation and basal Dripping Spring Quartzite measured in W½SW¼ sec. 6, T. 10 S., R. 3 E.; Dripping Spring Quartzite and Mescal Limestone measured in SE¼SE¼ sec. 1, T. 10 S., R. 2 E.; and Bolsa(?) Quartzite and lowest unit of Abrigo Formation measured in SE¼NW¼ sec. 1, T. 10 S., R. 2 E.)*

Cambrian

Abrigo Formation (lowest unit) :	Thickness (feet)
Sandstone, light-brown, light-gray to pale-red, very fine grained, partly dolomitic; weathers blocky; interbedded with platy, locally fossiliferous light-brown to grayish-red silty dolomite; unit forms steplike slope; base sharp and flat. (Note: Carpenter <sup>2</sup> included this unit in uppermost part of his Troy Quartzite)-----	44

<sup>2</sup> See footnote, p. C43.

### Cambrian—Continued

#### Bolsa(?) Quartzite:

	<i>Thickness (feet)</i>
Quartzite, light-gray to brownish-gray, fine-grained; crossbedded; partly dolomitic; fragments of small fossils; weathers blocky, interbedded with light-gray mudstone near middle and with medium-grained sandstone in lower third; forms cliff with steplike slope in middle third; base sharp and flat-----	76
Erosional surface(?)	
Quartzite, light-gray to light-brown to light-red; fine to medium grained; granule-sized particles near base; partly calcareous; partly crossbedded; weathers blocky; small fragments of fossils in upper part; forms cliff; 5-foot slope-forming, fine- to coarse-grained, light-gray to dark-red sandstone bed near base; base covered-----	124
Total Bolsa(?) Quartzite-----	200

### Unconformity

#### Precambrian

Basalt flows, black, vesicular; as much as 50 feet thick, but locally absent-----	0-50
---	------

#### Apache Group:

Mescal Limestone (not including diabase sills) :	
Dolomite, light- to dark-gray, partly brownish-gray, partly red; aphanitic; silty; weathers blocky; gray and red chert in nodules and thin stringers; light-gray chert beds in lower half; forms ledge-shelf slope in upper half of 78-foot cliff below middle and steplike slope near base; base flat, grades into underlying units-----	235
Limestone, light-gray to light-greenish-gray; aphanitic; weathers blocky; gray chert and siliceous limestone in nodules, thin stringers, and thin beds; flat-pebble conglomerate 44 feet above base; unit forms cliff, sloping near base; sharp and undulating-----	59
Mudstone, dark-yellowish-green to dark-gray; slightly calcareous; partly siliceous; weathers blocky to platy; forms weak steplike slope; base sharp and flat-----	41
Siltstone, dark-yellowish-green; weathers blocky to platy; 3-foot, gray to dark-yellowish-brown, finely crystalline, silty dolomite ledge at top; unit forms steplike slope; base sharp and flat-----	10
Total Mescal Limestone-----	345

Dripping Spring Quartzite (not including diabase sills) :

Upper member:	
Quartzite, light- to dark-gray, partly greenish-gray, partly brownish-gray; silty to coarse grained; partly arkosic; partly crossbedded; weathers blocky; slope-forming, platy-weathering, gray siltstone in 14-foot-thick bed 35 feet above base; upper 41 feet forms sloping cliff, lower 35 feet forms cliff; base sharp and flat-----	90
Siltstone, light-gray to greenish-gray, partly brownish-gray; weathers blocky; light-brownish-gray, fine-grained, partly arkosic quartzite in 1- to 3-foot beds in upper part; upper 54 feet forms cliff, lower 39 feet forms slope; base sharp, in contact with diabase intrusion (sill)-----	93

## Precambrian—Continued

## Apache Group—Continued

## Dripping Spring Quartzite—Continued

## Upper member—Continued

Mudstone, light-greenish-gray to dark-yellowish-green; weathers platy to soft; interbedded with ledge-forming, blocky-weathering, greenish-gray siltstone in upper 48 feet and lower 50 feet; interbedded with ledge-forming, blocky-weathering, light- to dark-gray to brownish-gray quartzite in middle 145 feet; unit forms slope, covered in 52-foot layer 50 feet above base; base sharp and flat-----

*Thickness  
(feet)*

295

Siltstone, grayish-green to dark-yellowish-brown; red in basal 30 feet; partly crossbedded; weathers platy to blocky; interbedded with slope-forming, greenish-gray to light-orange mudstone in middle part; unit forms weak steplike slope; base sharp and slightly undulating-----

117

Total upper member-----

595

## Middle member:

Quartzite, light-gray to brownish-gray; partly red near top; fine to medium grained; partly arkosic, partly calcareous; crossbedded; weathers blocky; ripple marks and rain-drop impressions at top of some beds near top; forms cliff and dip slopes; base covered-----

170

Quartzite, light-brown to light-gray; partly greenish gray; fine to coarse grained; partly arkosic, partly calcareous; weathers blocky; forms slope, covered at top and bottom, 13-foot sloping cliff 7 feet above base; base covered-----

36

Total middle member-----

206

## Barnes Conglomerate Member:

Conglomeratic quartzite, light-gray to brownish-gray to red; fine-grained to very coarse grained matrix; arkosic; partly calcareous; weathers blocky to massive; granule- to cobble-sized, rounded quartz and red chert fragments; forms sloping cliff; base sharp and undulating-----

24

Barnes Conglomerate Member-----

24

Total Dripping Spring Quartzite-----

825

## Pioneer Formation (not including diabase sills):

Siltstone, greenish-gray to reddish-purple; clayey near top to sandy near base; partly crossbedded; weathers massive, partly blocky; forms slope, some ledges near middle; base sharp and flat-----

175

Siltstone, purplish-gray; weathers massive; interbedded with grayish-purple and yellowish-gray quartzite; fine-grained; partly arkosic, arkosic ledge at top; weathers blocky; unit forms slope with ledges; base grades into underlying unit-----

97

Siltstone, grayish- to reddish-purple with green spots; weathers massive; slope-forming, gray and purple mudstone with green spots in 12-foot bed at top; ledge-forming, blocky-weather-

## Precambrian—Continued

## Apache Group—Continued

## Pioneer Formation—Continued

*Thickness  
(feet)*

ing, fine-grained, gray to brownish-gray quartzite in thin beds and lenses; unit forms slope. Conglomerate in 1-foot lens at base, greenish-to brownish-gray; fine-grained matrix; pebble-sized, white quartz fragments; forms weak ledge; base sharp and slightly undulating-----

78

Total Pioneer Formation----- 350

## Unconformity

## Pinal Schist

## Slate Mountains Section

*Generalized stratigraphic section of the Pioneer Formation, Dripping Spring Quartzite, and Mescal Limestone of the Apache Group of younger Precambrian age and the Bolsa(?) Quartzite of Cambrian age in the Slate Mountains, Pinal County, Ariz. (Based on composite section: Pioneer Formation and Barnes Conglomerate Member of Dripping Spring Quartzite measured in N 1/2 sec. 7, T. 10 S., R. 5 E.; Middle and upper members of Dripping Spring Quartzite and lower part of Mescal Limestone measured in SW 1/4 SW 1/4 sec. 6, T. 10, S., R. 5 E.; and upper part of Mescal Limestone and Bolsa(?) Quartzite measured near middle SE 1/4 sec. 1, T. 10 S., R. 4 E.)*

## Cambrian

## Abrigo Formation (lowest unit):

*Thickness  
(feet)*

Quartzite, light-gray to brownish-gray; very fine grained; crossbedded; partly calcareous; weathers platy to blocky; interbedded with fissile- to platy-weathering, light-greenish-gray mudstone; worm-burrow molds; unit forms steplike slope; base covered-----

104

## Bolsa(?) Quartzite:

Quartzite, gray, partly reddish-brown, partly purple to pink; fine grained, some granule-sized particles; mostly arkosic, some glauconite; partly crossbedded; weathers blocky; forms cliff; base sharp and flat-----

115

Sandstone, light-brown to pink, partly reddish-brown, partly gray; fine grained, some coarse-grained particles; grades laterally to quartzite; some quartzite beds; partly crossbedded; weathers blocky to soft; forms steplike slope; base sharp and flat-----

218

Sandstone, light-red to reddish-brown; fine to coarse grained; silty; partly crossbedded; weathers blocky to soft; forms slope with weak ledges; base sharp and slightly undulating-----

82

Total Bolsa(?) Quartzite-----

415

## Disconformity

## Precambrian

## Apache Group:

## Mescal Limestone (not including diabase sills):

Dolomite, dark-gray, partly grayish-red or brownish-gray; very finely crystalline; partly silty; weathers blocky; light-gray chert in nodules and thin bands; forms steplike slope; base covered-----

128

Precambrian—Continued		
Apache Group—Continued		
Mescal Limestone—Continued	<i>Thickness (feet)</i>	
Limestone, gray, partly brownish-gray; very fine ly crystalline; partly silty; weathers blocky; light-gray to pale-red chert in nodules and thin bands; forms steplike slope; base sharp and flat-----	49	
Dolomite, dark-yellowish-brown; very finely crys- talline; weathers blocky; light-gray to yellow- ish-brown chert in thin bands and beds; forms steplike slope; base covered-----	23	
Siltstone, reddish-brown to yellowish-brown; weathers massive; limestone in thin bands in upper part; chert in lower part; forms slope; base sharp and slightly undulating-----	35	
Total Mescal Limestone-----	235	
Dripping Spring Quartzite (not including diabase sills):		
Upper member:		
Quartzite, gray, partly grayish-red or greenish- gray; fine grained; arkosic; partly calcareous; partly crossbedded; weathers blocky; interbedded with slope-forming, fissile weath- ering, olive to gray to red mudstone; unit forms steplike slope; base covered-----	61	
Mudstone, red to dark-reddish-brown, weathers blocky to fissile; interbedded with ledge forming, platy-weathering, gray, red, and greenish-gray siltstone; unit forms slope; base covered-----		
Quartzite, gray, partly reddish-brown; very fine to medium grained; partly arkosic; partly crossbedded; weathers blocky; forms step- like slope; base grades into underlying unit--		
Mudstone, gray and reddish-brown, partly green- ish-gray; weathers fissile, partly soft; inter- bedded with ledge-forming, blocky-weathering, gray siltstone; unit forms slope; base covered--		
Siltstone, dark-greenish-gray, partly reddish- brown; weathers blocky; interbedded with ledge-forming, blocky-weathering crossbedded, fine- to coarse-grained, gray (partly with green- ish hue) and reddish-brown quartzite; unit forms slope with weak ledges; base sharp and flat-----	88	
Sandstone, dark-red; very fine grained; muddy; weathers blocky; forms slope; base sharp and flat-----	75	
Total upper member-----	528	
Middle member:		
Quartzite, pinkish-gray to red; very fine to me- dium grained; arkosic; partly calcareous in lower half; partly crossbedded; weathers blocky; ripple marks at top of some beds; forms cliff and dip slope; base sharp and flat--	367	
Quartzite, light-gray to pale-red; fine grained; arkosic; partly crossbedded; weathers blocky; granule- to pebble-sized quartzite fragments in lower half; forms cliff; base sharp and flat--	35	
Total middle member-----	402	
Precambrian—Continued		
Apache Group—Continued		
Dripping Spring Quartzite—Continued	<i>Thickness (feet)</i>	
Barnes Conglomerate Member:		
Conglomeratic quartzite, light-gray to pink; very fine grained to coarse-grained matrix; arkosic; partly crossbedded; weathers blocky; granule- to pebble-sized quartzite fragments in beds as much as 4 feet thick; forms cliff; base sharp and slightly undulating-----	45	
Total Barnes Conglomerate Member-----	45	
Total Dripping Spring Quartzite-----	975	
Pioneer Formation (not including diabase sills):		
Mudstone, reddish-purple to purple; weathers massive to fissile; interbedded with ledge-form- ing, platy- to blocky-weathering, greenish-gray, partly brownish-gray, siltstone; unit forms steplike slope; base sharp and flat-----	84	
Quartzite, gray, brownish-gray, or greenish-gray; very fine to medium grained; arkosic; partly crossbedded; weathers blocky; forms steplike slope; base covered-----	46	
Mudstone, dark-reddish-brown with light-green spots; weathers massive, partly soft; inter- bedded with ledge-forming, blocky-weathering, partly crossbedded, fine-grained, red, purple, and light-brown quartzite; unit forms slope with few ledges; base covered-----	310	
Total Pioneer Formation-----	440	
116 Unconformity		
Pinal Schist		
74		
<b>Waterman Mountains Section</b>		
<i>Generalized stratigraphic section of the Bolsa(?) Quartzite of Cambrian age in the Waterman Mountains, Pima County, Ariz. (Based on composite section measured in NW 1/4 sec. 36, T. 12 S., R. 8 E.)</i>		
Cambrian	<i>Thickness (feet)</i>	
Abrigo Formation (lowest unit):		
Mudstone, yellowish-brown; very silty, micaceous, and partly sandy; weathers massive; interbedded with ledge-forming, blocky-weathering, very fine to very coarse grained, yellowish-brown to reddish- brown sandstone; unit forms slope with few ledges; base sharp and slightly undulating-----	37	
Bolsa (?) Quartzite:		
Sandstone, light-red, partly brownish-gray; fine to coarse grained; partly crossbedded; weathers blocky; forms cliff; base grades into underlying unit -----	32	
Quartzite, light-gray to pink; fine grained, some gran- ule-sized particles; crossbedded; weathers blocky; forms cliff; base sharp and slightly undulating---	134	
Quartzite, light-gray to light-red; fine grained, some granule-sized particles in bands; crossbedded; weathers blocky; forms sloping cliff; base covered--	54	
Total Bolsa(?) Quartzite-----	220	
Unconformity		
Precambrian granite		

In the Vekol Mountains, the Apache Group includes the Pioneer Formation, the Dripping Spring Quartzite, the Mescal Limestone, and local flows of black basalt. All formations of the Apache have been intruded by diabase sills. The Apache Group is overlain disconformably by the Bolsa(?) Quartzite, which consists mostly of quartzite and sandstone, and the Bolsa(?) in turn is overlain conformably by the Abrigo Formation. The section in the Slate Mountains is similar to that of the Vekols, except that the Mescal is thinner, the basalt is absent, and the Bolsa(?) is thicker. In the Waterman Mountains, the Bolsa(?) is similar to the equivalent rocks in the Vekols. Rocks assignable to the redefined Troy Quartzite of younger Precambrian age have not been recognized at the localities described in this article, although some may be present in the Vekol Mountains (as discussed in a following paragraph).

The Bolsa(?) Quartzite in the Vekol, Slate,<sup>3</sup> and Waterman Mountains contains fragments of fossils, generally poorly preserved brachiopods, and worm borings. In each of the three areas, the unit is conformable with the overlying Abrigo Formation and rests unconformably on either rocks of the Apache Group or Precambrian granite. The fossils and the basal unconformity are regarded as sufficient evidence for assignment of a Cambrian, rather than a Precambrian, age to the clastic unit, and except in the Vekol Mountains, as discussed in the following paragraph, no contrary evidence is reported.

In the Vekol Mountains, however, Carpenter<sup>4</sup> found that the lower part of his Troy Quartzite—the Bolsa(?) of this report—is intruded by diabase, presumably of Precambrian age, and some question may remain regarding the age of the beds assigned to the Bolsa(?) in that area. Along the line of the measured section, the contact between the diabase and the overlying clastic unit is covered, and whether the diabase was intruded along the contact between Precambrian rocks and the clastic unit or whether the clastic unit rests on an eroded surface of the diabase is not clear. However, the diabase thins from about 200 to 20 feet within a few hundred feet near the measured section, and an eroded surface seems to be a more likely explanation than a rapidly thinning sill. Furthermore, small fragments of unidentified fossils in the uppermost 23-foot quartzite below the Abrigo certainly indicate that the quartzite is Cambrian rather than Precambrian. However, Carpenter<sup>4</sup> reports, without specifying the exact place, that "Diabase . . . penetrates the . . . Troy to within a few feet of the shale zone that separates the . . . massive cliff-forming Troy from the . . . crossbedded

fossiliferous member [the lowest unit of the Abrigo Formation of this report]." This observation by Carpenter obviously suggests a prediabase age—that is, Precambrian rather than Cambrian—for the clastic beds. It may be that both the Precambrian Troy and the Cambrian Bolsa(?) are present in the Vekol Mountains; however, because fossil fragments occur in so much of the unit, because we saw no diabase actually intruding the quartzite during our reconnaissance of the range or where we measured the sections, because no unconformity was recognized within those beds or between them and the overlying Abrigo Formation, and because the unit lies disconformably on basalt and the Mescal limestone, we consider the measured sections of the clastic unit below the Abrigo Formation in the Vekol Mountains to be of Cambrian age.

The Bolsa(?) Quartzite is about 200 feet thick in the Vekol Mountains, about 415 feet thick in the Slate Mountains, and about 220 feet thick in the Waterman Mountains. The upper 333 feet of the atypically thick section in the Slate Mountains is similar to the Bolsa(?) of the Waterman and Vekol Mountains, but the lower 82 feet is a pale-red to reddish-brown silty sandstone which was not seen in the other two ranges. Furthermore, the silty sandstone is not present everywhere in the Slate Mountains—the section measured by D. F. Hammer<sup>5</sup>, which is about 130 feet thicker (463 feet) than that reported here, does not include the lower red sandstone. If the basal red sandstone in the Slate Mountains is excluded, the differences in thickness of the Bolsa(?) in the three mountain ranges probably reflect deposition on a surface of low relief. A. W. Ruff<sup>5</sup> reports that the Bolsa(?) and Troy Quartzites in his area are 185 feet thick in the south-central part of the Waterman Mountains and only 95 feet thick 2 miles away at the northwestern end. Although much of the difference in thickness undoubtedly is due to relief on the Precambrian surface, some may be due to faulting, including thrusting, which is common. Locally the contact between the clastic unit and the underlying granite in the Waterman Mountains shows evidence of movement.

#### REFERENCES

- Darton, N. H., and others, 1924, Geologic map of the State of Arizona : Arizona Bur. Mines, scale 1 : 500,000.
- Darton, N. H., 1925, A résumé of Arizona geology : Arizona Bur. Mines Bull. 119, 298 p.
- 1932, Algonkian strata of Arizona and western Texas [abs.] : Washington Acad. Sci. Jour., v. 22, n. 11, p. 319.
- Dickinson, R. G., 1959, Cambrian and Ordovician systems in southeastern Arizona, in Arizona Geological Society Guidebook II: Arizona Geol. Soc. Digest, 2d ann., p. 21-24.

<sup>3</sup> W. G. Hogue; see footnote, p. C43.

<sup>4</sup> See footnote, p. C43.

<sup>5</sup> See footnote, p. C43.

- Hadley, J. B., 1944, Copper and zinc deposits in the Reward area, Casa Grande mining district, Pinal County, Ariz.: U.S. Geol. Survey Strategic Minerals Inv.
- Krieger, M. H., 1961, Troy Quartzite (Younger Precambrian) and Bolsa and Abrigo Formations (Cambrian), Northern Galiuro Mountains, southeastern Arizona: Art. 207 in U.S. Geol. Survey Prof. Paper 424-C, p. C160-C164.
- McClymonds, N. E., 1959a, Paleozoic stratigraphy of the Waterman Mountains, Pima County, Ariz., in Arizona Geological Society Guidebook II: Arizona Geol. Soc. Digest, 2d ann., p. 66-76.
- 1959b, Precambrian and Paleozoic sedimentary rocks of the Papago Indian Reservation, Ariz., in Arizona Geological Society Guidebook II: Arizona Geol. Soc. Digest, 2d ann., p. 77-84.
- Peterson, N. P., 1962, Geology and ore deposits of the Globe-Miami district, Gila and Pinal Counties, Arizona: U.S. Geol. Survey Prof. Paper 342, 151 p.
- Ransome, F. L., 1903, Geology of the Globe copper district, Arizona: U.S. Geol. Survey Prof. Paper 12, 168 p.
- 1904, Geology and ore deposits of the Bisbee quadrangle, Arizona: U.S. Geol. Survey Prof. Paper 21, 168 p.
- 1915, Paleozoic section of the Ray quadrangle, Arizona: Washington Acad. Sci. Jour., v. 5, p. 380-388.
- 1919, The copper deposits of Ray and Miami, Arizona: U.S. Geol. Survey Prof. Paper 115, 192 p.
- Shride, A. F., 1958, Younger Precambrian geology in southeastern Arizona [abs.]: Geol. Soc. America Bull., v. 69, no. 12, pt. 2, p. 1744.
- Wilson, E. D., and Moore, R. T., 1959, Geologic map of Pinal County, Arizona: Arizona Bur. Mines, scale 1:375,000.
- Wilson, E. D., and Moore, R. T., and O'Haire, R. T., 1960, Geologic map of Pima and Santa Cruz Counties, Arizona: Arizona Bur. Mines, scale 1:375,000.



## OCCURRENCE AND PALEOGEOGRAPHIC SIGNIFICANCE OF THE MAYWOOD FORMATION OF LATE DEVONIAN AGE IN THE GALLATIN RANGE, SOUTHWESTERN MONTANA

By CHARLES A. SANDBERG and WILLIAM J. McMANNIS,<sup>1</sup>  
Denver, Colo., Bozeman, Mont.

**Abstract.**—A channel-fill deposit of the generally marine Maywood Formation contains abundant *Bothriolepis* sp. fish remains and probably was deposited in brackish or fresh water of a bay or estuary. Related Upper Devonian deposits are present in southern Montana and northern Wyoming. They are closely associated with lithogenetically similar Lower Devonian deposits. Valleys previously inundated by an Early Devonian sea may have controlled and localized transgressions of the Late Devonian sea.

### OCCURRENCE IN THE GALLATIN RANGE

A sequence of yellowish-gray very silty dolomite interbedded with yellowish-brown dolomite, containing abundant well-preserved large fish plates of *Bothriolepis* sp., crops out about  $\frac{3}{8}$  mile north of the Squaw Creek Ranger Station on the west side of the Gallatin Range in southwestern Montana (fig. 1). Visible from U.S. Highway 191, this sequence forms an almost continuous 1,000-foot-long exposure overlying a northwest-trending cliff of Cambrian rocks 900 feet above the Gallatin River. Fish remains are most abundant at the south end of the outcrop in SW $\frac{1}{4}$ NE $\frac{1}{4}$ NW $\frac{1}{4}$  sec. 28, T. 4 S., R. 4 E., Gallatin County, Mont. The fossil-fish locality was discovered in the spring of 1961 by McMannis, who assisted the senior author in making a large collection a few months later.

The fish-bearing sequence was assigned tentatively to the Maywood(?) Formation by McMannis (1962). The marked similarity between the sequence and a measured section of the Maywood Formation at Milligan Canyon (fig. 2), 35 miles to the northwest, and the recent determination of the fish remains as *Bothriolepis* sp. by D. H. Dunkle now permit positive assignment of the Squaw Creek sequence to the Maywood Formation of

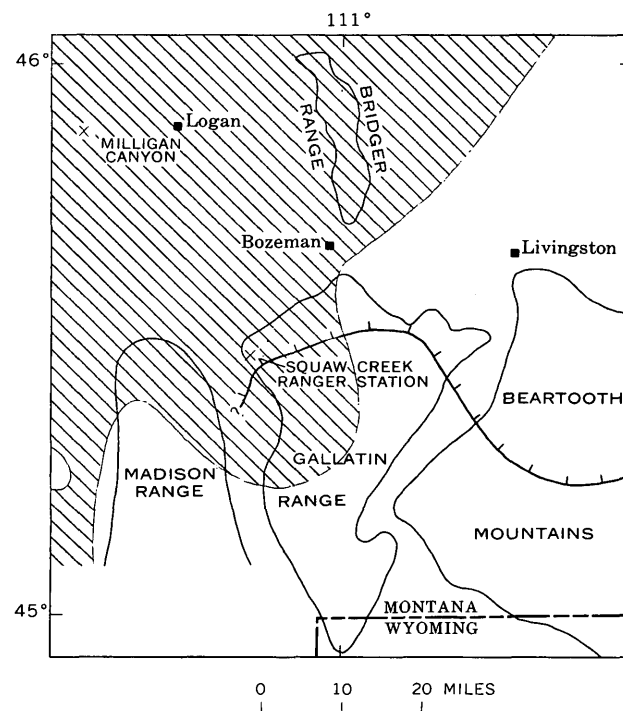


FIGURE 1.—Index map showing approximate southern limit of Maywood Formation (hatched line) and distribution of pre-Devonian rocks during Maywood deposition. Rocks directly underlying Devonian rocks are Bighorn Dolomite of Late Ordovician age (unshaded) and rocks of Late Cambrian age (shaded).

early Late Devonian age. The presence of *Bothriolepis* sp. suggests, however, that the Maywood of the Gallatin Range was deposited in marginal-marine brackish or fresh waters, whereas most known occurrences of the Maywood in the Logan area and farther north in Montana represent deposition in shallow, open, or slightly restricted marine waters.

<sup>1</sup> Montana State College.

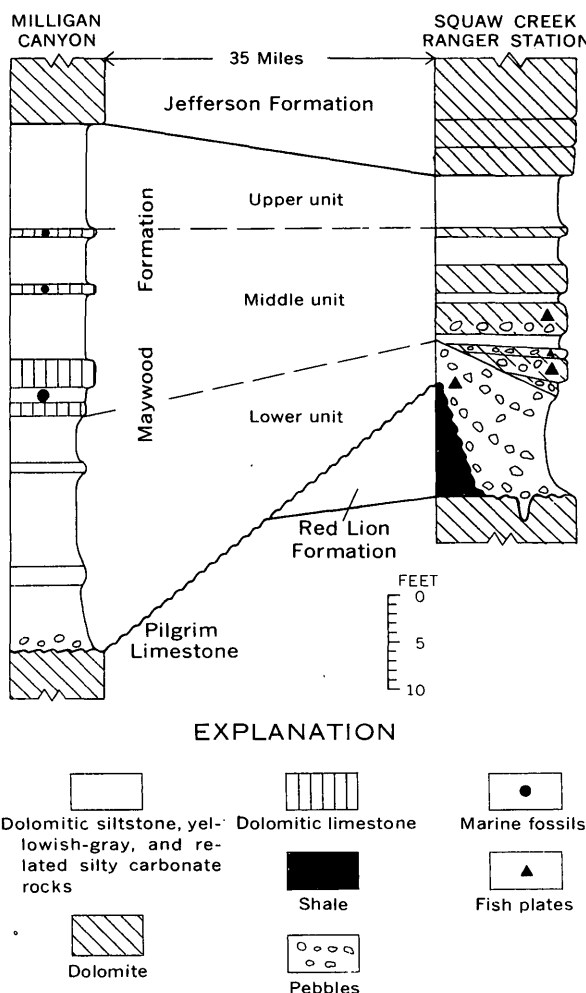


FIGURE 2.—Correlation of measured sections of Maywood Formation and adjacent rocks at Squaw Creek Ranger Station and Milligan Canyon, Mont.

At the fossil-fish locality and for about 600 feet to the north, the Maywood Formation rests unconformably on dolomite of the Pilgrim Limestone of Late Cambrian age along an irregular erosion surface displaying channels and solution crevices as much as 3 feet deep (McMannis, 1962, fig. 7). A wedge of greenish-gray shale of the Red Lion Formation of Late Cambrian age intervenes between the Maywood and Pilgrim farther north along the outcrop; the thickness of the shale increases to about 12 feet at the north end (fig. 2).

The Maywood Formation, which generally is conformably overlain by the Jefferson Formation, also of early Late Devonian age, was stated to be 61 feet thick at the Squaw Creek Ranger Station by McMannis (1962). However, correlation of this section with the bottom two units of the type section of the Jefferson

(Sandberg, 1962) at Logan, Mont., demonstrates that 27 feet of beds preferably assignable to the Jefferson was inadvertently included in the Maywood. Thus the Maywood actually has a maximum thickness of about 34 feet, at the south end of the outcrop.

The entire exposure near the Squaw Creek Ranger Station probably represents part of a wide, shallow channel-fill deposit. This is inferred from a slight northward thinning of the sequence and a corresponding lenticularity of the individual beds, as determined by a series of measured sections, and from the lithologic character of the rocks, as demonstrated by the following detailed section, measured at the fossil-fish locality:

*Measured section of the Maywood Formation,  $\frac{3}{8}$  mile north of the Squaw Creek Ranger Station, in SW $\frac{1}{4}$  NE $\frac{1}{4}$  NW $\frac{1}{4}$  sec. 28, T. 4 S., R. 4 E., Gallatin County, Mont. Measured by C. A. Sandberg and W. S. Alvarez.*

Maywood Formation:	<i>Thickness (feet)</i>
Dolomite, calcitic, very silty, yellowish-gray, pale-yellowish-orange, and grayish-yellow, microcrystalline. Interbedded with argillaceous dolomite. Contains scattered subangular granules and grains of chert. Weathers yellowish gray; thin bedded to platy; forms reentrant-----	$5\frac{1}{2}$
Dolomite, grayish-brown mottled with light-brown, very finely crystalline, rhombic, sugary textured, fetid. Weathers mottled light brownish gray and grayish orange; ledge forming-----	1
Dolomite, silty, dusky-yellow and light-olive-gray, microcrystalline. Weathers yellowish gray; platy to laminated; forms reentrant-----	3
Dolomite, pale-yellowish-brown and yellowish-brown, finely crystalline, rhombic, sugary textured. Weathers yellowish gray; ledge forming-----	3
Dolomite, silty, yellowish-gray to light-gray, cryptocrystalline. Weathers grayish yellow; platy to laminated; forms reentrant-----	1
Dolomite, yellowish-brown, dark-yellowish-brown, and grayish-brown, very finely crystalline, rhombic, sugary textured, limonitic. Bottom 2 ft. is silty and slightly glauconitic and contains scattered subangular pebbles of chert and small angular fragments of fish plates. Weathers pale yellowish brown; in 2 beds; ledge forming-----	$3\frac{1}{2}$
Dolomite, calcitic, silty, light- to dark-brownish-gray, and dark-yellowish-orange, microcrystalline, limonitic, slightly sandy. Weathers yellowish gray; platy to thinly laminated; forms reentrant; thins northwestward to $\frac{1}{2}$ ft at center of outcrop-----	$1\frac{1}{2}$
Dolomite, dark-yellowish-brown to brownish-gray, finely to very finely crystalline, slightly sandy and silty, very slightly glauconitic. Contains abundant fragmentary and whole fish plates as much as 5 in. in length and scattered subangular pebbles of chert. Large collection of <i>Bothriolepis</i> sp. from this bed. Weathers pale yellowish brown; forms upper bed of $3\frac{1}{2}$ -ft-thick ledge; pinches out apparently by onlap about 250 ft northwestward-----	1

Maywood Formation—Continued	<i>Thickness (feet)</i>
Dolomite, conglomeratic, yellowish-brown and variegated, finely to coarsely crystalline, slightly limonitic, slightly glauconitic, slightly sandy, slightly silty. Contains subangular to angular pebbles of chert, rounded flat pebbles of medium-dark-gray siltstone and light-olive-gray dolomite, and abundant fragmentary fish remains. Top 7 in. contains scattered whole fish plates, as much as 8 in. in length. Weathers pale yellowish brown; forms lower part of 3½-ft-thick ledge; pinches out apparently by onlap within 250 ft northwestward.	2½
Dolomite, silty, moderate-yellowish-brown mottled with yellowish-brown and dark-yellowish-orange, finely crystalline, slightly sandy, slightly glauconitic, slightly calcitic. Contains abundant subangular pebbles of chert, fragmentary fish remains, fragmentary carbonized plant remains, and spores. Basal contact is undulatory surface with relief of about 6 in. Weathers mottled yellowish gray, pale yellowish brown, and dark yellowish orange; forms reentrant; pinches out 25 ft northwestward.	1½
Dolomite, silty to very silty, conglomeratic, sandy, dusky-yellow, yellowish-gray, yellowish-orange, pale-yellowish-brown, and pale-olive, limonitic, slightly glauconitic, slightly calcitic. Grades in part to dolomitic siltstone. Contains subangular to subrounded pebbles of chert, rounded flat pebbles of medium-dark-gray siltstone and light-olive-gray dolomite, and small fragmentary fish plates of <i>Bothriolepis</i> sp. Interbedded with lenses of conglomerate composed of chert, dolomite, and siltstone pebbles. Basal few inches is loosely consolidated regolithic breccia composed of medium-dark-gray siltstone and greenish-gray and pale-olive shale. Weathers to yellowish-gray, yellowish-orange, and grayish-yellow smooth spheroidal surfaces studded with pebbles weathering grayish brown and dark yellowish brown. Upper 4 ft forms ledges; lower 6½ ft forms slope. Thickens to 16½ ft and forms cliff at center of outcrop; thins to 4 ft and forms partly covered slope at north end.	10½
Total thickness.	34

This sequence is divisible into three units summarized as follows: a lower unit, 10½ feet thick, composed of yellowish-gray very silty dolomite; a middle unit, 18 feet thick, consisting of 4 ledges of yellowish-brown dolomite separated by reentrants of yellowish-gray silty dolomite; and an upper unit, 5½ feet thick, composed of yellowish-gray very silty dolomite. Rounded pebbles of siltstone and dolomite and grains of glauconite derived from the underlying Cambrian rocks are common in the lower unit and bottom part of the middle unit. Subangular and angular pebbles of dense chert are common throughout, but their size decreases upward. The chert is largely light gray but includes some light- to medium-bluish-gray and a little medium-dark-gray and dark-bluish-gray chert. Lack of rounding of the resistant chert pebbles suggests that they were not transported far. A close probable source is

the chert-bearing Bighorn Dolomite of Late Ordovician age, whose erosional edge lies 10 to 20 miles east and south (fig. 1). Another possible source is the chert-bearing upper part of the Red Lion Formation, which is present within a few miles of the Squaw Creek locality.

The biota contained in the Squaw Creek section consists largely of fish and some carbonized plant remains and spores. Most of the fossils are in the bottom part of the middle unit, but fragmentary fish remains are scattered through the lower unit. The fish were tentatively identified as *Bothriolepis* sp. by D. H. Dunkle (written communication, June 27, 1963). The plant remains include an early arthrophyte (S. H. Mamay, written communication, Feb. 14, 1962), and the spores include a few trilete forms and possibly *Tasmanites* sp. (R. H. Tschudy, written communication, July 31, 1962).

The mixed biota suggests a marginal-marine brackish- or fresh-water environment for the Maywood Formation in the Gallatin Range. Although *Bothriolepis* sp. generally is considered an indicator of continental deposits, some of its occurrences in Wyoming have been interpreted as near-shore transgressive marine (Denison, 1951) or as marginal marine (Sandberg, 1963). The plant remains and trilete spores are continental, but *Tasmanites* sp. is marine.

#### OCCURRENCE IN THE LOGAN AREA

The 56-foot-thick section exposed on the north side of an unnamed gulley east of Milligan Canyon (fig. 2) in the northeast corner of sec. 1, T. 1 N., R. 1 W., Jefferson County, is representative of the Maywood Formation in the Logan, Mont., area. A more generalized section at the same locality was measured by Robinson (1963), who also recognized the three-fold subdivision of the Maywood there.

The lithologic character and succession of beds of the Maywood Formation at Milligan Canyon are similar to those of the Maywood at Squaw Creek in the Gallatin Range, but the biota differs greatly. The sequence at Milligan Canyon comprises a lower unit, 25 feet thick, composed of yellowish-gray silty dolomite; a middle unit, 20 feet thick, consisting of 4 ledges of light-olive-gray or medium-dark-gray fossiliferous dolomitic limestone separated by reentrants of yellowish-gray silty dolomitic limestone and dolomitic siltstone; and an upper unit, 11 feet thick, composed of yellowish-gray silty limestone and silty calcitic dolomite. Subrounded pebbles of quartzite are found only in the basal 1½ feet of the lower unit. These may have been derived from the Red Lion Formation, which contains

quartzite on Conrow Creek about 15 miles west of Milligan Canyon.

At Milligan Canyon, the biota, which is of early Late Devonian age, consists largely of brachiopods reported by Sandberg and Hammond (1958) and also includes echinoids, conodonts, ostracodes, and trochiliscids. The fossils are found in the middle unit and indicate an open-marine environment for at least this part of the sequence. The lower unit contains abundant salt casts at several nearby sections and probably was deposited in a brackish-water or slightly restricted marine environment. The upper unit, like that in the Gallatin Range, yields no positive indication of its depositional environment.

#### **PALEOGEOGRAPHIC INTERPRETATION**

The Maywood Formation of the Logan area is the correlative of the marine Souris River Formation, which is of Late Devonian age farther east in Montana (Sandberg and Hammond, 1958). The type Maywood, which is of Late (?) Devonian age in western Montana, has the same thickness, about 340 feet, as the Souris River at its center of accumulation in the Williston basin of northeastern Montana. Both formations may contain older Devonian beds in these areas, but the formations become younger and progressively thinner by transgressive onlap in the intervening area.

The relation of an isolated channel-fill deposit of the Souris River(?) Formation at Cottonwood Canyon, Wyo. (Sandberg, 1963), to the main body of the Souris River Formation provides a close parallel to the relation of the Maywood of the Gallatin Range to that of the Logan area. The deposit at Cottonwood Canyon, like the one at Squaw Creek, underlies the Jefferson Formation and contains a mixed biota that includes *Bothriolepis* sp. The Cottonwood Canyon deposit was interpreted by Sandberg (1963) to have been laid down in the upper reaches of a long, narrow estuary that extended into a retreating shoreline while the shallow Souris River sea transgressed westward and southward from the Williston basin. Similarly, the Squaw Creek deposit probably was laid down in an estuary or bay farther west along this same southward-retreating shoreline, after the Maywood sea had transgressed eastward from the Cordilleran seaway and coalesced with the Souris River sea somewhere in central Montana. To the north in northwestern Montana and western Alberta and farther south in western Wyoming, however, the major direction of transgression of the shallow early Late Devonian sea probably was eastward from the Cordilleran seaway.

The resulting distribution of the Maywood Formation is erratic. The Maywood may be very thin locally or entirely absent from small areas north of its approximate southern limit (fig. 1). These areas represent topographic highs on the landmass that existed in the region during much of Early and Middle Devonian time. They probably were islands during part or all of Maywood deposition. Conversely, however, isolated brackish- or fresh-water deposits of the Maywood may be more widespread than previously suspected in the former drowned coastal region south of the present known limit of the Maywood (fig. 1).

The widespread occurrence in southern Montana and northern Wyoming of isolated Upper Devonian basal channel-fill deposits, representing brackish- or fresh-water facies of the Maywood and Souris River Formations, is strongly suggested by regional paleogeography and is supported by some recently measured sections. Furthermore, several Upper Devonian channel-fill deposits recently were observed at the base of the Darby Formation of Late Devonian age in the Wind River Range of west-central Wyoming (J. F. Murphy, oral communication, July 1963; A. L. Benson, written communication, Aug. 12, 1963). These deposits contain *Bothriolepis* sp. and are related to the Maywood Formation, although they were deposited during direct eastward transgression of the Late Devonian sea in that area.

#### **PALEOGEOGRAPHIC RELATION OF UPPER AND LOWER DEVONIAN CHANNEL-FILL DEPOSITS**

Channel-fill deposits of the Beartooth Butte Formation of Early Devonian age also overlie the Bighorn Dolomite in the area of southern Montana and northern Wyoming where isolated Upper Devonian channel-fill deposits may be widespread. Some Maywood and related Upper Devonian basal channel-fill deposits have steep sides, coarse textures, grayish-red coloring, and scattered fish remains like some deposits of the Beartooth Butte Formation. Thus, unlike the basal beds of the Jefferson Formation, which generally are distinguishable from the Beartooth Butte on the basis of lithologic criteria (Sandberg, 1961, p. 1304), the Maywood and related deposits are not readily distinguishable from the Beartooth Butte without paleontologic determination of the fish remains.

Close association of Upper and Lower Devonian channel-fill deposits has been noted in several measured sections. At Cottonwood Canyon, Wyo., well-dated channel-fill deposits of the Souris River (?) Formation of Late Devonian age and of the Beartooth Butte For-

mation of Early Devonian age have been reported in about the same stratigraphic position and only a few hundred feet apart by Sandberg (1963). At Beaver Creek in the Big Belt Mountains, Mont., shallow-water marine beds of the Maywood Formation directly overlie a channel-fill deposit, which contains fish remains of probable Early Devonian age (Sandberg, 1961, p. 1306). At Livingston Peak, Mont., a brackish-water deposit of the Maywood Formation now has been recognized to directly overlie a channel-fill deposit of the Beartooth Butte Formation, previously reported by Sandberg (1961). Near Livingston Peak, two thin unfossiliferous channel-fill deposits at Yellowstone Canyon and Canyon Mountain, previously assigned to the Beartooth Butte by Sandberg (1961, fig. 1), now are considered to be Maywood.

The regional occurrence and local association of Upper and Lower Devonian channel-fill deposits in the same general stratigraphic setting suggest that some valleys, which previously had been inundated by the Early Devonian sea, served to localize and control the southward and eastward transgressions of the Late Devonian sea.

#### REFERENCES

- Denison, R. H., 1951, Late Devonian fresh-water fishes from the western United States: *Fieldiana Geology*, v. 11, no. 5, p. 221-261.
- McMannis, W. J., 1962, Devonian stratigraphy between Three Forks, Montana, and Yellowstone Park, in *Symposium, The Devonian System of Montana and adjacent areas*: Billings Geol. Soc. Guidebook 13th Ann. Field Conf., Sept. 1962, p. 4-12.
- Robinson, G. D., 1963, Geology of the Three Forks quadrangle, Montana: U.S. Geol. Survey Prof. Paper 370, 143 p.
- Sandberg, C. A., 1961, Widespread Beartooth Butte Formation of Early Devonian age in Montana and Wyoming and its paleogeographic significance: *Am. Assoc. Petroleum Geologists Bull.* v. 45, no. 8, p. 1301-1309.
- 1962, Stratigraphic section of type Three Forks and Jefferson Formations at Logan, Montana, in *Symposium, The Devonian System of Montana and adjacent areas*: Billings Geol. Soc. Guidebook 13th Ann. Field Conf., Sept. 1962, p. 47-50.
- 1963, Spirorbital limestone in the Souris River(?) Formation of Late Devonian age at Cottonwood Canyon, Bighorn Mountains, Wyoming: Art. 63 in U.S. Geol. Survey Prof. Paper 475-C, p. C14-C16.
- Sandberg, C. A., and Hammond, C. R., 1958, Devonian system in Williston basin and central Montana: *Am. Assoc. Petroleum Geologists Bull.*, v. 42, no. 10, p. 2293-2334.



## PETROGRAPHY OF THE BASEMENT GNEISS BENEATH THE COASTAL PLAIN SEQUENCE, ISLAND BEACH STATE PARK, NEW JERSEY

By DAVID L. SOUTHWICK, Washington, D.C.

**Abstract.**—An 8-foot core taken 3,873 to 3,881 feet below the land surface and about 75 feet below the base of the sedimentary rocks of the Coastal Plain consists of strongly foliated garnet-microcline-biotite-quartz-plagioclase veined gneiss close to migmatite in structure. The structures, textures, and minerals of this rock are described in detail. A K-Ar age of 235 m.y. on biotite suggests recrystallization during the late Paleozoic metamorphic event that affected parts of southeastern New England.

A test-drilling program at Island Beach State Park, N.J. (fig. 1), was undertaken by the U.S. Geological Survey in cooperation with the New Jersey Division of Water Policy and Supply to provide (1) geologic and hydrologic data pertaining to the ground-water resources of southern New Jersey, and (2) a sample of the crystalline basement rocks underlying the Coastal Plain. An exploratory borehole was drilled through the entire unconsolidated Coastal Plain sequence and into decomposed and fresh basement gneiss. A depth of 3,891 feet was reached. The unconsolidated rocks were drilled by conventional rotary methods, and a diamond coring bit producing core 3.85 inches in diameter was used in the fresh gneiss. An 8-foot section of core was recovered from a depth of 3,873 to 3,881 feet below the surface, or about 75 feet below the base of the Coastal Plain sedimentary rocks as delimited by Seaber and Vecchioli (1963). Eight sidewall cores were obtained from a section of decomposed gneiss lying between the base of the Raritan Formation and fresh basement rock (fig. 2).

The stratigraphic section of the Coastal Plain sequence at Island Beach (Upper Cretaceous to Recent) has been described by Seaber and Vecchioli (1963), and further water-resources studies of these rocks are in progress. The purpose of this article is to describe and interpret the pre-Cretaceous basement gneiss. Because of the scarcity of information on the rocks that

underlie the thicker parts of the Coastal Plain sequence, the gneiss is described in considerable detail.

### MEGASCOPIC DESCRIPTION OF THE BASEMENT GNEISS

The basement rock at Island Beach State Park is a veined gneiss approaching migmatite in character. It consists of two parts: a well-foiated dark-gray medium-grained garnet-microcline-biotite-quartz-plagioclase "body" (hereinafter called the paleosome<sup>1</sup>), and numerous virtually concordant, igneous-appearing stringers of quartz-feldspar alaskite and pegmatite ranging from about 1 to 20 cm in thickness (referred to as the neosome<sup>1</sup>). All the essential minerals can be easily identified with the naked eye. The paleosome consists of crystals 1–2 mm across; the quartz-feldspathic veinlets are generally somewhat coarser, and in the largest veinlet the crystals attain dimensions of 1–2 cm.

The paleosome is banded; individual layers a few millimeters thick differ in the ratio of biotite to quartz and feldspar. The quartz-feldspathic stringers are parallel to the banding, and all gradations exist between vaguely bounded millimeter-thick layers and lenses of quartz and plagioclase within the body of the gneiss to more sharply bounded, coarser quartz-microcline-plagioclase stringers a centimeter or two thick. If the core is assumed to be vertical, the banding dips 35–45°. Biotite flakes are imperfectly oriented parallel to it, giving foliation surfaces a lustrous sheen. A weak lineation of elongate biotite can be made out roughly parallel to the "strike" of the inclined foliation planes.

In addition to the gneissic banding, there is a second, far more subtle foliation consisting of short, discon-

<sup>1</sup> The migmatite terminology used here is that recommended by Dietrich and Mehnert (1961). The paleosome is the "older part of a composite rock (i.e., the remaining or pre-existing part)." The neosome is the "younger part of a composite rock (for example the injected, exuded, or metasomatically introduced material)."

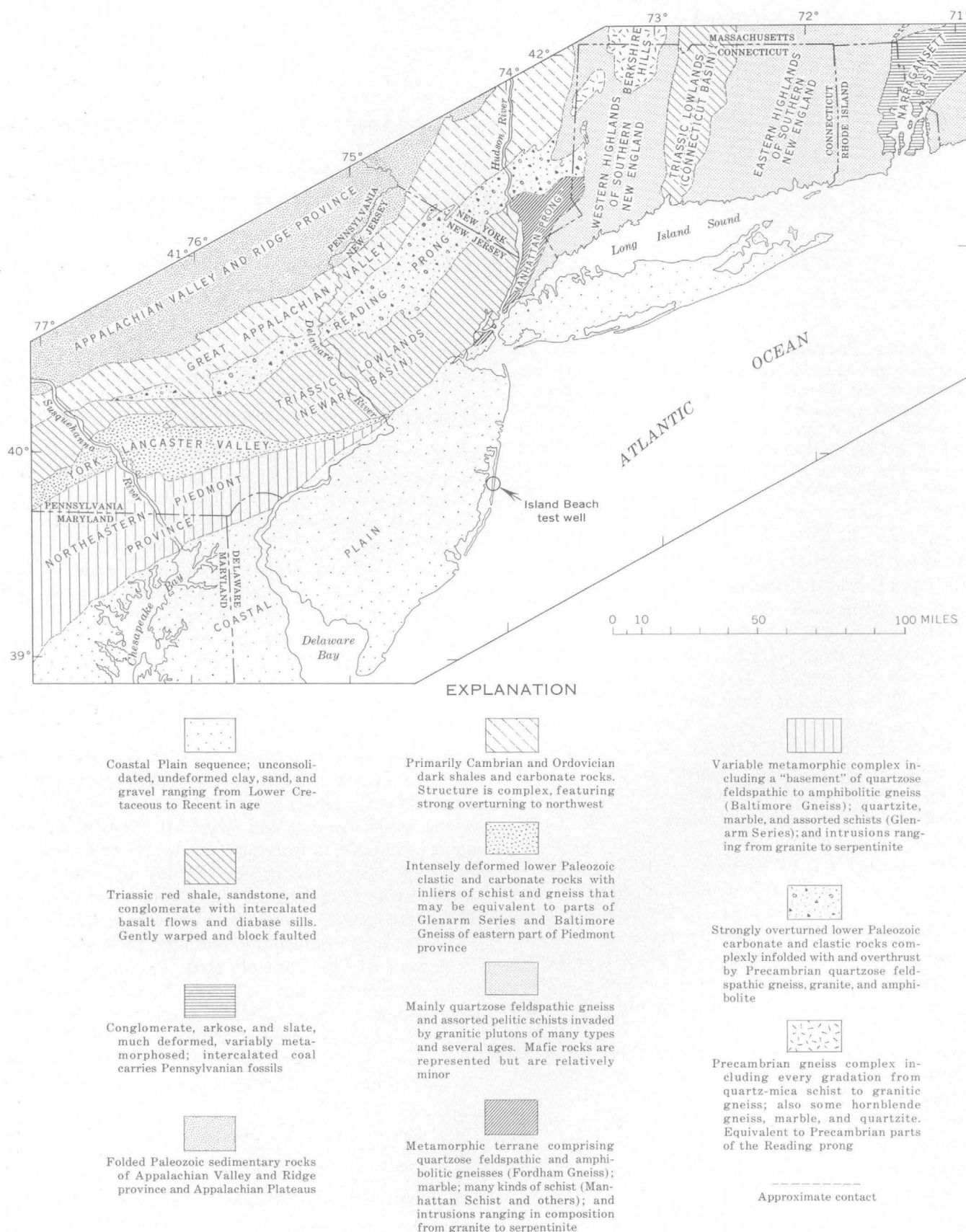


FIGURE 1.—Map showing the position of the Island Beach test well with respect to the major geologic subdivisions of the nearby Middle Atlantic States and southern New England.

tinuous shears carrying oriented biotite (visible only in two short sections of the core) and a vague "grain" of biotite flakes and elongate quartz crystals. Over most of the core this foliation dips in the same direction as the gneissic banding but at shallower angles ( $0\text{--}20^\circ$ ); locally it flattens and reverses. Possibly its intersection with the gneissic banding has produced the weak biotite lineation mentioned above.

The proportions of quartz, plagioclase, and microcline in the neosome vary greatly from stringer to stringer. Commonly the thick stringers ( $>5$  cm) are richer in microcline than are thin ones, but exceptions were noted. Some stringers exhibit rude compositional zoning. The central part consists of microcline and quartz with minor plagioclase and biotite; the marginal parts are rich in plagioclase and quartz and relatively poor in microcline. Most stringers thicker than about 1 cm are bordered by a narrow black rim composed of fine-grained biotite with a small proportion of plagioclase and quartz. These mafic borders range from about 0.5 mm to 1 cm in thickness, the thicker ones generally being associated with the thicker stringers. They pinch and swell, branch, and braid, and some are discontinuous. Elongate lenses of the same material occur in the central parts of some veins.

### GENERAL MINERALOGY

The following minerals were identified in the gneiss: plagioclase ( $An_{30}$ ), quartz, biotite, microcline (both perthitic and nonperthitic), garnet, muscovite, carbonate, chlorite, green amphibole, epidote, magnetite-ilmenite, apatite, zircon, sphene, tourmaline, and monazite. An average modal analysis of the paleosome is given in the accompanying table.

#### *Average modal analysis of the paleosome of the basement veined gneiss at Island Beach State Park, N.J.*

[From 6,337 points counted on 5 thin sections from different parts of the core]

Constituent	Percentage	Constituent	Percentage
Quartz	34.4	Sphene	Tr.
Plagioclase ( $An_{30}$ )	40.4	Epidote	Tr.
Microcline	3.6	Chlorite	0.1
Biotite	18.6	Tourmaline	Tr.
Garnet	.1	Granophyre	Tr.
Muscovite	.7	Myrmekite	Tr.
Carbonate	.6	Hydrothermal	
Opaque material	.2	assemblage <sup>1</sup>	1.0
Apatite	.2		
Zircon	Tr.	Total	100.0

<sup>1</sup> Hydrothermal assemblage is a fine mat of bleached, pinkish-yellow biotite, sericitic muscovite, and microcrystalline silica with or without chlorite, carbonate, powdery sphene, and shreds of deep blue-green amphibole.

### DESCRIPTIVE PETROGRAPHY

#### Paleosome

Plagioclase, the most abundant mineral of the paleosome, forms highly irregular crystals which are unzoned to very weakly zoned and are, as a rule, rather poorly twinned. Compositions, determined on the universal stage by the methods of Turner (1947) and Köhler (1941) using unpublished correlation curves compiled by T. L. Wright, range from  $An_{27}$  to  $An_{38}$ , with the largest grouping near  $An_{30}$ . The structural state is unequivocally ordered. All plagioclase is sericitized. Most crystals are lightly altered, but some are extensively replaced by white mica, dusty clinozoisite, albite, and quartz. There is no obvious compositional or structural control of the degree of sericitization.

Quartz occurs both as severely strained, anhedral individual grains up to 2 mm across and as fine-grained granular patches of unstrained crystals. The granular quartz commonly rims or invades large strained crystals, suggesting that it formed by cataclasis and recrystallization of the large grains. Elongate augen of recrystallized quartz parallel the foliation defined by oriented biotite.

Microline forms shapeless amoeboid grains which commonly are congregated in small patches or short trains. The crystals usually surround and engulf smaller crystals of quartz, plagioclase, and biotite. The distribution and textural relations suggest that microcline grew porphyroblastically and is younger than the other main minerals. A diffuse plaid twinning, never sharply defined, is characteristic of the microline in this rock. Most of the microline in the paleosome is nonperthitic.

Oriented biotite plates as much as 2 mm long and 0.1 mm thick are primarily responsible for the foliation of the rock. The biotite typically is pleochroic in shades of olive and drab greenish brown, but the colors vary slightly from place to place in the core. Locally the biotite is marginally altered to green chlorite, and in a few spots complete alteration to a mat of chlorite, muscovite, magnetite, and sphene has taken place. Biotite, as well as plagioclase and microcline, commonly shows evidence of mild bending and cracking.

Porphyroblasts of red-brown garnet up to 4 mm across are scattered throughout the paleosome. Typically they are subhedral and sieved with inclusions of quartz and biotite. A few show incipient alteration to green chlorite. The refractive index of the garnet is  $1.789 \pm 0.002$ , and the edge of the unit cell (determined from an X-ray diffraction pattern of garnet plus quartz and biotite inclusions) is 12.055 Å. These values cannot be fitted to any composition of anhydrous garnet.

The closest correspondence is to compositions between andradite and grossularite (Sriramadas, 1957), even though the cell edge is slightly longer than that of pure andradite. The anomalous cell edge could be due to hydration or other substitutions in the garnet structure (Chinner and others, 1960; Pistorius and Kennedy, 1960), or interference in the X-ray diffraction pattern caused by the inclusions.

Muscovite and carbonate form scattered large crystals, but more commonly they occur as a fine-grained mat together with chlorite, yellowish biotite, quartz, and granular opaque material. This assemblage forms discontinuous veinlets and vague defined patches that generally are associated with shear zones subparallel to the gneissic banding. Crosscutting veinlets also occur, however.

### Neosome

The neosome has an igneous rather than a metamorphic appearance. Typically the texture is coarse allotriomorphic granular with deeply embayed interlocking crystals of feldspar and quartz.

Microcline perthite is abundant in and characteristic of the neosome. It makes up 5 to 40 percent of each vein, in general forming a larger proportion of the thicker ones. Some very thin veinlets contain microcline crystals that are larger than the width of the veinlet. These crystals penetrate into the "wallrock" on both sides without disturbing its foliation; this suggests that they are porphyroblasts that grew by replacement. Wispy, regularly oriented lamellae of albite are estimated to make up 5–10 percent of the perthite. The composition of the unheated microcline host, determined by the X-ray method of Orville (1960), is  $\text{Or}_{93 \pm 1}$ . The obliquity, determined by the 131–131 method of Goldsmith and Laves (1954), is 0.87. The obliquity of "maximum" microcline of composition  $\text{Or}_{93}$  is 0.90; therefore the microcline host of the neosome perthite is probably close to "maximum" microcline.

The plagioclase of the neosome has a composition of  $\text{An}_{28}$ . It is virtually unzoned and rather poorly twinned. Both it and the microcline perthite are lightly dusted with sericite and show evidence of mild bending and cracking.

Quartz occurs in the same way as it does in the paleosome, forming large, strained individual grains and clusters of smaller recrystallized grains. The widely dispersed olive-brown biotite seems no different from that in the darker parts of the rock. All the main minerals are crosscut by narrow veinlets containing carbonate, muscovite, and a little quartz.

### DECOMPOSED INTERVAL

In the generalized log of the test well at Island Beach State Park, N.J., given by Seaber and Vecchioli (1963, p. B104–B105) a 64-foot section between the base of the Raritan Formation (depth 3,798 feet) and fresh basement gneiss (depth 3,862 feet) is described as "gneiss, biotite, weathered (saprolite?)." Petrographic study of eight samples from this interval (fig. 2) indicates that some of the material is not untransported saprolite, but is a poorly sorted, highly angular epiclastic sand.

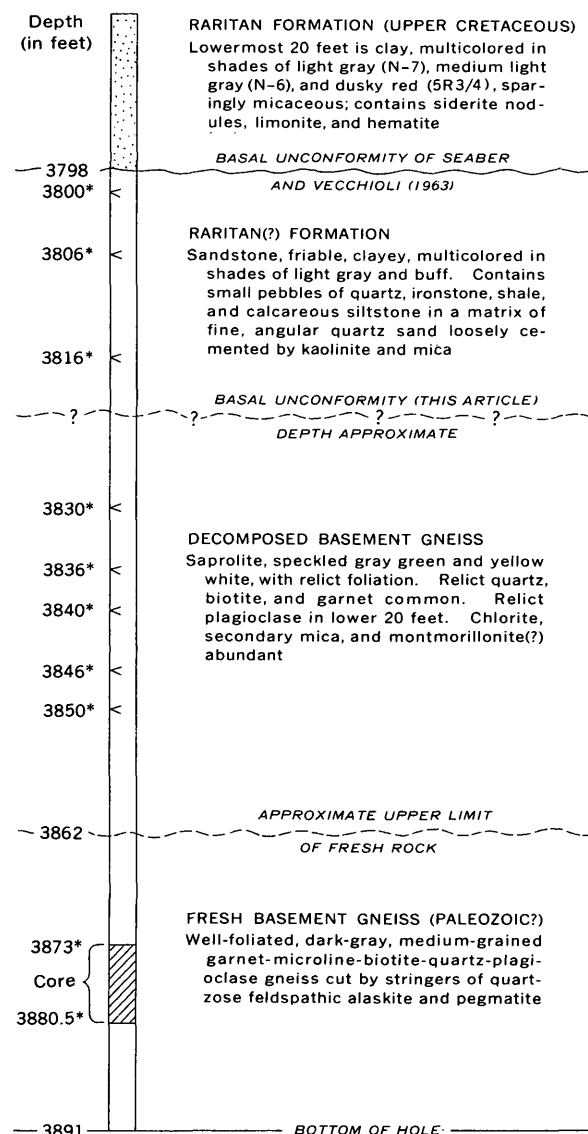


FIGURE 2.—Diagrammatic drawing of the lowermost 110 feet of the Island Beach test well. Numbers are depths below land surface (elevation approximately 10 feet). Depth measurements followed by asterisk are horizons at which samples were taken. Description of basal Raritan Formation (above 3,798 feet on this figure) from Gill, Seaber, Vecchioli, and Anderson (written communication, 1963).

The lowest five samples of the decomposed interval (3,850, 3,846, 3,840, 3,836, and 3,830 feet) are unquestionably derived from basement gneiss. They are soft, friable, speckled gray-green and yellow-white saprolite with well-preserved foliation and abundant megascopic biotite. Thin sections reveal the textures of the fresh gneiss somewhat blurred and distorted by alteration effects. Relict quartz (both large strained individual grains and recrystallized patches), biotite, garnet, apatite, and zircon are present in all five samples. Extensively sericitized feldspar can be made out only in the lowest two. The biotite is commonly fringed by a very fine grained, grass-green, weakly to strongly birefringent aggregate which appears to be a mixture of chlorite and montmorillonite. Sizable patches of the same material occur throughout the rock. The place of feldspar is taken by a fine mat of sericitic muscovite (possibly with some kaolinite) and a pale-brown dust of high refringence that may be finely divided clinozoisite.

The highest three samples of the interval (3,816, 3,806, and 3,800 feet) are tenacious clayey sand with scattered small pebbles. The color is streaky and uneven in shades of light gray and buff. The pebbles are subrounded to subangular and smaller than 1 cm in diameter. The majority are quartz, but iron-oxide-cemented sandstone, dark shale, calcareous siltstone, carbonate, and glauconite are also represented. The pebbles are distributed in a matrix consisting primarily of highly angular quartz silt and fine sand loosely cemented by a variable mixture of kaolinite, muscovite, pale-green chlorite, and iron oxides. Framework and cement are about equal in proportion. Besides quartz, clastic grains of perthite, microcline, epidote, greatly saussuritized plagioclase, carbonate, and "chert" occur in the framework but do not total more than 10 percent. Biotite is exceedingly scarce, and the deep-green chlorite and montmorillonite characteristic of the subjacent saprolite are absent.

The epiclastic textures, especially the rounded pebbles, suggest that at least the upper 18 feet of the "weathered gneiss" of Seaber and Vecchioli (1963, p. B104-B105) belongs to the lowermost part of the Raritan Formation rather than to the basement rocks (fig. 2). The material may be a combination of reworked, little-transported saprolite plus sand brought in from elsewhere, or it may be simply an immature sediment having no genetic connection with the underlying decayed rock.

The decomposed interval corresponds in position and general character to the "weathered zone" found on basement rocks beneath the sedimentary sequence of the Coastal Plain at many other localities. There is no new

evidence in the Island Beach profile bearing on the origin of this regional feature.

#### AGE

A potassium-argon age measurement was made on biotite from the paleosome of the Island Beach core by Richard Marvin of the Isotope Geology Branch, U.S. Geological Survey. An apparent age of 235 million years was obtained. A rubidium-strontium age determination on microcline from the neosome was attempted, but was unsuccessful. The biotite age is considered to be a minimum.

#### POSSIBLE REGIONAL GEOLOGIC AFFINITIES

While there is little point in attempting to correlate the gneiss at Island Beach with specific gneiss units in exposed crystalline complexes (the closest outcrops are over 50 miles away), it is of interest to speculate on the possible regional geologic relations. Figure 1 shows the position of the Island Beach test well with respect to the major geologic subdivisions of the Middle Atlantic States and southern New England. The map pattern suggests that rocks of the Piedmont province probably join rocks of the Manhattan prong and the New England highlands somewhere beneath the New Jersey coastal plain or its seaward extension. It is into this indefinite terrane that the Island Beach test well has penetrated.

On the basis of lithology, the gneiss at Island Beach fits equally well into all three provinces. Virtually identical vein gneisses are common in the eastern highlands of Connecticut; the Putnam Series as used by Sclar (1958) and Hebron Gneiss as used by Aitken (1951) are but two units in which they are found. The very complex Hartland Formation in the western highlands of Connecticut (Rodgers and others, 1959, p. 33-34) contains large tracts of migmatitic rocks. Veined gneisses occur in the Fordham Gneiss and to a lesser extent in the Manhattan Schist of the Manhattan prong (Prucha, 1956; Scotford, 1956; Fettke, 1914). Modal analyses indicate that most of the Fordham migmatites are more felsic than the Island Beach rock, but are otherwise similar (Scotford, 1956, p. 1172). The formation in the northeastern part of the Piedmont province most closely akin to the gneiss at Island Beach is the Precambrian Baltimore Gneiss (Knopf and Jonas, 1929, p. 143-146; C. A. Hopson, personal communication, 1963). The Baltimore Gneiss is an exceedingly complex mixture of well-layered paragneiss, banded gneiss, hornblende gneiss, amphibolite, migmatite, veined gneiss, augen gneiss, and uniform granitic gneiss. The veined gneiss phase is identical in all respects to the core from Island Beach.

The radiometric age of the biotite (235 m.y. minimum) may provide the only clue to the regional affinities of the Island Beach basement gneiss. This age is younger than any so far reported on biotite from the northeastern part of the Piedmont province or from the Manhattan prong, but corresponds well with the 230–250 m.y. dates obtained on biotite from the Narragansett basin area of southeastern New England (Tilton and others, 1958, 1959; Hurley and others, 1960; Long and Kulp, 1962). The available data suggest that parts of southeastern New England underwent a Permian-Carboniferous metamorphic event that did not affect (or was much weaker in) the northeastern part of the Piedmont province and the Manhattan prong. Possibly this event extended as far southwest as Island Beach. It is not unreasonable to project a belt of metamorphically related rocks along the curving regional strike of the Appalachians from Rhode Island and Connecticut to a point beneath the New Jersey coast (fig. 1).

To summarize, the basement veined gneiss at Island Beach, N.J., may have been metamorphosed at least once in common with rocks of the Narragansett basin area of southern New England. Whether or not this establishes a correlation in terms of total rock age remains a matter of considerable doubt. Because the biotite age may not record the first or only metamorphic event, it is possible that the gneiss at Island Beach is older "Piedmont" or "Manhattan" rock that was recrystallized in late Paleozoic time.

#### REFERENCES

- Aitken, J. M., 1951, Geology of a section of the Hebron Gneiss of eastern Connecticut: Connecticut State Geol. and Nat. Hist. Survey Bull. 78, 62 p.
- Chinner, G. A., Boyd, F. R., and England, J. L., 1960, Physical properties of garnet solid solutions: Carnegie Inst. Washington Year Book 59, p. 76–78.
- Dietrich, R. V., and Mehnert, K. R., 1961, Proposal for the nomenclature of migmatites and associated rocks: Internat. Geol. Cong., 21st, 1960, Copenhagen, pt. 26 (supp. vol.), p. 56–67.
- Fettke, C. R., 1914, The Manhattan Schist of southeastern New York and its associated igneous rocks: New York Acad. Sci. Annals, v. 23, p. 193–260.
- Goldsmith, J. R., and Laves, Fritz, 1954, The microcline-sanidine stability relations: Geochim. et Cosmochim. Acta, v. 5, p. 1–19.
- Hurley, P. M., Fairbairn, H. W., Pinson, W. H., and Faure, Gunter, 1960, K-A and Rb-Sr minimum ages for the Pennsylvanian section in the Narragansett Basin: Geochim. et Cosmochim. Acta, v. 18, p. 247–258.
- Knopf, E. B., and Jonas, A. I., 1929, The geology of the crystalline rocks of Baltimore County: Maryland Geol. Survey, Baltimore County Rept., p. 97–199.
- Köhler, A., 1941, Drehtischmessungen an Plagioklaszwillingen von Tief- und Hoch- temperaturopik: Min. petr. Mitt., v. 53, p. 159–179.
- Long, L. E., and Kulp, J. L., 1962, Isotopic age study of the metamorphic history of the Manhattan and Reading Prongs: Geol. Soc. America Bull., v. 73, p. 969–996.
- Orville, P. M., 1960, Powder X-ray method for determination of (Ab+An) content of microcline [abs.]: Geol. Soc. America, Program 1960 Ann. Mtg., p. 171–172.
- Pistorius, C.W.F.T., and Kennedy, G.C., 1960, Stability relations of grossularite and hydrogrossularite at high temperatures and pressures: Am. Jour. Sci., v. 258, p. 247–257.
- Prucha, J. J., 1956, Stratigraphic relationships of the metamorphic rocks in southeastern New York: Am. Jour. Sci., v. 254, p. 672–684.
- Rodgers, John, Gates, R. M., and Rosenfeld, J. L., 1959, Explanatory text for preliminary geological map of Connecticut, 1956: Connecticut Geol. and Nat. Hist. Survey Bull. 84, 64 p.
- Sclar, C. B., 1958, The Preston Gabbro and the associated metamorphic gneisses, New London County, Connecticut: Connecticut Geol. and Nat. Hist. Survey Bull. 88, 136 p.
- Scotford, D. M., 1956, Metamorphism and axial-plane folding in the Poundridge area, New York: Geol. Soc. America Bull., v. 67, p. 1155–1198.
- Seaber, P. R., and Vecchioli, John, 1963, Stratigraphic section at Island Beach State Park, New Jersey: Art. 26 in U.S. Geol. Survey Prof. Paper 475-B, p. B102–B105.
- Sriramadas, Aluru, 1957, Diagrams for the correlation of unit cell edges and refractive indices with the chemical composition of garnet: Am. Mineralogist, v. 42, p. 294–298.
- Tilton, G. R., Wetherill, G. W., Davis, G. L., and Hopson, C. A., 1958, Ages of minerals from the Baltimore Gneiss near Baltimore, Maryland: Geol. Soc. America Bull., v. 69, p. 1469–1474.
- Tilton, G. R., Davis, G. L., and Wetherill, G. W., 1959, Mineral ages in the Maryland Piedmont: Carnegie Inst. Washington Year Book 58, p. 171–174.
- Turner, F. J., 1947, Determination of plagioclase with the four-axis universal stage: Am. Mineralogist, v. 32, p. 389–410.



## OFFSHORE EXTENSION OF THE UPPER EOCENE TO RECENT STRATIGRAPHIC SEQUENCE IN SOUTHEASTERN GEORGIA

By MORRIS J. McCOLLUM and STEPHEN M. HERRICK, Atlanta, Ga.

*Work done in cooperation with the Georgia Department of Mines, Mining, and Geology*

**Abstract.**—Strata ranging in age from Recent to late Eocene were penetrated in test holes drilled 10 miles offshore from Savannah Beach, Ga. Study of the rock cores and cuttings reveals that the stratigraphic sequence is similar to that onshore but that the post-Miocene section is thinner.

During the summer of 1962, two test holes were drilled for the U.S. Coast Guard into the sediments beneath the ocean floor at lat  $31^{\circ}56'53\frac{1}{2}''$  N. and long  $80^{\circ}41'00''$  W., about 10 miles offshore from Savannah Beach, Ga. Rock cores and cuttings obtained by drilling were analyzed<sup>1</sup> to determine significant engineering properties for foundation design of a proposed "Texas-type" tower to replace the Savannah lightship. Samples from the borings were made available to the authors for geologic study, and as a result, the upper Eocene to Recent stratigraphic section has been extended offshore as far as the drilling site.

Previous to the test drilling, hydrographic and seismic surveys were made from Savannah Beach to, and in the vicinity of, the proposed tower site.<sup>2</sup> Both surveys were made simultaneously from a boat by means of a fathometer and sonar boomer. An electronic positioning apparatus was used to obtain horizontal control, and U.S. Coast Guard tide gages were used for vertical control.

The hydrographic survey showed that the ocean floor in the vicinity of the proposed tower site is from 49 to 55 feet below mean sea level. According to the seismic interpretation, in the area of the proposed tower site there is a north-trending linear zone of slight structural

disturbance and possible faulting. Although the seismic data were interpreted to indicate a small reef or shell bed in the sediments of late Miocene age, corroborative evidence for such was not observed in the samples from the offshore test holes. Correlated with pertinent information from a U.S. Geological Survey test hole (GGS 772, fig. 1), the seismic data indicate that the top of the lower Miocene limestone is an unconformity and is about 105 feet below sea level at the proposed tower site.

The geologic section on figure 1 shows the relation of the upper Eocene to Recent stratigraphic units in Chatham County, Ga., to those penetrated 10 miles offshore. The section extends southeasterly from a point about 7 miles northwest of Savannah, Ga., through Savannah and Savannah Beach to the proposed site of the tower. The onshore part of the section was modified from McCollum and Counts (1964). The indicated correlations are based principally on lithologic and paleontologic evidence supplemented by electric and gamma-ray logs. The fossils listed on the section are Foraminifera, and only selected guide species are shown.

Although all the onshore test holes were drilled through the Ocala Limestone, only the uppermost part of this stratigraphic unit was penetrated in the offshore hole (fig. 1). The Ocala, which consists of gray to buff fossiliferous limestone, is the source of most of the ground water pumped in the area. Its average thickness in Chatham County is about 400 feet.

Overlying the Ocala Limestone are undifferentiated rocks of Oligocene age. They consist predominantly of fossiliferous limestone inland but grade laterally to sandy limestone near the coast and to limy sand at the offshore site.

The sediments of Miocene age have been divided into three lithologic units. The lower Miocene sediments

<sup>1</sup> Walter E. Hanson and Co., 1962, Foundation engineering report for U.S. Coast Guard offshore structure, Savannah, Georgia: Springfield, Ill., unpub. rept.

<sup>2</sup> Norman Porter and Associates, 1962, Hydrographic and geological surveys for offshore structure project, Savannah, Georgia: New York, unpub. rept.

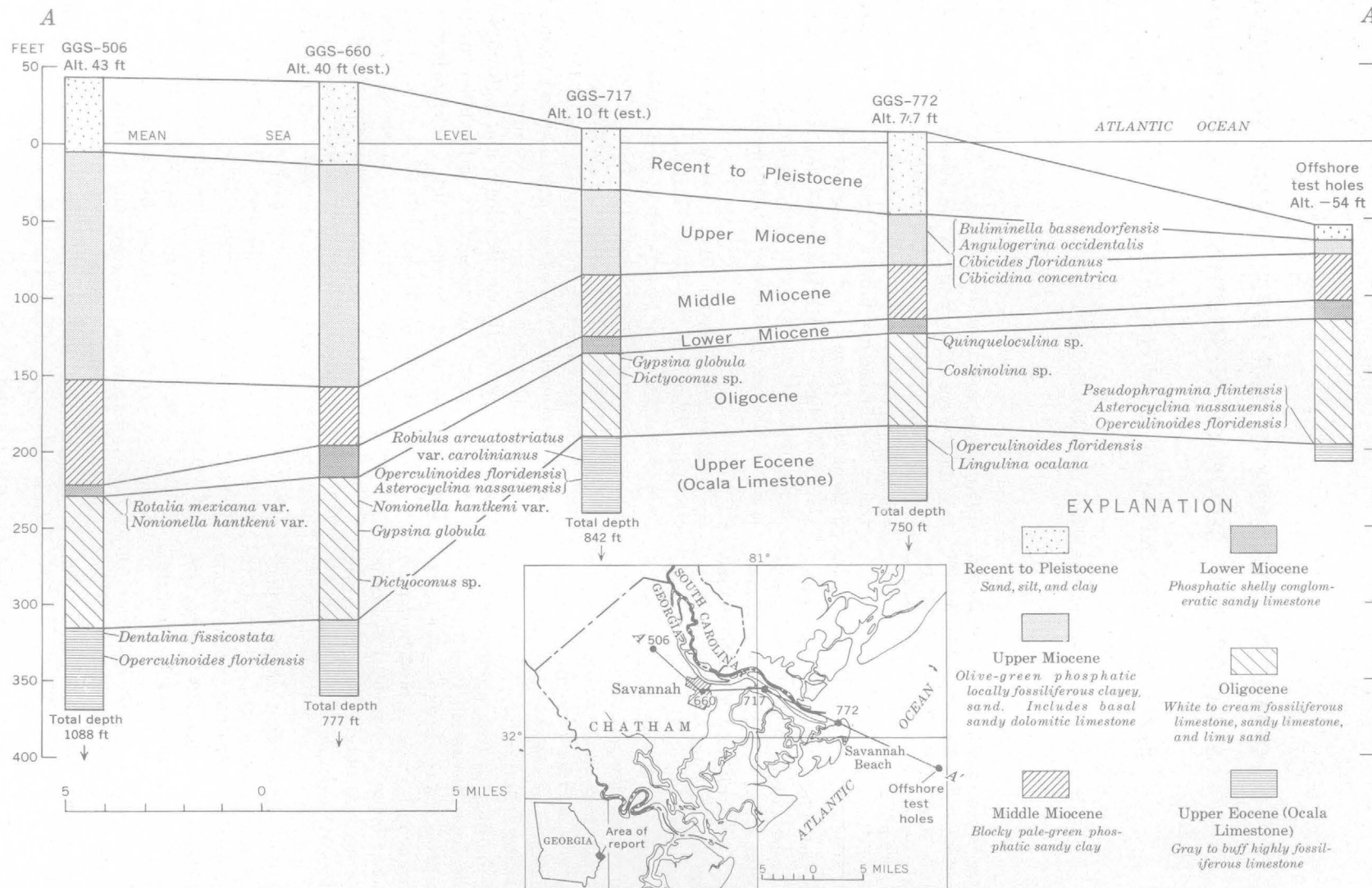


FIGURE 1.—Geologic section showing upper Eocene to Recent stratigraphic sequence in Chatham County, Ga., and 10 miles offshore.

consist of fossiliferous phosphatic conglomeratic sandy limestone. Unconformably overlying this limestone are middle Miocene sediments consisting of pale-green phosphatic sandy clay and clayey sand which are characteristically mottled because of isolated inclusions of clay. Separating the middle Miocene sand and clay from the upper Miocene sand and clay is a 1- to 2-foot layer of sandy dolomitic limestone which is considered to be a part of the upper Miocene sediments. The upper Miocene sandy clay and clayey sand are similar to those of the middle Miocene but generally are less consolidated and are not mottled. Foraminifera were found in upper Miocene sediments in test hole GGS 772, but none were found farther inland. No Foraminifera were found in Miocene deposits in the offshore test holes, probably because so little of the upper Miocene is present.

The post-Miocene sediments consist of terrace deposits (Pleistocene) composed mostly of sand, marsh deposits (Recent), and sandy barrier-island deposits underlain by sand of Pleistocene age, and of thin fossiliferous sand deposits offshore, which probably are of Recent age.

The top of the limestone (top of lower Miocene) dips

from east to west along the section; the dip is steepest between test holes GGS 717 and GGS 660, where it averages about 10 feet per mile. A contour map of the top of the limestone in the Savannah area (McCollum and Counts 1964), indicates a structural trough trending parallel to the coast and plunging to the south. The axis of the trough is approximately at GGS 506. A parallel high is shown on the structure-contour map east of the trough. The differences in the thickness of the recognized stratigraphic units in GGS 717 and GGS 660 indicate that downwarping of the trough may have begun in the Oligocene (or possibly even earlier) but that the principal downwarping occurred during the late Miocene. Other crustal movements are suggested by the landward dip of some and the seaward dip of other correlation lines between GGS 772 and the offshore test holes.

#### REFERENCE

McCollum, M. J., and Counts, H. B., 1964, Relation of salt-water encroachment to the major aquifer zones: U.S. Geol. Survey Water-Supply Paper 1613-D. [In press]



## UPPER EOCENE SMALLER FORAMINIFERA FROM SHELL BLUFF AND GRIFFIN LANDINGS, BURKE COUNTY, GEORGIA

By STEPHEN M. HERRICK, Atlanta, Ga.

*Work done in cooperation with the Georgia Department of Mines, Mining, and Geology*

**Abstract.**—Identification of microfossils from equivalent zones at Shell Bluff Landing and Griffin Landing, Ga., reveals lithologic and microfaunal differences that are explained through normal facies change. The Foraminifera are of late Eocene age and indicate that the fossil-bearing stratum correlates with the Moodys Branch Formation of Mississippi and Alabama and the lower Barnwell Formation of Georgia.

A bed containing abundant *Ostrea gigantissima* Finch is exposed along the west side of the Savannah River at Shell Bluff Landing and Griffin Landing, Burke County, Ga. (fig. 1). The small Foraminifera from this zone at Shell Bluff Landing have been described and figured by the author (Herrick, 1960). Samples were collected in 1963 from the equivalent bed at Griffin Landing, and the species found at both localities are listed in this article.

The oyster-bearing bed at Shell Bluff Landing, bed 6 of Cooke (1943, p. 57), consists of rather dense, indurated sand or very sandy and much leached limestone. A total of 11 genera and 20 species of Foraminifera were identified from this locality. The equivalent bed at Griffin Landing, bed 3 of Veatch and Stephenson (1911), consists of sandy calcareous clay or marl. Here the microfauna is much richer than at Shell Bluff Landing and includes 26 genera and 51 species of Foraminifera. The species identified and their relative abundance at both localities are indicated in the accompanying table.

In view of the fact that Shell Bluff Landing and Griffin Landing are only 10 miles apart ( $12\frac{1}{2}$  miles by river), the differences in the lithologies and microfaunas at the two localities are somewhat surprising. The known regional geologic picture for this part of Georgia indicates that when this oyster-bearing bed was deposited the shoreline trended northeast and was some-

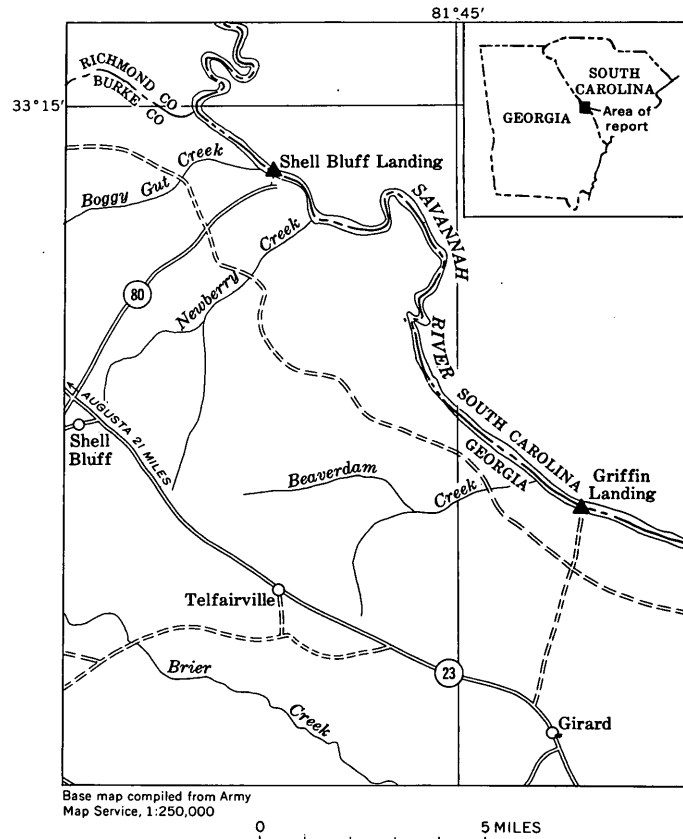


FIGURE 1.—Index map showing location of Shell Bluff Landing and Griffin Landing, Ga.

what northwest of the two fossil localities. Because Shell Bluff Landing is nearer the postulated shoreline, it seems reasonable to assume that at that site the depth of water was less and the average grain size of the sediments deposited was greater than at the Griffin Landing site. Apparently the ecological conditions

*Distribution and relative abundance of Foraminifera at Shell Bluff Landing and Griffin Landing, Burke County, Ga.*  
 [A, abundant; C, common; F, frequent; R, rare]

Foraminifera	Griffin Landing	Shell Bluff Landing (Herrick, 1960)
<i>Spiroplectammina mississippiensis</i>	R	-----
<i>Textularia cuyleri</i>	F	-----
<i>Planularia</i> sp. cf. <i>P. georgiana</i>	R	-----
<i>Marginulina triangularis</i>	-----	R
<i>Dentalina</i> sp. cf. <i>D. nasuta</i>	R	-----
<i>Guttulina lactea</i>	C	-----
sp. cf. <i>G. caudata</i>	R	-----
<i>irregularis</i>	-----	R
<i>Globulina minuta</i>	R	-----
<i>gibba</i>	-----	F
<i>Pyrulina albatrossi</i>	R	-----
<i>Pseudopolymorphina decora</i>	R	-----
<i>Sigmomorphina semitecta</i> var. <i>terquemiana</i>	C	F
<i>undulosa</i>	F	-----
<i>williamsoni</i>	-----	C
<i>Nonion advena</i>	A	-----
<i>inexcavatum</i>	A	-----
<i>planatum</i>	F	-----
<i>danvillensis</i>	C	-----
<i>micrum</i>	F	-----
<i>Nonionella jacksonensis</i> var. <i>compressa</i>	C	-----
<i>Elphidium texanum</i>	C	C
<i>Buliminella elegantissima</i>	R	-----
robertsi	R	-----
<i>Virgulina dibollensis</i>	R	-----
<i>zetina</i>	R	-----
<i>Bolivina spiralis</i>	C	-----
<i>jacksonensis</i> var. <i>striatella</i>	C	-----
<i>gracilis</i> ?	R	-----
<i>plicatella</i> ? var.	R	-----
<i>broussardi</i>	F	-----
<i>taylori</i>	F	-----
<i>Reussella eocena</i>	F	-----
<i>byramensis</i> ?	R	-----
<i>Angulogerina cooperensis</i>	A	-----
<i>vicksburgensis</i>	F	-----
<i>Spirillina vivipara</i>	R	-----
<i>Patellina advena</i>	R	-----
<i>Discorbis hemisphaerica</i>	F	R
<i>assulata</i>	C	-----
<i>alveata</i>	C	-----
<i>cocoaensis</i>	F	-----
<i>Valvularia jacksonensis</i>	A	-----
<i>texana</i>	R	-----
<i>Eponides</i> sp. cf. <i>E. cocoaensis</i>	R	-----
<i>jacksonensis</i> ?	R	-----
<i>Alabamina obtusa</i>	F	-----
<i>Globigerina ochitaeensis</i>	R	-----
<i>Anomalina jacksonensis</i> var. <i>texana</i>	C	-----
<i>granosa</i> var. <i>dibollensis</i>	R	-----
<i>Planulina cocoaensis</i>	R	-----
<i>Cibicides pseudoungerianus</i>	R	R
<i>lobatus</i> var.	C	-----
<i>mississippiensis</i>	R	-----
<i>americanus</i>	A	C
<i>americanus</i> var. <i>antiquus</i>	C	C
<i>danvillensis</i>	A	-----
<i>planococonvexus</i> <sup>1</sup>	A	C

<sup>1</sup> Previously identified as *Cibicides* cf. *refulgens* by Herrick (1960, p. 126).

were favorable for the large oysters at both localities, but the conditions at the Griffin Landing site were more favorable for the Foraminifera, a supposition suggested by the much more abundant microfauna identified from the latter site.

The large oyster, *Ostrea gigantissima* Finch, as noted

by Howe (1937, p. 362) and others, and the smaller Foraminifera constitute evidence for assigning a late Eocene age to the oyster-bearing bed at Shell Bluff Landing and Griffin Landing. Although no single diagnostic foraminiferal species was identified from Shell Bluff Landing the total microfauna found at this site was considered by Herrick (1960, p. 119) to be "not older than late Eocene . . . and possibly younger. . . ." The abundant foraminiferal fauna found at Griffin Landing constitutes strong additional evidence in support of a late Eocene age for the faunas at both these rather famous fossil localities.

The presence of an appreciable number of identical species permits correlation of these microfaunas with those reported from the type Moodys Branch Formation of Mississippi (Moodys Marl of former usage) (Cushman and Todd, 1945). Such species include *Guttulina irregularis*, *Globulina gibba*, *G. minuta*, *Sigmomorphina semitecta* var. *terquemiana*, *Nonion advena*, *N. inexcavatum*, *N. planatum*, *N. danvillensis*, *Nonionella jacksonensis* var. *compressa*, *Buliminella robertsi*, *Virgulina dibollensis*, *Bolivina jacksonensis* var. *striatella*, *B. gracilis*, *B. taylori*, *Reussella eocena*, *Angulogerina cooperensis*, *Discorbis hemisphaerica*, *D. assulata*, *D. alveata*, *Alabamina obtusa*, *Cibicides lobatulus*, *C. americanus* var. *antiquus*, and *C. planococonvexus*. Furthermore, the microfaunas from Shell Bluff Landing and Griffin Landing have several species in common with the Foraminifera from the Twiggs Clay Member of the Barnwell Formation in Houston County, Ga. (Herrick, 1944). Species occurring at Shell Bluff Landing or Griffin Landing and in the Twiggs Clay in Houston County include *Spiroplectammina mississippiensis* var., *Guttulina irregularis*, *Nonion advena*, *N. micrum*, *Buliminella elegantissima*, *Virgulina dibollensis*, *Bolivina gracilis*, *Angulogerina cooperensis*, *Discorbis assulata*, *D. alveata*, *Valvularia jacksonensis*, *Planulina cocoaensis*, and *Cibicides mississippiensis*.

#### REFERENCES

- Cooke, C. W., 1943, Geology of the Coastal Plain of Georgia: U.S. Geol. Survey Bull. 941, 121 p. [1944].  
 Cushman, J. A., and Todd, Ruth, 1945, Foraminifera of the type locality of the Moodys Marl Member of the Jackson Formation of Mississippi: Cushman Lab. Foraminiferal Research Contr., v. 21, pt. 4, p. 79-105, pls. 13-16.  
 Herrick, S. M., 1944, Southwestern Georgia field trip: Southeastern Geol. Soc. Guidebook 2d Field Trip, p. 47-48.  
 —— 1960, Small Foraminifera from Shell Bluff, Georgia: Bull. Am. Paleontology, v. 41, no. 187, p. 117-130, pls. 14-16.  
 Howe, H. V., 1937, Large oysters from the Gulf Coast Tertiary: Jour. Paleontology, v. 11, no. 4, p. 355-366, pl. 44.  
 Veatch, Otto, and Stephenson, L. W., 1911, Geology of the Coastal Plain of Georgia: Georgia Geol. Survey Bull. 26, 466 p.



## POST-PALEOCENE WEST ELK LACCOLITHIC CLUSTER, WEST-CENTRAL COLORADO

By LARRY H. GODWIN and DAVID L. GASKILL,  
Denver, Colo.

**Abstract.**—The West Elk Mountains are in part formed of silicic intrusions of stocks, dikes, sills, and laccoliths which intrude nearly 2,000 feet of the Wasatch Formation (Eocene). In structure and composition the West Elk laccolithic cluster is similar to the Colorado Plateau laccolithic clusters.

The West Elk laccolithic intrusions occupy about 500 square miles in northwestern Gunnison County, Colo. (fig. 1). The cluster forms the northern part of the West Elk Mountains and is adjacent to the large stocks in the Elk Mountains. The laccoliths are grouped around a dike swarm along a north-northeast-trending fracture zone at least 25 miles long. The laccoliths are large, from about 8 to 40 square miles in extent. They are asymmetric and in part discordant; most have bulged on one side. Small stocks at the north end of the fracture zone and sills are associated with the laccolithic cluster. The entire complex of igneous rocks is probably peripheral to a large buried batholith to the east.

In the West Elk Mountains, stocks, dikes, sills, and at least seven laccoliths intrude the Wasatch Formation of Eocene age. On the steep south face of Marcellina Mountain, baked and indurated Wasatch beds in contact with the laccolith are well exposed. In the Ruby Range, stocks and large dikes cut through nearly 2,000 feet of the Wasatch Formation and metamorphose it to dense hornfels and quartzite. No fossils have been found in the Wasatch Formation in this area. Leaves from the Ohio Creek Formation, which lies below the Wasatch Formation, indicate that the Ohio Creek is Paleocene in age (Gaskill, 1961). The basal conglomeratic unit, about 500 feet thick, of the Wasatch Formation as mapped in the Ruby Range may correlate with the unnamed Paleocene unit of Donnell (1961, p. 844) to the northwest. The remainder of the Wasatch, as mapped, is early Eocene. Thus, the time of emplacement of the

West Elk intrusions is clearly post-Paleocene and most likely post-early Eocene.

The igneous rocks range from quartz diorite to granite; six chemical analyses are given in the accompanying table. Minerals that comprise both the phenocrysts and the groundmass are quartz, potassic feldspar, plagioclase, hornblende, biotite, and magnetite. These minerals form equigranular and porphyritic rocks. The porphyritic rocks are composed of medium- to coarse-grained phenocrysts in a microgranular, felted,

*Chemical analyses of some igneous rocks from the West Elk Mountains, Colo.*

[Rapid rock analyses by P. Elmore, S. Botts, G. Chloe, L. Artis, and H. Smith  
Samples were analyzed by methods described by Shapiro and Brannock (1962)]

Constituent	Sample					
	1	2	3	4	5	6
SiO <sub>2</sub> -----	62.2	64.3	65.2	65.4	60.7	66.3
Al <sub>2</sub> O <sub>3</sub> -----	15.5	16.2	16.5	15.7	17.1	16.3
Fe <sub>2</sub> O <sub>3</sub> -----	2.0	2.8	2.7	2.6	3.9	2.8
FeO-----	2.2	1.9	2.1	1.8	2.0	1.9
MgO-----	1.3	1.3	1.1	1.1	1.7	1.1
CaO-----	4.1	4.2	3.4	3.3	4.5	3.4
Na <sub>2</sub> O-----	3.1	3.1	3.7	3.8	3.6	3.4
K <sub>2</sub> O-----	2.8	3.2	3.2	3.2	3.0	3.0
H <sub>2</sub> O-----	.98	.39	.20	.42	1.1	.18
H <sub>2</sub> O+-----	2.3	1.4	.99	1.1	1.1	.96
TiO <sub>2</sub> -----	.41	.47	.48	.52	.71	.46
P <sub>2</sub> O <sub>5</sub> -----	.30	.33	.32	.31	.45	.32
MnO-----	.08	.11	.11	.10	.16	.10
CO <sub>2</sub> -----	2.6	<.05	.08	.64	<.05	.13
Total-----	100	100	100	100	100	100

1. Granodiorite porphyry, from Ruby Anthracite Canyon laccolith, NW $\frac{1}{4}$ NW $\frac{1}{4}$  sec. 26, T. 13 S., R. 88 W., 6th P.M.
2. Granodiorite porphyry, from Marcellina Mountain laccolith, NE $\frac{1}{4}$ NW $\frac{1}{4}$  sec. 5, T. 13 S., R. 88 W., 6th P.M.
3. Quartz monzonite porphyry, dike, NW $\frac{1}{4}$ NW $\frac{1}{4}$  sec. 30 (approx.), T. 13 S., R. 87 W., 6th P.M.
4. Quartz monzonite porphyry, dike, NW $\frac{1}{4}$ NE $\frac{1}{4}$  sec. 8 (approx.), T. 14 S., R. 87 W., 6th P.M.
5. Dacite porphyry, dike, SE $\frac{1}{4}$ SW $\frac{1}{4}$  sec. 30 (approx.), T. 13 S., R. 87 W., 6th P.M.
6. Granodiorite, Ruby Peak stock, SW $\frac{1}{4}$ NW $\frac{1}{4}$  sec. 9 (approx.), T. 13 S., R. 87 W., 6th P.M.

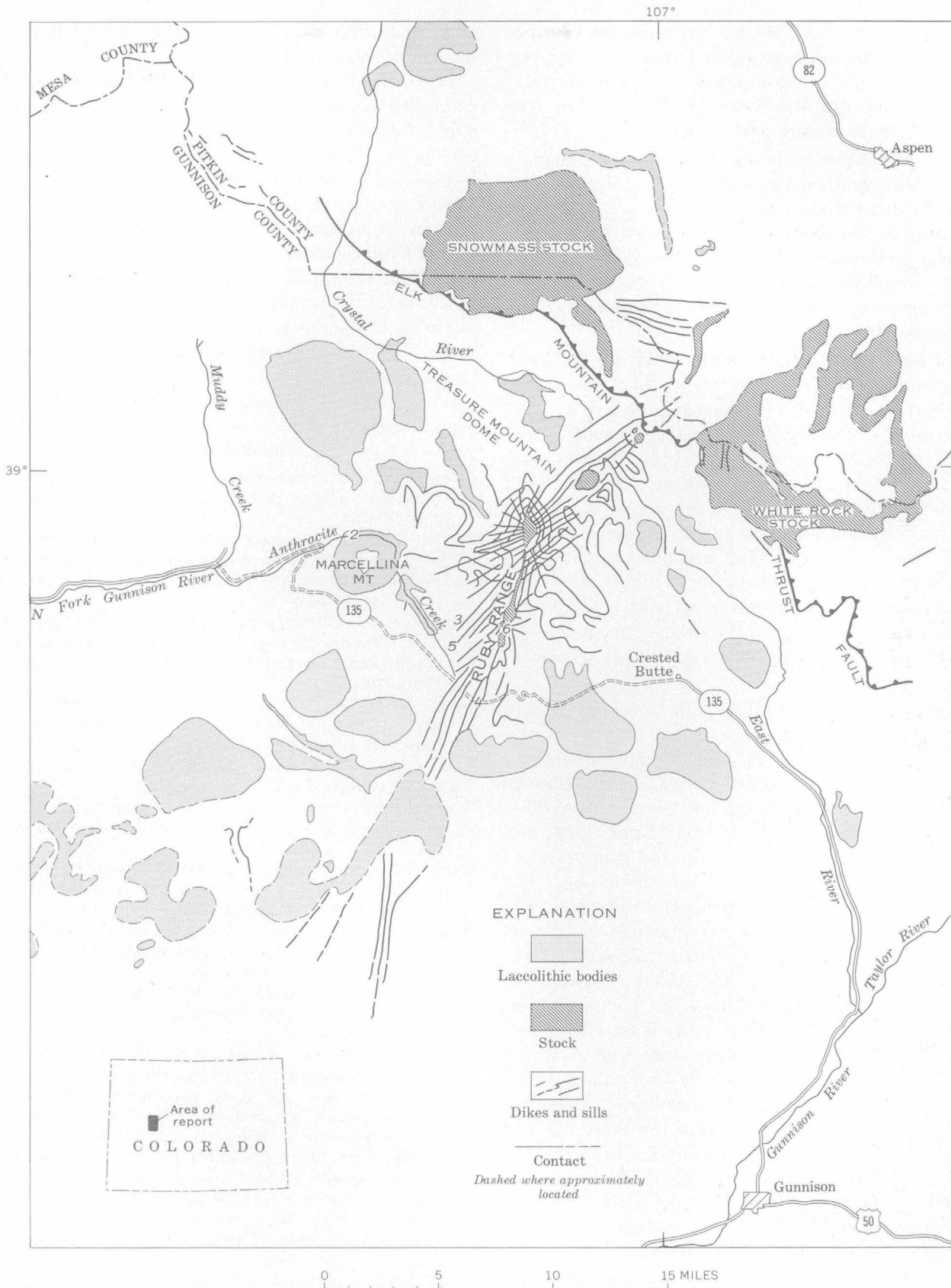


FIGURE 1.—Index map of the West Elk laccolithic cluster. Numbers refer to localities of analyzed intrusives described in table.

or graphic matrix. All the laccoliths are composed of porphyritic rocks; most are quartz monzonite porphyry. The stocks, which are composite, are predominantly medium-grained granitic rocks, but locally they may contain quartz monzonite porphyry.

A zone of contact metamorphism locally extends a mile from the small stocks, and mineralized zones containing lead-silver-zinc-gold deposits are associated with stocks in the Ruby Range. The extensive metamorphism and associated mineral deposits are missing near the laccoliths, where only narrow baked and indurated zones occur in the sedimentary rocks in contact with the laccoliths.

Structurally the northern part of West Elk Mountains is made up of primarily horizontal strata arched and broken by epizonal intrusions of stocks, sills, dikes, and laccoliths. The structural pattern is complicated by the Treasure Mountain dome and the Elk Mountain thrust fault at the north end of the mountains. Field relations indicate that the primary structure was caused by a virtually continuous intrusion of igneous rocks. The Elk Mountain thrust fault seems to antedate some of the laccolithic intrusions but is probably associated with the earlier phases of igneous activity. The Treasure Mountain dome apparently resulted from the emplacement of a pluton about the same time as the intrusion of the laccoliths.

Igneous rocks from the West Elk laccolithic cluster are similar in texture, color, and composition to specimens from the Colorado Plateau laccolithic clusters. Many of the igneous rocks from the Colorado Plateau laccolithic mountains have been described (Cross, 1894; Eckel, 1949; Hunt and others, 1953; Hunt, 1958; and Witkind, 1958), and they contain the same mineral assemblages observed in the West Elk Mountains. The chemical analyses of igneous rocks from the West Elk Mountains shown in the table also resemble analyses of rocks from laccolithic clusters of the Colorado Plateau (Witkind, 1958; Hunt and others, 1953). In addition to the similar rock compositions, the metamorphism and basically simple structure in the West Elk Mountains are similar to the metamorphism and structure in the laccolithic mountains of the Colorado Plateau. The strong resemblance suggests a similar environment.

Three notable differences between the West Elk and Colorado Plateau laccolithic mountains are: (1) the larger area of the West Elk cluster of laccoliths; (2) the generally larger size of many of the individual West Elk laccoliths; and (3) the general arrangement of the West Elk laccoliths adjacent to a central fracture zone intruded by small composite stocks. These differences

may reflect the stage of laccolithic intrusion and the amount of subsequent erosion.

The similarities of the West Elk laccolithic cluster and other laccolithic mountains of the Colorado Plateau might indicate a similar time of emplacement. Some geologists (Cross, 1894; Eckel, 1949; Hunt, 1956; Larsen and Cross, 1956; Shoemaker, 1956) have postulated a similar age of intrusion for all laccolithic mountains in the region. Of these workers, about half prefer a Late Cretaceous age and the others prefer a Tertiary age. The West Elk laccoliths intrude post-Paleocene rocks; thus, the postulated Tertiary age for laccolithic intrusion in the region (Cross, 1894; Larsen and Cross, 1956; Hunt, 1956) is supported. The postulated Late Cretaceous age of the intrusion (Eckel, 1949; Shoemaker, 1956) is denied, at least for the West Elk Mountains.

#### REFERENCES

- Cross, C. W., 1894, The laccolitic mountain groups of Colorado, Utah, and Arizona: U.S. Geol. Survey 14th Ann. Rept., pt. 2, p. 157-241.
- Donnell, J. R., 1961, Tertiary geology and oil-shale resources of the Piceance Creek basin between the Colorado and White Rivers, northwestern Colorado: U.S. Geol. Survey Bull. 1082-L, p. 835-891.
- Eckel, E. B., 1949, Geology and ore deposits of the La Plata district, Colorado, with sections by J. S. Williams, F. W. Galbraith, and others: U.S. Geol. Survey Prof. Paper 219, 179 p. [1950].
- Gaskill, D. L., 1961, Age of the Ohio Creek conglomerate, Gunnison County, Colorado: Art. 96 in U.S. Geol. Survey Prof. Paper 424-B, p. B230-B231.
- Hunt, C. B., 1956, Cenozoic geology of the Colorado Plateau: U.S. Geol. Survey Prof. Paper 279, 99 p.
- , 1958, Structural and igneous geology of the La Sal Mountains, Utah: U.S. Geol. Survey Prof. Paper 294-I, p. 305-364.
- Hunt, C. B., Averitt, Paul, and Miller, R. L., 1953, Geology and geography of the Henry Mountains region, Utah: U.S. Geol. Survey Prof. Paper 228, 234 p. [1954].
- Larsen, E. S., Jr., and Cross, C. W., 1956, Geology and petrology of the San Juan region, southwestern Colorado: U.S. Geol. Survey Prof. Paper 258, 303 p.
- Shapiro, Leonard, and Brannock, W. W., 1962, Rapid analysis of silicate, carbonate, and phosphate rocks: U.S. Geol. Survey Bull. 1144-A, 56 p.
- Shoemaker, E. M., 1956, Structural features of the central Colorado Plateau and their relation to uranium deposits, in Page, L. R., Stocking, H. E., and Smith, H. B., compilers, Contributions to the geology of uranium and thorium by the U.S. Geological Survey and Atomic Energy Commission for the United Nations International Conference on Peaceful Uses of Atomic Energy, Geneva, Switzerland, 1955: U.S. Geol. Survey Prof. Paper 300, p. 155-170.
- Witkind, I. J., 1958, The Abajo Mountains, San Juan County, Utah, in Intermountain Assoc. Petroleum Geologists Guidebook, 9th Ann. Field Conf., Guidebook to the geology of the Paradox Basin (Colorado Plateau), 1958: p. 60-65.



## CHEMISTRY OF GREENSTONE OF THE CATOCTIN FORMATION IN THE BLUE RIDGE OF CENTRAL VIRGINIA

By JOHN C. REED, JR., Denver, Colo.

**Abstract.**—Four analyses of greenstone from the Blue Ridge outcrop belt of the Catoctin Formation indicate that the greenstone may have been derived from tholeiitic basalt, but that it has  $\text{Na}_2\text{O}/\text{K}_2\text{O}$  ratios characteristic of spilite. The spilitic character is probably the result of low-grade regional metamorphism rather than submarine eruption.

The Catoctin Formation is a sequence of interlayered metavolcanic and metasedimentary rocks of late Precambrian(?) age that underlies sedimentary rocks of Early Cambrian(?) age in the Blue Ridge anticlinorium in Virginia (fig. 1) and the Catoctin Mountain anticlinorium in Maryland and southern Pennsylvania. In the Blue Ridge, which forms the northwestern flank of the anticlinorium in Virginia, the volcanic rocks rest unconformably on plutonic basement rocks of Precambrian age, or are separated from them by a thin unit of locally derived sedimentary rocks. On the southeast flank of the anticlinorium in central Virginia the Catoctin Formation is interlayered with, and underlain by, metasedimentary rocks of late Precambrian(?) age.

The volcanic rocks of the Catoctin Formation in Virginia are predominately metabasalt, although Keith (1894), Bloomer and Bloomer (1947), and Bloomer and Werner (1955) also report some metandesite. In Maryland and southern Pennsylvania, felsic volcanic rocks are widespread in the formation.

The metabasalt of the Catoctin Formation is greenstone and greenschist, consisting typically of albite, chlorite, actinolite, epidote, magnetite, and smaller amounts of sphene, leucoxene, and calcite. Relict grains of pyroxene (both augite and pigeonite) and grains of calcic plagioclase partially replaced by albite occur locally in the flows and in greenstone dikes that cut plutonic basement rocks and apparently fed the Catoctin flows (Bloomer and Werner, 1955; Reed, 1955). On the southeast flank of the Blue Ridge anticlinorium the volcanic rocks are locally amphibolite

containing oligoclase, biotite, and hornblende (Brown, 1958).

The greenstone commonly displays well-preserved volcanic textures (Nickelsen, 1956; Bloomer and Werner, 1955; Reed, 1955). Amygdules are abundant and generally are filled with epidote, quartz, albite, or chlorite. Columnar joints are preserved locally in several places in the outcrop belt on the northwestern flank of the Blue Ridge anticlinorium (Reed, 1955; Furcron, 1934), and are reported by Nelson (1962) in one area near Charlottesville on the southeastern limb of the anticlinorium. Pillow structure has nowhere been reported.

Pods and knots of fine-grained epidote-quartz rock are widespread in the greenstone, and veins of epidote and quartz are locally abundant. Many of the pods and knots apparently formed by replacement of greenstone without important changes in volume, for they commonly display gradational contacts, and contain amygdules and relicts of the original basaltic fabric preserved by the quartz-epidote mosaic (Reed, 1955).

Bloomer and Bloomer (1947) inferred that the greenstone of the Catoctin Formation in central Virginia is a "plateau andesite" altered to propylite by deuterio hydrothermal solutions. Later, Bloomer (1950) and Bloomer and Werner (1955) suggested that the Catoctin greenstone is a spilite because of its mineralogy and chemical composition. Brown (1958) agrees with this interpretation, at least for the greenstone that he studied on the southeast flank of the Blue Ridge anticlinorium in the Lynchburg area. He points out that there the greenstone of the Catoctin Formation is interlayered with geosynclinal sedimentary rocks, presumably marine, and is associated with ultramafic rocks and with quartzite that he suggests may be metamorphosed radiolarian chert.

Reed (1955) concluded that the greenstone of the Catoctin Formation in the Luray area, on the northwest flank of the anticlinorium, is a subaerially extruded

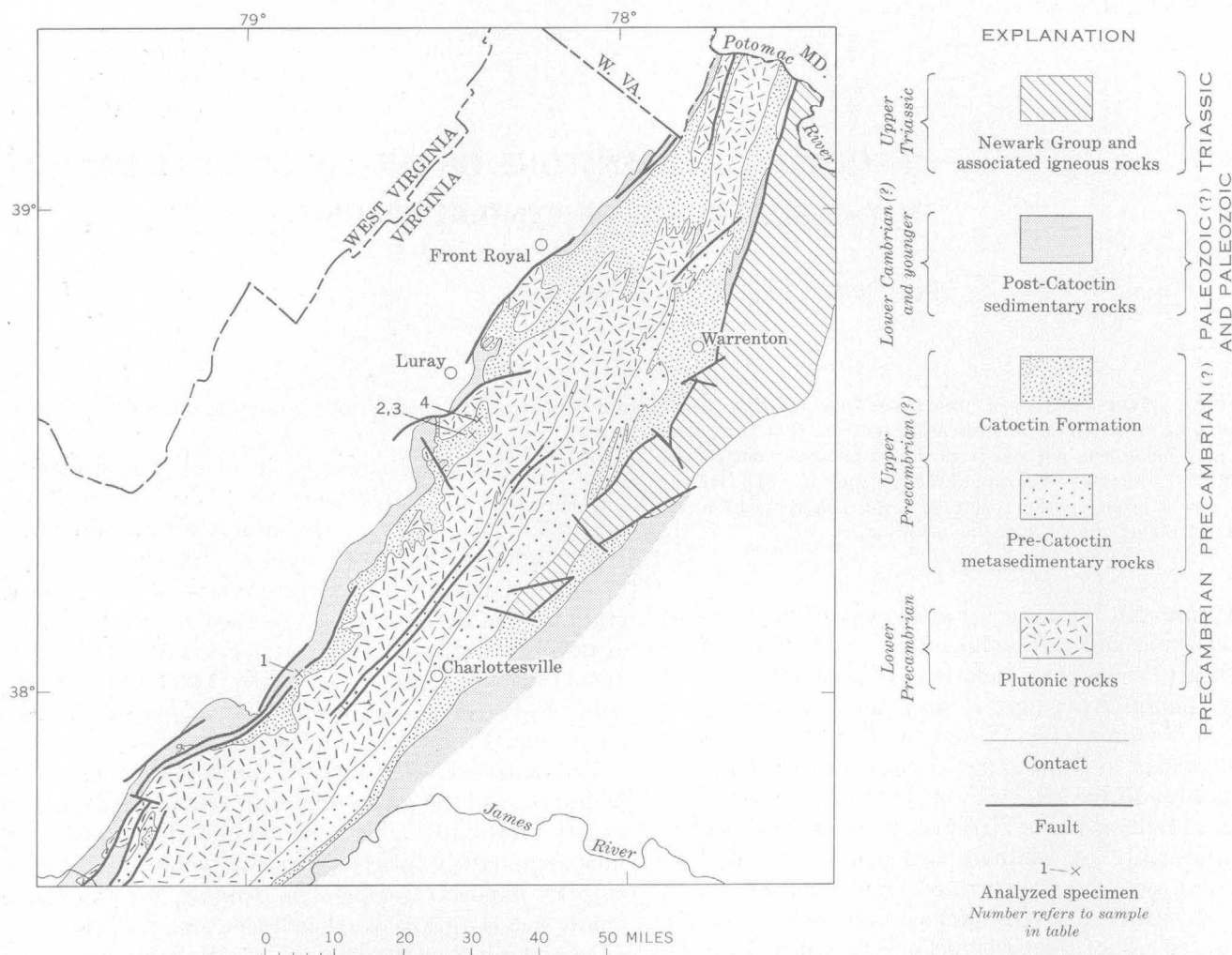


FIGURE 1.—Geologic map of the Blue Ridge anticlinorium in Virginia, showing sources of analyzed rocks (1, 2, 3, 4). Generalized from geologic map of Virginia (Virginia Division of Mineral Resources, 1963).

tholeiitic basalt regionally metamorphosed under low-grade conditions. He cites the areal extent of individual flows, thinness of breccia zones between flows, presence of columnar jointing, and absence of pillow structure as evidence for subaerial eruption. He believed that the original lava was a tholeiitic basalt because of the widespread preservation of intersertal or intergranular textures, and the occurrence of relict augite and pigeonite in the greenstone and relict labradorite in feeder dikes.

Bloomer and Werner (1955) and Reed (1955) cite previously published chemical analyses in support of their respective conclusions, but no modern chemical

analyses of greenstone from the Catoctin Formation in Virginia were available to them. The purpose of this article is to present four new analyses of Catoctin greenstone, and to discuss briefly their bearing on the interpretation of the origin of the greenstone. One of the analyzed specimens is from the area studied by Bloomer and Werner (1955), and three are from the area studied by Reed (1955) (fig. 1). The analyses are presented in the accompanying table. Uncertainties in the minor-element analyses are large, but the data are included for comparison with the minor-element analyses published by Bloomer and Bloomer (1947).

*Composition of four samples of greenstone from the Catoctin Formation in Virginia*

[Major oxides by standard rock analysis, Christel L. Parker, analyst; minor elements by semiquantitative spectrographic analysis, J. C. Hamilton, analyst]

Constituent	Sample				
	1	2	3	4	Average of 1-4
<b>Major oxides (in weight percent)</b>					
SiO <sub>2</sub> -----	45.27	48.91	46.00	48.08	47.1
Al <sub>2</sub> O <sub>3</sub> -----	14.38	14.86	14.86	14.08	14.5
Fe <sub>2</sub> O <sub>3</sub> -----	6.55	6.53	6.52	3.13	5.7
FeO-----	8.28	6.84	9.05	7.58	7.9
MgO-----	6.00	5.70	6.91	5.83	6.1
CaO-----	5.95	6.35	4.87	9.01	6.5
Na <sub>2</sub> O-----	4.58	4.45	4.57	3.90	4.4
K <sub>2</sub> O-----	.55	.63	.12	.88	.5
H <sub>2</sub> O+-----	3.24	2.89	3.81	2.93	3.2
H <sub>2</sub> O-----	.13	.11	.12	.09	.1
TiO <sub>2</sub> -----	4.09	2.27	2.63	1.97	2.7
P <sub>2</sub> O <sub>5</sub> -----	.56	.26	.31	.20	.3
MnO-----	.33	.22	.26	.20	.25
CO <sub>2</sub> -----	.09	.03	.02	2.18	.6
Cl-----	.01	.01	.01	.00	.01
F-----	.07	.04	.04	.05	.05
Subtotal-----	100.08	100.10	100.10	100.11	
Less O-----	.03	.02	.02	.02	
Total-----	100.05	100.08	100.08	100.09	
<b>Minor elements (in weight percent)<sup>1</sup></b>					
Ba-----	0.03	0.05	0.01	0.05	
Be-----	.0001	0	0	0	
Co-----	.005	.005	.005	.005	
Cr-----	.007	.015	.005	.015	
Cu-----	.0005	.015	.02	.007	
Ga-----	.003	.002	.003	.003	
La-----	.003	0	0	0	
Nb-----	0	0	.001	0	
Ni-----	.005	.005	.005	.007	
Sc-----	.003	.005	.005	.005	
Sr-----	.05	.015	.01	.02	
V-----	.07	.05	.05	.05	
Y-----	.005	.005	.005	.003	
Zr-----	.015	.01	.01	.007	
<b>Minerals (visually estimated volume percent)</b>					
Albite-----	35	40	40	35	
Chlorite-----	35	20	30	25	
Epidote-----	5	10	<1	15	
Actinolite-----	5	-	<1	10	
Pyroxene-----	<1	20	20	-	
Magnetite-----	10	5	5	5	
Sphene and leucoxene-----	10	5	5	5	
Carbonate-----	<1	-	-	5	

<sup>1</sup> Results are reported in percent to the nearest number in the series 1, 0.7, 0.5, 0.3, 0.2, 0.15, and 0.1, etc., which represent approximate midpoints of group data on a geometric scale. The assigned group for semiquantitative results will include the quantitative value about 30 percent of the time. Elements looked for and not detected: Ag, As, Au, B, Bi, Cd, Ce, Ge, Nf, Ng, In, Li, Mo, Pd, Pt, Re, Sb, Sn, Ta, Te, Th, Tl, U, W, Zn, Pr, Nd, Sm, Eu.

1. Fine-grained schistose greenstone containing ragged laths of cloudy albite as much as 0.5 mm long and a few grains of partly chloritized pyroxene in a felted mosaic of chlorite, actinolite, epidote, magnetite, sphene, and carbonate. Plagioclase is finely twinned and some is faintly zoned. A faint relict texture is preserved. Cleavage is defined by alinement of albite laths, actinolite, and chlorite and magnetite aggregates. The rock is cut by a few irregular veinlets of coarse epidote and carbonate. Collected from roadcut on east side of U.S. Highway 250, 0.3 mile north of interchange with the Blue Ridge Parkway in Rockfish Gap, Waynesboro quadrangle, Virginia. See Bloomer and Werner (1955, pl. 1), and Dietrich and Lowry (1955, p. 35). Field No. 63 SNP-1; USGS Lab. No. D 100118.
2. Massive porphyritic greenstone with well preserved relict intergranular texture consisting of albite laths 0.5 mm long and partly chloritized pyroxene about 0.25 mm in diameter in a matrix of chlorite, epidote, magnetite, and sphene. Scattered plagioclase phenocrysts (now albite) as much as 5 mm long. Collected from roadcut on east side of Skyline Drive, 0.75 mile S. 35° W. of summit of Hawksbill, Stony Man quadrangle, Virginia. See Reed (1955, pl. 1, and pl. 2, fig. 4). Field No. 63 SNP-2; USGS Lab. No. D 100119.
3. Massive greenstone with well-preserved relict intergranular texture consisting of albite laths 0.25 to 0.5 mm long and partly chloritized pyroxene in a matrix of chlorite, magnetite, sphene, and leucoxene. A few phenocrysts of plagioclase (now albite) as much as 2 mm long. Collected from roadcut on east side of Skyline Drive, about 200 feet south of sample 2. See Reed (1955, pl. 1). Field No. 63 SNP-3; USGS Lab. No. D 100120.
4. Fine-grained schistose greenstone displaying conspicuous columnar jointing. Felted microcrystalline mosaic of albite, chlorite, epidote, actinolite, carbonate, magnetite, sphene, and leucoxene, containing a few laths of albite and small grains of pyroxene, but displaying no relict texture. Cliff on east side of the Appalachian Trail 0.15 mile northeast of Hawksbill Gap, Stony Man quadrangle, Virginia. See Reed (1955, pl. 1). Field No. 63 SNP-4; USGS Lab. No. D 100121.

The variation diagrams on figure 2 compare the analyzed Catoctin greenstone with published analyses of unmetamorphosed basalt and with average compositions of tholeiitic basalt, olivine basalt, and theoleiitic andesite given by Nockolds (1954). The tholeiitic basalt of the Columbia Plateau is chosen for comparison because its field relations and petrography are similar to those inferred for the Catoctin lavas in the Luray, Va., area (Reed, 1955), and because modern analyses illustrating the range of variation within geographic and stratigraphic subdivisions are available (Waters, 1961; Hamilton, 1963). The proportions of silica, alumina, magnesia, and potash in the Catoctin greenstone are in the same range as in the Columbia River Basalt and most closely resemble those of the Picture Gorge flows of Waters (1961). The content of titania and total iron oxides is higher in some of the Catoctin analyses, but the most striking differences are the consistently higher proportion of soda and consistently lower proportion of

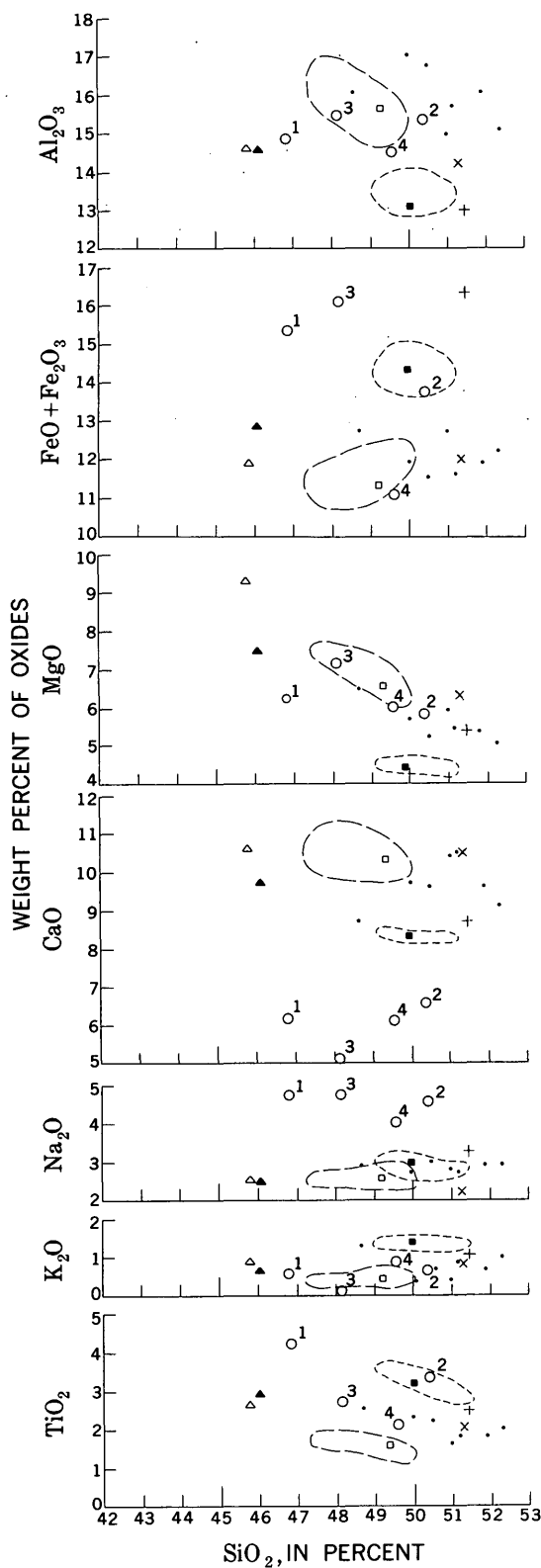


FIGURE 2.—Variation diagrams showing the weight percentage of oxides in greenstone of the Catoctin Formation compared with the percentage in unmetamorphosed basalt. Analyses recalculated free of  $\text{CaCO}_3$  and volatile material.

lime in the Catoctin greenstone. The wide range in composition among the basalts of the Columbia Plateau shows that comparison of a small number of analyses with worldwide averages such as those of Nockolds (1954) is probably inconclusive. The general chemical similarities between the analyzed greenstone and basalt of the Columbia Plateau is consistent with the conclusion that the greenstone is derived from tholeiitic basalt, as was suggested by Reed (1954) on the basis of field and petrographic evidence. However, the chemical data are insufficient to conclusively distinguish them from olivine basalt or tholeiitic andesite, especially in view of the lack of knowledge of possible changes in bulk composition during metamorphism. The  $\text{Na}_2\text{O}/\text{CaO}$  ratios of the analyzed Catoctin greenstone are very different from those of normal basalt or andesite and show that chemically the greenstone is spilite, as first suggested by Bloomer (1950).

The spilitic character of the greenstone is evidently not a result of submarine eruption, because three of the analyses are from the area where Reed (1955) has shown that the flows were subaerial. Spilitization apparently is related to low-grade regional metamorphism, and may have resulted either from introduction of soda from an outside source, or from metamorphic segregation within the volcanic sequence during which soda was concentrated in the greenstone and lime segregated in the epidote pods, quartz-epidote veins, and amygdaloidal fillings.

#### EXPLANATION

- $\circ^1$  Greenstone of the Catoctin Formation  
(Number refers to sample in table)
- $+$  Average of 26 tholeiitic andesites (Nockolds, 1954)
- $\circ$  Columbia River Basalt from Riggins quadrangle, Idaho (Hamilton, 1963)
- $\triangle$  Average of 96 samples of olivine basalt (Nockolds, 1954)
- $\blacktriangle$  Average olivine basalt from the Snake River Plain (Waters, 1961)
- $\times$  Average of 137 samples of tholeiitic basalt (Nockolds, 1954)
- $\square$  Average and range of late Yakima and Ellensburg flows, Columbia River Basalt (Waters, 1961)
- $\square - \square$  Average and range of Picture Gorge flows, Columbia River Basalt (Waters, 1961)

## REFERENCES

- Bloomer, R. O., 1950, Late Pre-Cambrian or lower Cambrian formations in central Virginia: Am. Jour. Sci., v. 248, p. 753-783.
- Bloomer, R. O., and Bloomer, R. R., 1947, The Catoctin formation in central Virginia: Jour. Geology, v. 55, p. 94-106.
- Bloomer, R. O., and Werner, H. J., 1955, Geology of the Blue Ridge region in central Virginia: Geol. Soc. America Bull., v. 66, p. 579-606.
- Brown, W. R., 1958, Geology and mineral resources of the Lynchburg quadrangle, Virginia: Virginia Div. Mineral Resources Bull. 74, 99 p.
- Dietrich, R. V., and Lowry, W. D., 1955, Geological features along U.S. Routes 11, 29 and 250 in Virginia, pt. II, Washington, D.C., and Point of Rocks, Maryland, to Staunton, Virginia, *in* Russell, R. J., ed., Guides to southeastern geology: Geol. Soc. America, p. 29-42.
- Furcron, A. S., 1934, Igneous rocks of the Shenandoah National Park area: Jour. Geology, v. 42, p. 400-410.
- Hamilton, Warren, 1963, Columbia River Basalt in the Riggins quadrangle, western Idaho: U.S. Geol. Survey Bull. 1141-L, 37 p.
- Keith, Arthur, 1894, Geology of the Catoctin belt: U.S. Geol. Survey 14th Ann. Rept., pt. 2, p. 285-395.
- Nelson, W. A., 1962, Geology and mineral resources of Albemarle County: Virginia Div. Mineral Resources Bull. 77, 92 p.
- Nickelsen, R. P., 1956, Geology of the Blue Ridge near Harpers Ferry, West Virginia: Geol. Soc. America Bull., v. 67, p. 239-207.
- Nockolds, S. R., 1954, Average chemical compositions of some igneous rocks: Geol. Soc. America Bull., v. 65, p. 1007-1032.
- Reed, J. C., Jr., 1955, Catoctin formation near Luray, Virginia: Geol. Soc. America Bull., v. 66, p. 871-896.
- Virginia Division of Mineral Resources, 1963, Geologic map of Virginia: scale 1: 500,000.
- Waters, A. C., 1961, Stratigraphic and lithologic variations in the Columbia River Basalt: Am. Jour. Sci. v. 259, p. 583-611.



## OCCURRENCE AND ORIGIN OF LAUMONTITE IN CRETACEOUS SEDIMENTARY ROCKS IN WESTERN ALASKA

By J. M. HOARE, W. H. CONDON, and W. W. PATTON, JR.,  
Menlo Park, Calif.

**Abstract.**—Laumontitized sedimentary rocks of Cretaceous age which are easily recognized by their distinctive mottled or spotted appearance crop out over an area of at least 2,000 square miles in western Alaska. Most of the laumontite is thought to have formed diagenetically through the reaction of water rich in calcium carbonate with tuffaceous material of acid or intermediate composition.

In the course of regional mapping in western Alaska, laumontitized<sup>1</sup> sandstones have been mapped over an area of at least 2,000 square miles. This is probably the largest known occurrence of this calcic zeolite in North America. Deposits of similarly zeolitized sedimentary rocks of probable comparable size have been recognized in Russia (Zaporozhtseva, 1960). The zeolitized rocks discussed here form part of a thick sequence of clastic sedimentary rocks which were deposited in the Koyukuk geosyncline (fig. 1) in mid-Cretaceous (Albian and Cenomanian?) time.

Geophysical data indicate that the sedimentary section in the deeper parts of the geosyncline may be as much as 20,000 to 30,000 feet thick. The section consists of dark-gray, fine-, medium-, and some coarse-grained graywacke sandstones interbedded with equal or greater amounts of siltstone and shale. In the southwestern part of the geosyncline this thick sequence of rocks can be divided into three mappable lithologic units on the basis of whether the sandstones are calcareous, noncalcareous, or laumontitized (fig. 2). Most of the rocks mapped as calcareous effervesce freely when treated with cold dilute hydrochloric acid, but many rocks in the unit are noncalcareous or slightly calcareous. Conversely, the rocks mapped as noncalcareous include some rocks that are at least weakly calcareous. The laumon-

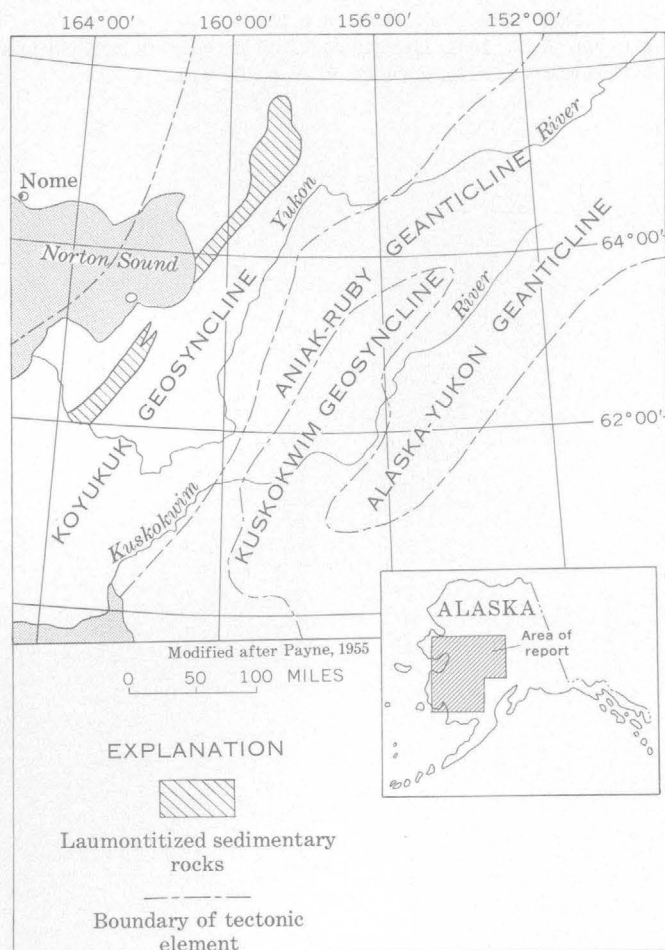


FIGURE 1.—Map showing occurrence of laumontitized sedimentary rocks in west-central Alaska.

tized unit contains an equal or greater amount of calcareous and noncalcareous sandstone that contains little or no laumontite. The thickness of the laumontitized strata cannot be determined accurately because the

<sup>1</sup> The ideal, alkali-free formula for laumontite is  $\text{Ca}_4\text{Al}_8\text{Si}_{16}\text{O}_{48} \cdot 16\text{H}_2\text{O}$  (Coombs, 1952, p. 825); however, it usually also contains some sodium and potassium.

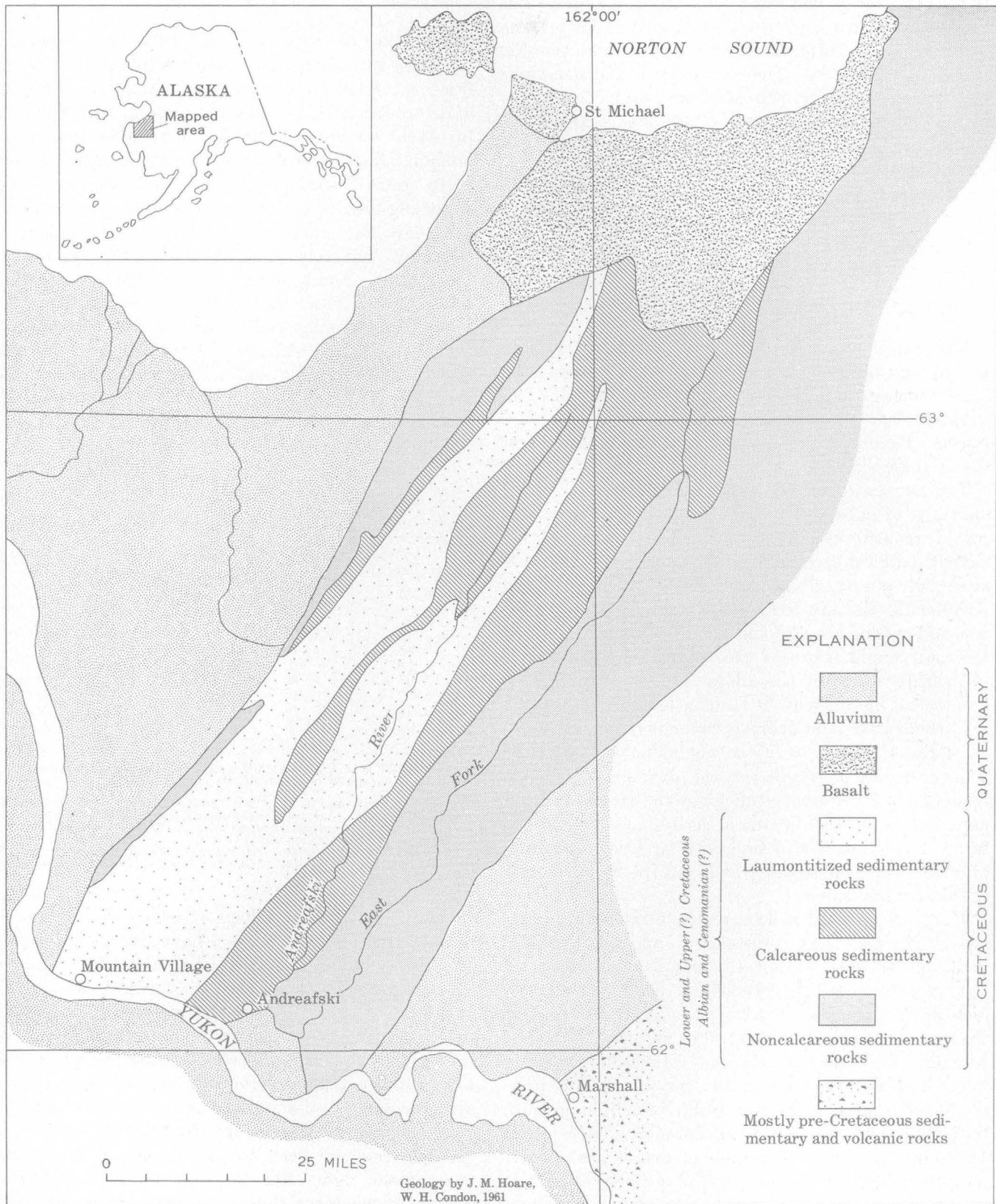


FIGURE 2.—Map showing distribution of laumontitized sedimentary rocks in the southwestern part of the Koyukuk geosyncline, western Alaska.

rocks are highly deformed and poorly exposed, but they probably are 2,000 to 5,000 feet thick. These three mappable units form northeast-trending belts parallel to the regional strike. The stratigraphic and structural relationships of these belts of strata are uncertain. In many places the laumontitized sandstones appear to overlie the calcareous sandstones. However, the intimate association of laumontitized and calcareous sandstones near the head of Andreafski River suggests that they may also in part grade into each other and that the laumontitized sandstones are at least locally a facies of the calcareous sandstones.

#### DESCRIPTION OF LAUMONTITE-BEARING ROCKS

Medium- to coarse-grained sandstones in the laumontitized sequence are generally more highly altered than are the finer grained sandstone and siltstone. This fact suggests that porosity and permeability may be important factors in determining the amount of alteration in these clastic rocks.

The laumontitized sandstones are fairly well sorted mixtures of subangular and subrounded mineral and rock fragments in a poorly defined matrix containing chloritized biotite, sericite, and laumontite. The clasts are chiefly quartz, albite, chert, and fragments of finely porphyritic volcanic detritus. Epidote, apatite, pyroxene, and sphene are very minor constituents. Much of the matrix and many of the fragments could not be identified. Some of the albite is partly replaced by laumontite, but most of the laumontite occurs as cement.

Carbonitized plant debris is common in the laumontitized rocks as well as in the nonlaumontitized rocks. The occurrence of fragile vertical plant stems in highly laumontitized calcareous tuff suggests that the tuff was deposited in a shallow-water environment. Shallow-water deposition is also suggested by local occurrence of mud cracks in shales which are interbedded with the altered sandstones.

The laumontitized rocks are recognizable in the field because the dark-gray sandstones are spotted or mottled with lighter gray areas. In finer grained rocks the lighter gray spots are well-defined ovoids less than  $\frac{1}{4}$  inch in greatest dimension. In coarser grained rocks the spots are less well-defined; they merge with the surrounding dark-gray matrix and with each other. In more highly altered strata the spots make up practically all the rock and the result is a light gray or buff rock with an earthy appearance, mottled with vague darker areas. The spots or ovoids are oriented with their long dimensions parallel to the bedding. In more massive strata the orientation of the spots may be the only apparent indication of bedding.

#### X-RAY STUDIES

A number of representative specimens from each of the three lithologic units were studied by X-ray diffraction methods. The purpose of this study was first to determine if laumontite was present, and if present, to obtain semiquantitatively the relative amounts of laumontite, quartz, calcite, and plagioclase in the rocks.

No special techniques were used in preparing and analyzing the diffraction samples. The laumontite undoubtedly lost much of its water, and the diffraction peaks are probably those of leonardite rather than laumontite. The spacing of the diffraction lines obtained from the Alaskan material (see accompanying table) agrees quite well with the data obtained by Coombs (1952, p. 822), except for the strongest peak at 9.41, (110) face. Coombs' data were obtained using a powder camera which apparently did not record this low-angle peak that is shown on later diffractographs (Neumann and others, 1957, pl. I).

#### *X-ray diffraction data for laumontite (leonardite)*

[Only the 7 most intense lines shown]

Air-dried leonardite <sup>1</sup>		Air-dried laumontite <sup>2</sup> (leonardite?)	
d (Å)	I <sup>3</sup>	d (Å)	I <sup>3</sup>
		9.41	10
6.88	6	6.81	6
4.18	10	4.15	7
3.67	4	3.65	3
3.52	10	3.51	4.5
3.28	3	3.25	3.5
3.04	4	3.03	3

<sup>1</sup> Coombs, 1952, p. 822, specimen 192, Hungary. Analysis was by means of a powder camera which apparently did not record the highest intensity line (9.41) because of its low angle.

<sup>2</sup> Specimen 61A-Hr 1010, lat 62°16' W., long 163°5'8" N., Kwiguk 1:250,000-scale quadrangle, Alaska. X-ray powder not purified, contains minor amounts of quartz, albite, chlorite, and carbonized plant detritus. Analysis on wide-range diffractometer, Ni-filtered CuK $\alpha$  radiation, ( $\lambda=1.54050$  Å).

<sup>3</sup> Line intensities do not compare well because the line of strongest intensity, 9.41, was not recorded for the Hungarian specimen, and the Alaskan specimen contains crystalline impurities.

Data from X-ray analysis of whole-rock diffraction powders show that, almost without exception, the presence of laumontite is indicated by the development of light-gray ovoids in the dark-gray sandstones and siltstones or by more complete alteration of the dark-gray rocks to light-olive-gray rocks. None of the dark-gray sandstones that are not mottled appear to contain more than 2 percent laumontite and most of them none at all. Several of the weakly laumontitized and non-laumontitized specimens came from beds lying between strongly laumontitized strata. Separate X-ray analyses of the light- and dark-colored fractions of the laumontitized rocks show that most, if not all, of the laumontite is in the light-colored fraction. Thin sec-

tions show that the darker fraction contains relatively more chlorite and biotite.

The X-ray data also show that albite and oligoclase are the only feldspars plentiful enough to be detected by this method of analysis. Of these, albite is by far the more common feldspar in both altered and unaltered rocks. The anorthite content of the feldspar in selected specimens was estimated from the spacing of the (131), (1 $\bar{3}$ 1), and (220) reflection peaks (Smith and Yoder, 1956, p. 634). Oligoclase was identified only in the unaltered rocks. The composition of the albite is variable, but in general it appears to be less calcic in rocks containing appreciable amounts (10 to 20 percent) of laumontite. Coombs (1954, p. 71) points out that lime-free albite in sediments may owe its composition to albitization of andesine. Some of the albite in these rocks may be derived from older volcanic rocks which are commonly albitized, but the close correlation between the occurrence of laumontite and albite suggests that much of it formed in place.

### ORIGIN

The laumontitized rocks of western Alaska appear to be similar in many respects to rocks recently described (Zaporozhtseva, 1960) in the Lena coal basin, Russia, where laumontitized sedimentary rocks are developed on a regional scale. Laumontitized rocks form three separate stratigraphic intervals in a sedimentary sequence 2,500 to 3,000 meters thick for a distance of more than 1,000 km (Zaporozhtseva, 1960, p. 58). In discussing the diagenetic origin of the laumontite, Zaporozhtseva emphasizes the chemistry of the formative medium and either ignores or tacitly assumes such important factors as availability of reactive volcanic glass, porosity, and depth of burial. She believes that the laumontite formed while the sediments were still unconsolidated and concludes (Zaporozhtseva, 1960, p. 58) that

The widespread occurrence of laumontite \* \* \* is attributable to the uniform circumstances of sedimentation over a vast territory, where the formation of calcic zeolite took place in silt deposits of a desalinized basin, as well as in alluvial(?) deposits, during the diagenetic stage.

She points out (Zaporozhtseva, 1960, p. 56) that

The availability of the starting material for the formation of zeolites in the ooze of reservoirs is a fairly frequent phenomena. Yet, it is common that zeolites do not always crystallize thereby. It may be assumed that they are very sensitive to the formative medium, the details of which are unclear (concentration of the components in solution, chemical activity, the amounts of organic matter, carbonic acid, oxygen, the concentration of hydrogen ions, and so on).

It is probable that the laumontitized sandstones of

western Alaska developed in a manner analogous to that described by Zaporozhtseva.

Staining with sodium cobaltinitrite solution reveals that the laumontitized rocks contain no more than a trace of potash feldspar. However, many of the non-laumontitized rocks contain as much as 5 percent potash feldspar and a few as much as 20 percent.

The writers believe that the laumontite formed through the interaction of unstable volcanic debris, probably glass, with water of the appropriate composition. This manner of formation has been suggested by Bradley (1929, p. 2-5) for the analcime in the Tertiary Green River Formation, by Coombs (1954, p. 79) for analcime and heulandite in the Taringatura sediments in New Zealand, and by Hay (1963, p. 246) for authigenic zeolites in late Pleistocene sediments.

The following observations suggest that tuffaceous material of siliceous or intermediate composition is a prime requisite to the formation of laumontite in these rocks: (1) mottled laumontitized sandstone beds grade laterally into laumontitized tuffs; (2) the intercalation of laumontitized and nonlaumontitized strata within the laumontitized unit is more easily explained by intermittent incorporation of tuffaceous material of pyroclastic or epiclastic origin in the sandstone than by postulating differential effects of load metamorphism; (3) the apparent lack of laumontite and tuffs in the underlying(?) calcareous and noncalcareous units, although they do contain abundant albite and calcic feldspars and were deeply buried, suggests that the laumontite formed at the expense of tuffaceous material rather than by the hydration of plagioclase.

Of equal importance in the genesis of laumontite is the composition of the water in which the volcanic debris was deposited. Bradley's (1929) observations indicate that the formative medium was alkaline. His observations are supported by experimental evidence showing that (1) alkaline waters are capable of reacting with siliceous volcanic material, and (2) zeolites can be synthesized under alkaline conditions. However, Coombs (1960, p. 348) reports that zeolites exist at Wairakei, New Zealand, in waters made slightly acid by carbon dioxide and that zeolites have been formed artificially from obsidian in waters of the same composition.

These contrasting facts are made more understandable by Hemley's work (Hemley and others, 1961, p. 340), which points out the fundamental importance of equilibrium constants or critical ion ratios (in this instance the activities of  $\text{Ca}^{+2}$  and  $\text{Na}^{+1}$  relative to  $\text{H}^{+1}$ ). Thus, the reaction by which laumontite was formed could have taken place in either alkaline or slightly acid

solutions, depending upon the concentrations of the reacting ions. However, in this specific environment the combined effects of solution of calcareous material and of hydrolysis of unstable volcanic ash could be expected to lead to somewhat alkaline conditions even in the presence of acid-forming decaying plant material.

Laumontitized strata have not been recognized in sedimentary deposits of about the same age which were laid down in the adjacent Kuskokwim geosyncline (fig. 1). The apparent lack of laumontite in these deposits is largely attributed to the fact that they contain few calcareous strata and little or no tuff or tuffaceous sandstone. That the Kuskokwim geosynclinal deposits are mostly deeper water deposits containing relatively little carbonitized plant trash is probably also significant in explaining why laumontite is so abundant in the Koyukuk geosyncline and apparently lacking in the Kuskokwim geosyncline.

#### REFERENCES

Bradley, W. H., 1929, The occurrence and origin of analcrite and meerschaum beds in the Green River formation of Utah, Colorado and Wyoming: U.S. Geol. Survey Prof. Paper 158-A, p. 1-7.

- Coombs, D. S., 1952, Cell size, optical properties and chemical composition of laumontite and leonardite: Am. Mineralogist, v. 37, p. 812-830.
- 1954, The nature and alteration of some Triassic sediments from Southland, New Zealand: Royal Soc. New Zealand Trans., v. 82, pt. 1, p. 65-109.
- 1960, Lower grade mineral facies in New Zealand, in Petrographic provinces, igneous and metamorphic rocks: Internat. Geol. Cong., 21st, Copenhagen, 1960, Proc., pt. 13, p. 339-351.
- Hay, R. L., 1963, Stratigraphy and zeolitic diagenesis of the John Day Formation of Oregon: California Univ., Dept. Geol. Sci. Bull., v. 42, no. 5, p. 199-262.
- Hemley, J. J., Meyer, Charles, and Richter, D. H., 1961, Some alteration reactions in the system  $\text{Na}_2\text{O}\text{-Al}_2\text{O}_3\text{-SiO}_2\text{-H}_2\text{O}$ : in U.S. Geol. Survey Prof. Paper 424-D, p. D338-D340.
- Neumann, Henrich, Sverdrup, Thor, and Saebo, P. Chr., 1957, X-ray powder patterns for mineral identification III, silicates: Av Handlinger Utgitt av Det Norske Videnskaps-Akademii I, Oslo I. Mat. Naturv. Klass, no. 6, 18 p., 38 pl.
- Payne, T. G., 1955, Mesozoic and Cenozoic tectonic elements of Alaska: U.S. Geol. Survey Misc. Geol. Inv. Map I-84, scale 1:5,000,000.
- Smith, J. R., and Yoder, H. S., Jr., 1956, Variations in X-ray powder diffraction patterns of plagioclase feldspars: Am. Mineralogist, v. 41, p. 632-647.
- Zaporozhtseva, A. S., 1960, On the regional development of laumontite in Cretaceous deposits of Lena coal basin: Acad. Sci. USSR Izv., geol. ser., no. 9, p. 52-59. [English ed.]



## CLAY MINERALS FROM AN AREA OF LAND SUBSIDENCE IN THE HOUSTON-GALVESTON BAY AREA, TEXAS

By JOHN B. CORLISS<sup>1</sup> and ROBERT H. MEADE,  
La Jolla, Calif., Woods Hole, Mass.

*Work done in cooperation with the  
National Aeronautics and Space Administration*

**Abstract.**—X-ray diffraction study of the clay-size fraction of eight fine-grained samples from a core hole in sediments of Pleistocene age at Clear Lake, Harris County, Tex., indicates a clay-mineral assemblage of montmorillonite, illite, chlorite, and kaolinite. In each sample, more than half the clay-mineral assemblage is montmorillonite.

A core hole drilled 20 miles southeast of Houston, Tex., (fig. 1) as part of the engineering testing program for the new facility of the National Aeronautics and Space Administration at Clear Lake, penetrated 963 feet of sand and clay of Pleistocene age. Eight samples of fine-grained sediments were selected from the core for clay-mineral analysis. The position of the samples in the geologic section and the relative proportions of the clay minerals in each sample, as determined by X-ray diffraction analysis, are shown on figure 2. Montmorillonite is the principal constituent, but lesser amounts of illite, chlorite, and kaolinite occur in all samples.

The core hole is near the center of the broad area of rapid land subsidence shown on figure 2. The subsidence appears to be due to changes in effective overburden loads that are related to the withdrawal of confined ground water and a substantial decline of artesian head (Winslow and Doyel, 1954; Winslow and Wood, 1959). The clay-mineral assemblage is similar to that found in fresh-water-bearing sediments underlying areas of rapid subsidence in the San Joaquin and Santa Clara Valleys of California. Compared to the other common clay minerals, montmorillonite is particularly sensitive to changes in pressure; perhaps the predomi-

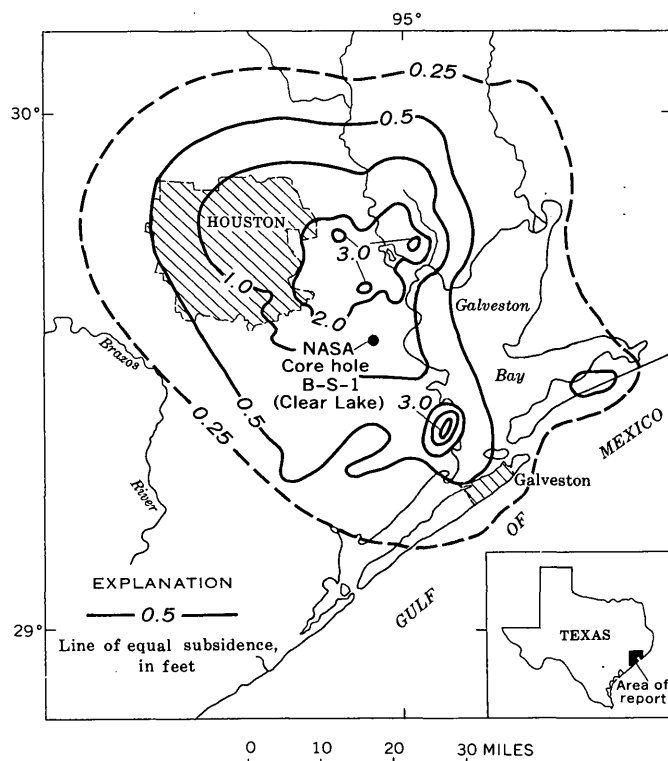


FIGURE 1.—Map showing land-surface subsidence in the Houston-Galveston Bay area, 1943-59, and the location of NASA core hole B-S-1. Lines of equal subsidence are from U.S. Coast and Geodetic Survey measurements. Compiled by Brian Myers.

nance of montmorillonite in these clay-mineral assemblages accounts in part for the marked response of the sediments (compaction and subsidence of the land surface) to changes in the effective overburden load.

<sup>1</sup> Scripps Institution of Oceanography.

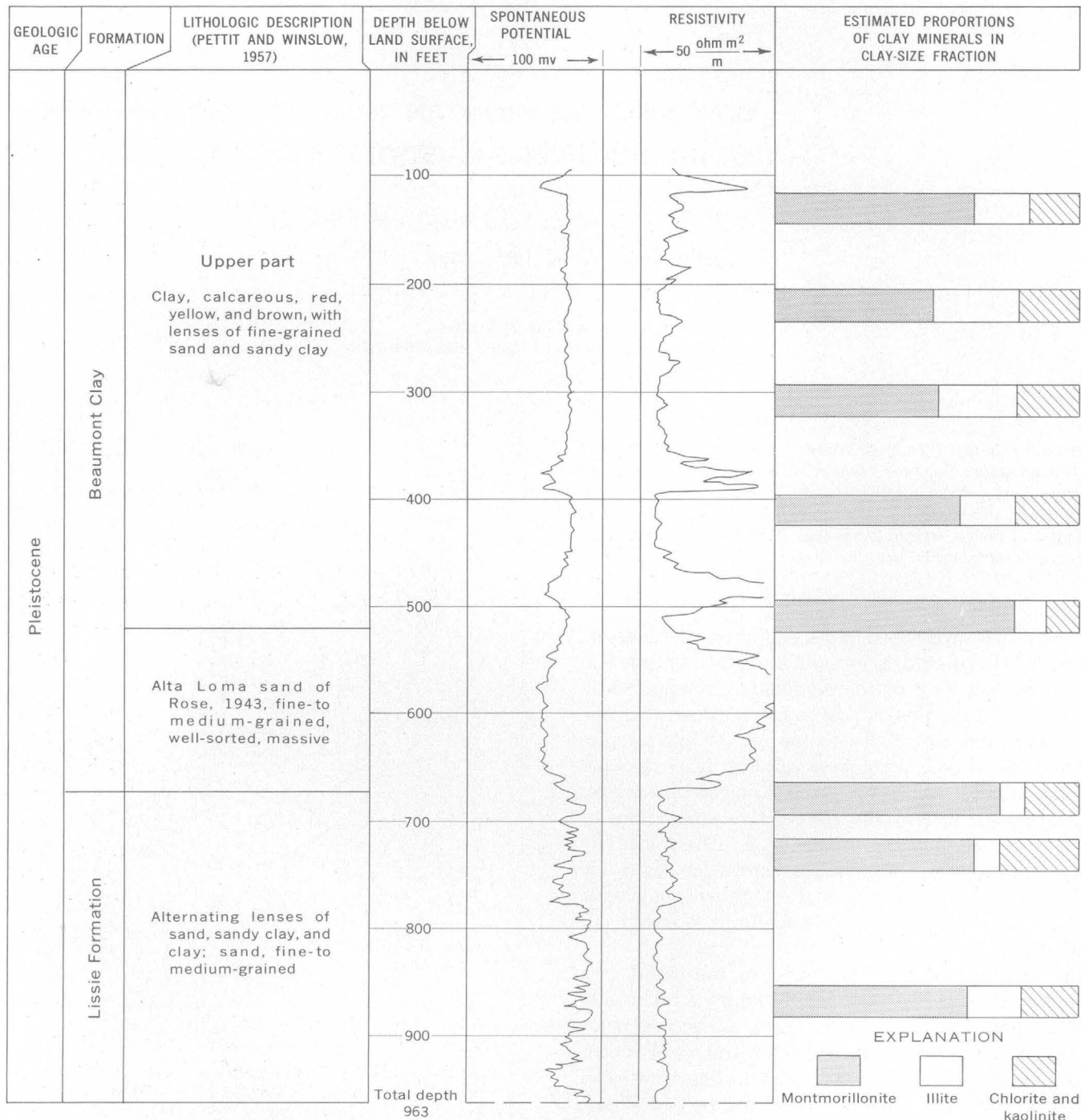


FIGURE 2.—Electric log, lithology, and clay mineralogy of the sediments penetrated by NASA core hole B-S-1, Clear Lake, Harris County, Tex. Lithologic descriptions from Pettit and Winslow (1957).

The cores, taken with a double-tube Dension core barrel, were stored in air-tight jars. Samples from eight selected fine-grained sections of the core were prepared as follows:

(1) Five grams of sample was placed in 150 milliliters of distilled water, stirred briefly, and dispersed in an ultrasonic generator for about an hour (no chemical dispersing agent added).

(2) Concentrated slurries of two size fractions—0.1 to 0.2 and 0.2 to 2.0 microns—were separated out by centrifuging.

(3) The slurries were placed on finely porous ceramic slides by means of a dropper, and the water was sucked out through the slide by a vacuum pump. This produced an aggregate of clay-mineral particles oriented with their basal surfaces parallel to the slide.

*Basal X-ray-reflection criteria used to identify clay minerals*

Treatment of sample	Criteria for clay-mineral identification after various steps of treatment			
	Montmorillonite	Illite	Chlorite	Kaolinite
Air drying-----	Broad reflections at 15 Å and 5.0 Å; diffuse band 3.1–3.3 Å. 15-Å reflection much more intense than the others.	Integral series related to 9.9 Å: 5.0 Å, 3.3 Å. 5.0-Å reflection less intense than the other two.	Integral series related to 14 Å: 7 Å, 4.7 Å, 3.5 Å. 7-Å and 3.5 Å reflections much more intense than the others. 14-Å reflection obscured by montmorillonite reflection.	Reflections at 7.0–7.1 Å and 3.5 Å. 3.5 Å reflection is separated slightly from the corresponding chlorite reflection.
Exposing to ethylene glycol.	Integral series related to 17 Å: 8.5 Å, 5.6 Å, 3.5 Å. 17-Å reflection much more intense than the others.	----do----	----do----	Do.
Heating at 400°C for 1 hour.	Nearly integral series related to 9.8 or 9.9 Å: 5.0 Å, 3.1–3.3 Å.	As above, presumably: reflections obscured by montmorillonite reflections.	As above, except that faint reflection at 14 Å now visible.	Do.
Heating at 550°C for 1 hour.	----do-----	----do-----	14-Å reflection enhanced; other orders absent.	No reflections.

These oriented aggregates were then treated in four steps:

- (1) Dried in air,
- (2) Exposed to ethylene glycol vapors at 60°C for 1 hour,
- (3) Heated to 400°C for 1 hour, and
- (4) Heated to 550°C for 1 hour.

After each step, an X-ray diffraction pattern was run using a Norelco diffractometer with a Brown linear recorder.

These diffraction patterns were examined to identify the clay minerals present and to estimate their relative proportions. The criteria used in identifying the minerals are listed in the accompanying table. Tentatively it is assumed that the relative proportions of the clay minerals in a sample are represented by the ratios of the intensities (areas) of certain selected reflections on the diffraction patterns of the sample. The estimated relative proportions of montmorillonite and illite are determined by comparing the intensities of the 9.9-Å (angstrom units) reflections before and after heating to 400°C. Chlorite and kaolinite are considered together because their reflections coincide, making it difficult to differentiate them quantitatively. The estimated ratio of chlorite and kaolinite to illite is determined by the ratio of the intensities of the 7-Å and 10-Å reflection after the ethylene-glycol treatment.

The estimated average composition of the 0.2–2.0 $\mu$  fractions of all 8 samples is 65 percent montmorillonite, 15 percent illite, and 20 percent chlorite plus kaolinite. The composition of the finer 0.1–0.2 $\mu$  fraction is similar to that of the coarser 0.2–2.0 $\mu$  fraction (given in fig. 2), except for a slightly larger proportion of montmorillonite in the finer size fraction of most of the samples.

The Layne-Texas Co., under supervision of McClelland Engineers, Inc., drilled the core hole for the U.S. Army Corps of Engineers, who in turn made the cores available for the clay-mineral studies. We are grateful to Leonard A. Wood of the U.S. Geological Survey who arranged for transmittal of the cores, supplied background material for the illustrations, and reviewed the article.

**REFERENCES**

- Pettit, B. M., Jr., and Winslow, A. G., 1957, Geology and ground-water resources of Galveston County, Texas: U.S. Geol. Survey Water-Supply Paper 1416, 157 p., 23 pls., 13 figs.
- Rose, N. A., 1943, Progress report on the ground-water resources of the Texas City area, Texas: Texas Board Water Engineers, duplicated rept.
- Winslow, A. G., and Doyel, W. W., 1954, Land-surface subsidence and its relation to the withdrawal of ground water in the Houston-Galveston Region, Texas: Econ. Geology, v. 49, no. 4, p. 413–422.
- Winslow, A. G., and Wood, L. A., 1959, Relation of land subsidence to ground-water withdrawals in the upper Gulf Coast region, Texas: Mining Engineering, v. 11, no. 10, p. 1030–1034.



## ATTAPULGITE FROM CARLSBAD CAVERNS, NEW MEXICO

By WILLIAM E. DAVIES, Washington, D.C.

**Abstract.**—The clay mineral attapulgite occurs in well-cemented cave fill found in a maze of small solution pockets and tubes in the Lower Cave, Carlsbad Caverns, N. Mex. Two varieties of clay are present: gray to olive-green clay, mainly montmorillonite; and pink clay composed of approximately equal parts of attapulgite and montmorillonite. Both varieties are found in the same area, grade one into another, and contain as much as 15 percent quartz. The pink clay contains 32 percent calcite, which forms a strong bond that prevents dispersion. The gray clay disperses readily.

Attapulgite, general composition  $(\text{OH}_2)_4 (\text{OH})_2 \text{Mg}_5\text{Si}_8\text{O}_{20} \cdot 4\text{H}_2\text{O}$ , is a clay mineral commonly associated with soils derived from limestone; however, its presence in cave deposits has not been reported previously. In 1956 a deposit of well-cemented, fine-grained cave fill was examined in the Lower Cave, Carlsbad Caverns, N. Mex. This deposit had been previously described (Good, 1957), but the clay minerals were not identified. The clay occurs in a maze of small solution pockets and tubes about 150 meters east of the old ladder entrance to Lower Cave.

The clay in the tubes and pockets originally filled the openings completely, but shrinkage and slumping have left small voids between the clay and the roof of the pockets. The clay is broken by irregular fractures into fragments 5 to 15 centimeters on a side. The deposit contains two kinds of clay which are easily distinguished by their color: one is pink and the other gray to olive green. Both varieties occur in the same locality and commonly grade one into another. The pink clay is dense, hard, and breaks with a conchoidal fracture. It is very resistant to crushing and fracturing and withstands the repeated blows of an ordinary geologic pick.

Attempts to disperse the pink clay in water were to no avail. Samples left in water at room temperature for 2 years absorbed no water, and the strength of the clay was not altered. The green clay dispersed readily in water, forming small silt-sized flakes.

Laboratory tests showed that the pink clay contained 32 percent calcite, which apparently acted as a cement,

thereby preventing dispersal of the clay. After removal of the calcium carbonate by dissolving it in hydrochloric acid, the insoluble residue consisted primarily of clay (85 percent) with small proportions of silt and sand (15 percent). No heavy minerals were observed in the clay. X-ray examination of the silt ( $62-2\mu$ ) and the clay ( $<2\mu$ ) fractions of the acid-insoluble material showed the following minerals (estimate of quantities are based on the relative intensities of the diffracted lines):

Mineral	Parts in ten
Attapulgite	5
Montmorillonite	4
Kaolinite (?)	Trace
Quartz	Trace
Feldspar	Trace

In the silt-sand fraction the composition is estimated as follows:

Mineral	Parts in ten
Quartz	5
Attapulgite	3
Kaolinite (?)	1
Feldspar	Trace

Additional examination with an electron microscope confirmed the presence of attapulgite and showed that the attapulgite in the silt-sand fraction consists of aggregates of very fine grained fibers.

The pink clay (before removal of calcium carbonate) had the following engineering properties:

Liquid limit	89 percent <sup>1</sup>
Plastic limit	45 percent <sup>1</sup>
Field moisture equivalent	123 percent <sup>1</sup>
Shrinkage limit	8 percent <sup>1</sup>
Shrinkage ratio	21
Specific gravity	2.20

<sup>1</sup> Moisture content in percent of dry unit weight.

Compared with attapulgite not containing calcite (White, 1949) these values are low. Plastic limit is generally in the order of 116 percent and liquid limit 177 percent.

The gray to olive-green clay consists of montmorillonite, quartz, a small amount of halloysite, and some disordered kaolinite. Calcite was not detectable.

The occurrence of the clays gives some clue to their origin. The pink clay occurs in an exposed position where small phreatic tubes connect with larger passages. The gray to olive-green clay occurs in phreatic tubes behind the pink clay. It is probable that the development of attapulgite and the cementation by calcite in the exposed clay occurred during a period when the Lower Cave was inundated by waters rich in carbonates.

Of possible practical importance is the strong cemen-

tation imparted to the clay by the calcium carbonate present in the raw sample. Such bonding, where attapulgite is present, may be applicable as a simple, cheap means of stabilizing clay surfaces.

Laboratory identification of the attapulgite from the Carlsbad Caverns was made by John C. Hathaway and Dorothy Carroll, U.S. Geological Survey.

#### REFERENCES

- Good, J. M., 1957, Noncarbonate deposits of Carlsbad Caverns: Natl. Speleological Soc. Bull. 19, Oct., p. 20.  
White, W. A., 1949, Atterberg plastic limits of clay minerals: Am. Mineralogist, v. 34, no. 7-8, July-Aug., p. 508-512.



## DIAGRAM FOR DETERMINING MINERAL COMPOSITION IN THE SYSTEM $\text{MnCO}_3\text{--CaCO}_3\text{--MgCO}_3$

By WILLIAM C. PRINZ, Washington, D.C.

**Abstract.**—In the system  $\text{MnCO}_3\text{--CaCO}_3\text{--MgCO}_3$ , index of refraction increases toward  $\text{MnCO}_3$  and the spacing of the strongest X-ray line ( $d_{(211)}$ ) increases toward  $\text{CaCO}_3$ . Variations in these properties are combined to produce a diagram for determining the composition of relatively iron-free minerals in the system.

In the system  $\text{MnCO}_3\text{--CaCO}_3\text{--MgCO}_3$ , index of refraction increases toward  $\text{MnCO}_3$  and the spacing of the strongest X-ray line ( $d_{(211)}$ ) increases toward  $\text{CaCO}_3$ . Variation in the index of refraction of the ordinary ray with composition in the system has been presented by Wayland (1942, pl. 1), and Winchell and Winchell (1951, fig. 61); Goldsmith and Graf (1960, fig. 6) show the variation in the spacing of the  $d_{(211)}$  plane. These data are here combined (fig. 1) and yield a useful chart for determining the composition of minerals within the system. A similar diagram for determining the composition of dolomite containing as much as 10 percent  $\text{FeCO}_3$  has been published by Zen (1956, fig. 1).

Variation in the spacing of the  $d_{(211)}$  plane with composition in the series  $\text{MnCO}_3\text{--CaCO}_3$  has also been determined by Erenburg (1959), and a chart for determining composition in the system  $\text{CaCO}_3\text{--MgCO}_3$  by X-ray methods has been presented by Harker and Tuttle (1955, p. 277, fig. 2). Data in both these papers agree closely with those given by Goldsmith and Graf (1960) and shown here (fig. 1).

Natural material is known from the calcite half of the series  $\text{MnCO}_3\text{--CaCO}_3$ , but except at high temperatures, a gap exists between  $\text{CaMn}(\text{CO}_3)_2$  and  $\text{MnCO}_3$ . The series  $\text{MnCO}_3\text{--MgCO}_3$  is continuous (Goldsmith and Graf, 1960), but natural material is rare. That the  $\text{MgCO}_3\text{--CaCO}_3$  series is discontinuous is well known.

Iron carbonate, which when pure has  $n_o=1.875$  and  $d_{(211)}=2.791 \text{ \AA}$ , is the most common other phase that occurs in this system; its presence in a mineral would cause the composition as shown by the diagram (fig. 1)

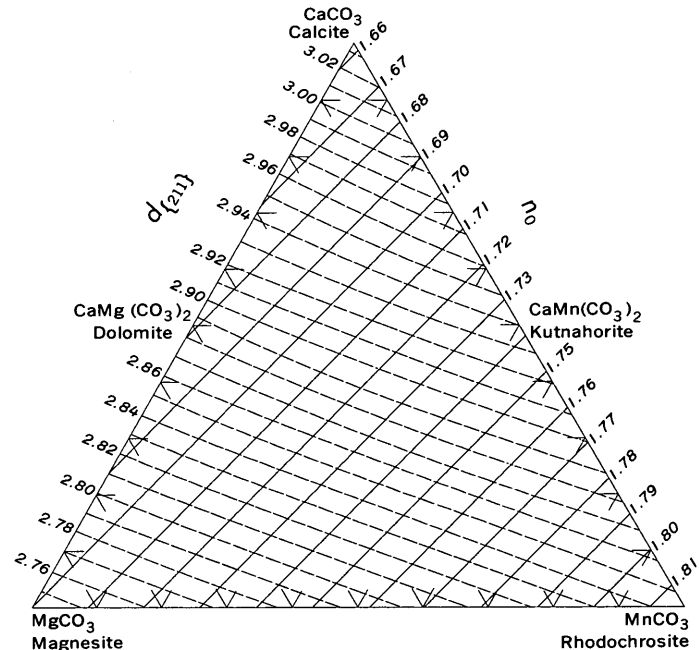


FIGURE 1.—Variation in index of refraction of the ordinary ray ( $n_o$ —solid lines) and spacing (in angstrom units) of the strongest X-ray line ( $d_{(211)}$ —dashed lines) with composition (molecular percent) in the system  $\text{MnCO}_3\text{--CaCO}_3\text{--MgCO}_3$ . X-ray data from Goldsmith and Graf (1960, fig. 6); optical data from Wayland (1942, pl. 1) and Winchell and Winchell (1951, fig. 61).

to be displaced toward the  $\text{MnCO}_3$  and  $\text{MgCO}_3$  corners. Data presented by Zen (1956) and Howie and Broadhurst (1958) for dolomite and ankerite and by Frondel and Bauer (1955) for kutnahorite suggest that the accuracy of the diagram around dolomite and kutnahorite is good if the amount of  $\text{FeCO}_3$  in the mineral is less than 1 percent, that it is usable but less reliable if the amount is 2 percent, and that accuracy would be poor for samples containing more than 3 percent  $\text{FeCO}_3$ .

A search of the literature for analytical data to check the validity of other parts of the diagram proved unre-

warding. Most papers give composition and index of refraction but not X-ray data. Published analyses that give both are generally of relative pure end members in the system; these data fit very well.

Both index of refraction of the ordinary ray and the spacing of the strongest X-ray line are easily and quickly measured, so the diagram should prove useful in determining the composition of relatively iron-free minerals in the system. Perhaps with more data it will be possible to refine this diagram and to construct similar ones to include  $\text{FeCO}_3$ .

#### REFERENCES

Erenburg, E. G., 1959, Continuous isomorphism in the  $\text{CaCO}_3$ - $\text{MnCO}_3$  system: Russian Jour. Inorganic Chemistry (translation of Zhurn. Neorg. Khim.), v. 4, p. 859-861.

- Frondel, Clifford, and Bauer, L. H., 1955, Kutnahorite, a manganese dolomite,  $\text{CaMn}(\text{CO}_3)_2$ : Am. Mineralogist, v. 40, p. 748-760.
- Goldsmith, J. R., and Graf, D. L., 1960, Subsolidus relations in the system  $\text{CaCO}_3$ - $\text{MgCO}_3$ - $\text{MnCO}_3$ : Jour. Geology, v. 68, p. 324-335.
- Harker, R. I., and Tuttle, O. F., 1955, Studies in the system  $\text{CaO}$ - $\text{MgO}$ - $\text{CO}_2$ : Am. Jour. Sci., v. 253, p. 209-224, 274-282.
- Howie, R. A., and Broadhurst, F. M., 1958, X-ray data for dolomite and ankerite: Am. Mineralogist, v. 43, p. 1210-1214.
- Wayland, R. G., 1942, Composition, specific gravity, and refractive indices of rhodochrosite from Butte, Montana: Am. Mineralogist, v. 27, p. 614-628.
- Winchell, A. N., and Winchell, Horace, 1951, Elements of optical mineralogy, pt. 2. descriptions of minerals, 4th ed.: New York, John Wiley and Sons.
- Zen, E-an, 1956, Correlation of chemical composition and physical properties of dolomite: Am. Jour. Sci., v. 254, p. 51-60.



## LITHIUM ASSOCIATED WITH BERYLLIUM IN RHYOLITIC TUFF AT SPOR MOUNTAIN, WESTERN JUAB COUNTY, UTAH

By DANIEL R. SHAWE, WAYNE MOUNTJOY, and WALTER DUKE,  
Denver, Colo.

**Abstract.**—Lithium content of bedded rhyolitic tuff is unusually high at the Roadside beryllium deposit, Spor Mountain, Utah. Li<sub>2</sub>O averages 0.22 percent in 18 representative samples and is concentrated in clay fractions during sizing. It is probably present chiefly in montmorillonite. Though perhaps not of economic importance by itself, the lithium may well be abundant enough to be a byproduct if the deposit is worked for beryllium.

Unusually large amounts of lithium have been detected in samples from a beryllium deposit in bedded rhyolitic tuff at the Roadside claims, Spor Mountain, in western Juab County, Utah. The rhyolitic tuff contains numerous crystals of quartz and sanidine, and pebbles of carbonate rock. The tuff is hydrothermally altered and as a result also contains opal, chalcedony, montmorillonite, calcite, fluorite, manganese oxide, and bertrandite (Be<sub>4</sub>Si<sub>2</sub>O<sub>7</sub>(OH)<sub>2</sub>) (Staatz, 1963, p. M27). Li<sub>2</sub>O content ranges from 0.04 to 0.43 percent; its average value is 0.22 percent in 18 samples that are representative of tuff exposed in a pit dug to develop the beryllium deposit at the south end of the Roadside No. 5 claim. The Li<sub>2</sub>O content and BeO content of the 18 samples are given in table 1. Several of the samples contain very little beryllium, yet carry appreciable lithium, indicating that lithium mineralization was more widespread than beryllium mineralization.

Lithium was determined by a flame photometric method, employing a standard-addition technique similar to that described by Grimaldi (1960). The sample was completely dissolved by digestion in hydrofluoric and perchloric acids, thus facilitating accurate determination of lithium.

The lithium probably is in montmorillonite, which is the only clay mineral recognized in the Spor Mountain beryllium deposits according to Staatz and Griffitts (1961, p. 946) and Staatz (1963, p. M28). This view is supported by the data of table 2 which show that the lithium is most abundant in the clay-size fractions of

TABLE 1.—Li<sub>2</sub>O and BeO analyses of 18 samples from the Roadside No. 5 claim

[Li<sub>2</sub>O determined by flame photometer method by Wayne Mountjoy, 1963. BeO determined by photo-neutron activation method by Walter Duke, 1963]

Sample No.	Laboratory No.	Field No.	Li <sub>2</sub> O (percent by weight)	BeO (percent by weight)
1	D111323	DRS-27-63	0.25	0.84
2	D111324	DRS-28-63	.32	1.07
3	D111325	DRS-30-63	.27	1.25
4	D111326	DRS-31-63	.19	.10
5	D111327	DRS-32-63	.11	.56
6	D111329	DRS-34-63	.16	.016
7	D111330	DRS-35-63	.23	.011
8	D111332	DRS-37-63	.30	1.05
9	D111333	DRS-38-63	.08	1.00
10	D111334	DRS-39-63	.18	.15
11	D111335	DRS-40-63	.07	.073
12	D111337	DRS-42-63	.08	.005
13	D111339	DRS-44-63	.28	.70
14	D111343	DRS-48-63	.04	.41
15	D111371	DRS-76-63	.35	1.15
16	D111379	DRS-84-63	.36	.81
17	D111388	DRS-93-63	.43	.008
18	D111389	DRS-94-63	.28	.12

TABLE 2.—Li<sub>2</sub>O, BeO, and F analyses of two samples, and Li<sub>2</sub>O and F analyses of three size fractions of the two samples, Roadside No. 5 claim

[Li<sub>2</sub>O determined by flame photometer method by Wayne Mountjoy, 1963. Fluorine determined volumetrically by W. D. Goss, 1963. BeO determined by photo-neutron activation method by Walter Duke, 1963]

Sample No.	Laboratory No.	Field No.	Approximate size range (diameter)	Li <sub>2</sub> O (percent by weight)	F (percent by weight)	BeO (percent by weight)
1	D112129	DRS-30-63.	(Total sample)	0.24	1.34	1.25
2	D112130	DRS-30-63C.	>0.05mm	.12	.76	----
3	D112131	DRS-30-63M.	.05mm-5μ	.33	1.87	----
4	D112132	DRS-30-63F.	<5μ	.39	1.88	----
5	D112133	DRS-92-63.	(Total sample)	.19	1.90	.006
6	D112134	DRS-92-63C.	>.05mm	.13	.96	----
7	D112135	DRS-92-63M.	.05mm-5μ	.21	1.17	----
8	D112136	DRS-92-63F.	<5μ	.38	3.10	----

two samples. Several published articles have called attention to the high lithium content of some montmorillonite (1 percent Li<sub>2</sub>O in hectorite, Ross and Hendricks, 1945, p. 27, 35, 38), and it has been suggested that such material may become a source of lithium (Norton and Schlegel, 1955, p. 336, 341).

Lithium is commonly associated with beryllium in magmatic deposits, and the same may apply to hydrothermal deposits. Staatz and Griffitts (1961, table 1) report as much as 700 parts per million lithium (0.13 percent Li<sub>2</sub>O) locally in berylliferous fluorite nodules from the Spor Mountain area, but the amount of lithium shown for the Roadside samples (table 1, this article) has heretofore not been detected in the Spor Mountain beryllium deposits. A berylliferous deposit described by McAnulty and Levinson<sup>1</sup> in the Honeycomb Hills, similar to the deposits at Spor Mountain, and about 20 miles west has an average of about 480 ppm lithium (0.09 percent Li<sub>2</sub>O) in 14 samples.

<sup>1</sup> W. N. McAnulty and A. A. Levinson, 1963, Rare alkali and beryllium mineralization in volcanic tuffs, Honeycomb Hills, Juab County, Utah: Paper presented at Geol. Soc. America Annual Meeting, New York.

The lithium grade of the Roadside deposit does not appear to be high enough to make the deposit economically valuable for lithium alone. Conventional lithium mines in pegmatite ordinarily have at least 1.0 percent Li<sub>2</sub>O (Norton and Schlegel, 1955, p. 344). If the Roadside deposit is worked for beryllium, however, lithium is likely to be recoverable as a byproduct.

#### REFERENCES

- Grimaldi, F. S., 1960, Dilution-addition method for flame spectrophotometry: Art. 225 in U.S. Geol. Survey Prof. Paper 400-B, p. B494-B495.  
Norton, J. J., and Schlegel, D.M., 1955, Lithium resources of North America: U.S. Geol. Survey Bull. 1027-G, p. 325-350.  
Ross, C. S., and Hendricks, S. B., 1945, Minerals of the montmorillonite group: U.S. Geol. Survey Prof. Paper 205-B.  
Staatz, M. H., 1963, Geology of the beryllium deposits in the Thomas Range, Juab County, Utah: U.S. Geol. Survey Bull. 1142-M, 36 p.  
Staatz, M. H., and Griffitts, W. R., 1961, Beryllium-bearing tuff in the Thomas Range, Juab County, Utah: Econ. Geology, v. 56, p. 941-950.



## A GEOCHEMICAL INVESTIGATION OF THE HIGH ROCK QUADRANGLE, NORTH CAROLINA

By ARVID A. STROMQUIST,<sup>1</sup> AMOS M. WHITE,<sup>2</sup> and JOHN B. McHUGH<sup>1</sup>

*Work done in cooperation with the  
North Carolina Department of Conservation and Development, Division of Mineral Resources*

**Abstract.**—Silt to clay-sized alluvium was sampled from 55 streams, each draining an area of about 2 square miles. Because transport of the alluvium has been minimal, the results of chemical analyses are considered to be areally representative. Rapid colorimetric methods of analysis indicated slight, but significant, enrichment of copper, nickel, and zinc in alluvium of the western half of the quadrangle. These results are compatible with the pattern of mineralization as indicated by the prospects and mines near Silver Hill on the northwest, Gold Hill on the west, and Georgeville on the southwest.

Stream alluvium was sampled in the High Rock quadrangle, North Carolina (fig. 1), and analysed for copper, lead, zinc, nickel, tungsten, and molybdenum by rapid geochemical methods. Results of the analyses are comparable to those of similar investigations in nearby areas. All metal values in the stream alluvium are low, but the concentration of samples having a slightly anomalous metal content in the western part of the quadrangle suggests a trend of increasing abundance of copper and zinc in that direction.

The High Rock quadrangle is underlain by rocks of the Carolina slate belt (Laney, 1910, 1917; Pogue, 1910; Stuckey, 1928, Stromquist and Conley, 1959; Conley, 1962a and 1962b) and is near the faulted complex of plutonic rocks of the Charlotte belt (King, 1955) that truncate slate-belt rocks on the west (fig. 1). Rocks of the Kings Mountain belt (King, 1955, map) lie to the west of the Charlotte belt. East of the slate belt are sedimentary rocks of the Newark Group and of the Coastal Plain. Lowlands of the High Rock quadrangle range in altitude from 500 to 600 feet above sea level. Flat Swamp Mountain, the most pronounced ridge in the quadrangle, attains an altitude of 1,200 feet; other ridges and hills are as much as 800 feet high. Volcanic and intrusive rocks form the ridges and highlands of

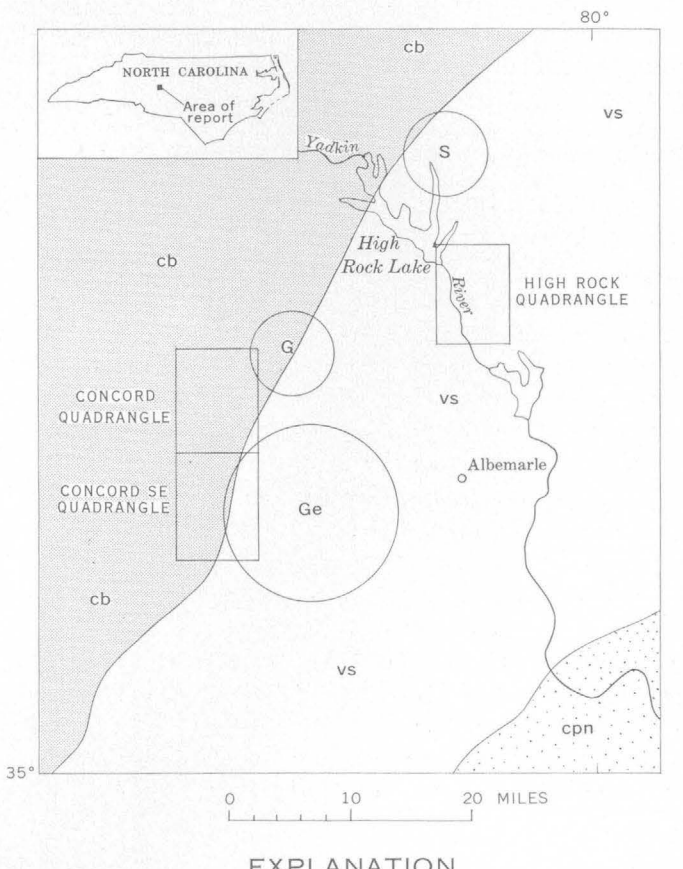


FIGURE 1.—Geologic sketch map of a part of south-central North Carolina, showing location of quadrangles and mining areas. Geology generalized from geologic map of North Carolina (Stuckey and Conrad, 1958) and from King (1955). Circles indicate groups of mines and prospects; letters designate area: S, Silver Hill; G, Gold Hill; Ge, Georgeville.

<sup>1</sup> Denver, Colo.

<sup>2</sup> Washington, D.C.

the area, whereas sedimentary rocks constitute the lowlands. Rocks in the High Rock quadrangle comprise rhyolitic and basaltic flows and tuffs interbedded with tuffaceous argillite, and argillaceous tuff, all of Ordovician age (White and others, 1963). Gabbroic sills and stocks, probably of Paleozoic age (King, 1955, p. 349), intrude the volcanic and sedimentary rocks and occupy about 2 percent of the area. The rocks have weathered to saprolite in some places, but nowhere in the quadrangle is saprolite more than a few feet thick, and in many places the streams flow on hard rock. The thickness of saprolite in the High Rock area contrasts sharply with that in the Concord area, where Bell and Overstreet (Bell and Overstreet, 1960; Overstreet and Bell, 1960) report saprolite developed to depths of 125 feet.

The geochemical analyses were made on samples of fine-grained alluvium from 55 small streams, each draining an area of 2 square miles or less, whose drainage basins cover 63 percent of the quadrangle (fig. 2). Each sample consisted of about 100 grams of clayey and silty alluvium taken upstream from the flood plains of the principal streams into which the 55 streams emptied. The sampling of small drainage basins limits the source of metals in the alluvium to the basin sampled. Except in areas of pervasively fractured rocks, ground water probably has distributed dissolved solids only short distances in rocks of the Piedmont province in North Carolina, for according to LeGrand (1958, p. 179), "The linear distance between the point where a drop of water first reaches the water table and the point where it is discharged at a spring or seepage area is almost everywhere less than a mile, and commonly less than half a mile." According to Hawkes (1957, p. 306) a clay sample, rather than sand or gravel, is likely to have adsorbed metallic ions from the water in which it was transported. Colorimetric field methods of chemical analysis (Ward and others, 1963) were used by John B. McHugh and W. W. Janes of the U.S. Geological Survey in determining the abundance of copper, lead, zinc, nickel, tungsten, and molybdenum in the 55 silt and

clay samples. The methods are sensitive, rapid (as many as 30 determinations per day), and accurate to  $\pm 30$  percent.

Figure 3 shows the frequency distribution of the elements looked for. Copper was reported to the nearest 10 ppm, and lead, zinc, and nickel were reported to the nearest 25 ppm. All 55 samples were below the limits of detection with respect to molybdenum (<4 ppm) and tungsten (<20 ppm); most were below the limits of detection with respect to lead (<25 ppm). Hence results for molybdenum, tungsten, and lead are not significant. With respect to nickel, two samples contained at least 50 ppm and one contained 75 ppm (fig. 3); all three samples came from near the northwest corner of the quadrangle (fig. 2). Because of this clustering of the nickel "highs" these results have been considered of "odd" significance and are shown on figure 2.

The arithmetic mean of the results for zinc is about 50 ppm and that for copper is slightly more than 30 ppm (fig. 3). Figure 2 indicates, with chemical symbols, those basins in which the alluvium sampled contains at least 75 ppm zinc and 40 ppm copper. On the basis of an analytical error of  $\pm 30$  percent, 75 ppm zinc is a borderline "anomaly" and a result of 40 ppm copper could be a submarginal one. Nevertheless, these questionable small anomalies indicate a slight metal enrichment in the western half of the quadrangle (fig. 2) and suggest a trend of increasing mineralization northward, westward, and southwestward, toward the mines and prospects clustered about Georgeville, Gold Hill, and Silver Hill (fig. 1). What relations, if any, the pattern of metal enrichment may bear to the south-plunging anticline shown on figure 2 is obscure. This fold has a wave length of about 10–12 miles and projects toward the Gold Hill district.

Although this article reports only the preliminary results of a geochemical study in the High Rock quadrangle, the authors believe that study of a larger area in this part of North Carolina will bear out more strongly the trends shown here.

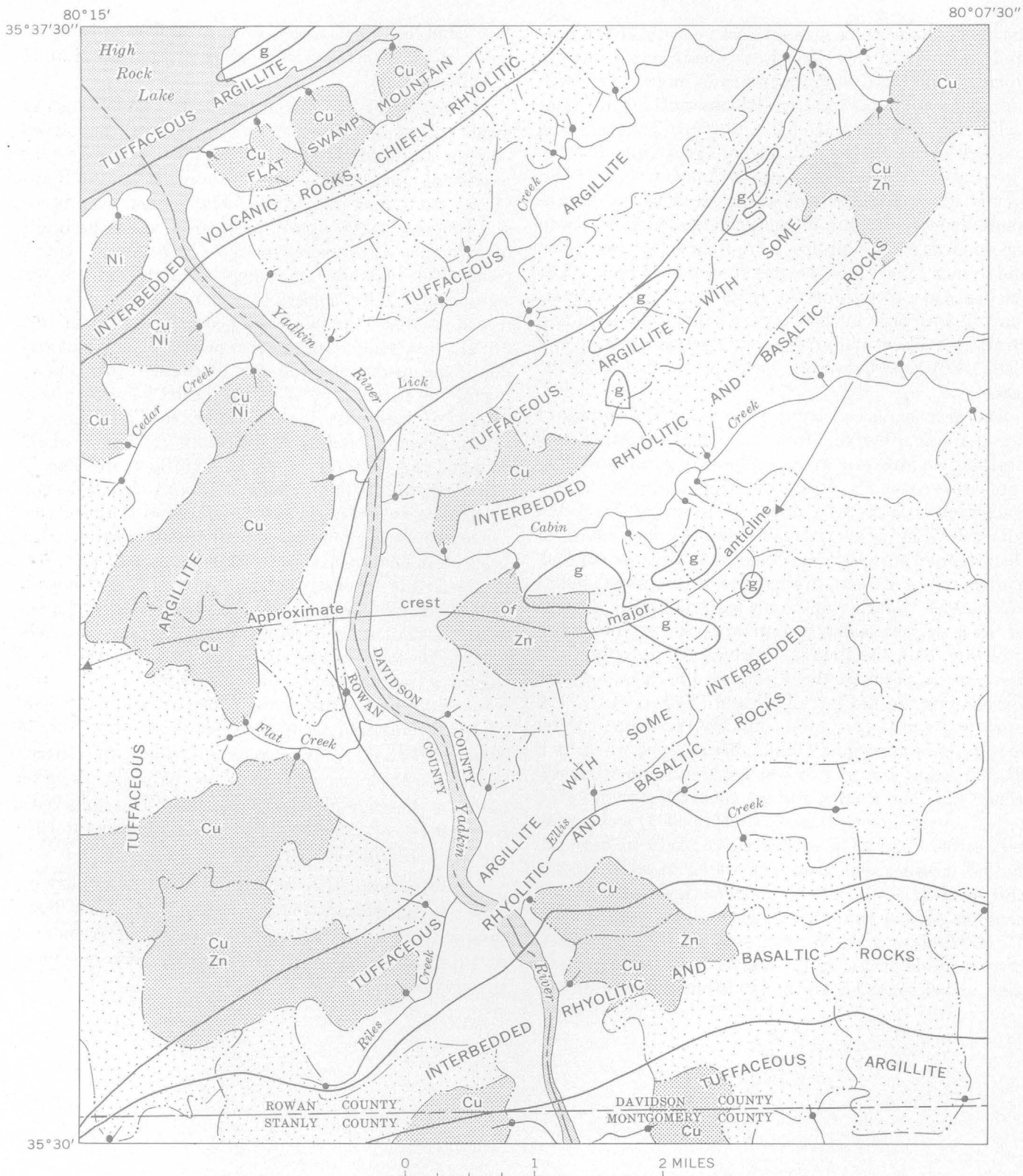


FIGURE 2.—Geochemical map of High Rock quadrangle, North Carolina, showing generalized lithology and the major geologic structure. Stippled areas are sampled drainage basins; heavy stipple designates basins in which samples contain at least 40 ppm copper (*Cu*), 75 ppm zinc (*Zn*), and 50 ppm nickel (*Ni*). Dots indicate sampled localities. Areas underlain by gabbro are indicated by *g*.

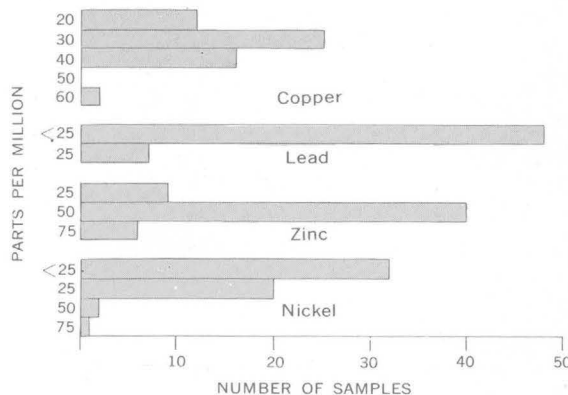


FIGURE 3.—Frequency distribution of copper, lead, zinc, and nickel in 55 samples of stream alluvium, High Rock quadrangle, North Carolina. Values for molybdenum and tungsten, not shown on diagram, were <4 and <20 ppm, respectively.

#### REFERENCES

- Bell, Henry, 3d, and Overstreet, W. C., 1960, Geochemical and heavy-mineral reconnaissance of the Concord quadrangle, Cabarrus County, North Carolina: U.S. Geol. Survey Mineral Inv. Field Studies Map MF-234.
- Conley, J. F., 1962a, Geology of the Albemarle quadrangle, North Carolina: North Carolina Dept. Conserv. and Devel., Div. Mineral Resources Bull. 75, 26 p., map.
- 1962b, Geology and mineral resources of Moore County, North Carolina: North Carolina Dept. Conserv. and Devel., Div. Mineral Resources Bull. 76, 40 p., map.
- Hawkes, H. E., Jr., 1957, Principles of geochemical prospecting: U.S. Geol. Survey Bull. 1000-F, p. 225-355.
- King, P. B., 1955, A geologic section across the southern Appalachians—an outline of the geology in the segment in Tennessee, North Carolina, and South Carolina, in Russell, R. J., ed., Guides to southeastern geology: Geol. Soc. America, p. 332-373, map in pocket.
- Laney, F. B., 1910, The Gold Hill mining district of North Carolina: North Carolina Geol. and Econ. Survey Bull. 21, 137 p.
- 1917, The geology and ore deposits of the Virgilina district of Virginia and North Carolina: North Carolina Geol. and Econ. Survey Bull. 26, 175 p.
- LeGrand, H. E., 1958, Chemical character of water in the igneous and metamorphic rocks of North Carolina: Econ. Geology, v. 53, no. 2, p. 178-189.
- Overstreet, W. C., and Bell, Henry, 3d, 1960, Geochemical and heavy-mineral reconnaissance of the Concord SE quadrangle, Cabarrus County, North Carolina: U.S. Geol. Survey Mineral Inv. Field Studies Map MF-235.
- Pogue, J. E., Jr., 1910, Cid mining district of Davidson County, North Carolina: North Carolina Geol. and Econ. Survey Bull. 22, 144 p.
- Stromquist, A. A., and Conley, J. F., 1959, Geology of the Albemarle and Denton quadrangles, North Carolina: Carolina Geol. Soc. Field Trip Guidebook, 36 p.
- Stuckey, J. L., 1928, The pyrophyllite deposits of North Carolina: North Carolina Dept. Conserv. and Devel., Div. Mineral Resources, 62 p.
- Stuckey, J. L., and Conrad, S. G., 1958, Explanatory text for the geologic map of North Carolina: North Carolina Dept. Conserv. and Devel., Div. Mineral Resources Bull. 71, p. 3-51, map.
- Ward, F. N., Lakin, H. W., Canney, F. C., and others, 1963, analytical methods used in geochemical exploration by the U.S. Geological Survey: U.S. Geol. Survey Bull. 1152, 100 p.
- White, A. M., Stromquist, A. A., Stern, T. W., and Westley, Harold, 1963, Ordovician age for some rocks of the Carolina slate belt in North Carolina: Art. 87 in U.S. Geol. Survey Prof. Paper 475-C, p. C107-C109.



## EVALUATION OF WEATHERING IN THE CHATTANOOGA SHALE BY FISCHER ASSAY

By ANDREW BROWN and IRVING A. BREGER,  
Northport, Ala., Washington, D.C.

*Abstract.*—Weathering of the Chattanooga Shale leads to oxidation of the organic matter. On Fischer assay this is reflected by increased yields of water and decreased yields of oil. Decrease in oil/water ratios, when plotted against water yields, provides an index for evaluating the degree of weathering to which the shale has been exposed. Low ratios are indicative of a high degree of weathering.

The pyrolytic oil yield of the Chattanooga Shale was determined on a large number of samples during studies of the shale as a possible source of uranium (Swanson, 1960). Brown (1956) had earlier reported the yields of oil from various parts of the shale. Analyses indicate a yield of 9 to 10 gallons of oil per ton over much of the area investigated—an oil content too low to be of present economic significance; in addition, the analyses provide information on the loss of oil yield in surface samples as a consequence of weathering processes. Fischer assays (Stanfield and Frost, 1949) of the black parts of the shale (the Gassaway Member and the lower unit of the Dowelltown Member) were made on samples from 13 surface exposures of different types, on samples from 5 drill holes that penetrated the shale at depths of from 136 to 360 feet, and on a sample from the abutment of a dam in southern Kentucky where the shale is far enough below the original land surface to be considered below the zone of surface oxidation and weathering.

The area covered by the study, shown in figure 1, is a belt extending about 80 miles northeast from Cannon County, Tenn., into southern Kentucky along the strike of the Chattanooga Shale. Throughout this area the evidence is strong that the black parts of the shale, where unaffected by weathering, will yield 9 to 10 gallons of oil per ton as shown by Fischer assay. About 10 miles south of this area the oil yield of the shale drops rather sharply to 5 to 6 gallons per ton, and 25 or 30 miles to the southeast, in Walden Ridge, Tenn., the yield is only 1 to 3

gallons per ton. North and northwest of the area, data are insufficient to permit tenable conclusions.

The lower unit of the lower or Dowelltown Member of the Chattanooga, which contains about 18 percent organic matter, is 5 to 6 feet thick south of the approximate latitude of Cookeville, Tenn. (fig. 1), but it thins northward and disappears as an identifiable unit about halfway between Cookeville and the Kentucky State line. Above it is the upper or gray unit of the Dowelltown, which contains less than 10 percent organic matter and yields only 2 to 3 gallons of oil per ton; analyses of this unit are not included in the data given. The upper Dowelltown has an average thickness of about 10 feet in the southern part of the mapped area but, like the lower unit, thins and disappears as an identifiable unit in northern Tennessee. The upper or Gassaway Member contains 20 to 25 percent organic matter and is or has been present throughout all the mapped area. It is thickest, about 21 feet, near locality 73 (fig. 1), but thins in all directions, becoming 11 to 13 feet thick at localities 88 and 101 to the south and southwest, and 13 to 17 feet thick near the Kentucky State line. North of that line, however, it thickens again to about 30 feet at locality 12.

In the area discussed, the oil yield of the lower unit of the Dowelltown Member is approximately the same as that of the Gassaway Member, and data from both units are given in the accompanying table. The data include assays of shale from the Gassaway Member at 19 localities and of shale from the lower unit of the Dowelltown Member at 13 localities, all in the southern part of the mapped area.

The Chattanooga Shale does not contain oil as such, its oil being derived from the carbonaceous constituents known as kerogen (Breger, 1961) on destructive distillation. The Fischer assays give not only the oil yield, but the water yield as well. Inasmuch as all samples are dried at 105° C before assay, the water shown is

*Oil and water yields and oil/water ratios of surface and subsurface samples of the Chattanooga Shale in parts of Tennessee and southern Kentucky*

[Localities are arranged generally from north to south and are shown on figure 1]

Locality No.	Unit <sup>1</sup>	Thickness (feet)	Yield (gallons per ton)				Oil/water ratios	
			Surface samples		Subsurface samples		Surface samples	Subsurface samples
			Oil	Water	Oil	Water		
12 <sup>2</sup>	G	29.10			10.4	4.0		2.6
16	G	17.65	5.6	6.0			0.9	
22	G	13.23	8.6	6.1			1.4	
27	G	17.82	6.3	8.0			.8	
58	G	17.93	9.2	5.8			1.6	
60	G	16.79	7.9	7.7			1.0	
64	G	19.58	9.5	5.6			1.7	
	DL	5.15	8.2	4.8			1.7	
66	G	17.27	5.2	6.8			.7	
	DL	6.05	3.2	7.8			.4	
73	G	21.51	11.1	7.0			1.6	
	DL	5.59	10.6	3.4			3.0	
C211	G	11.5			8.2	2.7		3.0
	DL	2.0			9.8	3.1		3.2
C37	G	17.43			11.6	3.3		3.5
	DL	3.11			8.8	3.6		2.5
C77	G	15.45			9.7	3.6		2.7
	DL	5.74			8.2	3.4		2.4
78	G	18.45	4.6	10.9			.4	
	DL	4.80	1.0	10.8			.1	
87	G	16.50	8.3	7.2			1.2	
	DL	6.47	10.0	4.6			2.2	
92	G	15.09	7.0	6.4			1.1	
	DL	6.10	5.1	7.7			.7	
C93	G	14.70			10.7	2.6		4.1
	DL	6.46			9.0	3.2		2.7
C94	G	14.00			10.8	2.1		5.1
	DL	5.85			10.3	2.8		3.7
88	G	13.42	9.6	9.0			1.1	
	DL	10.38	12.3	4.3			3.0	
101	G	13.35	8.7	4.6			1.9	
	DL	7.33	4.1	7.4			.6	

<sup>1</sup> G, Gassaway Member; DL, Lower unit, Dowelltown Member.

<sup>2</sup> Southern Kentucky; all other localities in northern Tennessee.

derived from the organic matter and, in part, from the clay constituents.

Oil and water yields obtained by Fischer assay of 32 samples of Chattanooga Shale are shown in the accompanying table and are plotted on figure 2. Examination of the points on figure 2 shows that a wide spread exists in values for outcrop samples, and that oil yields are generally higher and water yields lower for deep or core samples than for outcrop samples. These observations suggest that oxidation or weathering of the shale has led to decreased oil yield and increased water yield as shown by Fischer assay. Although the higher water yield might have resulted from oxidation of the organic matter, it could also be explained on the basis of hydration of the clay minerals in the shale. Inasmuch as the mineral content of these shale samples is generally constant, and the clay is primarily hydromica (Bates and Strahl, 1957) it seems likely that the water obtained on assay originates in the oxidized organic matter.

Oil yield, water yield, and the oil/water ratio shown by Fischer assay of 32 samples are listed in the table, and the relation between the water yield and the oil/water ratio is shown graphically on figure 3. For the subsurface samples of presumably unweathered shale (the subsurface localities, and locality 12), the oil yield ranges from 8.2 to 11.6 gallons per ton, the water yield from 2.1 to 4.0 gallons per ton, and the oil/water ratio from 2.5 to 5.1. For surface samples the range in yield is much wider; 1.0 to 12.3 gallons of oil per ton, and 3.4 to 10.9 gallons of water; the oil/water ratio ranges from 0.1 to 3.0. For all subsurface samples the average oil yield is 9.8 gallons per ton, the average water yield, 3.1, and the oil/water ratio, 3.2. For the surface samples the average values are 8.5 gallons of oil, 6.8 gallons of water, and an oil/water ratio of 1.3.

Unlike the rather consistent oil yield from subsurface samples, the yield from surface exposures differs in outcrops of different types. The highest yields are from the Gassaway Member at locality 73 where the

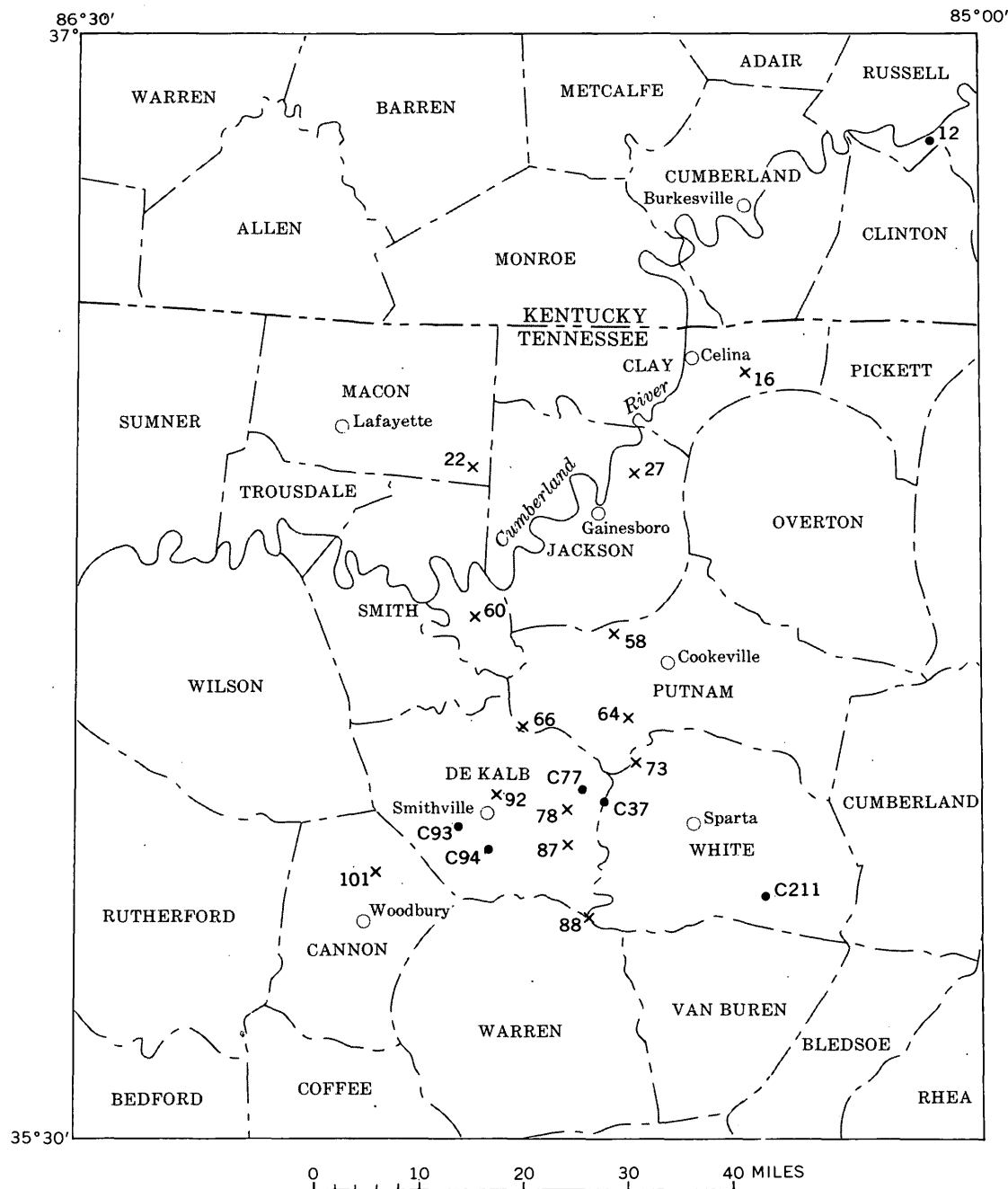


FIGURE 1.—Sketch map showing localities from which samples of the Chattanooga Shale were selected for analysis. Dot, subsurface locality; X, surface locality. Results of analyses are shown in the accompanying table.

rock is exposed in a waterfall, and from the Dowelltown Member at localities 73, 87, and 88, all of which are in the beds of perennial streams. The highest oil/water ratio (3.0) of all surface samples is from the lower unit of the Dowelltown at localities 73 and 88; the next highest (2.2) from the lower Dowelltown at locality 87.

Samples of both the Gassaway and Dowelltown Members from locality 64, and of the Gassaway Member at localities 87 and 88, were taken in bluffs protected to some extent by overhanging ledges of Fort Payne Chert. The oil yield at these exposures ranges from 8.2 to 9.6 gallons per ton, the water yield from 4.8 to 9.0 gallons, and oil/water ratio from 1.1 to 1.7. Compared to sub-

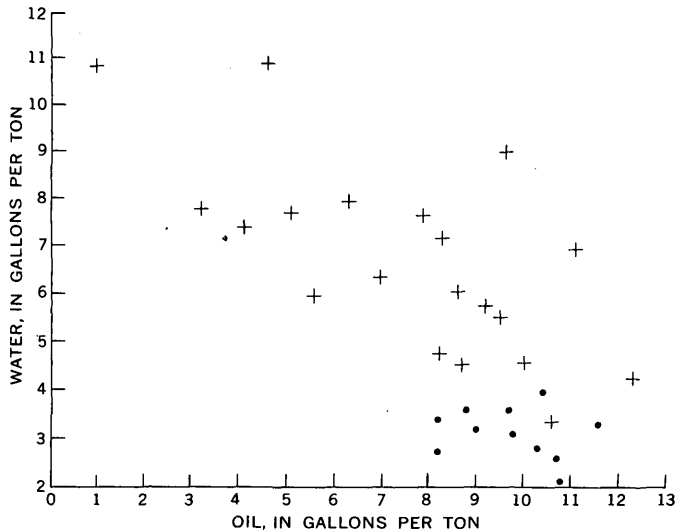


FIGURE 2.—Oil and water yields shown by Fischer assay of 32 samples of Chattanooga Shale. Dot, subsurface sample; cross, surface sample.

surface samples, the shale has acquired considerable water, but has lost little if any of its oil yield.

Nine of the surface localities (16, 22, 27, 58, 60, 66, 78, 92, and 101) are in old roadcuts where the present shale outcrop is nowhere more than a few tens of feet behind the original outcrop; the roads have been cut into steep hillsides, and the shale has been exposed to weathering for decades or centuries. Shale from these roadcuts shows the lowest oil yield, the highest water yield, and the lowest oil/water ratio of all localities studied.

The range in oil yield of the nine roadcut samples is from 1.0 to 9.2 gallons per ton, and the water yield ranges from 5.8 to 10.9 gallons per ton; the oil/water ratio is from 0.1 to 1.9. The lowest oil yield is in the surface shale from locality 78, which may be compared with that from drill hole C77, 0.3 mile to the north. The two samples from the outcrop show oil yields of 1.0 to 4.6 gallons per ton and oil/water ratios of 0.1 and 0.4; the two samples from the drill hole show oil yields of 9.7 and 8.2 gallons per ton and oil/water ratios of 2.7 and 2.4.

On the assumption, which seems well founded, that the shale at depth in the area shown in figure 1 yields 9 to 10 gallons of oil per ton and shows an oil/water ratio of about 2.5, certain conclusions as to the effect of weathering on the oil yield of the rock can be drawn. All surface exposures have acquired some additional water, but where the oil/water ratio is between 1.0 and 2.5 the apparent loss of oil yield is small. As weathering continues, however, to the point where the water yield is about the same or more than the oil yield, with

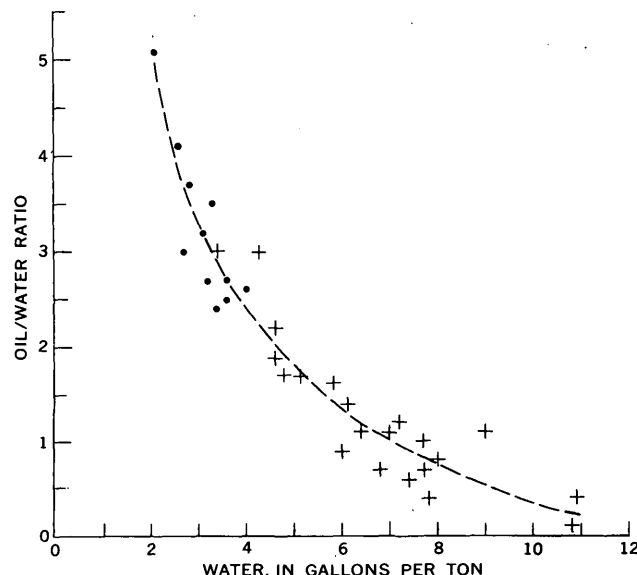


FIGURE 3.—Water yield and oil/water ratio shown by Fischer assay of subsurface (dot) and surface (cross) samples of Chattanooga Shale.

oil/water ratios of 1.0 or less, the continued addition of water is accompanied by loss of some of the kerogen in the rock, possibly through oxidation.

It is recognized that only subsurface samples are reliable indicators of the oil yield of rocks such as the Chattanooga Shale. The oil/water ratios of the rock from surface exposures in limited areas, however, can be used as a qualitative guide to loss through weathering. In the area here discussed, and in comparable areas where the yield and the oil/water ratio at depth are known with reasonable certainty, an oil/water ratio of 1.0 or less indicates that an appreciable amount of the oil yield has been lost through weathering.

#### REFERENCES

- Bates, T. F., and Strahl, E. O., 1957, Mineralogy, petrography and radioactivity of representative samples of Chattanooga shale: Geol. Soc. America Bull., v. 68, p. 1305-1313.
- Breger, I. A., 1961, Kerogen, in McGraw-Hill Encyclopedia of Science and Technology: New York, McGraw-Hill.
- Brown, Andrew, 1956, Uranium in the Chattanooga Shale of eastern Tennessee, in Page, L. R., Stocking, H. E., and Smith, G. B., compilers, Contributions to the geology of uranium and thorium by the United States Geological Survey and Atomic Energy Commission for the United Nations International Conference on Peaceful Uses of Atomic Energy, Geneva, Switzerland, 1955: U.S. Geol. Survey Prof. Paper 300, p. 457-462.
- Stanfield, K. E., and Frost, I. C., 1949, Method of assaying oil shale by a modified Fischer retort: U.S. Bur. Mines Rept. Inv. 4477, 13 p.
- Swanson, V. E., 1960, Oil yield and uranium content of black shales: U.S. Geol. Survey Prof. Paper 356-A, 44 p.



## MEASUREMENT OF RELATIVE CATIONIC DIFFUSION AND EXCHANGE RATES OF MONTMORILLONITE

By THOMAS E. BROWN, Denver, Colo.

**Abstract.**—To broaden the understanding of the effects of clay minerals on the quality of water, a technique was developed for determining the rate of cation exchange between a clay mineral and a contacting solution, together with the rate of cation diffusion into the clay and the solution. The technique consists of mounting the clay on a glass slide, converting the clay to a mono-ionic form, and then bring it into contact with a solution containing the cation that is to be exchanged. Mounting the clay on a glass slide permits instantaneous separation of the clay from the solution and therefore permits rate measurements for very brief intervals of time.

---

Clay minerals, with their cation-adsorption and exchange properties, have the ability to modify the chemical quality of contacting solutions. The change in the chemical quality of a solution resulting from contact with a clay mineral or group of clay minerals is directly related to: (1) the quantity and type of clay minerals in contact with the solution, (2) the quantity and types of cations originally adsorbed on the clay minerals, (3) the composition of the solution before contact with the clay minerals, and (4) the length of time that the solution is in contact with the clay minerals.

The first three variables can be evaluated by available techniques, but the fourth variable and its relation to the other three presents more of a problem.

Numerous workers have studied the rates of cation exchange between various clay minerals and neutral salt solutions. Gedroiz (1914), Cernsecu (1931), Borland and Reitemeier (1950), Lacy (1954), Faucher and Thomas (1954), Doepler and Young (1962), and Haagsma and Miller (1963) have described various aspects of ion exchange of clay minerals. A common difficulty of most workers who have studied exchange reaction rates is in the establishment of brief times of contact between the clay mineral and a solution.

The author has devised a simple technique by which contact between a clay mineral and a solution can be held to a time interval as brief as 1 second. The use of

clay mounted on glass slides permits a clean and easy separation of the clay from a contacting solution. The technique involves an initial saturation of the clay with a particular cation and subsequent treatment of the clay with a different cation for a measured interval of time.

A montmorillonite (Wyoming bentonite) was selected for this study. A suspension of the  $<2\mu$ -diameter fraction of the clay was prepared, and 2.5-milliliter volumes of the suspension were pipeted onto 26  $\times$  46 millimeter glass slides and allowed to dry. To convert the montmorillonite to a calcium form in which calcium occupied the interlayer, the slides were soaked in 1.0*N* calcium chloride solution for 15 minutes. X-ray diffraction analyses of random samples of the converted montmorillonite confirmed that calcium occupied the interlayer of the clay mineral.

The selection of calcium as the initial interlayer cation was based on the following considerations:

(1) Calcium montmorillonites are relatively abundant in nature.

(2) Calcium montmorillonites are characterized by two water layers in their interlayer position and, consequently, are easily recognized by the 15.4-Å (angstrom) spacing of the *d*(001) planes at 50-percent relative humidity.

(3) Montmorillonites have a marked preference for calcium over most monovalent cations. Thus, it was possible to contrast the exchange rates of less preferred cations (for example, potassium, sodium, and rubidium) with a more preferred cation (for example, cesium) when displacing calcium from a montmorillonite.

(4) Calcium can be determined quite easily and accurately in small quantities ( $<1.0$  parts per million).

Alkali metals were selected to displace calcium on the montmorillonites for two reasons:

(1) Only calcium and magnesium are more commonly adsorbed than the alkali metals on montmorillonites in nature.

(2) At 50-percent relative humidity, the single hydration level of alkali metals in the interlayer position of a montmorillonite results in a characteristic 12.4 Å spacing of the  $d(001)$  planes, as contrasted with the 15.4 Å spacing for calcium montmorillonite.

After the samples of clay (on slides) had soaked for 15 minutes in 1.0*N* calcium chloride solution, they were removed from the solution, rinsed thoroughly in distilled water, and then placed individually into separate 50-ml beakers filled with distilled water. Ten minutes of soaking effectively removed extraneous calcium chloride from the samples.

Next, the samples of clay were transferred from the distilled water to 50-ml beakers filled with a solution of the desired cation. After remaining submerged in the continuously agitated cation solution for a predetermined time, the samples were removed and then rinsed in distilled water. Calcium exchange was determined by measuring the calcium content of the cation solution, using the method given in Rainwater and Thatcher (1960, p. 127).

The question arises as to the ability of montmorillonite to remain on a glass slide during immersion in various salt solutions, especially when such solutions are being vigorously agitated. Usually, there was no apparent loss of clay from the slide during the entire treatment procedure. Occasional groups of slides had to be discarded when the clay would not adhere during immersion in the different salt solutions. This lack of adherence of the clay resulted from too large a quantity of the clay being present on the slide. Measurements were not made to determine the optimum thickness of the mounted clay. Slide-mounted kaolinite, illite, vermiculite, and nonmonomineralic clay-sized stream sediments were also checked as to their stability in agitated salt solutions and were found to be equally as stable as montmorillonite.

Total cation exchange for each of a group of three calcium-saturated samples of clay prepared at the same time was determined after the slides had remained submerged in a 0.1*N* cesium chloride solution for relatively long periods of time, usually 1, 2, or 3 hours. When the amount of calcium displaced from each of the three samples was in good agreement, complete exchange was assumed. Invariably, the agreement among the samples was good ( $\pm 5$  percent). These data also substantiated the assumption that weight differences among specimens prepared at the same time from the same suspension of clay were negligible. Knowing the total cation exchange and the quantity of clay on a slide, one can easily calculate the cation-exchange capacity of the clay.

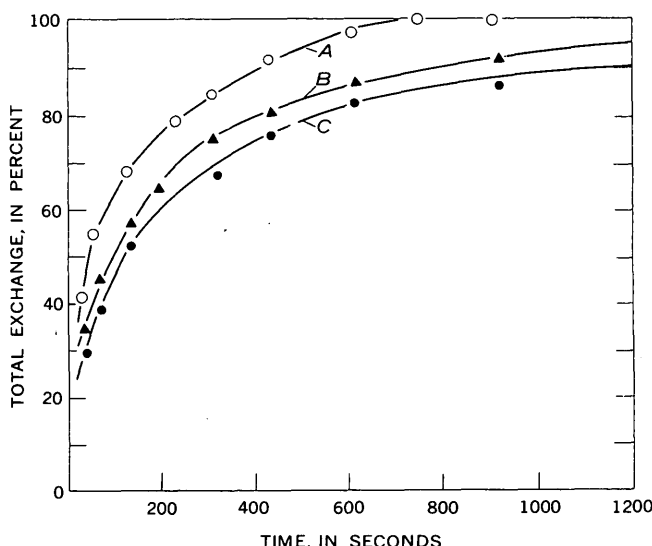


FIGURE 1.—Rate curves for displacement of calcium from slide-mounted montmorillonite by various alkali metals. A, agitated 0.025*N* CsCl solution; B, agitated 0.025*N* RbCl solution; and C, agitated 0.025*N* KCl solution.

Exchange reactions between calcium montmorillonite and potassium or cesium cations resulted in the fixation of appreciable quantities (>10.0 percent of total exchange) of the latter two cations. Cation fixation was the principal reason for not reusing the clay samples mounted on the glass slides.

Figure 1 illustrates the rate at which cesium, rubidium, and potassium in mechanically agitated solutions displace calcium on a montmorillonite. The curves show the combined effect of exchange reaction rate and gross diffusion of different cations on the clay. "Gross diffusion" is used herein to indicate the combined effect of cationic diffusion in solution and counterdiffusion of different cations on the adsorbent. "Counterdiffusion" is defined by Husted and Low (1954, p. 344) as the simultaneous diffusion of two different cations in opposite directions. Diffusion within the clay is anisotropic, and the two principal paths of diffusion are: (1) parallel to the  $d(001)$  planes, and (2) perpendicular to the  $d(001)$  planes along crystallite edges.

Boyd and others (1947), in their work on "organic zeolites", determined the exchange-rate controlling mechanism to be either diffusion in or through the adsorbent and (or) diffusional transport across a thin liquid film enveloping the particle. They discounted the chemical exchange of different cations on the adsorbent as a rate-influencing factor.

Diffusion in or through the adsorbent, if a major factor, would manifest itself if mounted clays having different clay thicknesses were subjected to the same treat-

ment for the same time interval. The standard clay suspension (thick) was then diluted 100 percent to form a relatively thin clay suspension (thin) from which slides were made.

Combined exchange and diffusion rates were measured for thick and thin clay samples in both agitated and nonagitated solutions. The effect of solution agitation, maintained by a magnetic stirrer, on the rate curves is shown on figure 2.

The facts that both thick and thin samples when immersed in agitated solution yielded results that fell on the same rate curve (*A*), and that this curve is markedly displaced with respect to the separate rate curves for thin (*B*) and thick (*C*) samples in unagitated solutions suggest that the measured exchange rates are in part functions of the mobility of ions in solution and (or) the diffusion of cations across the particle-enveloping film. The separation between curves *C* and *D* is attributed to rapid depletion of exchanging cations in the unstirred solution next to the clay, with the result that a small amount of clay undergoes total exchange more rapidly than a large amount of clay.

One of the principal benefits derived in using samples of clay mounted on slides is the ease with which X-ray diffraction studies can be coordinated with rate studies. Figure 3 illustrates the diffraction results obtained in the calcium montmorillonite to cesium montmorillonite transition. The X-ray diffraction tracings illustrated on figure 3 were obtained at an approximate 20-percent relative humidity, with the exception of tracing *A*, which was obtained at 50-percent relative

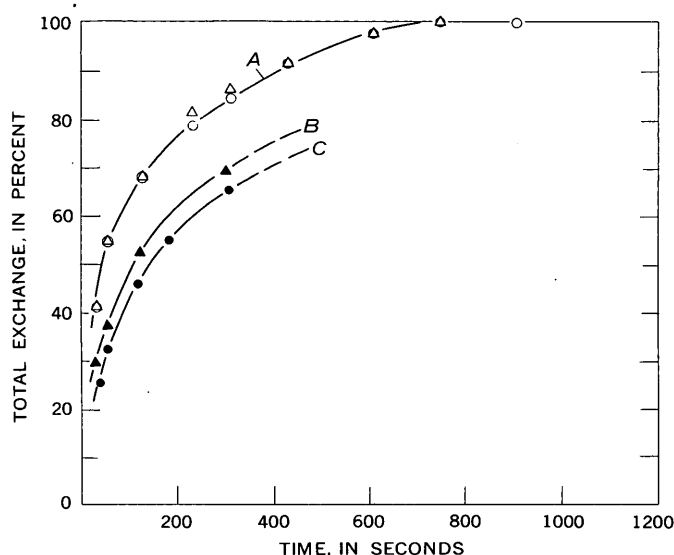


FIGURE 2.—Effect of solution agitation on rate curves for calcium clay-cesium solution exchange. *A*, agitated solution for both thick (open triangles) and thin (open circles) clay slides; *B*, nonagitated solution for thin clay; and *C* nonagitated solution for thick clay.

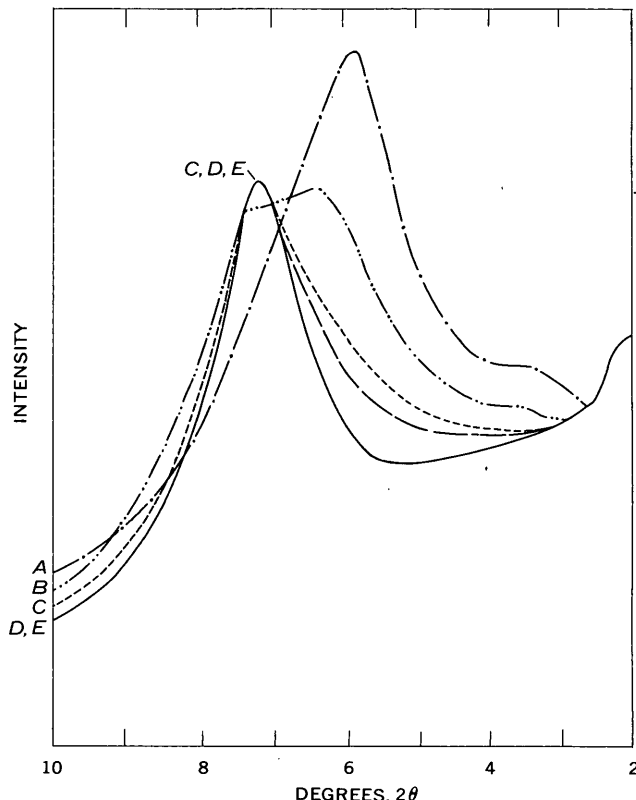


FIGURE 3.—Smoothed X-ray diffraction tracings of the calcium montmorillonite to cesium montmorillonite transition, showing region of the  $d(001)$  peak. *A*, 100-percent calcium montmorillonite; *B*, 71.5-percent calcium montmorillonite; *C*, 40.9-percent calcium montmorillonite; *D*, 9-percent calcium montmorillonite; and *E*, 100-percent cesium montmorillonite. (Ni-filtered  $\text{CuK}\alpha$  radiation).

humidity. This would account for the similarity of the  $d(001)$  peaks for tracing *C*, *D*, and *E*.

Figure 3 is also noteworthy in that it emphasizes two facts previously reported by many workers in the field of clay mineralogy, namely: (1) qualitative analysis of the interlayer cation of montmorillonite should not be based solely on the position of the  $d(001)$ , and (2) a controlled humidity is essential when studying montmorillonites with X-ray diffraction. In this work, a humidity control was not available and, consequently, ambient values were recorded.

Temperature effects on cation exchange can be measured with the aid of a constant-temperature bath. Studies on montmorillonite in the temperature range from 24° to 48°C. showed that the rate of exchange increased significantly as the temperature of the solution increased. All experimental work reported in this article was done at room temperature (about 26°C).

The technique described in this article applies not only to montmorillonite but also to other clay minerals. The rate of cation exchange between clay minerals and solutions and the diffusion of cations in the clay min-

erals and solutions indicate the effect that these earth materials have on quality of water. In addition, rate studies may provide a means of differentiating various clay minerals in stream sediments.

#### REFERENCES

- Borland, J. W., and Reitemeier, R. F., 1950, Kinetic exchange studies on clays with radioactive calcium: *Soil Sci.*, v. 69, p. 251-260.
- Boyd, G. E., Schubert, J., and Adamson, A. W., 1947, The exchange adsorption of ions from aqueous solutions by organic zeolites; pt. 2. Kinetics: *Am. Chem. Soc. Jour.*, v. 69, p. 2836-2848.
- Cernescu, N. C., 1931, Kationenumtausch und Struktur: *Inst. Geol. Romaniei Anuar.*, v. 16 p. 777-859. (Chem. Abs., v. 29, 3897, 1935.)
- Doebler, R. W., and Young, W. A., 1962, Some conditions affecting the adsorption of quinoline by clay, in Swineford, Ada, ed., National Conference on Clays and Clay Minerals, 9th, Lafayette, Indiana, 1960, Proc.: New York, Pergamon Press, p. 468-483.
- Faucher, J. A., and Thomas, H. C., 1954, Adsorption studies on clay minerals; pt. 4. The system montmorillonite-cesium-potassium: *Jour. Chem. Physics*, v. 22, p. 258-261.
- Gedroiz, K. K., 1914, Colloidal chemistry as related to soil science; pt. 2. Rapidity of reaction exchange in soil; the colloidal condition of the soil saturated with various bases; and the indicator method of determining the colloidal content of the soil: *Zhur. opty. agron. [USSR]*, v. 15, p. 181-205. (Translated by S. A. Waksman and distributed by U.S. Dept. Agriculture.)
- Haagsma, T., and Miller, M. H., 1963, The release of non-exchangeable soil potassium to cation-exchange resins as influenced by temperature and exchangeable ion: *Soil Sci. Soc. America Proc.*, v. 27, p. 153-156.
- Husted, R. F., and Low, P. F., 1954, Ion diffusion in bentonite, *Soil Sci.*, v. 77, p. 343-353.
- Lacy, W. J., 1954, Decontamination of radioactively contaminated water by slurring with clay: *Indus. Eng. Chemistry*, v. 46, p. 1061-1065.
- Rainwater, F. H., and Thatcher, L. L., 1960, Methods for collection and analysis of water samples: U.S. Geol. Survey Water-Supply Paper 1454, 301 p.



## PRELIMINARY STRUCTURAL ANALYSIS OF EXPLOSION-PRODUCED FRACTURES, HARDHAT EVENT, AREA 15, NEVADA TEST SITE

By F. N. HOUSER and W. L. EMERICK, Denver, Colo.

*Work done in cooperation with the U.S. Atomic Energy Commission*

**Abstract.**—The HARDHAT nuclear explosion was detonated at a depth of 950 feet in a granodiorite and quartz monzonite stock. Postshot studies, conducted in the station-1500 tunnel at radial distances of from 430 to 520 feet from the center of the detonation, showed that many explosion-produced fractures (1) differ in orientation from pre-explosion fractures, (2) are related to directions of shear and tension resulting from stress originating at the detonation point, and (3) indicate by their orientation that the direction of propagation of the stress wave was deflected to the southeast from the normal as a result of a predominant set of preexplosion joints.

The HARDHAT nuclear explosion, with an approximate yield of 5 kilotons, was detonated on February 15, 1962, at a depth of 950 feet in granitic rock of the Climax stock (Houser and Poole, 1960). The Climax Stock consists predominantly of an older granodiorite and a younger porphyritic quartz monzonite in which aplite dikes are locally common. Although the proportions of essential minerals vary appreciably in the two granitic rocks, the differences are not enough to greatly affect the bulk chemistry. Hydrothermal alteration in the granodiorite and quartz monzonite has formed small amounts of clay, sericite, albite, orthoclase, pyrite, and quartz. The stock is exposed over an area of about 1½ square miles and probably has a minimum thickness of at least 15,000 feet.

Prior to the event, the station-1500 tunnel, herein called the 1500 tunnel for convenience, extended directly toward the U15a drill hole at a depth of 783 feet (elevation 4,253 feet) for a distance of 616 feet from the bottom of the station-1500 shaft (fig. 1). The end of the tunnel was 181 feet horizontally and 89 feet vertically from the shot point, which was at an elevation of 4,164 feet. The postshot structural features exposed in the

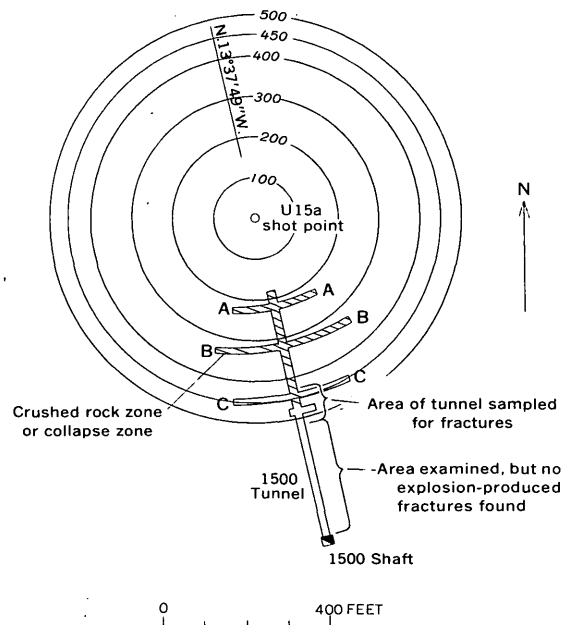


FIGURE 1.—Generalized map of the 1500 tunnel used in the HARDHAT event, showing zones crushed and collapsed by the U15a explosion.

1500 tunnel were mapped in May 1962, by W. L. Emerick, J. W. Hasler, R. P. Snyder, and W. H. Laraway.

### COMPARISON OF EXPLOSION-PRODUCED FRACTURES WITH THE PRE-HARDHAT NATURAL FRACTURES

The two most conspicuous sets of explosion-produced fractures have the following average orientations: N. 42° W. (strike), 88° NE. (dip); and N. 65° W., 71° SW. (sets A and B respectively, fig. 2). Three less obvious groups of similarly oriented joint sets have the following average attitudes: N. 72° W. (strike), 85° NE. (dip); N. 70° E., 88° SE.; and N. 65° E., 50° NW.

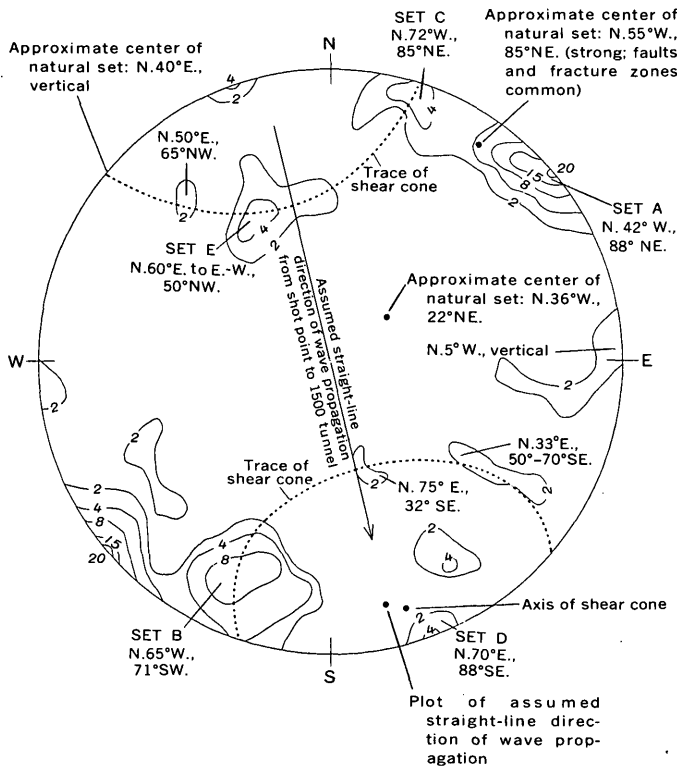


FIGURE 2.—Contour diagram of 51 poles of explosion-produced fractures mapped in the 1500 tunnel. All plots are on the upper hemisphere of an equal-area projection; contour intervals are in percent. Preexplosion fractures are referred to as "natural." Modified by annotation from contour diagram by Emerick, Snyder, and Bowers (written communication, 1962).

(sets *C*, *D*, and *E*, respectively, fig. 2). It can be seen that none of the attitudes agrees with the three predominant preexplosion natural fracture sets of N. 55° W. (strike), 85° NE. (dip); N. 36° W., 22° NE., and N. 40° E., vertical dip. The explosion-produced set striking N. 42° W., and dipping 88° NE. is the only one that is close (about 13°) to a preexplosion set in attitude. This one set in the explosion-produced group of fractures is nearly parallel to a tension direction related to the stress-propagation direction in the vicinity of the tunnel, and its prominence may be attributed to its near relationship to the preexplosion set striking N. 55° W. and dipping 85° NE. The preexplosion set striking N. 36° W., and dipping 22° NE. is not represented in any way in the observed postshot fractures, and only a few individual postexplosion joints are near in attitude to the moderately strong preexplosion set striking N. 40° E. and dipping vertically.

#### EXPLOSION-PRODUCED SHEAR AND TENSION FRACTURES

It is to the less pronounced explosion-produced fractures that we must turn to define the relation between

the tension and shear fractures and the direction of propagation of the stress wave (fig. 2).

The fractures parallel to shear directions related to the direction of propagation are defined by 6 partly linear groups that comprise about 115° of the total 360° of the cone of shear. Although these groups are of low fracture density, they are designated "sets" on figure 2 for convenience in annotation only. The moderately pronounced set *B*, striking N. 65° W. and dipping 71° SW., includes shear fractures, but it defines only part of a cone of shear, the approximate center of which is the stress-wave propagation direction. Explosion-produced fractures of five other general orientations further define the cone of shear. The attitudes of these are in the vicinity of (1) N. 75° E. (strike), 32° SE. (dip); (2) N. 33° E., 50°–70° SE.; (3) N. 50° E., 65° NW., (4) N. 60° E. to E-W., 50° NW.; and (5) N. 72° W., 85° NE. (fig. 2). Most of these fractures are joints, but explosion-produced faults are also common in the N. 65° W. (strike), 71° SW. (dip) (set *B*) and N. 70° E., 88° SE. (set *D*) groups. It is believed that the pronounced concentration of shear fractures with the general attitude of N. 65° W. (strike) and 71° SW. (dip) (set *B*) were formed where a shear direction could avail itself of preexplosion natural fractures, probably belonging to the set striking N. 55° W. and dipping 85° NE.

The trace of the cone of shear defined by these six groups is shown by lines of dots in figure 2. Points on this trace are at generally approximately equal angular distances from the polar plot of the direction of the stress wave. The trace is asymmetric with respect to the center of the plot because the explosion occurred in a direction at about negative 12° below the interval of tunnel surveyed and represented on figure 2.

The explosion-produced tension fractures approximately perpendicular to the direction of propagation of the stress wave are indicated as striking about N. 70° E. and dipping 88° SE. (set *D*). Tension fractures approximately parallel to the direction have two main attitudes: N. 42° W. (strike), 88° NE. (dip) (set *A*) and N. 5° W., vertical dip. Most of these tension fractures have orientations of the first of the above types and were influenced probably by the pronounced natural fracture set striking N. 55° W. and dipping 85° NE.

#### DIRECTION OF PROPAGATION OF STRESS WAVE

The 1500 tunnel is oriented parallel to, and 89 feet above, a horizontal radial line projected from the HARD-HAT shot point, as shown in figures 1 and 3. The interval of tunnel in which fractures were measured is between 430 and 520 feet from the point of detonation.

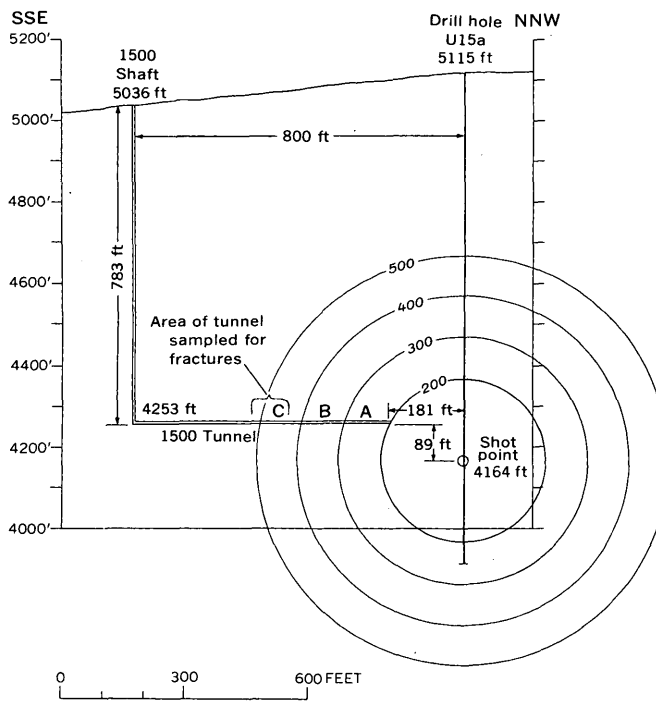


FIGURE 3.—Generalized section of the 1500 tunnel, showing relation of the tunnel to shot point.

The average angle between the tunnel interval examined and the shot point is  $12^\circ$  from the horizontal, but ranges from  $13^\circ$  at the end near the shot (430 feet) to  $11^\circ$  at the limit of fracturing (520 feet).

Features of the explosion-produced fractures suggest that the stress wave did not pass parallel to the straight-line direction from the shot point to the tunnel, at the midpoint in the radial-distance interval of 430 to 520 feet. Rather, the stress wave was deflected slightly to the southeast. Four features which indicate this horizontal change in direction are:

- (1) The average counterclockwise deflection of about  $6^\circ$  of the shear fractures that strike approximately perpendicular to the line of the tunnel.
- (2) The average counterclockwise deflection of about  $7^\circ$  of the tension fractures that strike approximately perpendicular to the line of the tunnel.
- (3) The approximately  $3^\circ$  clockwise deflection of the center of the trace of the cone of shear as defined by the interpreted shear fractures.
- (4) The approximately  $9^\circ$  clockwise deflection of the bisectrix of the tensional fractures approximately parallel to the theoretical direction of propagation. The bisectrix is used here rather than the average because it is thought that the

high frequency of the set striking N.  $42^\circ$  W. and dipping  $88^\circ$  NE. (set A, fig. 2) is due to the strong preexplosion set striking N.  $55^\circ$  W. and would unduly influence such an average.

The reason for the horizontal deflection of  $3^\circ$  to  $9^\circ$  is thought to lie in the implied tendency of the stress waves to parallel the very strong preexplosion set striking N.  $55^\circ$  W. and dipping  $85^\circ$  NE. The average angles of incidence of an assumed straight-line stress-wave propagation to the fractures striking N.  $55^\circ$  W. and dipping  $85^\circ$  NE. would be  $42^\circ$  horizontally and  $70^\circ$  vertically. The only other preexplosion set worthy of consideration is that striking N.  $40^\circ$  E. and dipping vertically. This set was found by pretest surface and subsurface mapping to be somewhat less open than the set striking N.  $55^\circ$  W. and only about a third as frequent in occurrence.

#### SUMMARY

It is concluded that new, postshot fractures (1) differ in attitude from the preexplosion natural fractures, (2) are related to directions of shear and tension resulting from stress originating at the detonation point, and (3) indicate by their orientation that the direction of propagation of the stress wave was deflected  $3^\circ$  to  $9^\circ$  to the southeast from the normal as a result of a predominant set of preexplosion joints.

This may be the first well-illustrated example for estimating the influence of preexisting fractures on the distortion of a shock wave in a rock medium. Examples of deflection in strain are often observed in nature, but frequently the direction of stress is unknown or surmised. Here at the site of the HARDHAT event the source is known.

For any future experiments in the Climax stock, in which the direction of stress-wave propagation would be critical in interpreting effects, consideration should be given to the orientation and frequency of existing natural fracture systems so as to minimize their influence. Those parts of stress waves moving in horizontal or nearly horizontal directions approximately parallel to the average strikes of the N.  $55^\circ$  W. and N.  $40^\circ$  E. natural sets should be influenced the least in the manner described in this report.

#### REFERENCE

Houser, F. N. and Poole, F. G., 1960, Preliminary geologic map of the Climax stock and vicinity, Nye County, Nevada: U.S. Geol. Survey Misc. Geol. Inv. Map I-328, 2 sheets.



## SEISMICITY OF THE LOWER EAST RIFT ZONE OF KILAUEA VOLCANO, HAWAII, JANUARY 1962–MARCH 1963

By ROBERT Y. KOYANAGI, Hawaiian Volcano Observatory

**Abstract.**—Eight-hundred and forty small, shallow earthquakes from the lower eastern part of the Kilauea east rift zone were recorded at Pahoa between January 1962 and March 1963. Ninety-four percent of these earthquakes, including some that were felt, were smaller than magnitude 2. The largest was of magnitude 4.0. Instability of the flank of Kilauea south of the east rift zone is indicated by the concentration of foci south of the surface trace of the rift zone.

Following the brief eruption of Kilauea along the central part of its east rift zone in September 1961 (Moore and Richter, 1962), frequent earthquakes emanated from the lower part of the rift zone and adjacent southeast flank of the volcano for many months. Earthquakes from this region, lat 19°21' N. to 19°33' N. and long 154°46' W. to 155°06' W. (fig. 1), that occurred from January 1962 through March 1963 were studied to determine what light they might shed on the structure of this portion of the volcano.

The seismograph at Pahoa recorded 840 earthquakes ranging in magnitude from 0.5 to 4.0 on the Richter scale during this period. At Pahoa these earthquakes were characterized by strong, sharp first motion, high frequency (5 to 10 cycles per second), and short total duration ( $\frac{1}{2}$  to 2 minutes). Almost all the quakes produced compressional first motion at Pahoa.

Earthquakes of magnitude 2 or greater were generally well recorded on the Kilauea seismic network and at Hilo, as well as at Pahoa (fig. 1) (see also Krivoy and others, 1963; Koyanagi and others, 1963; Okamura and others, 1963; Okamura and others, 1964; and Krivoy and others, 1964, for a description of stations and instruments of the seismic network). Foci were determined from P arrival times interpreted on the basis of traveltimes obtained from the March 7, 1955, earthquake in southeast Hawaii (Eaton, 1962, fig. 2, model B). The very large number of smaller quakes that originated within 15 to 20 kilometers of Pahoa

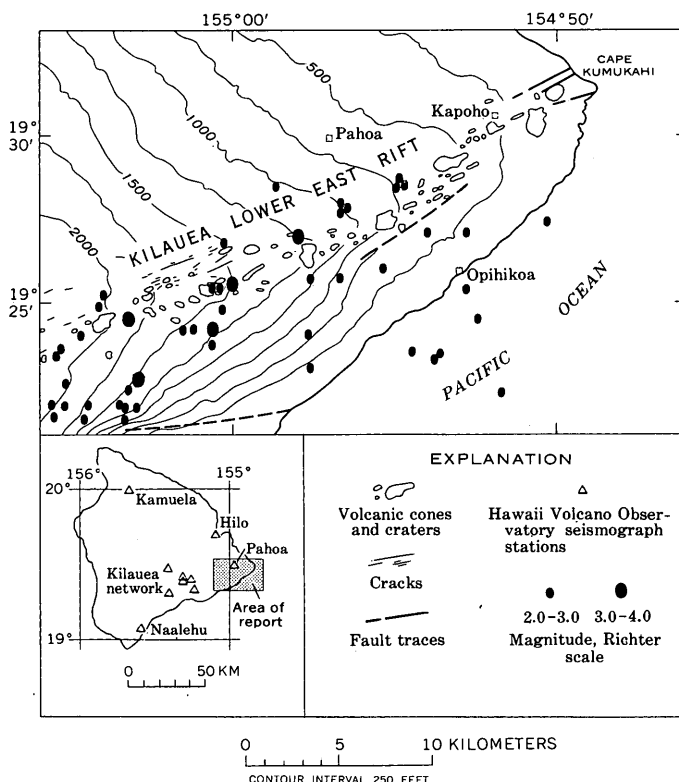


FIGURE 1.—Plot of earthquake epicenters (elongated dots) along the lower east rift zone of Kilauea, during January 1962–March 1963. Cones, craters, cracks, and fault traces after Stearns and Macdonald (1946).

were poorly recorded at other stations, where their first arrivals were often indistinct.

Epicenters of quakes of magnitude 2.0 and greater are plotted on figure 1. Most of these quakes came from depths of 3 to 8 km. The two deepest quakes of the group had magnitudes of 2.5 and 2.8 and originated at a depth of about 12.5 km at lat 19°22' N., long 155°03' W. Several deeper earthquakes (about 45 km) occurred a few kilometers southwest of the region considered here (Koyanagi, 1964).

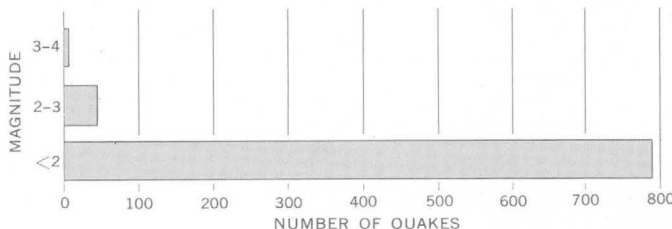


FIGURE 2.—Magnitudes of quakes along the Kilauea lower east rift recorded at Pahoa during January 1962–March 1963. The smallest earthquakes from this region that could be discerned on the Pahoa seismograms had magnitudes of about 0.5.

Of the 840 quakes recorded at Pahoa, 790 (94.0 percent) were smaller than magnitude 2.0 (fig. 2). Forty-five (5.4 percent) had magnitudes of 2.0 to 3.0; and five (0.6 percent) had magnitudes of 3.0 or greater.

The largest earthquake of the group was of magnitude 4.0. It took place 14 km southwest of Pahoa at a depth of about 5 km on January 7, 1962. It was felt throughout the island, but no damage was reported. Several earthquakes smaller than magnitude 2.0, presumably from the immediate vicinity of Pahoa or Kapoho, were felt as sharp vibrations lasting only 1 or 2 seconds by residents of these communities.

The number of quakes recorded at Pahoa per week (fig. 3) ranged from 0 to 58. Periods of increased seismic activity alternating with relatively quiet periods occurred at intervals of 3 to 7 weeks. The most striking feature of the curve is the 2 months of very low seismic activity on the lower east rift zone after the brief eruption of Kilauea in and near Aloia Crater on the upper

east rift zone during December 7–10, 1962. This period of inactivity was terminated at the end of February 1963 by 2 weeks of frequent earthquakes; 48 quakes were recorded during the week that ended on March 11.

When considered in the context of events at Kilauea following the 1960 flank eruption near Kapoho (Richter and Eaton, 1960), the high level of seismic activity along the lower east rift zone from January 1962 through March 1963 appears to be closely related to the rapid refilling of the shallow reservoir beneath the Kilauea summit (Eaton, 1962) that began in the autumn of 1960. Also, the drop in reservoir pressure caused by the small eruption in December 1962 seems temporarily to have relieved stresses usually applied through the fluid core of the rift zone to the lower (eastern) part of the rift zone.

The preponderance of shallow earthquakes and the absence of foci deeper than about 12 km indicate that the lower part of the rift zone is confined largely to the pile of volcanic rocks on the ocean floor and that it does not penetrate the mantle. Lateral transmission of magma demonstrated in recent flank eruptions (Eaton, 1962) also supports the idea of a shallow rift zone.

The asymmetry in the distribution of earthquakes, with the rift zone itself being the northern limit of concentrated epicenters, shows the instability of Kilauea's southeast flank, which is broken by numerous normal faults that approximately parallel the rift zone and have downward displacement on the seaward blocks.

The author wishes to express sincere appreciation to Jerry P. Eaton, U.S. Geological Survey, for his suggestions and assistance in organizing this article.

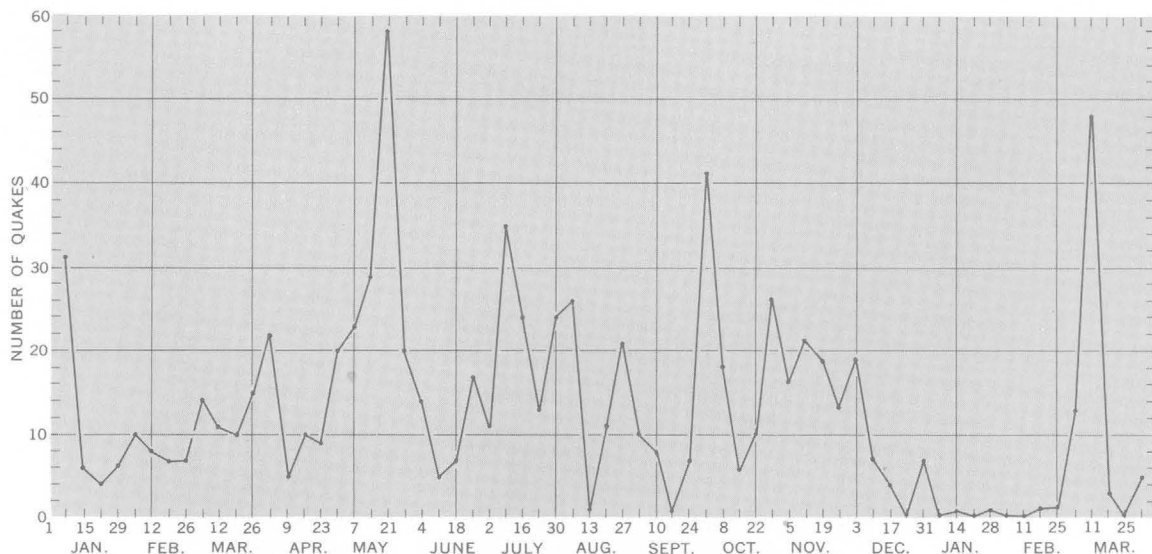


FIGURE 3.—Weekly frequency of earthquakes along the lower east rift zone recorded at Pahoa, January 1962–March 1963.

**REFERENCES**

- Eaton, J. P., 1962, Crustal structure and volcanism in Hawaii, in Macdonald, G. A., and Kuno, Hisachi, eds., Crust of the Pacific Basin: Am. Geophys. Union, Geophys. Mon. 6, p. 13-29.
- Koyanagi, R. Y., 1964, Hawaiian seismic events during 1962: Art. 144 in U.S. Geol. Survey Prof. Paper 475-D, p. D112-D117.
- Koyanagi, R. Y., Krivoy, H. L., and Okamura, A. T., 1963, Hawaiian Volcano Observatory summary: U.S. Geol. Survey Hawaiian Volcano Observatory Summary 25, (Jan., Feb., and March 1962).
- Krivoy, H. L., Koyanagi, R. Y., and Okamura, A. T., 1963, Hawaiian Volcano Observatory summary: U.S. Geol. Survey Hawaiian Volcano Observatory Summary 24, (Sept., Oct., and Dec. 1961).
- Krivoy, H. L., Koyanagi, R. Y., Okamura, A. T., and Kojima, George, 1964, Hawaiian Volcano Observatory summary: U.S. Geol. Survey Hawaiian Volcano Observatory Summary 28, (Oct., Nov., and Dec. 1962). [In press]
- Moore, J. G., and Richter, D. H., 1962, The 1961 flank eruption of Kilauea Volcano, Hawaii [abs.]: Trans. Am. Geophys. Union, 43, p. 446.
- Okamura, A. T., Koyanagi, R. Y., and Krivoy, H. L., 1963, Hawaiian Volcano Observatory summary: U.S. Geol. Survey Hawaiian Volcano Observatory Summary 26, (April, May, and June 1962).
- Okamura, A. T., Kojima, George, and Yamamoto, Akira, 1964, Hawaiian Volcano Observatory summary: U.S. Geol. Survey Hawaiian Volcano Observatory Summary 27, (July, Aug., and Sept. 1962).
- Richter, D. H., and Eaton, J. P., 1960, The 1959-60 eruption of Kilauea Volcano: The New Scientist, v. 7, p. 994-997.
- Stearns, H. T., and Macdonald, G. A., 1946, Geology and groundwater resources of the Island of Hawaii: Hawaii Div. Hydrography Bull. 9, 363 p.



## PALEOLATITUDINAL AND PALEOGEOGRAPHIC DISTRIBUTION OF PHOSPHORITE

By RICHARD P. SHELDON, Denver, Colo.

**Abstract.**—Recent phosphorite has been shown to occur at warm latitudes, between the equator and the 40th parallels. Ancient phosphorite commonly is found at much higher latitudes. When occurrences of ancient phosphorite are located according to their virtual geomagnetic poles, their resulting paleolatitudinal distribution closely matches the latitudinal distribution of young phosphorite. Also, the paleogeographic setting of ancient phosphorite matches the geographic setting of young phosphorite. Thus, the combined study of paleomagnetic and paleogeographic data will aid in the search for ancient phosphorite.

V. E. McKelvey (1963) has shown that Recent and upper Tertiary phosphorite is a fairly common sediment, but that it occurs only in certain geographic positions. It is deposited in warm climates between the 40th parallels, mainly on the west coasts of continents, but also in small part on the other coasts.

Older phosphorite shows no such clear-cut geographic distribution. For an extreme example, Mississippian and Triassic phosphorite occurs on the north slope of the Brooks Range in Alaska, north of the Arctic Circle (Patton and Matzko, 1959).

This difference in distribution between young (late Tertiary to Recent) and old (pre late Tertiary) phosphorite suggests either that the warm climatic belts at one time extended to higher latitudes than at present, or that the positions of the climatic belts have changed with respect to the continents. In order to test these alternatives, the distribution of ancient phosphorite has been plotted with respect to the virtual geomagnetic poles at the time of its deposition. With this orientation, the difference in latitude at the time of deposition between the young and old phosphorite disappears, suggesting that the positions of climatic belts have changed with respect to the continents.

Thus, a new approach to the exploration for ancient phosphorite is possible. Study of the paleogeography in the proper paleolatitude of each geologic system of each continent may reveal many areas favorable for the existence of phosphate deposits.

This article is an outgrowth of the phosphate research of the U.S. Geological Survey, largely under the direction of V. E. McKelvey. Many people have been helpful in supplying data and in criticizing the article. In particular I would like to thank V. E. McKelvey, Warren Hamilton, J. B. Cathcart, F. G. Poole, Cleaves Rogers, and E. R. Cressman of the U.S. Geological Survey, T. M. Cheney of Nicol Industrial Minerals, and L. T. Grose of Colorado College.

### LATITUDINAL DISTRIBUTION OF YOUNG PHOSPHORITE

McKelvey (1963, fig. 2) showed the distribution of Recent phosphorite in the ocean and pointed out that geologically young phosphorite has a similar distribution. His data are given in table 1, together with those for a few occurrences of upper Tertiary phosphorite, and are plotted in graphical form on figure 1. The

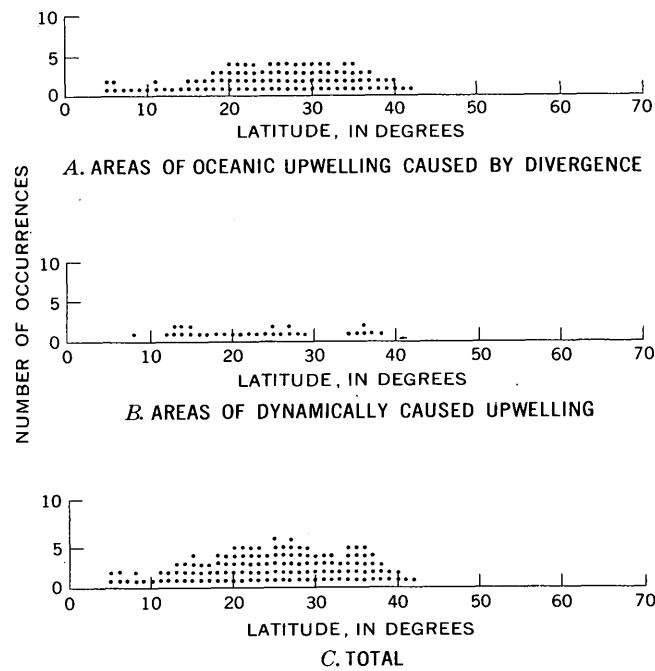


FIGURE 1.—Distribution of young (Recent and late Tertiary) phosphorite.

TABLE 1.—*Distribution of young phosphorite*

Area	Latitude	Source of data
<b>RECENT PHOSPHORITE</b>		
Deposited in areas of oceanic upwelling caused by divergence		
Southwestern North America	25°–42° N	McKelvey (1963).
Western South America	5°–40° S	Do.
Venezuela	11° N	Do.
Northwest Africa	15°–32° N	Do.
Southwest Africa	18°–35° S	Do.
Ghana, Africa	5° N	Do.
Australia	20°–23° S	Do.
Deposited in areas of dynamically caused oceanic upwelling		
Red Sea	12°–27° N	McKelvey (1963).
Southern India	8° N	Do.
Brazil	36°–38° S and 13°–15° S	Do.
Southern Florida	25° N	Do.
North Carolina	34° N	Do.
<b>UPPER TERTIARY PHOSPHORITE</b>		
Deposited in areas of oceanic upwelling caused by divergence		
California (Monterey Formation, Miocene)	34°–37° N	Bramlette (1946).
Sechura, Peru (Miocene)	6° S	T. M. Cheney (oral communication, 1961).
Deposited in areas of dynamically caused oceanic upwelling		
Florida (Hawthorn Formation, Miocene)	27°–29° N	Cathcart and others (1953).
North Carolina (Miocene)	35°–36° N	J. B. Cathcart (oral communication, 1962).

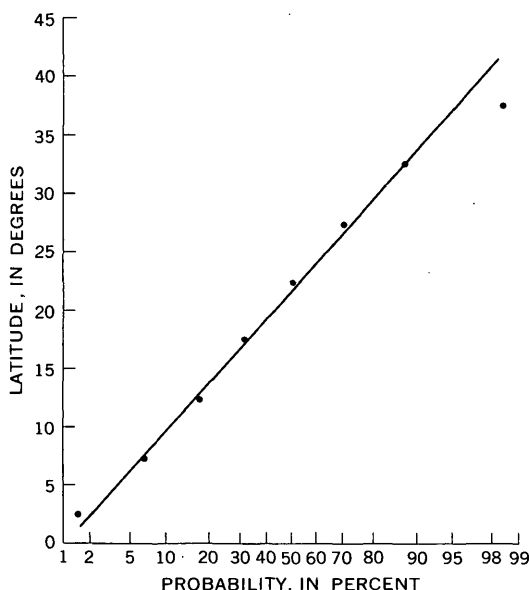


FIGURE 2.—Probability graph of the distribution of young (late Tertiary and Recent) phosphorite.

732-760 O-64—8

graph was constructed by taking the range latitude of each area of phosphorite deposition and plotting one point for each degree of latitude covered. This is equivalent to random sampling on a grid pattern, and the graph is a frequency diagram.

The results give an approximately bell-shaped distribution with a mean latitude of about 23° and a range of from 5° to 42°. These data when plotted on a probability graph (fig. 2) approximate a straight line, showing that the data approach a normal distribution.

### PHOSPHORITE DEPOSITION

Most Recent phosphorite is deposited in areas of oceanic upwelling caused by divergence (Kazakov, 1937; McKelvey and others, 1953), which generally are found in the trade-wind belt where surface waters are blown offshore by the trade winds and where the offshore current is augmented by the Coriolis force. Deeper, cold phosphorus-rich ocean water wells up to take the place of the seaward-moving surface water. In general, this upwelling occurs on the west coasts of continents, on the north coasts of continents in the northern hemisphere, and on the south coasts of continents in the southern hemisphere. The latitudinal distribution of Recent and upper Tertiary phosphorite is shown in figure 1C. The geographic setting of the Recent deposits off the coast of California and Baja California is shown in figure 3.

Some phosphatic sediment is deposited in areas of dynamic upwelling (McKelvey, 1963). For example, off the south coast of Florida the deep-flowing Florida Current is forced up over the shallow submarine part of the Florida Peninsula (Sverdrup and others, 1946) and probably is the cause of the deposition of minor amounts of phosphorite (fig. 3). The latitudinal distribution of this type of phosphorite is shown in figure 1B.

Geologically young phosphorite commonly is found in rocks exposed adjacent to areas of modern oceanic upwelling (McKelvey, 1963). For example, the phosphorite in the Monterey Formation of Miocene age in California (Bramlette, 1946) is located next to the modern upwelling associated with the California Current (fig. 3), the Miocene phosphorite in the southeastern United States (J. B. Cathcart, oral communication, 1963) is located next to the areas of dynamically caused upwelling associated with the Florida Current (fig. 3), and the Miocene phosphorite of the Sechura Desert in Peru (T. M. Cheney, oral communication, 1961) is located next to the modern upwelling associated with the Peru Current (fig. 4). There is little doubt that these geologically young phosphorites were deposited by upwelling currents, just as the Recent phosphatic sediment offshore is being deposited by the modern upwelling currents.

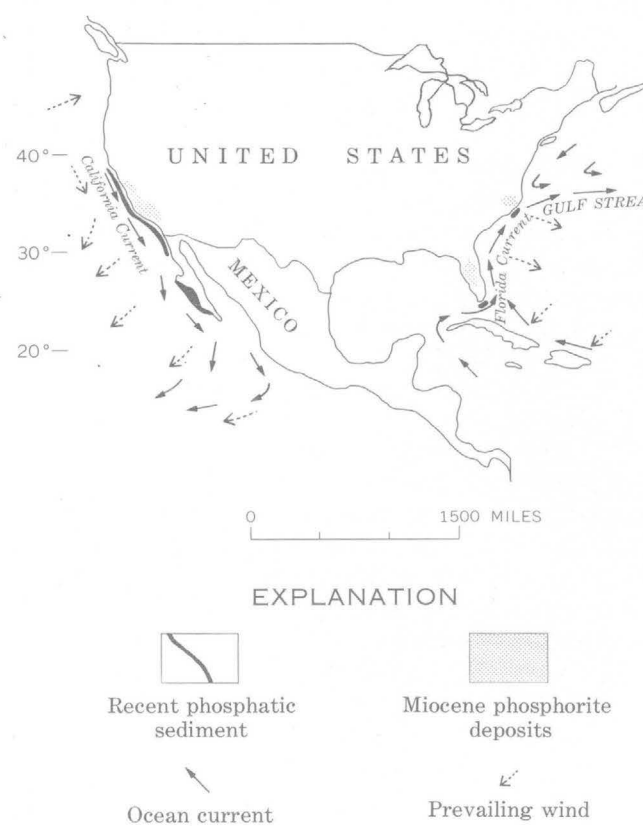


FIGURE 3.—Recent and upper Tertiary phosphorite of North America. After Sverdrup and others (1946), McKelvey (1963), Bramlette (1946), Cathcart and others (1953), and B. F. d'Anglejan (written communication, 1963).

In areas of both dynamic oceanic upwelling and upwelling caused by divergence, the basic cause of the deposition of apatite, the mineral forming marine phosphorite, is the warming and decrease in pressure of cold phosphorus-rich waters. Kazakov (1937) showed that a rise in pH will saturate the water with respect to apatite, and J. R. Kramer (written communication, 1962) has shown that a rise of temperature alone also will saturate the water. These two factors partly are interrelated in that a rise in temperature drives off  $\text{CO}_2$ , resulting in a rise in pH. Thus the distribution of phosphorite in the warmer latitudes is predictable and appears to be ruled out for colder higher latitudes, much as is the case for autochthonous calcium carbonate sedimentation (Rodgers, 1957).

In summary, phosphorite is deposited in warm latitudes, mostly between the 40th parallels. Most phosphorite is found in areas of oceanic upwelling caused by divergence, which is found in the trade-wind belt on the west coast of continents, on the north coast of continents in the northern hemisphere, and on the south coast of continents in the southern hemisphere. Some phosphorite is found in areas of dynamically caused up-

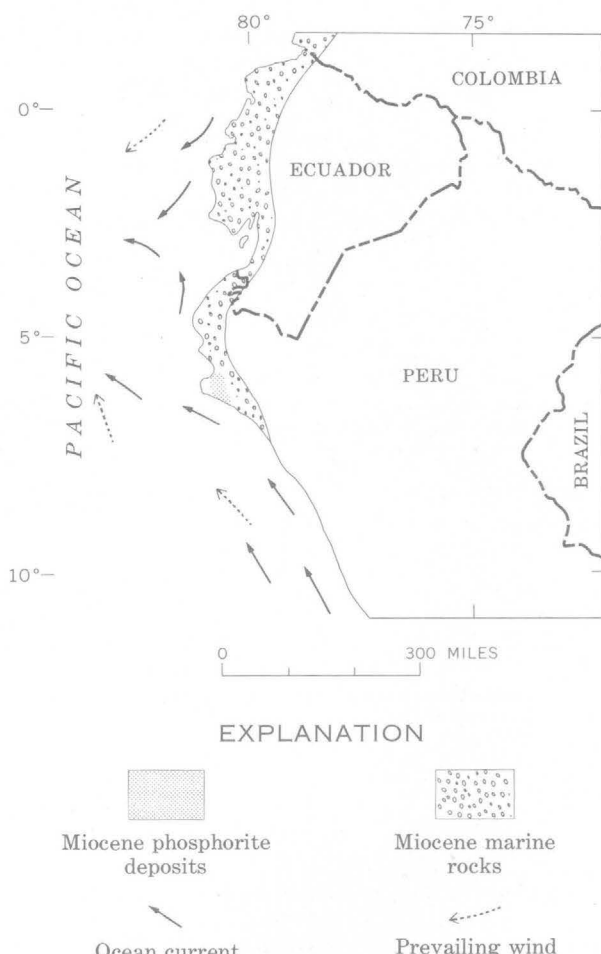


FIGURE 4.—Miocene phosphorite of Sechura, Peru. After T. M. Cheney (oral communication, 1961), Sverdrup and others (1946), and Harrington (1962).

welling which can occur on the east coast of continents and in special geographic settings.

#### DISTRIBUTION OF ANCIENT PHOSPHORITE

Ancient phosphorite (table 2) has a much different latitudinal distribution than does young phosphorite. The distribution of ancient phosphorite (fig. 5A) does not appear to be a normal distribution; the range of known latitudes is from  $6^{\circ}$  to  $70^{\circ}$ . The processes now operating to form phosphorite could not have operated to form ancient phosphorite in its present positions. Thus, the ancient climatic belts either must have been drastically different than now, or the climatic belts must have moved with respect to the continents, or both. This dilemma has arisen with respect to other climate indicators (see the various articles in Nairn, 1961; and Runcorn, 1962). The anomalous paleoclimatic evidence from evaporite, bauxite, bioherm, and glacial deposits largely has been resolved by recent

TABLE 2.—*Present distribution and paleolatitudes of ancient phosphorite*

Locality	Age and formation	Present location		Paleolatitude	Source
		Latitude	Longitude		
Tennessee and Kentucky, U.S.A.	Ordovician, Trenton and Maysville Groups.	34°–37° N	86°–87° W	12°–13° S	Smith and Whitlatch (1940).
Idaho, U.S.A.	Ordovician, Swan Peak Formation.	42° N	111° W	9° N	Mansfield (1927).
Brooks Range, Alaska, U.S.A.	Mississippian, Lisburne Group.	68°–69° N	151°–157° W	30°–31° N	Patton and Matzko (1959).
Utah, U.S.A.	Mississippian, Brazer Formation.	41°–43° N	111°–112° W	3°–5° N	Cheney (1957).
Idaho, Wyoming, Mon- tana, and Utah, U.S.A.	Permian, Phosphoria Formation.	39°–47° N	108°–115° W	3°–9° N	McKelvey and others (1959).
Alberta, Canada	Permian, Rocky Moun- tain Group.	50°–51° N	115° W	15° N	McGugan and Rapson (1961).
Brooks Range, Alaska, U.S.A.	Triassic, Shublik Formation.	69°–70° N	144°–146° W	42° N	Patton and Matzko (1959).
North-central Mexico	Jurassic, La Caja and La Casita Formations.	23°–26° N	102°–104° W	15°–18° N	Rogers and others (1961).
Huancayo, Peru	Jurassic, Sincos Shale	11°–12° S	75°–76° W	4°–6° S	T. M. Cheney and L. T. Grose (oral communi- cation, 1963).
Brazil	Cretaceous, Gramame and Maria Farinha Formations.	6°–7° S	35° W	3°–4° S	The British Sulphur Corp. (1961).
Turkey and northwest Syria.	Late Cretaceous, Kara- bogaz Formation.	36°–37° N	37°–40° E	21°–22° N	Sheldon (report in preparation).
Syria	Late Cretaceous	34°–35° N	38°–39° E	19°–20° N	Cayeux (1939, p. 283); C. L. Wendel (written communication, 1963).
Iraq	do	34° N	36° E	16° N	C. L. Wendel (written communication, 1963).
Israel	do	30°–32° N	35° E	12°–14° N	Bentor (1953).
Jordan	Cretaceous and Eocene	31°–32° N	36° E	14°–15° N	McKelvey (oral com- munication, 1958).
Egypt	Cretaceous	26°–27° N	28°–34° E	8°–9° N	Cayeux (1941).
Algeria and Tunisia	Cretaceous and Eocene	34°–36° N	0°–10° E	18°–20° N	Do.
Libya	do	31° N	15° E	14° N	G. H. Goudarzi (written communication, 1963; Desio, 1943).
Morocco	do	32°–33° N	8°–9° W	15°–16° N	Cayeux (1950).

studies (Irving, 1956; Blackett, 1961; Opdyke, 1962, p. 41–66) by relocating the localities with reference to their paleolatitudes as determined from magnetic studies.

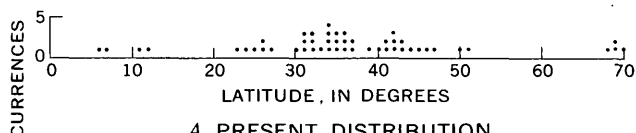
#### PALEOLATITUDINAL DISTRIBUTION OF ANCIENT PHOSPHORITE

The paleolatitudes of the early Tertiary and older phosphorite, as determined from selected paleomagnetic results, are shown on figure 5B. Its mean paleolatitude is lower than that of young phosphorite and its distribution does not appear to be normal. However, the range of ancient phosphorite is from 3° to 42° paleolatitude, which closely corresponds to the range of latitude of young phosphorite. The lack of normality may be due to the small sample and the lack of a randomizing element in the selection of the phosphorite.

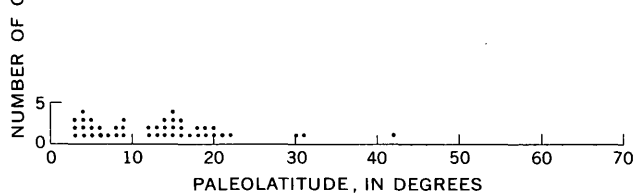
The correspondence between the latitudes of young phosphorite and the paleolatitudes of ancient phosphorite is close enough, in view of the inexactness of

paleomagnetic data and poor sampling, to explain the anomalous present distribution of phosphorite by the shifting of climatic belts relative to the continents.

The virtual geomagnetic poles used in the study are listed in table 3. The virtual geomagnetic pole most closely corresponding to the age of each phosphorite



A. PRESENT DISTRIBUTION



B. PALEODISTRIBUTION

FIGURE 5.—Present distribution and paleodistribution of ancient (early Tertiary and older) phosphorite.

was used, providing that determination of the pole is reasonably reliable. Where several determinations are available an average was taken, and for the Upper Cretaceous to Eocene pole for Africa, the pole was interpolated between the Cretaceous and Recent geomagnetic poles.

TABLE 3.—Virtual geomagnetic poles

Age	Latitude	Longitude	Source
North America			
Early Jurassic	83° N	63° E	Cox and Doell (1960), Jurassic pole 20.
Triassic	56.5° N	105° E	Opdyke in Runcorn (1962, table 2).
Permian (Leonard).	41° N	127° E	Cox and Doell (1960), Permian pole 55.
Late Mississippian and Early Pennsylvanian (used for Utah phosphorite).	30° N	133° E	Cox and Doell (1960), Carboniferous pole 49.
Mississippian (used for Alaska phosphorite).	35° N	132° E	Cox and Doell (1960), average of Mississippian poles 43, 47, 49.
Ordovician	20° N	153° E	Collinson and Runcorn (1960).
Africa and Arabia			
Late Cretaceous and Eocene.	75° N	170° W	Cox and Doell (1960), Cretaceous pole 13. Interpolated be- tween Cretaceous and Recent poles.
South America			
Cretaceous	65.5° N	118° W	Creer (1962).
Jurassic	78° N	126° W	Creer (1958, 1962), Serra Geral pole.

In all examples the present position of the phosphorite was used in the conversion to paleolatitudes, except for Mississippian and Triassic phosphorite of northern Alaska. In an analysis of the geology around the Arctic Ocean, Warren Hamilton (written communication, 1963) has postulated that the northern part of Alaska was detached from the Victoria and Melville Island region in late Mesozoic time and was rotated counter-clockwise to its present position. Hamilton's evidence for this is based largely on stratigraphy. The Brooks Range miogeosyncline appears to be closely related to the Verkhoyansk miogeosyncline of Siberia, and if the miogeosynclines are restored to continuity, the Triassic and Mississippian phosphorite is moved to a paleolatitude about 10° lower than that obtained by calculating from its present position relative to interior North America.

### PALEOGEOGRAPHY OF ANCIENT PHOSPHORITE

Paleolatitudinal distribution of ancient phosphorite is similar to the latitudinal distribution of young phosphorite. Geographic settings of ancient and modern phosphorite also appear to correspond. The paleogeographic settings of most occurrences of the ancient phosphorite listed in table 2 are shown in figures 6 through 11, and in each occurrence, the basic paleogeographic elements are the same. These occurrences of phosphorite are located in paleogeographic positions where trade winds and the Coriolis force would operate in concert to produce maximum oceanic upwelling of the divergent type.

Independent climatic evidence, where available, is shown on each figure; in general it consists of paleo-wind directions deduced from eolian crossbedding studies, and the occurrence of evaporite deposits. Some of these are less well known than others, so that much work remains to be done to substantiate the paleogeographic details. But the consistency of the results makes it appear that the generalizations concerning the geography of young phosphorite can also be applied to ancient phosphorite.

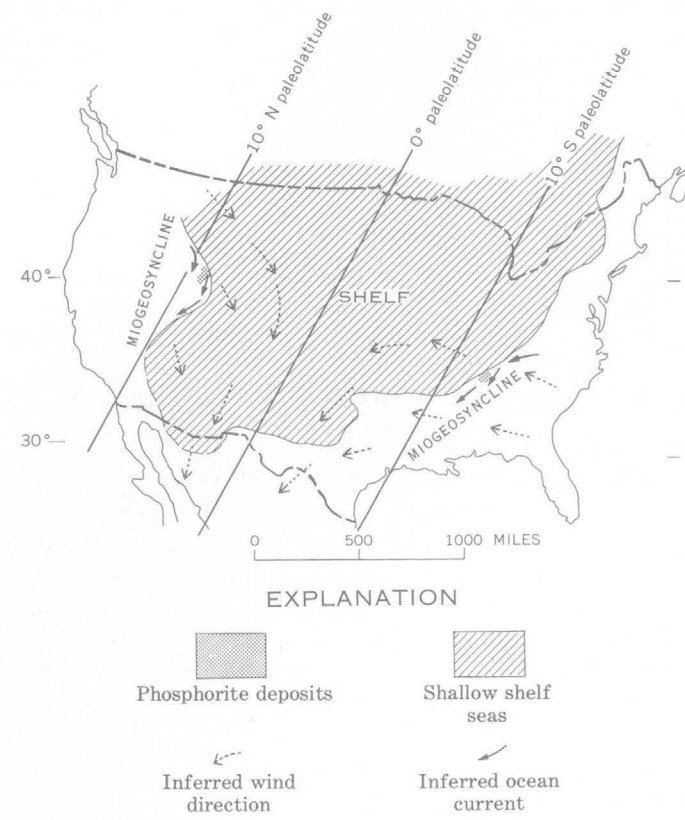
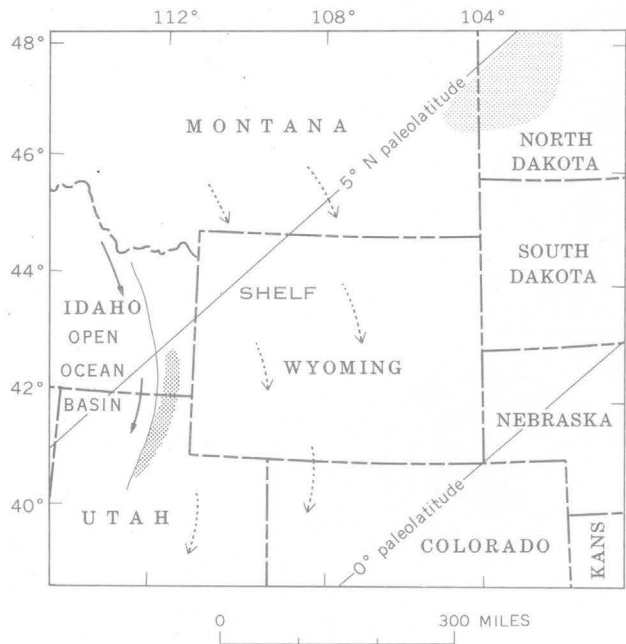


FIGURE 6.—Ordovician phosphorite in the United States. After Mansfield (1927), Smith and Whitlatch (1940), and Sloss and others (1960).



#### EXPLANATION

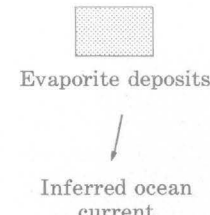
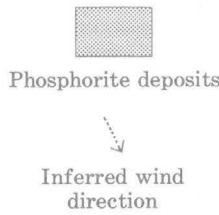
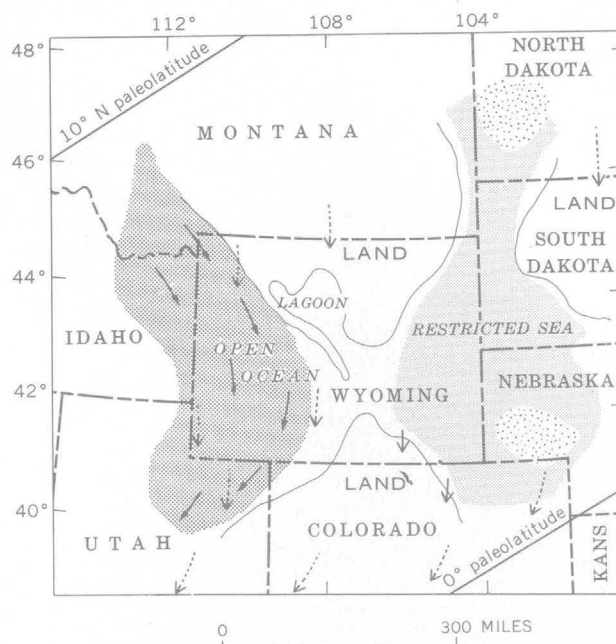


FIGURE 7.—Upper Mississippian phosphorite, Utah, U.S.A.  
After Cheney (1957).

#### CONCLUSIONS

The distribution of ancient phosphorite can be explained in terms of processes known to form modern phosphorite only if there has been polar wandering or continental drift or both. When plotted against its paleomagnetic latitudes, ancient phosphorite shows a distribution and paleogeography similar to those of young phosphorite, so that the warmer latitudes and the trade-wind belts of the past may have been through-



#### EXPLANATION

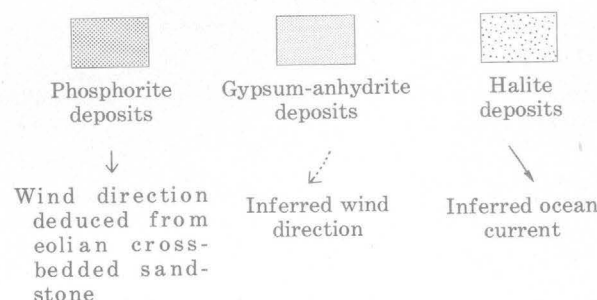
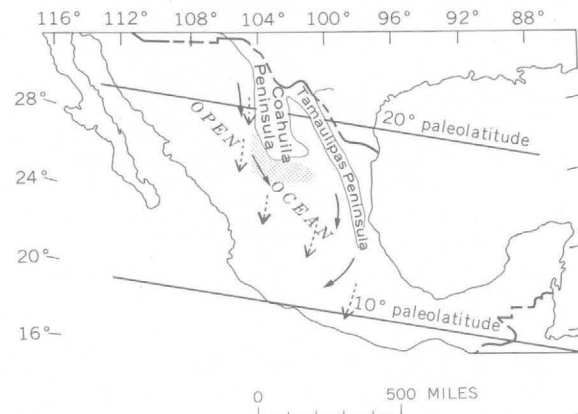
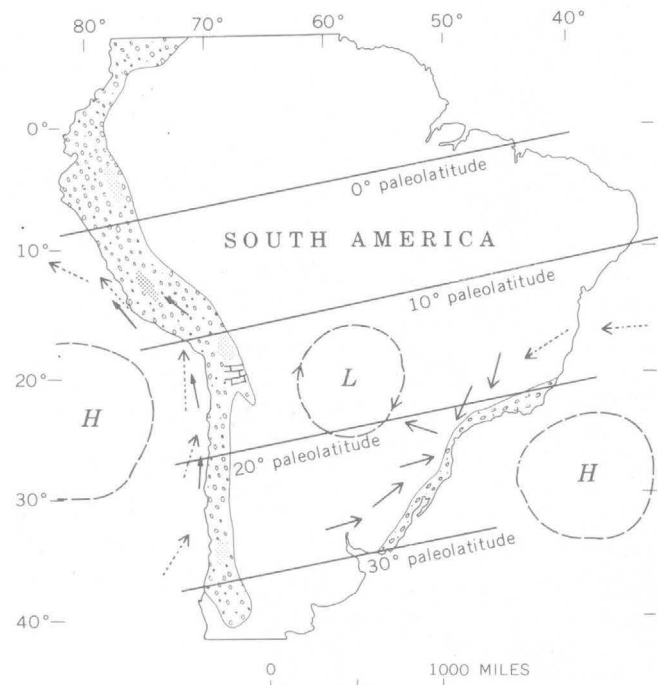


FIGURE 8.—Permian phosphorite in the northwestern United States. After McKelvey and others (1959), Sheldon and others (1961), R. F. Wilson and E. K. Maughan (oral communications, 1960).

out most of geologic time as narrow as at present, and they probably always fell within the 40th parallels. Potential phosphogenic provinces (Sheldon, report in preparation) can perhaps be recognized on the basis of paleogeographic and paleomagnetic studies, and the search for phosphorite can be narrowed accordingly.

**EXPLANATION**

Phosphorite deposits  
 Evaporite deposits  
 Bioherm  
 Marine Jurassic rocks  
 Inferred ocean currents  
 Inferred wind direction

FIGURE 10.—Jurassic phosphorite, north-central Mexico. After Rogers and others (1961) and C. L. Rogers (written communication, 1963).

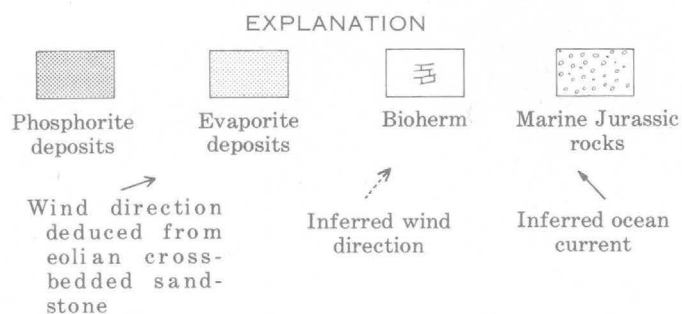


FIGURE 9.—Jurassic phosphorite, Huancayo, Peru. H, permanent barometric high area; L, permanent barometric low area. After T. M. Cheney and L. T. Grose (oral communications, 1962), Bigarella and Salamuni (1961), and Harrington (1962).

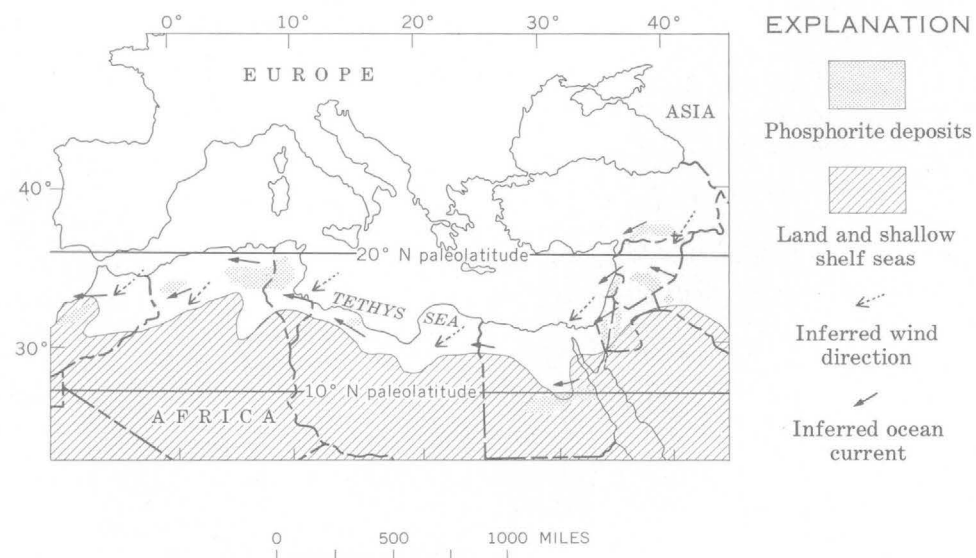


FIGURE 11.—Upper Cretaceous and Eocene phosphorite, North Africa and the Middle East. After Cayeux (1939, 1941, 1950), Klemme (1958), Sheldon (report in preparation), C. L. Wendel (written communication, 1963), and G. H. Goudarzi (written communication, 1963).

## REFERENCES

- Bentor, Y. K., 1953, Relations entre la tectonique et les dépôts de phosphates dans le Neguev Israelien: Internat. Geol. Cong., 19th, Algiers, Comptes rendus, sec. 11, pt. 11, p. 93-101.
- Bigarella, J. J., and Salamuni, Riad, 1961, Early Mesozoic wind patterns as suggested by dune bedding in the Botucatu sandstone of Brazil and Uruguay: Geol. Soc. America Bull., v. 72, p. 1089-1106.
- Blackett, P. M. S., 1961, Comparison of ancient climates with ancient latitudes determined from rock magnetic measurements: Proc. Royal Soc., A, v. 263, p. 1-3.
- Bramlette, M. N., 1946, The Monterey Formation of California and the origin of its siliceous rocks: U.S. Geol. Survey Prof. Paper 212, 57 p.
- Catheart, J. B., Blade, L. V., Davidson, D. F., and Ketner, K. B., 1953, The geology of the Florida land pebble phosphate deposits: Internat. Geol. Cong., 19th, Comptes rendus, sec. 11, pt. 11, p. 77-91.
- Oayoux, Lucien, 1939, Les phosphates de chaux sedimentaires de France (France métropolitaine et d'outre-mer): Services de la carte géologique de la France, Etudes des gîtes minéraux de la France, v. I, Paris, Imprimerie Nationale, p. 1-349.
- 1941, Les phosphates de chaux sedimentaires de France (France métropolitaine et d'outre-mer): Bureau de documentation minière, v. II, Paris, Imprimerie Nationale, p. 351-659.
- 1950, Les phosphates de chaux sedimentaires de France (France métropolitaine et d'outre-mer): Services de la carte géologique de la France, Etudes des gîtes minéraux de la France, v. III, Paris, Imprimerie Nationale, p. 661-1019.
- Cheney, T. M., 1957, Phosphate in Utah and an analysis of the stratigraphy of the Park City and Phosphoria Formations, Utah: Utah Geol. and Mineralog. Survey Bull. 59, 54 p.
- Collinson, D. W., and Runcorn, S. K., 1960, Polar wandering and continental drift; evidence from paleomagnetic observations in the United States: Geol. Soc. America Bull., v. 71, p. 915-958.
- Cox, Allan, and Doell, R. R., 1960, Review of paleomagnetism: Geol. Soc. America Bull., v. 71, p. 645-768.
- Creer, K. M., 1958, Preliminary paleomagnetic measurements from South America: Annales de Géophysique, v. 14, no. 3, p. 373-390.
- 1962, Paleomagnetic data from South America: Jour. of Geomagnetism and Geoelectricity, v. 13, nos. 3 and 4, 154-165.
- Desio, Ardito, 1943, L'esplorazione mineraria della Libia: Collezione Scientifica e Documentaria Dell'Africa Italiana, Istituto per gli Studi di Politica Internazionale, Milano, 333 p.
- Harrington, H. J., 1962, Paleogeographic development of South America: Am. Assoc. Petroleum Geologists Bull., vs. 46, no. 10, p. 1773-1814.
- Irving, E., 1956, Palaeomagnetic and palaeoclimatological aspects of polar wandering: Geofisica Pura e Applicata, vs. 33, p. 23-41.
- Kazakov, A. V., 1937, The phosphorite facies and the genesis of phosphorites, in Geological investigations of agricultural ores USSR: Sci. Inst. Fertilizers and Insectofungicides Trans. (USSR), no. 142, p. 95-113. [Special issue in English published for 17th Internat. Geol. Cong.]
- Klemme, H. D., 1958, Regional geology of circum-mediterranean region: Am. Assoc. Petroleum Geologists, v. 42, no. 3, pt. I, p. 477-512.
- Mansfield, G. R., 1927, Geography, geology, and mineral resources of part of southeastern Idaho: U.S. Geol. Survey Prof. Paper 152, 453 p.
- McGugan, Alan, and Rapson, J. E., 1961, Stratigraphy of the Rocky Mountain Group (Permo Carboniferous), Banff Area, Alberta: Jour. Alberta Soc. Petroleum Geologists, v. 9, no. 3, p. 73-106.
- McKelvey, V. E., 1963, Successful new techniques in prospecting for phosphate deposits: Science, Technology, and Development, United States papers prepared for the United Nations Conference on the application of science and technology for the benefit of the less developed areas, v. II, p. 163-172.
- McKelvey, V. E., Swanson, R. W., and Sheldon, R. P., 1953, The Permian phosphate deposits of Western United States: Internat. Geol. Cong., 19th Comptes rendus, sec. 11, pt. 11, p. 45-64.
- McKelvey, V. E., Williams, J. S. Sheldon, R. P., Cressman, E. R., Cheney, T. M., and Swanson, R. W., 1959, The Phosphoria, Park City and Shedhorn Formations in the Western phosphate field: U.S. Geol. Survey Prof. Paper 313-A, 47 p.
- Nairn, A. E. M., 1961, Descriptive palaeoclimatology: New York, London, Interscience Publishers, 380 p.
- Opdyke, N. D., 1962, palaeoclimatology and continental drift, in Runcorn S. D., Continental Drift: New York, London, Academic Press, p. 41-66.
- Patton, W. W., and Matzko, J. J., 1959 Phosphate deposits in northern Alaska: U.S. Geol. Survey Prof. Paper 302-A, p. 1-17.
- Rodgers, John, 1957, The distribution of marine carbonate sediments, in Regional aspects of carbonate deposition: Soc. of Econ. Paleontologists and Mineralogists, Spec. Pub. 5, p. 2-13.
- Rogers, C. L., Cserna, Zoltan de, Tavera, Eugenio Van Vloten, Rogers Ojeda, Jesus, 1961, Reconocimiento geológico y depósitos de fosfatos del norte de Zacatecas y áreas adyacentes en Coahuila, Nuevo Leon y San Luis Potosí: Consejo de Recursos Naturales No Renovables Bol. 56, 322 p.
- Runcorn, S. K., 1962, Continental Drift: New York, London, Academic Press, 338 p.
- Sheldon, R. P., Maughan, E. K., and Cressman, E. R., 1961, Sedimentation in Wyoming and adjacent areas during Leonard (Permian) time [abs.] Geol. Soc. America Spec. Paper 68, p. 100-101.
- Sloss, L. L. Dapples, E. C., and Krumbein, W. C., 1960, Lithofacies maps: New York, John Wiley and Sons, Inc., 108 p.
- Smith, R. W., and Whitlatch, G. I., 1940, The phosphate resources of Tennessee: Tennessee Div. Geol. Bull. 48, 444 p.
- Sverdrup, H. U., Johnson, M. W., and Fleming, R. H., 1946, The oceans: New York, Prentice-Hall, Inc., 1087 p.
- The British Sulphur Corp. Ltd., 1961, World survey of phosphate deposits: London, The British Sulphur Corp. Ltd., v. I-VI.



## RECONNAISSANCE OF ZEOLITE DEPOSITS IN TUFFACEOUS ROCKS OF THE WESTERN MOJAVE DESERT AND VICINITY, CALIFORNIA

By RICHARD A. SHEPPARD and ARTHUR J. GUDE 3d,  
Denver, Colo.

*Abstract.*—Vitric material in tuffaceous rocks of Tertiary age in the Mojave Desert is generally altered partly or wholly to zeolites, clay minerals, potash feldspar, and (or) silica minerals. The most abundant zeolite is clinoptilolite, but beds rich in analcime, erionite, and phillipsite have been found. Mordenite is a minor constituent of some beds. Potentially economic deposits of clinoptilolite, analcime, and erionite are listed.

In recent years there has been accelerated interest in natural zeolites for industrial use. This article reports the results of a reconnaissance of potentially economic deposits in the western part of the Mojave Desert. Some of the more important products for which zeolites are used are: water softeners, desiccants for various liquids and gases, carriers for certain curing agents and catalysts (O'Connor and others, 1959), hydrocarbon separators, and decontaminators of radioactive wastes containing cesium<sup>137</sup> (Brown, 1962). These uses depend upon the ion exchange and sieve properties of zeolites. Industry now uses synthetic zeolites almost exclusively, but as economic methods are developed to convert natural material into a commercial product, large natural deposits may become important.

Since the early studies of Bradley (1928) and Ross (1928), zeolites have been found to be common diagenetic minerals in tuffs and tuffaceous sediments (Defeyes, 1959). Clinoptilolite (commonly reported as heulandite) and analcime are by far the most common zeolites reported, although erionite (recently shown to be identical to offretite (Hey and Fejer, 1962)), phillipsite, and mordenite are known from several localities. Only rarely is chabazite or natrolite reported.

Prior to this reconnaissance, a few scattered zeolite occurrences were reported from tuffaceous rocks of Tertiary age in the Mojave Desert and vicinity. Kerr and Cameron (1936) described clinoptilolite in an altered tuff 5 miles east of Tehachapi Pass, where it comprises

10 percent or less of the rock. In their study of the Hector bentonite deposit, Ames and others (1958) found analcime and clinoptilolite in altered tuff beds associated with the bentonite. Benda and others (1960) identified analcime and heulandite (probably clinoptilolite) from several cores drilled near Kramer, Calif., and Smith and others (1958, p. 1070) reported beds of analcime-crystal sand from the Kramer borate district.

Although zeolitized tuffs generally cannot be positively recognized in the field, the following properties are characteristic of the material: (1) conchoidal to subconchoidal fracture, (2) chalky rather than vitreous appearance, (3) relatively low porosity, and (4) moderate hardness. Tuffs which are altered to mainly montmorillonite also have most of these properties but generally lack the conchoidal fracture and have a characteristic "pop corn" coating on weathered surfaces. Silicified tuffs commonly show a conchoidal fracture but are much harder than zeolitized ones. Color is not a criterion for identification, for although more than half of the zeolitized tuffs of the Mojave are white to light gray, many are pastel shades of red, green, or yellow.

Unaltered tuffs and tuffaceous rocks of Tertiary age are rare in the Mojave Desert. Some tuffs contain minor remnants of vitric material and a few contain vitric particles that are altered only along their peripheries. Even though a tuff may be completely altered, the pyroclastic texture is generally well preserved by the diagenetic minerals. A hand lens is adequate to confirm the pyroclastic nature of most altered tuffaceous rocks, but fine-grained tuffs and rocks that contained a small amount of vitric material can be correctly identified only in thin section.

The identification of individual zeolite minerals is generally not possible in the field, owing to their very fine crystallinity. Some zeolites in altered tuffs are so

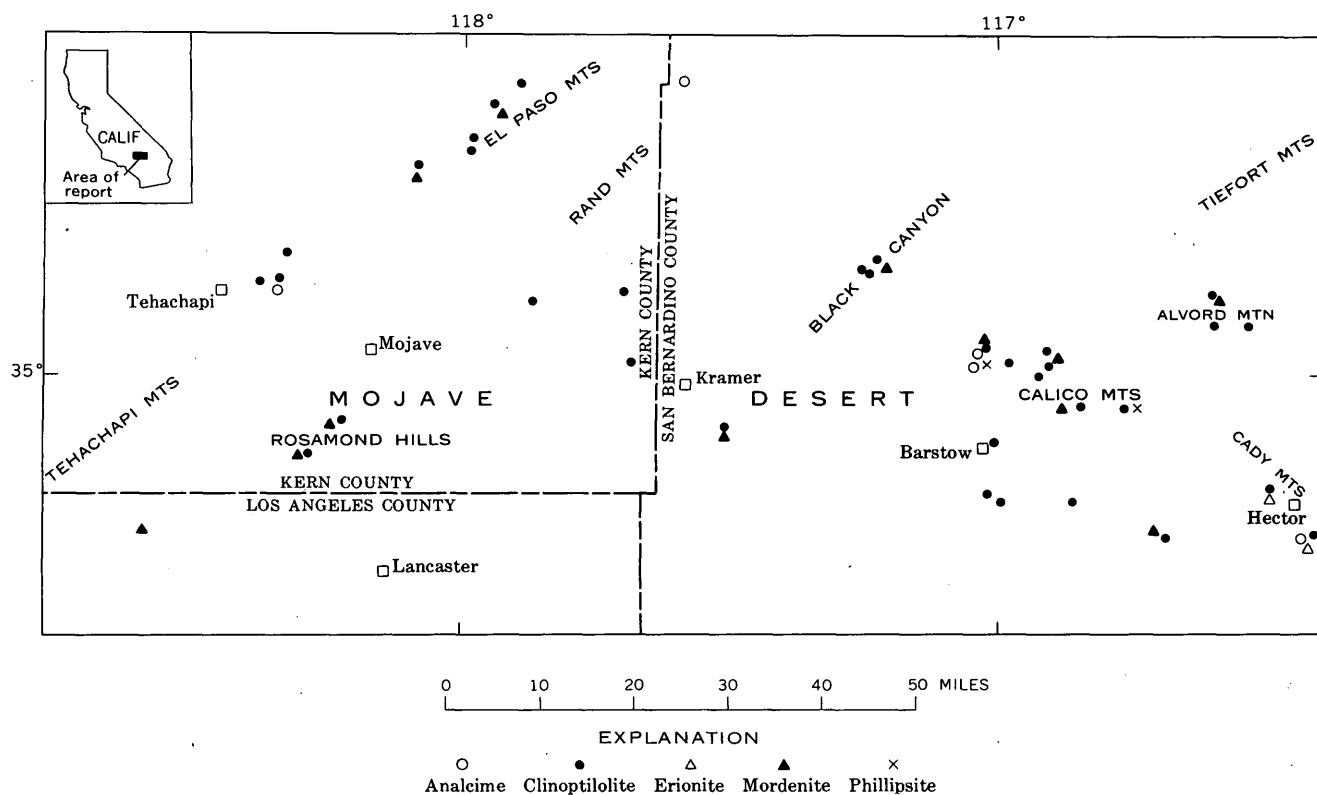


FIGURE 1.—Map of the western Mojave Desert, Calif., showing occurrences of zeolites in tuffaceous rocks found during reconnaissance described in this article.

finely crystalline that even the necessary optical parameters cannot be obtained for positive identification. X-ray powder techniques, however, are well suited for identification because the zeolites need not be separated from the other rock constituents (Deffeyes, 1959). A concentration as low as 10 percent generally can be detected on diffractometer traces.

The zeolites of altered tuffaceous rocks of the Mojave Desert are commonly associated with other diagenetic minerals, such as clay minerals (mainly montmorillonite), potash feldspar, and (or) a silica mineral. In addition, the zeolitized rocks may contain pyrogenic crystals and cognate lithic fragments. Inasmuch as many of the tuffs have been reworked, they may also contain plutonic and metamorphic rock fragments and their constituent minerals that were derived from highlands surrounding the depositional basins. The amount of zeolite in altered tuffaceous rocks is variable and, in part, dependent upon the amount of vitric material originally present. Beds that are nearly monomineralic were deposited as vitric tuffs containing

only a negligible percentage of crystal and lithic fragments.

Those zeolite occurrences found during this reconnaissance are shown on figure 1. Clinoptilolite, analcime, and erionite occur either as nearly monomineralic beds or in association with other zeolites and diagenetic minerals. Mordenite is present in many places, but generally this zeolite comprises less than 25 percent of the rock and is associated with clinoptilolite. Phillipsite so far has been found only in the Rainbow Basin north of Barstow and the southeast flank of the Calico Mountains, where it is associated with clinoptilolite and montmorillonite.

Those formations of Tertiary age that contain zeolites in potentially minable quantities are listed in the accompanying table. The altered tuff beds are more than a foot thick and contain at least 80 percent zeolite at each of the localities listed. When ways to utilize natural zeolite are discovered through industrial technology, these deposits in the Mojave Desert will provide large supplies.

*Localities of potentially economic zeolite deposits in the western Mojave Desert and vicinity, California*

Formation and member	Zeolite	Locality
Ricardo Formation, Member 2 (Dibblee, 1952).	Clinoptilolite.	El Paso Mountains, Last Chance Canyon, sec. 17, T. 29 S., R. 38 E.
Ricardo Formation, Member 4 (Dibblee, 1952).	-----do-----	El Paso Mountains, NE $\frac{1}{4}$ sec. 18, T. 29 S., R. 38 E.
Barstow Formation.	Analcime.	Vicinity of Rainbow Basin, sec. 24, T. 11 N., R. 2 W.
	Clinoptilolite.	Black Canyon, secs. 10 and 11, T. 32 S., R. 44 E., and vicinity of Rainbow Basin, sec. 24, T. 11 N., R. 2 W.
Unnamed formation.	-----do-----	Southern flank of Cady Mountains, SW $\frac{1}{4}$ sec. 31, T. 9 N., R. 5 E.
Unnamed formation.	Erionite.	Southern flank of Cady Mountains, SW $\frac{1}{4}$ sec. 6, T. 8 N., R. 5 E.
Gem Hill Formation.	Clinoptilolite.	Vicinity of Gem Hill, SE corner, T. 10 N., R. 13 W.
Pickhandle Formation of Bowen (1954).	-----do-----	Black Canyon, sec. 1, T. 32 S., R. 44 E.
Spanish Canyon Formation.	-----do-----	Alvord Mountain, head of Spanish Canyon, sec. 30, T. 12 N., R. 4 E., and southeast flank of Clews Ridge, NW $\frac{1}{4}$ sec. 3, T. 11 N., R. 4 E.

## REFERENCES

- Ames, L. L., Jr., Sand, L. B., and Goldich, S. S. 1958, A contribution on the Hector, California, bentonite deposit: Econ. Geology, v. 53, p. 22-37.
- Benda, W. K., Erd, R. C., and Smith, W. C., 1960, Core logs from five test holes near Kramer, California: U.S. Geol. Survey Bull. 1045-F, p. 319-393.
- Bowen, O. E., 1954, Geology and mineral deposits of Barstow quadrangle, San Bernardino County, California: California Div. Mines Bull. 165.
- Bradley, W. H., 1928, Zeolite beds in the Green River Formation: Science, v. 67, p. 73-74.
- Brown, R. E., 1962, The use of clinoptilolite: Ore Bin, v. 24, p. 193-197.
- Deffeyes, K. S., 1959, Zeolites in sedimentary rocks: Jour. Sed. Petrology, v. 29, p. 602-609.
- Dibblee, T. W., Jr., 1952, Geology of the Saltdale quadrangle, California: California Div. Mines Bull. 160, p. 1-43.
- Hey, M. H., and Fejer, E. E., 1962, The identity of erionite and offretite: Mineralog. Mag., v. 33, p. 66-67.
- Kerr, P. F., and Cameron, E. N., 1936, Fuller's earth of bentonitic origin from Tehachapi, California: Am. Mineralogist, v. 21, p. 230-237.
- O'Connor, F. M., Thomas, T. L., and Dunham, M. L., 1959, Chemical-loaded molecular sieves—new approach to faster cures: Indus. and Eng. Chemistry, v. 51, p. 531-534.
- Ross, C. S., 1928, Sedimentary analcite: Am. Mineralogist, v. 13, p. 195-197.
- Smith, G. I., Almond, H., and Sawyer, D. L., 1958, Sassolite from the Kramer borate district, California: Am. Mineralogist, v. 43, p. 1068-1078.



## ORE CONTROLS AT THE KATHLEEN-MARGARET (MACLAREN RIVER) COPPER DEPOSIT, ALASKA

By E. M. MacKEVETT, JR., Menlo Park, Calif.

*Work done in cooperation with the Defense Minerals Exploration Administration*

**Abstract.**—The Kathleen-Margaret copper prospect, near the terminus of the MacLaren Glacier on the southern flank of the Alaska Range, explores north-striking quartz veins that cut greenstone and contain subordinate bornite and chalcopyrite. The quartz veins are near an eastward-striking fault zone. Copper values in the largest and richest known vein apparently diminish northward away from the fault zone–vein intersection.

This article supplements and updates a report by Chapman and Saunders (1954), who described the Kathleen-Margaret copper prospect during the early stages of its development, and is largely an outgrowth of investigations made under the auspices of the DMEA (Defense Minerals Exploration Administration). The article is based mainly on geologic mapping of the underground workings at a scale of 1 inch equals 20 feet and on examination of several thin sections and polished sections. The writer participated in three brief examinations of the prospect in 1957 and 1958 for the DMEA and made an additional 2-day examination in 1960. Emphasis in this article is placed on the structure and local geologic setting of the ore deposit as determined from exposures in the underground workings. Little new information concerning the areal geology at the prospect has been obtained since the work of Chapman and Saunders (1954).

Information in the DMEA files has been drawn upon freely, and grateful acknowledgment is made to those who participated in the DMEA program at the prospect, particularly to R. M. Chapman, Fred Barker, and A. E. Weissenborn of the U.S. Geological Survey, and to E. W. Parsons of the U.S. Bureau of Mines.

The prospect is in the southern part of the central Alaska Range, about 10 miles north of the Denali Highway (fig. 1). It is in the Mount Hayes B-6 quadrangle (U.S. Geological Survey 1:63,360 topographic series,

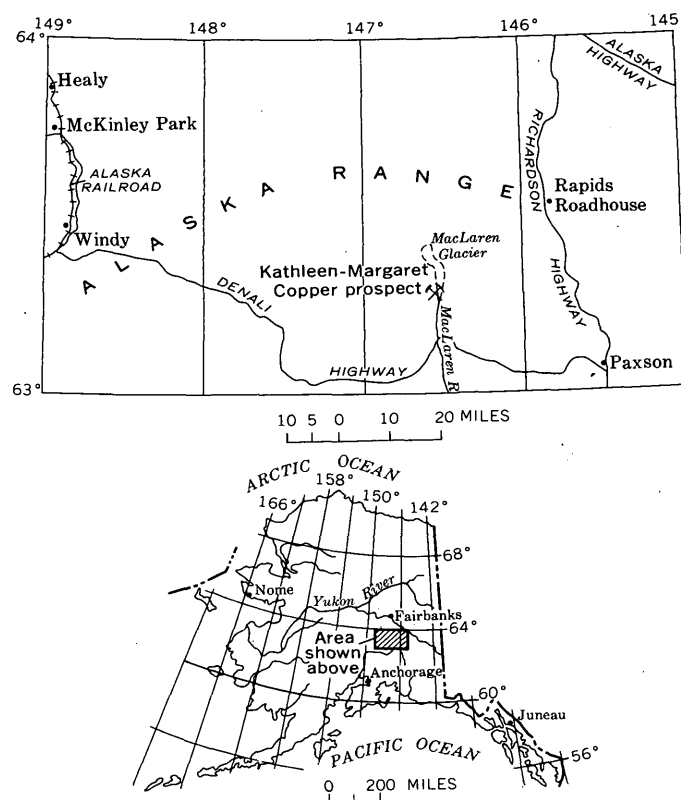


FIGURE 1.—Index map showing the location of the Kathleen-Margaret copper prospect.

1951), approximately 1 mile west of the terminus of the MacLaren Glacier, at an altitude of about 4,000 feet. Access is most practical by small aircraft, which can utilize a landing strip on the flats of the MacLaren River about 1½ miles southeast of the prospect. The prospect is also accessible from the Denali Highway by foot or amphibious vehicle.

A road, approximately 1½ miles long and suitable for tractors and four-wheel-drive vehicles, connected the prospect with a base camp on the river flats about half a mile northwest of the airstrip. Both the road and the camp buildings are now in disrepair (R. M. Chapman, written communication, 1963).

The MacLaren River copper deposit probably has been known since 1918 (Martin, 1920, p. 20), but its early history is sketchy. F. S. Pettyjohn, Jr., relocated the copper-bearing quartz veins in 1952 while associated with E. O. Albertson in a prospecting venture. The prospect was explored, partly under DMEA sponsorship, between 1953 and 1959, by an adit and connecting underground workings totaling about 800 feet (fig. 2), by diamond drilling, and by shallow trenching. Most of the trenches sloughed and became partly filled with surficial debris soon after they were excavated. Approximately 2 tons of ore, estimated to contain between 1 and 2 percent copper, was stockpiled at the property in 1960.

The Kathleen-Margaret prospect is in the altered volcanic rock (greenstone) that is extensively distributed along the southern flank of the central part of the Alaska Range and throughout nearby terranes (Moffit, 1912, pl. 2). This rock constitutes a thick sequence, mainly of lava flows, and was considered by Moffit (1912, p. 30) to be of late Carboniferous or Early or Middle Triassic age. Little geologic mapping has been done in the region since Moffit's pioneering reconnaissance. Undoubtedly, detailed geologic mapping would reveal more complicated geology than has been recognized by reconnaissance methods and would disclose diverse lithologies and structures. Most of the ground at the prospect is covered by low vegetation and by unconsolidated surficial debris.

The dominant rock at the prospect is greenstone that forms a flow sequence dipping southward gently. The greenstone is greenish gray, very fine grained, and is composed largely of secondary minerals. Most of it is cut by numerous veinlets and some is porphyritic and (or) amygdaloidal. Thin sections of the greenstone consist largely of altered plagioclase, epidote, and chlorite. Quartz, calcite, and actinolite are less abundant, and sphene, opaque minerals and their alteration products, and prehnite(?) are uncommon. Scattered specks of chalcopyrite are rare constituents of some of the greenstone. The amygdules and veinlets contain epidote, chlorite, calcite, and quartz. The porphyritic greenstone consists of phenocrysts of altered plagioclase, as much as 2 mm long, in a felty groundmass that is rich in altered plagioclase less than 0.1 mm long. The primary texture in much of the greenstone has been obliterated during alteration.

The greenstone is cut locally by hypabyssal rocks, by several discontinuous quartz veins (some containing copper minerals), and by numerous faults.

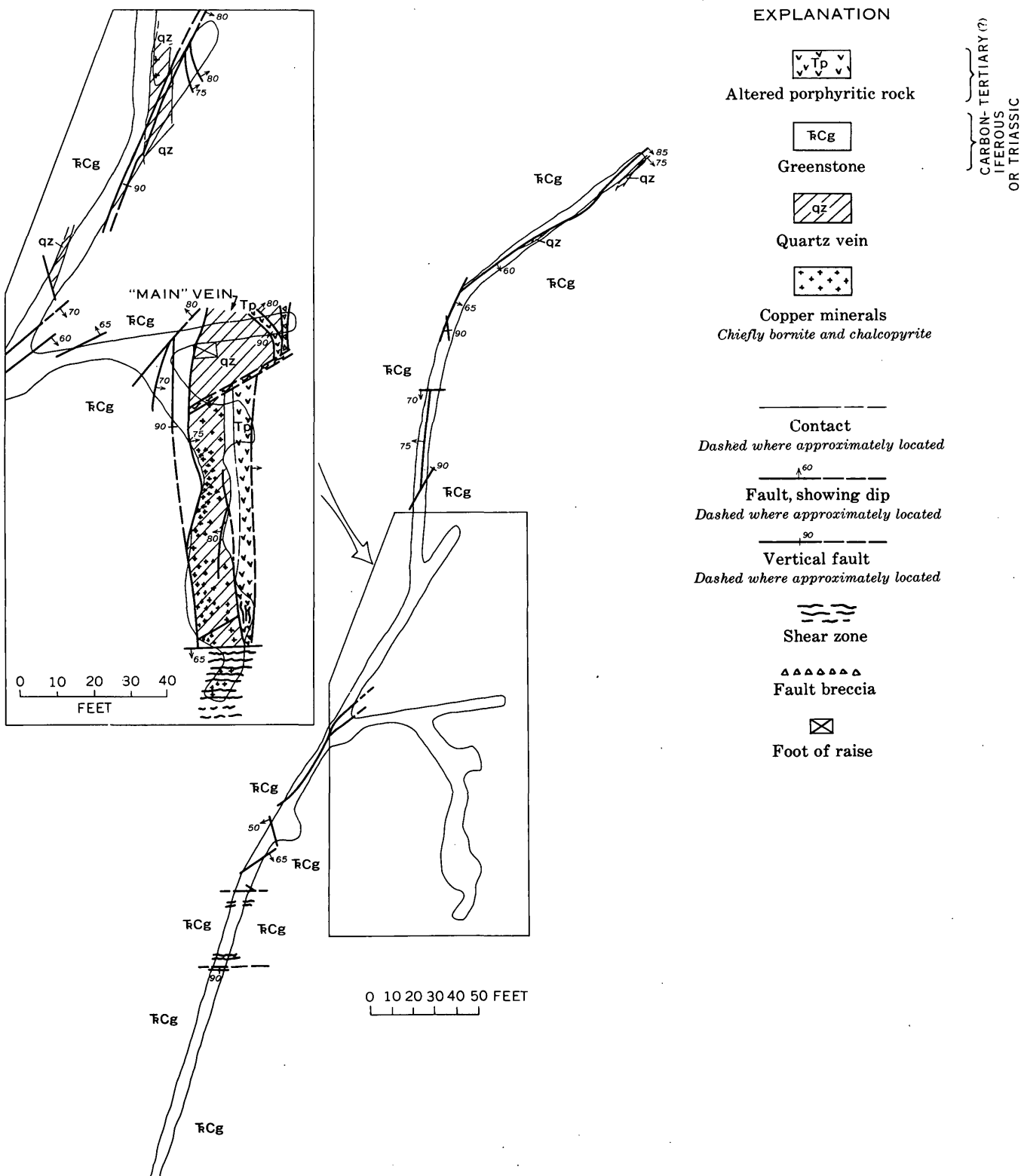
The hypabyssal rocks consist of diabase and a highly altered porphyritic rock. The diabase is known only from a few outcrops where it commonly forms sills as much as 20 feet thick and is slightly altered. It is fine grained, has a diabasic texture, and consists chiefly of pyroxene (augite?), plagioclase, and uralitic hornblende in nearly equal amounts. Its lesser constituents are secondary iron oxides that are mainly alteration products of opaque minerals, and clay minerals. Quartz-chlorite-epidote veinlets cut some of the diabase.

A narrow altered porphyritic dike is exposed in the underground workings along a fault a few feet from a mineralized quartz vein, the "main" vein (fig. 2). Rock making up the dike is light gray and contains medium-grained phenocrysts of altered feldspar in a fine-grained groundmass that is rich in plagioclase and calcite. Phenocrysts constitute about 25 percent of the rock's volume. They are largely altered to calcite, chalcedony, epidote, and clay minerals. Subordinate constituents in the groundmass are apatite, altered opaque minerals, and chlorite. The rock is cut by numerous veinlets containing epidote, calcite, iron oxides, and quartz. Both the diabase and the porphyritic dike are probably Tertiary in age, although field evidence for their age assignment is meager.

Faults are numerous and well exposed in the underground workings, but little is known of their areal distribution.

A steep fault zone, which strikes eastward and whose component fractures dip between 65° S. and vertical, and several steep subsidiary faults that strike north-eastward are exposed in the underground workings (fig. 2). The fault zone is about 35 feet thick and is characterized by abundant gouge and breccia. The subsidiary faults commonly contain minor gouge and, uncommonly, breccia. The "main" quartz vein is cut by the fault zone and is partly bounded by north-striking faults that dip nearly vertically.

Several copper-bearing quartz veins crop out at the prospect (fig. 3), but they commonly are not traceable along strike for more than 100 feet because of inherent discontinuities or poor exposures. Most of the veins strike nearly north, dip vertically or steeply east or west, and range from a few inches to about 20 feet in thickness. Only one of the veins, the "main" vein, is large enough and rich enough to have encouraged exploration. It has been explored by both the underground workings and by some of the surface cuts. The copper content of the "main" vein diminishes northward from the intersection between the vein



Base map from MacLaren River  
Copper Corporation, 1957

Geology mapped by A. E. Weissenborn,  
E. M. MacKevett, Jr., G. O. Gates, and  
E. W. Parsons, 1957, 1958

FIGURE 2.—Geologic map of the level workings, Kathleen-Margaret prospect.

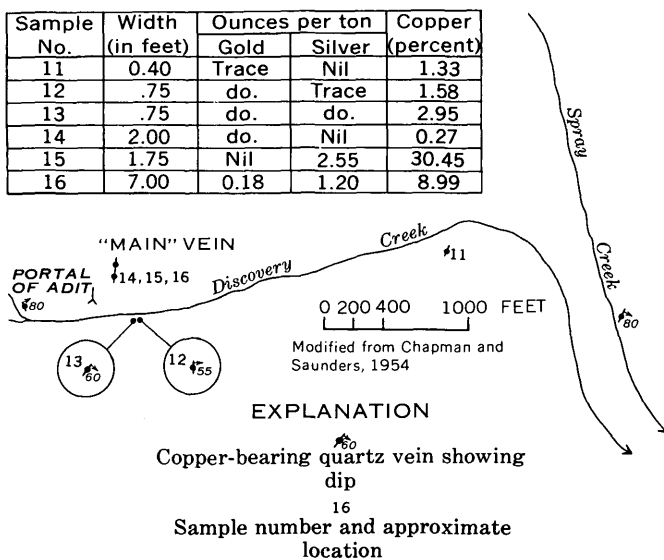


FIGURE 3.—Location and sampling data of outcrop samples, Kathleen-Margaret prospect.

and the fault zone (fig. 2). The small quartz bodies that are exposed in the northern part of the adit may be parts of the "main" vein, in which case a size diminution of the vein to the north is also indicated. The "main" vein is not known with certainty south of the fault zone, although the two small quartz veins south of Discovery Creek that were sampled by Chapman and Saunders (fig. 3, Nos. 12 and 13) may be branches of an offset segment of the "main" vein.

The veins consist largely of quartz in the form of strained anhedral crystals between 1 and 2 mm in diameter. Much of the quartz is fractured and cut by a system of calcite veinlets that intersect approximately at right angles. The veinlets contain minor quantities of quartz along with the calcite. Most of them are less than 0.1 mm thick. Irregular masses of chalcopyrite and bornite, mostly a few millimeters but as much as several centimeters across, cut and replace the early quartz, and are also cut by the calcite veinlets.

Bornite and chalcopyrite are intimately associated throughout most of the ore, with chalcopyrite forming irregular blebs in bornite-rich samples and the converse prevailing in the chalcopyrite-rich samples. Bornite is the most abundant sulfide mineral in most of the ore. Surface coatings of malachite are conspicuous in some of the vein outcrops and also on breccia fragments within the pervious fault zone.

The grade of ore ranges from a few tenths of a percent to about 30 percent copper, but commonly it is between 1 and 5 percent. The ore also contains minor values in silver and traces of gold. The zone of richest ore, about 60 feet long, 5 feet wide, and 100 feet high, extends northward from the fault zone and is adjacent to the west wall of the "main" vein.

The diminution in copper values in the "main" quartz vein northward from the fault zone suggests that the fault zone may have been significant in the ore genesis. Possibly the copper-bearing solutions ascended a conduit formed at the intersection between the fault-controlled "main" vein and the incipient fault zone and found receptive hosts in the adjacent fractured vein quartz. The copper minerals may have been derived from late-stage fluids associated with the porphyry dike. The process of ore formation probably was part of a sequence involving (1) the formation of the "main" vein and similar veins by quartz deposition in open spaces formed by previous fracturing; (2) fracturing of the vein quartz; (3) intrusion of the porphyry dike; (4) deposition of chalcopyrite and bornite in the quartz vein near the fault zone during the initial stage of development of the fault zone; (5) additional faulting, particularly along the fault zone; (6) deposition of calcite-rich veinlets in the quartz vein; and (7) mobilization and deposition of the secondary copper minerals in the fault zone and outcrops of the veins contemporaneous with recurrent movements along the fault zone.

All the known copper-bearing veins at the prospect are near the projection of the east-striking fault zone, which tends to strengthen the belief that the fault zone had a role in the ore formation. However, additional field and laboratory work should be done before a theory on the genesis of the MacLaren River deposits can be advanced with reasonable assurance.

## REFERENCES

- Chapman, R. M., and Saunders, R. H., 1954, The Kathleen Margaret (K-M) copper prospect of the upper MacLaren River, Alaska: U.S. Geol. Survey Circ. 332, 5 p.
- Martin, G. C., 1920, The Alaskan mining industry in 1918: U.S. Geol. Survey Bull. 712-A, p. 1-52.
- Moffitt, F. H., 1912, Headwater regions of the Gulkana and Susitna Rivers, Alaska, with accounts of the Valdez Creek and Chistochina placer districts: U.S. Geol. Survey Bull. 498, 82 p.



## CAVITIES, OR "TAFONI," IN ROCK FACES OF THE ATACAMA DESERT, CHILE

By KENNETH SEGERSTROM and HUGO HENRÍQUEZ <sup>1</sup>  
Denver, Colo., Santiago, Chile

*Work done in cooperation with the Instituto de Investigaciones Geológicas de Chile  
under the auspices of the Agency for International Development, U.S. Department of State*

**Abstract.**—Cavities that resemble certain "niches" in rocks of the southwestern United States and "tafoni" of the Mediterranean area are well developed in granitoid rocks and argillite bordering the Atacama Desert along the coast of northern Chile. Similar cavities are developed to a minor degree in granitoid rocks in the Andes. Differential wetting and drying, hydration of feldspar to clay minerals, and removal of waste by wind are believed to be the causal processes.

Hollowed-out exfoliated blocks and similarly sculptured bedrock outcrops are picturesque landscape features of the Atacama Desert of northern Chile. Exceptionally fine cavities are developed in spheroidally weathered granitoid rocks of the area near Caldera (approximate 27° S.), along the marine terrace that borders most of the coast of northern Chile, but occurrence of the cavities is not restricted to the coastal area, nor to granitoid rocks. Similar cavities are also found in the foothills of the Andes, and in the high Cordillera (fig. 1), in both granitoid rocks and in argillite.

Openings in the rock are of all sizes from pits a few centimeters in depth and diameter to caves large enough to shelter several people (fig. 2). The smaller cavities tend to develop on sloping surfaces, where they form a wafflelike pattern (fig. 3). The large caves develop in vertical faces. The shapes of the cavities are typically spheroidal (Segerstrom, 1962, fig. 93.4), but ellipsoidal and spiral-like forms (fig. 4) are common. A few of the openings have perforated the opposite wall of some outcrops, forming windows or small natural bridges. Many of the cavities are in pairs resembling owl's eyes. Walls around the openings are almost paperthin in places; at other places they are more than a meter thick. Intersections of the cavities with each other and with

the outer surfaces of the rock have produced monoliths and other bizarre forms; the appearance of some outcrops is reminiscent of Swiss cheese.

Exposure of the cavities is not restricted to a single orientation nor to a small range of orientations, but the largest openings tend to be on the windward side (west to southwest) of bedrock outcrops or exfoliated blocks. The cavities are in rock surfaces ranging in steepness from vertical to gently sloping and may be found either in the base or top of the exposure; however, the largest openings are in vertical or nearly vertical faces and near the base of the outcrops.

### TAFONI IN AREAS OUTSIDE CHILE

The Corsican term "tafoni" (singular, "tafone") has been adopted for cavities in rock faces (Penck, 1894, p. 214) and is a suitable term for cavities observed in the Atacama Desert. The term has had wide acceptance in foreign literature (Cotton, 1948, p. 8–11, pl. III), particularly in French, where the spelling is "tafoni," and in German-language publications. Oddly enough, this useful term does not appear in American literature or even in those glossaries and dictionaries that have been published in the United States.

Tafoni in granitic rocks have been described from many arid and semiarid regions of the world. Low granite hills on the east side of Rogers playa, in the Mojave Desert of southeastern California (Blackwelder, 1929, fig. 4), are pitted with cavities apparently identical with those of Chile. Tafoni in granite are also cited from the Tule and Tinajas Altas Mountains of Arizona ("niches", Bryan, 1923, p. 49), the Sierra de Dolores of west Texas (Walther, 1892, p. 58), and from the islands of Elba (Wilhelmy, 1958, p. 159–163), Corsica (Kvelberg and Popoff, 1937), and Sardinia

<sup>1</sup> Geologist, Instituto de Investigaciones Geológicas de Chile.

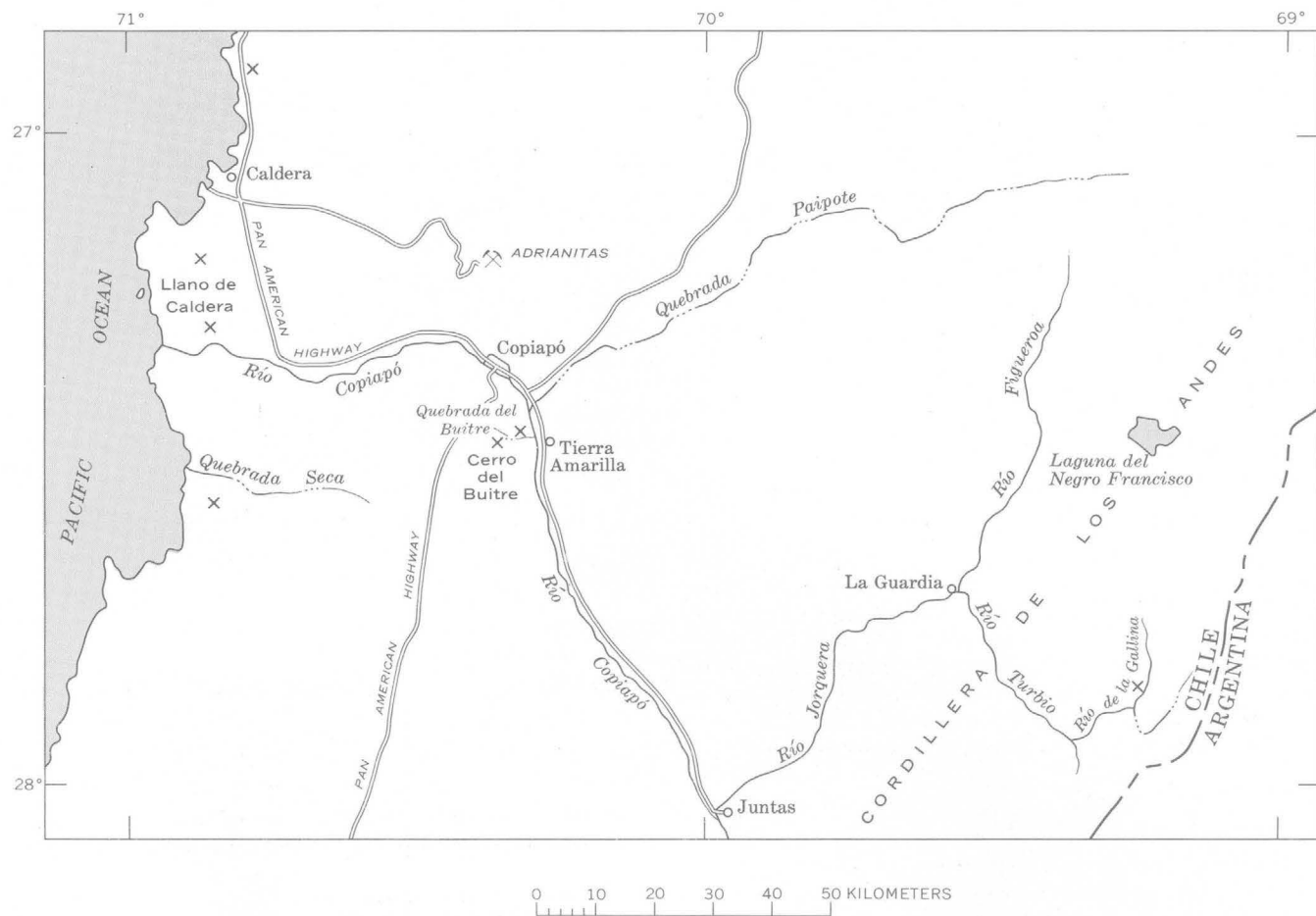


FIGURE 1.—Index map of Chile between lat 27° and 28° S. X, tafoni localities.

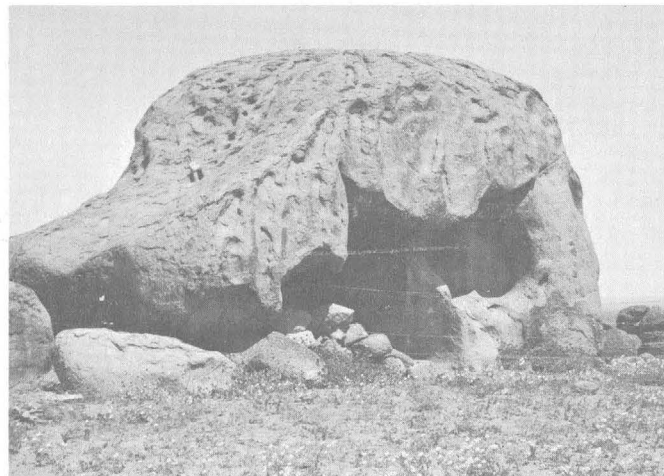


FIGURE 2.—Large cave in granite about 15 km south-southwest of Caldera. Scale is shown by the human hand that projects from a small cavity in the roof.

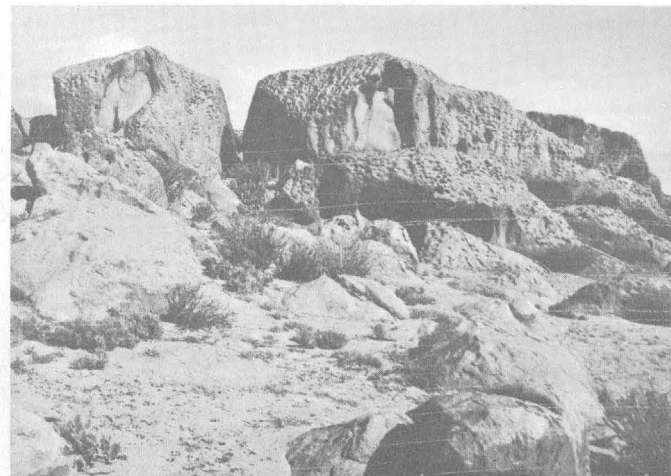


FIGURE 3.—Cavities in granite 19 km north of Caldera. The smaller pits exhibit a wafflelike pattern on sloping faces of the outcrop.

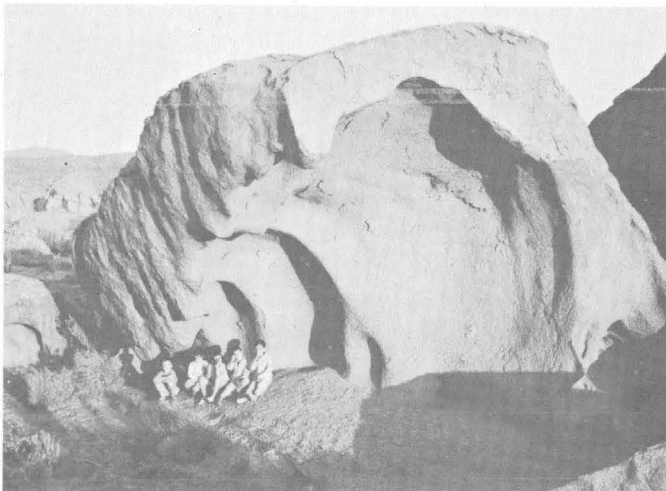


FIGURE 4.—Spiral-like series of cavities in a granitic outcrop about 19 km north of Caldera.

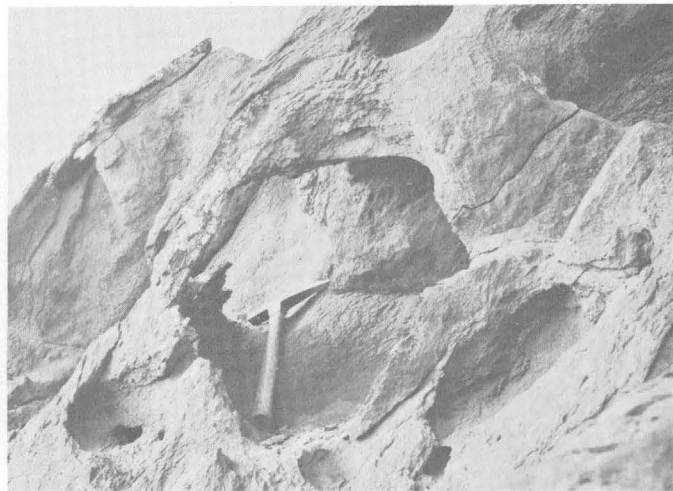


FIGURE 5.—Cavities in well-foliated argillite near Quebrada Seca, 56 km south of Caldera.

(Pelletier, 1962, p. 192-193). Other tafoni-in-granite localities have been reported in northern Portugal (Neiva, 1940), the central Sahara (Schwarzbach, 1954), Korea (Wilhelmy, 1958, p. 152), northeastern Brazil (Tricart and Cailleux, 1960), and Uruguay and western Argentina (Wilhelmy, 1958, p. 170-175).

Tafoni are also found in other types of rock. The cavities have developed in rhyolite tuff and conglomerate of the southwestern United States (Blackwelder, 1929, p. 393 and fig. 1), trachyphonolite lava of the Ahaggar volcano of north Africa (Termier and Termier, 1960, fig. 50), and volcanic breccia of the North Island of New Zealand (Bartrum, 1936; Cotton, 1942, pl. III-1). Bryan (1923, p. 51) describes niches in conglomerate in Arizona, and Cotton (1948, pl. III-2) depicts tafoni in conglomerate in New Zealand.

Cavities in rock faces of the cold deserts at polar latitudes have similarly been termed "tafoni." In northwest Greenland the hollows are in diabase sills (Davies and others, 1963, fig. 16), in southern Greenland they form in granite (Nordenskjöld, 1914, p. 517), and on the western slope of the Hekla-Hook Mountains in Spitzbergen they are found in siliceous rock (Blanck and others, 1928, p. 669). In Antarctica, granite and gneiss glacial erratics exhibit tafoni as much as a meter or more in depth in Victoria Valley, where the mean annual precipitation is 70 to 100 millimeters (Calkin and Cailleux, 1962). Cavernous weathering of boulders has also been described from other localities in Antarctica (Philippi, 1912; Nichols, 1953; Avsyuk and others, 1956). Locally, through overlapping, the pits have produced mushroomlike and other bizarre skeletal forms (Calkin and Cailleux, 1962; Nordenskjöld, 1914).

### TAFONI IN NORTHERN CHILE

The tafoni near Caldera, Chile, are in granitoid rocks, of generally homogeneous composition and texture, composed of plagioclase, quartz, orthoclase, and biotite, with minor accessory minerals. The grains range in size from 0.5 to 2.5 mm. Xenoliths of diorite and gabbro are present, but their exposures are of relatively small extent.

Near Quebrada Seca the pits are in argillite (figs. 1 and 5), but they are not as large and abundant as those which have been formed in the granitoid rocks near Caldera.

Tafoni are also found in the foothills of the Andes (for example, Quebrada del Buitre) or in the high Cordillera (fig. 1). A low hill of weathered granodiorite on the north side of the Quebrada del Buitre, 4 km west of Tierra Amarilla (fig. 1) is covered with a lag deposit, several hectares in extent, that consists of exfoliated blocks of homogeneous, coarse-grained granodiorite as much as 3 or 4 meters in diameter. Many of the blocks, particularly those which are on the top and windward sides of the hill, contain round cavities a meter or more in diameter resembling the potholes of a riverbed (Segerstrom and Ruiz, 1962, p. 62). Some of the blocks are completely perforated.<sup>1</sup> The cavities are developed in outcrop faces of diverse orientation, but most of the largest ones open toward the southwest, or windward side. On the northern summit of the Cerro del Buitre, 3.7 km west of the Quebrada del Buitre

<sup>1</sup> R. I. Tilling, 1962, Batholith emplacement and contact metamorphism in the Paipote-Tierra Amarilla area, Atacama province, Chile: Yale Univ., Ph. D. dissert., 202 p.

locality and about 600 m higher, a block of fine-grained granite is perforated by a natural hole 30 centimeters in diameter. In the Cordilleran valley of the Río de la Gallina (fig. 1), at an altitude of 3,600 m above sea level, large boulders of pyroxene diorite porphyry contain rounded cavities as much as 75 cm in diameter.

The climate of the western and central parts of the Atacama Desert is dry and temperate in the winter, dry and subtropical in the summer; the slightly less arid eastern part is cool to cold at altitudes above 2,000 m. Throughout the area there are greater differences of temperature between day and night than between winter and summer. During most nights a fog called "camanchaca" forms over the coastal area, drifts inland up the principal valleys to altitudes of 750 m or more above sea level, and is usually not dissipated until mid-morning. Typically the afternoons are clear and windy, with the prevailing winds from the west-southwest. In summer the winds often attain high velocities. At dusk the west wind dies and is often supplanted by an east wind, of much less velocity. At Copiapó (fig. 1) the average temperatures range from 23°C in summer to 13°C in winter, and the maximum and minimum temperatures are 32°C and -2°C. During the period 1911-60 the mean annual precipitation at Copiapó was only 25 mm (Segerstrom and Ruiz, 1962, p. 11). Rainfall along the coast is little if any greater than that at Copiapó (altitude 380 m), but at high altitudes in the eastern part of the area shown in figure 1 the precipitation is perhaps 3 or 4 times as great, practically all of it in the form of snow.

Tafoni observed in the Atacama Desert tend to have damp interiors and dry exteriors much of the time, because of shading of the interior and exposure of the exterior to the sun. Near the coast and in Quebrada del Buitre, where the cavities are best developed, the source of moisture is early morning fog; at higher altitudes the source is not known. The interior walls are scaly and crumbly, whereas the exterior surface of the rock is sound. The hard faces of outcrops are fresh and not noticeably impregnated with iron; the relatively soft inside walls exhibit thin coatings of white clay minerals on many of the feldspar grains. In the granite there is no readily visible joint control of cavities, nor do textural and compositional differences seem to be influential. Fine-grained mafic inclusions in the granite, likewise, have no apparent relation to the distribution of tafoni. The less homogeneous argillite, on the other hand, exhibits some bedding-plane control of the tafoni.

#### CAUSES OF TAFONI

The formation of tafoni has been ascribed to the following physical processes by the authors who have been

cited: scouring by wind, beating of rain, insolation, freezing and thawing, differential expansion and contraction of curved surfaces, differential humidity between exterior and interior of cavities, and burrowing by animals. Chemical processes believed to be responsible for cavities in rock faces are solution of certain minerals, crystallization of salt introduced by sea air, case hardening of the exterior by impregnation with iron oxide, and hydration of feldspar and other minerals with related chemical changes. Some authors maintain that the size, shape, and orientation of tafoni are controlled by joint systems, bedding, foliation, and other structures, as well as by small differences in texture and composition of the rock. It has been held that formation of the hollows takes place either in a coastal climate which is periodically damp and subject to frequent winds or one with long dry seasons and high temperatures (Wilhelmy, 1956, p. 55).

A plausible hypothesis which has been advanced for development of the rock cavities in the southwestern United States seems equally applicable to the Chilean occurrences. The explanation is in part the same as that which has been advanced for exfoliation; namely, that the hydration of feldspar and other minerals plays a major role (Blackwelder, 1925, p. 793). Dampness promotes hydration, and hydration may produce new minerals of larger volume (principally clay minerals); hence, rupture due to katamorphism is more prevalent in moist rocks than in dry rocks (Blackwelder, 1925, p. 805-806). Normally, sunshine dries out the lower part of the cavity sooner than the more shady upper part, thus favoring the inward and upward growth of the cavity (Blackwelder, 1929, p. 396). The results of fieldwork in Corsica and detailed petrographic studies of Corsican samples suggest that cavity formation in granite is a result of differential expansion and contraction of curved surfaces; that is, a physical process more than a chemical one (Kvelberg and Popoff, 1937). Once a cavity has started, differential humidity and a resulting hydration probably could produce the required differential expansion and contraction of concentric "shells" in the wall surrounding the cavity.

Wind may assist in removing the debris, but it is probably a minor agent in development of the cavities (Bryan, 1923, p. 49). In the Atacama Desert and in the southwestern United States the abrasive action of windblown sand has produced polishing, pitting, and grooving of outcrops and boulders (Segerstrom, 1962, fig. 93.2; Blackwelder, 1929, fig. 3), but such phenomena are absent in the tafoni of those regions. Despite statements that the rocks were hollowed out by sandblasting (Segerstrom, 1962, p. 91 and 93), the conclusion is inescapable that the role of the wind is more important

in the removal of particles already loosened by other processes than in actual abrasion of the inner walls of niches (Bryan, 1923, p. 49; Blackwelder, 1929; Tricart and Cailleux, 1960).

In closing, the authors wish to acknowledge the help of Roland Pascoff, of the Instituto de Geografía, Santiago, Chile, who supplied numerous bibliographical references.

#### REFERENCES

- Avsyuk, G. A., Markov, K. K., and Shumsky, P. A., 1956, Geographical observations on an Antarctic "oasis": Moscow, U.S.S.R. Natl. Comm. for Internat. Geophys. Year 1957-58, Acad. Sci., Antarctic Council, 69 p.
- Bartrum, J. A., 1936, Honeycomb weathering of rocks near the shoreline: New Zealand Jour. Sci. and Technology, p. 593-600.
- Blackwelder, Eliot, 1925, Exfoliation as a phase of rock weathering: Jour. Geology, v. 33, p. 793-806.
- 1929, Cavernous rock surfaces of the desert: Am. Jour. Sci., 5th ser., v. 17, p. 393-399.
- Blanck, E., Rieser, A., and Mortensen, Hans, 1928, Die wissenschaftlichen Ergebnisse einer bodenkundlichen Forschungsreise nach Spitzbergen im Sommer 1926: Chemie der Erde, v. 3, p. 588-698.
- Bryan, Kirk, 1923, Erosion and sedimentation in the Papago country, Arizona, with a sketch of the geology: U.S. Geol. Survey Bull. 730-B, p. 19-90.
- Calkin, P., and Cailleux, Andre, 1962, A quantitative study of cavernous weathering (taffonis) and its application to glacial chronology in Victoria Valley, Antarctica: Zeitschr. f. Geomorph., v. 6, p. 317-324.
- Cotton, G. A., 1948, Climatic accidents in landscape making, a sequel to landscape as developed by the process of normal erosion: New York, John Wiley and Sons, Inc, 354 p.
- Davies, W. E., Krinsley, D. B., and Nicol, A. H., 1963, Geology of the North Star Bugt area, northwest Greenland: Copenhagen, Meddeleser om Grønland, v. 162, no. 12, 68 p.
- Kvelberg, Irma, and Popoff, Boris, 1937, Die Tafoni-Verwitterungsscheinung: Riga, Acta Universitatis Latviensis, Fac. of Chem., ser. 4, no. 6, p. 129-370.
- Neiva, J. M., 1940, Alguns aspectos erosivos dos granitos do Norte de Portugal: Publ. do Museu e Laboratório Mineralógico e Geológico da Fac. de Ciências do Porto, v. 14, p. 1-8.
- Nichols, R. L., 1953, Geomorphology of Marguerite Bay, Palmer Peninsula, Antarctica: Washington, U.S. Office of Naval Research, Ronne Antarctic Research Exped., Tech. Rept. 12, 151 p.
- Nordenskjöld, Otto, 1914, Einige Zuge der physischen Geographie und der Entwicklungsgeschichte Sudgrönlands: Geogr. Zeitschr., p. 425-441, 505-524, 628-641.
- Pelletier, Jean, 1962, Le relief de la Sardaigne: Annales de Géographie, no. 384, p. 192-193.
- Penck, Albrecht, 1894, Morphologie der Erdoberfläche: Stuttgart, v. 1.
- Philippi, E., 1912, Geologische Beschreibung des Gaussbergs: Deutsche Südpolarexpedition, 1901-03, hrsg., v. E. v. Drygalski, v. 2, p. 47-71.
- Schwartzbach, Martin, 1954, Geologie in Bildern; eine Einführung in die Wissenschaft von der Erde: Wittlich, Georg Fischer Verlag, 132 p.
- Segerstrom, Kenneth, 1962, Deflated marine terrace as a source of dune chains, Atacama province, Chile: Art 93 in U.S. Geol. Survey Prof. Paper 450-C, p. C91-C93.
- Segerstrom, Kenneth, and Ruiz, Carlos, 1962, Geología del cuadrángulo Copiapo: Santiago, Instituto de Investigaciones Geológicas, Carta Geológica de Chile, v. 3, no. 1, 115 p.
- Termier, Henri, and Termier, Genevieve, 1960, Érosion et sédimentation: Paris, Masson, 412 p.
- Tricart, Jean, and Cailleux, Andre, 1960, Le modelé des régions sèches: Paris, Centre de Documentation Universitaire, 308 p.
- Walther, Johannes, 1892, Die nordamerikanischen Wüsten: Berlin, Verhandl. d. Ges. f. Erdkunde, p. 52-65.
- Wilhelmy, Herbert, 1956, Cavernous rock surfaces (taffoni) in semi-arid and arid climates: Internat. Geog. Cong., 18th, Rio de Janeiro, Abstracts of Papers, p. 55-56.
- 1958, Klimamorphologie der Massenersteine: Braunschweig, Westermann Verlag, 238 p.



## NEGAUNEE MORAINE AND THE CAPTURE OF THE YELLOW DOG RIVER, MARQUETTE COUNTY, MICHIGAN

By KENNETH SEGERSTROM, Denver, Colo.

**Abstract.**—The Negaunee moraine of Wisconsin age borders the Yellow Dog Plains on the Upper Peninsula of Michigan and marks a zone where ice blocked the preexisting drainage to the north and east. A glacial stream that drained southward to Dead River was captured in postglacial time by the east-flowing Yellow Dog River. Headward cutting of the north-flowing Salmon Trout River now threatens to capture headwaters of the Yellow Dog River.

The Yellow Dog Plains, a terracelike sandy area about 10 miles long and 2 to 3 miles wide, is an eye-catching topographic feature among the generally knobby landforms northwest of Marquette, on the Upper Peninsula of Michigan (fig. 1). A steep escarpment lacking bedrock exposures drops to the north as much as 400 feet below the surface of the plains, and a highland to the south—marked by dozens of rock knobs—rises as high as 400 feet above the plains. A narrow lowland at the base of the escarpment is bordered to the north by a belt of granitic hills known as the Huron Mountains. As explained below, a gap in the southern highland near Pinnacle Falls formerly permitted a glacial stream to discharge southward along Mulligan Plains, but drainage is now directed north and east—via the Salmon Trout and Yellow Dog Rivers (figs. 1 and 2).

The drainage history, beginning with the ice-contact origin of the plains and concluding with postglacial drainage changes, is summarized below.

The highly irregular escarpment and the lowland at its base were mapped by Leverett (1929, pl. 1) as part of a morainal belt extending from Marquette to Keweenaw Bay, a little west of the area of figure 1. This belt, currently termed the Negaunee moraine (Flint and others, 1959), is on the western limb of the Green Bay Lobe of Wisconsin Drift (Martin, 1957), and it is assigned to the Mankato Stade. The vaguely defined Negaunee moraine, although marked locally by kame-and-kettle topography, is characterized by its negative geomorphic aspect. Thus, it is not a typical end

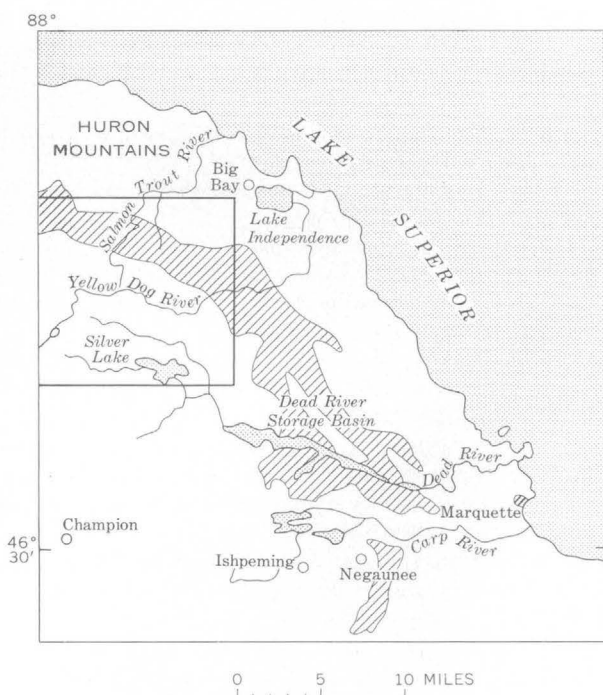


FIGURE 1.—Index map of area northwest of Marquette, Mich., showing location of area of figure 2 (outlined). Shaded area is Negaunee moraine, after Martin (1957).

moraine, a “ridgelike accumulation of drift built along any part of the margin of a glacier” (Flint, 1957, p. 131 and fig. 7-19). Near the Yellow Dog Plains the moraine is part of a thick accumulation of sand and other materials, locally studded with kames or pitted with small kettles; elsewhere, it consists mostly of thin drift dotted with numerous bedrock knobs and a few small gravelly kames.

Near the Yellow Dog Plains there is a pronounced change in size of particles in the Negaunee moraine. The materials at the base of the escarpment to the north are extremely heterogeneous; particles of all sizes are present, but in only a few places is clay sufficiently

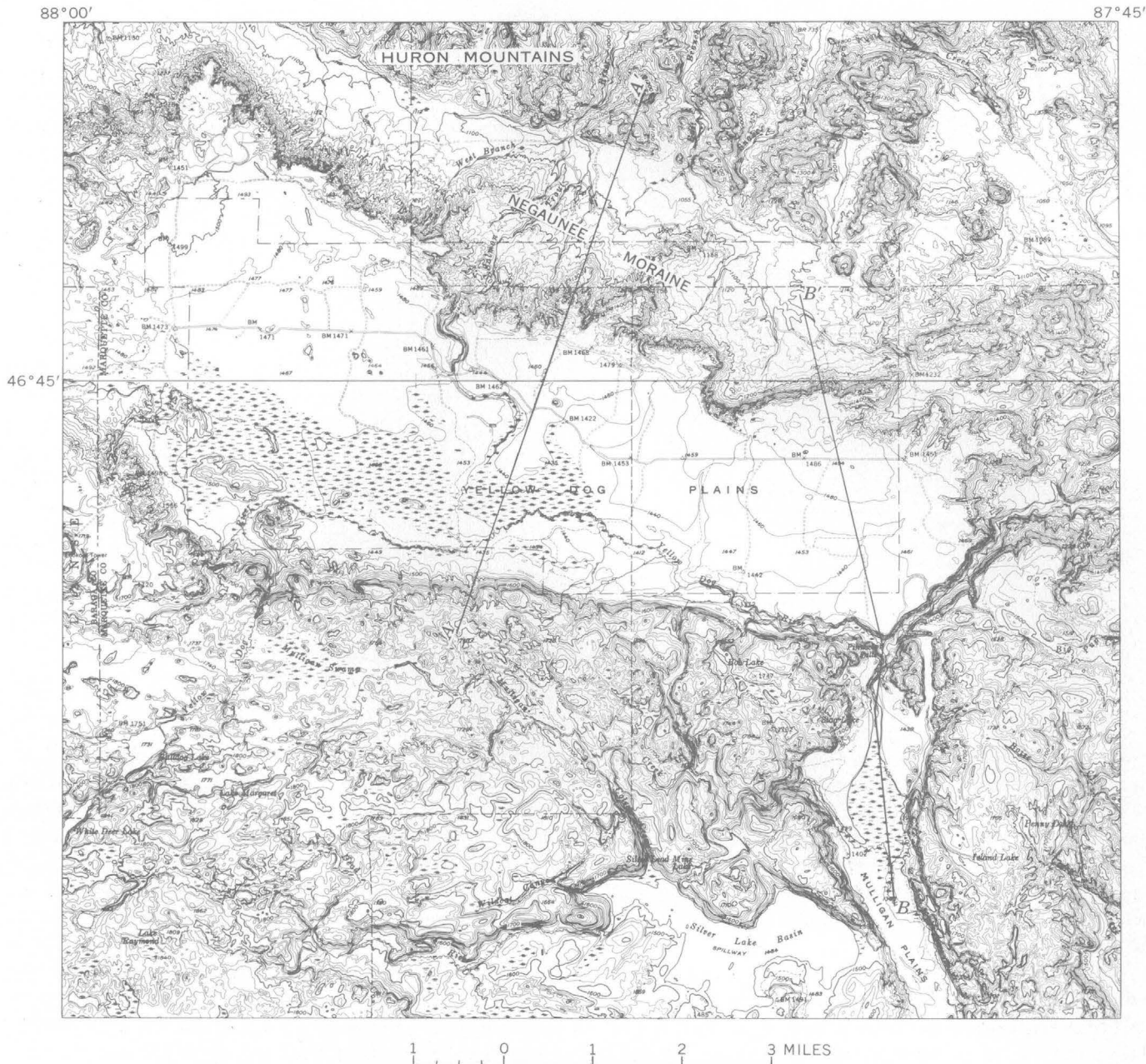


FIGURE 2.—Topographic map of Yellow Dog Plains and vicinity, showing location of sections *A-A'* and *B-B'*. From U.S. Geological Survey Huron Mountain and Champion 15-minute quadrangle maps.

abundant to cement the materials to a hard, typically till-like consistency. Southward, the morainal materials grade into coarse- and medium-grained sand containing scattered cobbles and boulders at the upper edge of the escarpment (fig. 3).

On the Yellow Dog Plains the boulders diminish in number southward, and the sand becomes finer and better sorted. Near the southern edge of the plains no boulders are seen, and very little of the surficial material is finer or coarser than medium-grained sand.

The late-glacial history of the area is generally as follows: Prior to the last glaciation the ancestral Yellow Dog River evidently flowed eastward in a broad valley eroded in slate and bordered on the north and south by relatively hard crystalline rocks. During the Mankato(?) Stade the area was covered by a continental glacier of unknown thickness. Locally the ice was thickest over the valley immediately south of the Huron Mountains; therefore, during stagnation the margin of the glacier temporarily stood there. Melt

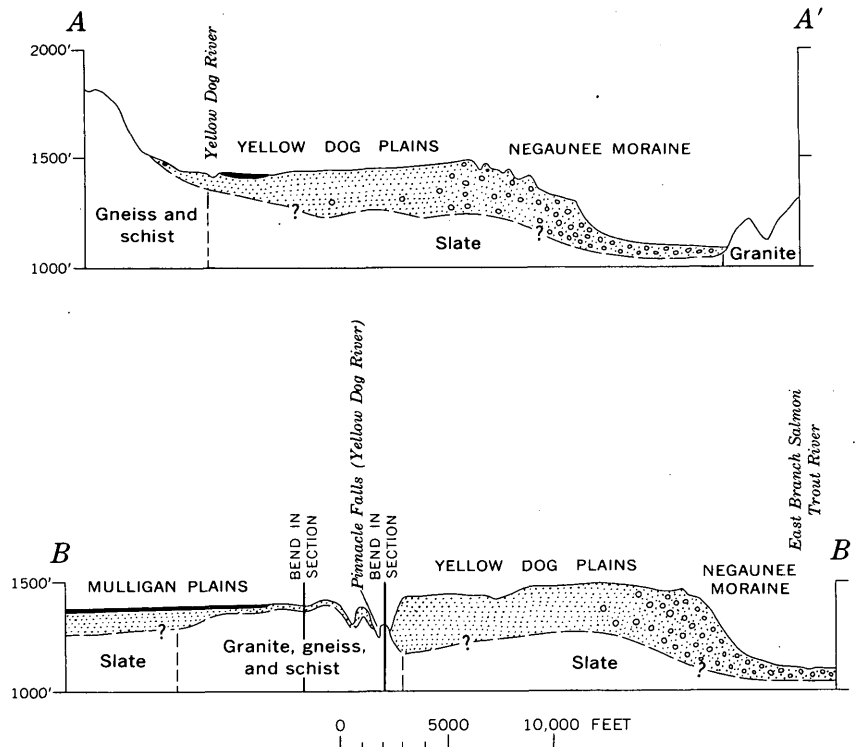


FIGURE 3.—Cross sections A-A' and B-B'. Location of sections is shown on figure 2. Swamp deposits shown as solid black. Vertical exaggeration about  $\times 10$ .

water deposited kames on the underlying ground-moraine surface, and spilling southward constructed a broad kame terrace—the Yellow Dog Plains. The flow of melt water was obstructed by the high bedrock hills to the south, causing brief ponding, until increasing depth of the water permitted it to breach a gap near the present Pinnacle Falls. Erosion of the gap resulted in drainage of the lake.

Along the north and east edges of the kame terrace, where glacial and outwash materials were interlayered, bedding features were largely destroyed through collapse caused by melting of the underlying blocks of stagnant ice. This produced debris slopes ranging in steepness from  $15^\circ$  or  $20^\circ$  near the top of the section to  $1^\circ$  or  $2^\circ$  near the bottom, accounting for the concave-upward profile at the ragged edge of the plain. The Negaunee moraine was thus formed; locally it consists of debris slopes interrupted by scattered kames and kettles.

The capture of the Yellow Dog River came about as follows: After the terrain between the Yellow Dog Plains and Lake Superior was deglaciated, the former

drainage systems were reactivated. The Salmon Trout and Yellow Dog Rivers reexcavated their old channels or incised new ones in their drift-covered lower valleys and soon cut headward into the Negaunee moraine. The steep slope of the moraine resulted in unusually rapid headward cutting by streams consequent on the newly exposed land surface. Meanwhile, the glacial drainage—southward through the Mulligan Plains to the Dead River—survived briefly, but with the loss of melt water this drainage system must have become very sluggish and was therefore a less effective cutting agent than the revived Yellow Dog River to the northeast.

Inevitably, through stream capture, most of the drainage of the Yellow Dog Plains was diverted eastward, and the Yellow Dog River acquired its present course. The river, superposed upon the sand plain, cut into bedrock at the present Pinnacle Falls. This indicates that the present river channel occupies a position on the shoulder of the ancestral valley (fig. 3, section B-B'). Near Pinnacle Falls the river has cut an exceptionally steep, narrow gorge that extends down-

stream for about 2 miles. Except at the falls, the walls of the gorge are almost entirely sand, and they slope as much as  $26^{\circ}$  or  $27^{\circ}$  (the angle of repose for this material is about  $33^{\circ}$ ).

With disappearance of the ice from the Huron Mountains and Negaunee moraine area, the Salmon Trout River cut headward across the plains. Because the divide between this stream and the Yellow Dog River is today less than 20 feet high and the Salmon Trout is at a lower elevation, beheading, or capture, of the Yellow Dog River is imminent.

#### REFERENCES

- Flint, R. F., 1957, Glacial and Pleistocene geology: New York, John Wiley, 553 p.
- Flint, R. F., chm., and others, 1945, Glacial map of North America: Geol. Soc. America Spec. Paper 60.
- 1959, Glacial map of the United States east of the Rocky Mountains: New York, Geol. Soc. America.
- Leverett, Frank, 1929, Moraines and shore lines of the Lake Superior Basin: U.S. Geol. Survey Prof. Paper 154-A, 72 p.
- Martin, H. M., 1957, Map of the surface formations of the northern peninsula of Michigan: Michigan Geol. Survey Pub. 49.



## ANCIENT LAKE IN WESTERN KENTUCKY AND SOUTHERN ILLINOIS

By WARREN I. FINCH, WILDS W. OLIVE, and EDWARD W. WOLFE,  
Paducah, Ky.; Menlo Park, Calif.

*Work done in cooperation with the Kentucky Geological Survey*

**Abstract.**—Elongate, narrow, round-crested gravel ridges with accordant crests at an altitude of about 355 feet above sea level suggest that during late Pleistocene time a lake occupied the valley of the Ohio River and its tributaries near the confluence of the Ohio and Tennessee Rivers.

Accordant gravel ridges found in the valleys of the Ohio, Tennessee, and Clarks Rivers in an area extending at least 40 miles up the Ohio and Tennessee Rivers from Metropolis, Ill., indicate that a lake flooded these valleys below an altitude of 355 feet at some time in the late Pleistocene. The evidence consists of elongate, narrow, round-crested ridges believed to represent former bay-mouth bars and beach ridges, composed of gravel, which rest on presumed lacustrine deposits of loess-like silt. The crests of the ridges are accordant at altitudes of slightly more than 350 feet, 5 to 20 feet above an extensive silt deposit whose upper surface lies at altitudes between 330 and 350 feet and which presumably represents an old lake bed. The distribution of the ridges is shown on figure 1.

Most of the ridges are along the margins of the old lake bed through which the Ohio, Tennessee, and Clarks Rivers flow, and most cross the mouths of the tributaries of these rivers. Typically, a long segment abuts against the downriver wall, and a short segment abuts against the upriver wall; the tributary flows between the two segments (fig. 2). A swale 2 or 3 feet below the general level of the crestline is common where the long segment joins the valley wall. Other gravel ridges are found at the base of adjoining upland slopes and are separated from the uplands by a swale 2 or 3 feet below the general level of the ridge crestline. The ridges are generally 200 to 500 feet wide, a few hundred feet to as much as a mile long, and 5 to 20 feet high.

The gravel of the ridges consists chiefly of poorly sorted subrounded chert pebbles and cobbles rarely larger than 3 inches in diameter, and sparse small rounded quartz pebbles. Matrix material generally is clay or silt, but the gravel in some ridges is nearly free of matrix material. Gravel also occurs in widespread continental deposits of Pliocene(?) and Pleistocene age, which blanket adjacent uplands, but this older gravel has a matrix dominantly composed of sand and is easily distinguished from the ridge deposits.

The gravel ridges overlie silt and clay deposits, which are believed to be of lacustrine origin. At depth these deposits contain sand and gravel in varying quantities, which may be in part alluvial in the Tennessee, Ohio, and Clarks River valleys. Drill holes west and northwest of Symsonia penetrated as much as 73 feet of unconsolidated material below gravel ridge deposits. None of the ridges are capped by loess, although Peorian Loess (Leighton and Willman, 1950) forms an extensive blanket on the adjacent uplands.

Shaw (1911, p. 484; 1915, p. 147) described similar features, which he identified as beach ridges that developed in a lake of late Quaternary age near Madisonville, Ky., 65 miles east-northeast of Paducah. Bay-mouth bars similar in form to those of the ancient lake are currently accumulating along the edges of Kentucky Lake, which was impounded in 1945. One of the bars is shown on figure 3. Although the modern bars are similar in form to the ancient bars, they differ in composition in that they are composed of angular chert rubble derived from erosion of wave-cut scarps in residuum of Paleozoic rocks, whereas the older bars are composed of subrounded chert gravel evidently derived mainly from erosion of Pliocene(?) and Pleistocene continental deposits. The bases of the modern bars are above an altitude of 350 feet and their crests rarely rise more

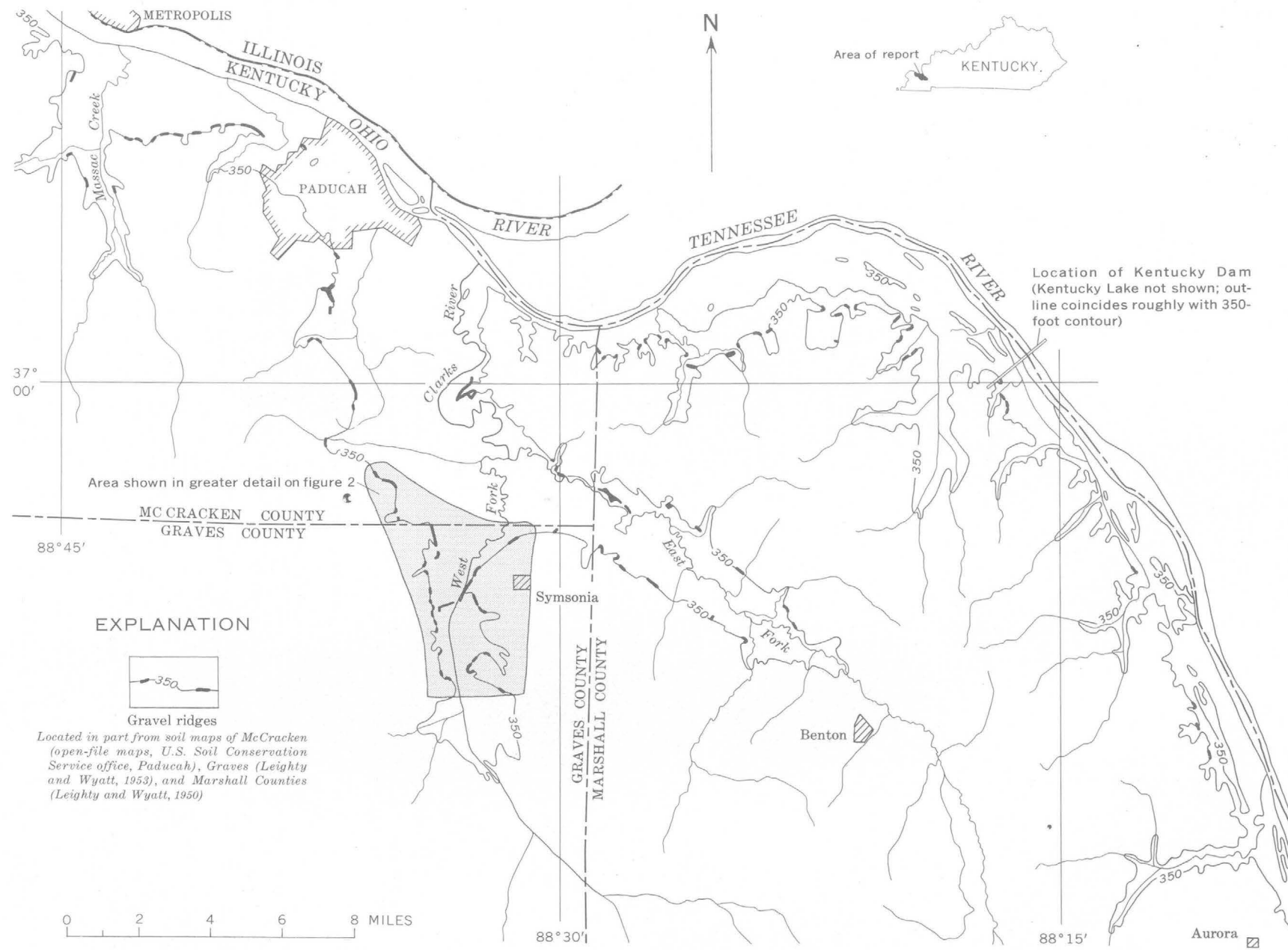


FIGURE 1.—Location of gravel ridges and the 350-foot contour in McCracken, Graves, and Marshall Counties, Ky.

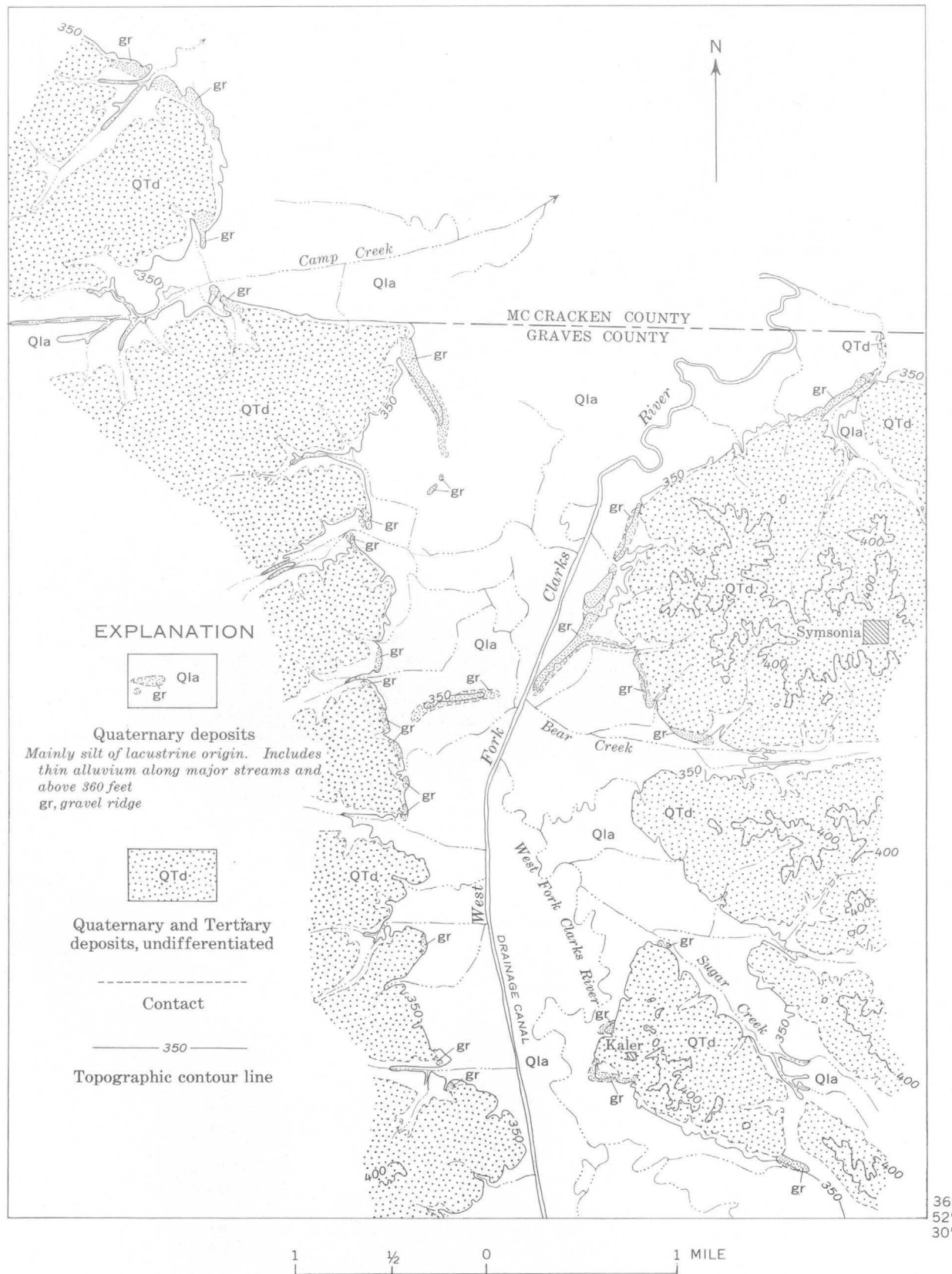


FIGURE 2.—Lacustrine deposits in part of the Symsonia quadrangle, Kentucky.



FIGURE 3.—Modern gravel bar across a small bay of Kentucky Lake, east of Aurora, Ky. (photograph taken during low water level).

than 1 or 2 feet above the normal level of Kentucky Lake, 359 feet above sea level.

The approximate shoreline of the ancient lake in part of western Kentucky is indicated by the 350-foot contour as shown on figure 1. Although gravel ridges have been observed at an altitude of about 350 feet along the margins of the Ohio River lowlands in southern Illinois, the ridges have not been mapped; therefore, the extent of the lake in Illinois is not shown on figure 1. The lake probably extended down the Ohio to the vicinity of Metropolis, 6 to 8 miles northwest of Paducah, as indicated by the distribution of the distinctive gravel ridges.

The relation of ridge deposits to upland and lacustrine deposits is illustrated on figure 2. The bay-mouth bars extending across the valley of the West Fork of Clarks River may have developed subsequent to the beach-ridge deposits farther upstream. A succession in the development of these deposits could have been caused by deltaic deposition above the bars which

caused shoal water, the site of gravel bar development, to migrate toward the middle of the lake.

The townsite of Kaler is on an island hill surrounded by lacustrine deposits and accompanying ridge deposits, a type of feature that also was noted in the area of ancient lakes described by Shaw (1915, p. 156).

The cause and exact age of the lake are unknown. The lake may have formed during the diversion of the Ohio River through the Metropolis Gap from its former Cache Valley course (Fisk, 1944, p. 39-40). Another possibility is that the Ohio may have been impounded near Metropolis either by rapid alluviation or by faulting. Absence of loess on the gravel ridges indicates a fairly young age, probably late Wisconsin. The surface on which Paducah is situated, which is well within the area of the ancient lake, is described by Ray (1963, p. B127) as a terrace deposit that may be of Mankato age.

#### REFERENCES

- Fisk, H. N., 1944, Geological investigation of the alluvial valley of the lower Mississippi River: Vicksburg, Miss., Mississippi River Comm., 78 p.
- Leighton, M. M., and Willman, H. B., 1950, Loess formations of the Mississippi Valley: *Jour. Geology*, v. 58, no. 6, p. 599-623; Illinois Geol. Survey Rept. Inv. 149.
- Leighty, W. J., and Wyatt, C. E., 1950, Soil survey of Marshall County, Kentucky: U.S. Dept. Agriculture, Ser. 1938, no. 29, 109 p.
- , 1953, Soil survey of Graves County, Kentucky: U.S. Dept. Agriculture, Ser. 1941, no. 4, 139 p.
- Ray, L. L., 1963, Quaternary events along the unglaciated lower Ohio River valley: Art. 33 in U.S. Geol. Survey Prof. Paper 475-B, p. B125-B128.
- Shaw, E. W., 1911, Preliminary statement concerning a new system of Quaternary lakes in the Mississippi basin: *Jour. Geology*, v. 19, p. 481-491.
- , 1915, Newly discovered beds of extinct lakes in southern and western Illinois and adjacent States: *Illinois Geol. Survey Bull.* 20, p. 139-157.



## OUTLINE OF PLEISTOCENE GEOLOGY OF MARTHA'S VINEYARD, MASSACHUSETTS

By CLIFFORD A. KAYE, Boston, Mass.

**Abstract.**—Six glacial drifts and the deposits of one interglaciation are recognized on Martha's Vineyard. It is thought that these represent Nebraskan Glaciation, Aftonian Interglaciation, and Kansan, early Illinoian, late Illinoian, early Wisconsin, and late Wisconsin Glaciations. In addition, the terminal moraine of middle Wisconsin Glaciation is nearby, at the Elizabeth Islands, and the periglacial effects of this ice sheet are preserved on Martha's Vineyard. The Pleistocene stratigraphy was worked out independently of earlier work and is in remarkably close agreement with the conclusions reached by Fuller and Woodworth a half century ago.

The following discussion and the diagrammatic cross section (fig. 2) summarize the major conclusions that the author has reached concerning the stratigraphic divisions of the Pleistocene deposits of Martha's Vineyard, an island just off the coast of Massachusetts. The conclusions are the result of a field study begun in 1957 that will be reported on more fully later.

Early workers on the glacial deposits of the southern New England islands recognized the existence of a complex stratigraphic sequence of drifts. Fuller (1914) distinguished 7 drift units and 1 interglacial unit on Long Island, comprising all 4 glacial stages of the Pleistocene. Woodworth and Wigglesworth (1934) recognized approximately the same sequence on Martha's Vineyard. However, the conclusions of these earlier workers were later questioned (for example, Flint, 1947, p. 296), and in recent decades most publications on the Pleistocene geology of eastern North America have tried to explain all deposits as the product of Wisconsin Glaciation.

The writer approached the geology of Martha's Vineyard with few preconceptions, working independently of the results of earlier writers. He soon became convinced, however, that deposits and structural effects of several ice sheets that apparently represent a wide time range are present. The problem of arranging the drifts in stratigraphic order was complicated by the fact that most of the deposits are fragmentary. No single exposure contains the entire section, and the

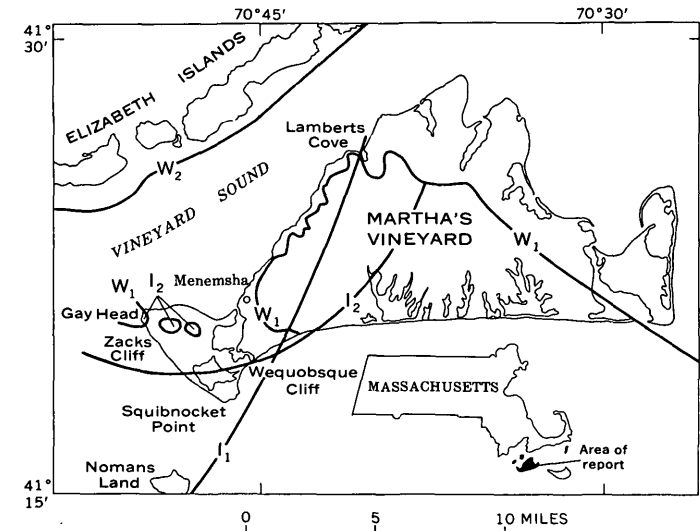


FIGURE 1.—Map of Martha's Vineyard and surrounding islands, showing localities and inferred ice margins referred to in text. Ice markings: I<sub>1</sub>, early Illinoian; I<sub>2</sub>, late Illinoian; W<sub>1</sub>, early Wisconsin; and W<sub>2</sub>, middle Wisconsin. See figure 1 of the following article (p. C141) for location of mapped moraines on Martha's Vineyard.

stratigraphic sequence had to be put together piecemeal by a series of comparisons between widely separated outcrops. Moreover, the deposits are almost everywhere very much deformed by glacially produced thrust faulting and some folding. Thus, deposits that were laid down as much as several miles apart have been telescoped together by the glacial imbrication. This complicated the recognition of facies differences and variations of the type to be expected within a single drift. A series of value judgments had to be made as to whether differences in adjacent deposits were due to faulting, differences in age, or compositional and textural variations within a single drift.

When all the fragments were pieced together, however, there was strong evidence of 6 drifts and the periglacial effects of a 7th glaciation, thought to be that which produced the nearby Elizabeth Islands moraine several miles to the northwest (fig. 1). Moreover,

sediments deposited during an interglaciation are present, and the weathering and erosional effects of several other interglaciations have been deduced. This confirms the deductions of Fuller (1914) and Woodworth and Wigglesworth (1934) as to the number of drifts and interglacial deposits present. The writer differs with these earlier workers, however, on the stratigraphic position of some of the deposits; therefore, in the following brief account only stage names are used.

The drifts were assigned ages by matching them with all the known major glacial stages and substages of the upper Mississippi Valley, working back from the late Wisconsin and taking into account the lengths of interglacial intervals as suggested by weathering effects and interglacial deposits. It is recognized that this method leaves much to be desired as a means of correlation, and therefore must be considered as a provisional interpretation, at best. Nonetheless, it is apparent that Martha's Vineyard possesses one of the most complete sections of Pleistocene deposits known, and possibly the most complete and varied within the confines of such a small area (81 sq mi).

#### NEBRASKAN DRIFT

Nebraskan drift consists of a till that has been recognized at only one locality on Martha's Vineyard, the eastern part of Wequobsque Cliff (fig. 1), where it overlies greensand of Miocene age and attains a maximum exposed thickness of 20 feet. It is very compact and well graded in the clay to fine-gravel size range; clasts larger than 3 inches are very rare. It is light gray (dry) or medium gray (moist), and is massive in the upper part but thinly banded or stratified in the lower part. About 97 percent of the coarse clasts in the till consist of quartz pebbles and nodular rocks derived from Tertiary and Cretaceous coastal-plain sediments, which are exposed on Martha's Vineyard; thus only 3 percent are derived from crystalline rocks of the New England upland. This is significant because the percentage of crystalline rocks of New England upland provenance increases in successively younger tills. The sand, silt, and clay show by their mineral composition that they, too, are largely reworked coastal-plain sediments.

At two places in the cliff the upper part of the till has been profoundly altered by weathering to a maximum depth of 13 feet beneath sand of early Illinoian age. This old truncated regolith (which, like most interglacial weathering profiles, has been partially to completely removed by later glacial erosion) is nearly white. Study of the clay mineralogy by John Hathaway, U.S. Geological Survey, showed that the regolith is considerably richer in kaolinite than the unweathered

till from which it was derived. Little can be deduced about the direction of movement of the Nebraskan ice, although dark-gray phyllite pebbles in the till, which resemble rocks in southern Rhode Island, suggest south-southeast or east-southeast movement. There is no evidence indicating the maximum extent of the ice sheet. This till was not recognized by Woodworth and Wigglesworth and may not have been exposed in their day.

#### AFTONIAN DEPOSITS

Deposits of probable Aftonian age consist of several bodies of quite dissimilar sediments that are thought to represent both marine and nonmarine depositional facies in a coastal area (fig. 2). In eastern Wequobsque Cliff there is a bright pistachio-colored greensand interbedded with quartzose gravel (the content of crystalline rock pebbles is about 2 percent of the total pebbles) containing reworked Miocene shark teeth and other fossils. In Wequobsque Cliff these sediments overlie the Nebraskan till. The greensand does not resemble the Miocene greensand or the glauconitic fine sand of Late Cretaceous age, both of which crop out on the island. The glauconite may therefore be authigenic; an attempt is being made to date it by the potassium-argon method. Cropping out in the central part of Gay Head Cliff is a massive bed that consists mainly of reworked Miocene and Cretaceous sand, gravel, and fossils, which in part is loosely cemented by phosphate. This peculiar bed was called the Aquinnah Conglomer-

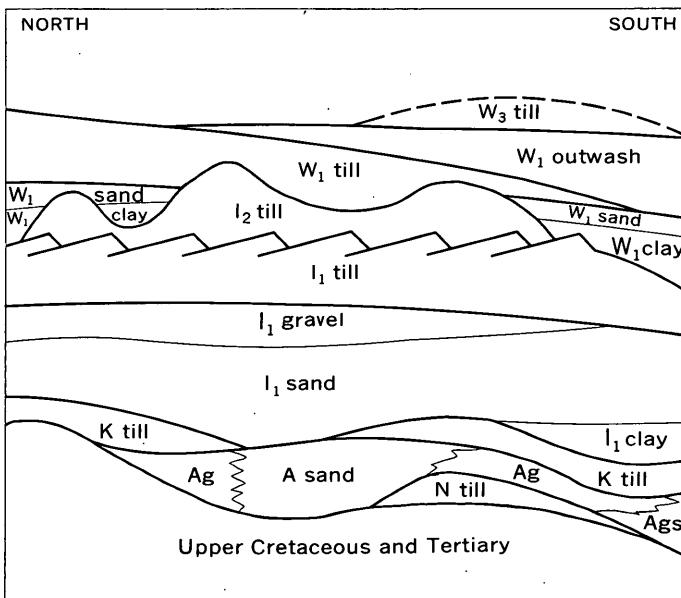


FIGURE 2.—Diagrammatic north-south cross section through Martha's Vineyard, showing succession of drifts and their spatial relationships. Symbols: *N*, Nebraskan; *A*, Aftonian; *K*, Kansan; *I<sub>1</sub>*, early Illinoian; *I<sub>2</sub>*, late Illinoian; *W<sub>1</sub>*, early Wisconsin; *W<sub>3</sub>*, late Wisconsin; *gs*, greensand; *g*, gravel. The serrated contact between early Illinoian and late Illinoian till indicates imbrication of all older deposits by late Illinoian ice.

ate by Woodworth and Wigglesworth (1934), and although it strongly resembles the Miocene deposits of Gay Head, its Pleistocene age was established by the finding of the bone of a Pleistocene horse. This odd sediment is probably talus that accumulated on the lower slopes of a sea cliff that was cut into Miocene and Upper Cretaceous sediments in Aftonian time. In the southern part of Gay Head it can be seen grading into greensand and quartzose gravel very similar to those of Wequobsque Cliff. In south and central Gay Head these sediments unconformably overlie white clayey coarse sand of the Raritan Formation of Late Cretaceous age; in some places they underlie Kansas till, and in others sand of early Illinoian age.

The Aquinnah Conglomerate and the greensand-quartzose gravel complex are not found in the northern part of Gay Head. Instead, a massive ferruginous clay and fossiliferous glauconitic sand lie between Miocene greensand and Kansan drift. Mollusks from the sand were studied by Dall (1894), who dated them as Pliocene. More recently Raup and Lawrence (1963), working with another collection of shells, considered the fauna to be Pleistocene. Further study is being carried on to resolve the difference of opinion. At this stage of the study, one can only suggest that if these deposits are Pleistocene in age they probably are equivalent to the greensand and gravel to the south.

#### KANSAN DRIFT

Kansan drift is found at several places in Gay Head Cliff overlying the Aquinnah Conglomerate, the Pliocene or Pleistocene fossiliferous sand, or where this is missing, Upper Cretaceous or Miocene sediments. It is also exposed in the cliff in the northern end of Lamberts Cove and in several sand and gravel pits in the interior of the western part of the island. It is a compact, medium-gray to greenish-gray till that is poor in cobbles and boulders. However, a lag deposit of boulders, mostly of crystalline rocks (termed the "Dukes boulder bed" by Woodworth and Wigglesworth, 1934), marks the stratigraphic position of the Kansan drift in a few places in Gay Head Cliff. The content of crystalline rocks in the till is higher than in the Nebraskan till, but nodular sedimentary rocks (siderite, dolomite, limestone, and phosphorite) from the coastal-plain sediments make up 60-80 percent of the clasts larger than 1 inch. In the lag gravel the content of crystalline rocks is higher, mainly because these rocks are generally harder and more durable than the nodular rocks. In Lamberts Cove Cliff, Kansan till is oxidized beneath its contact with overlying sand of the Illinoian drift to a depth of more than 40 feet. In the northern part of Gay Head, lag pebbles and boulders of Kansan till are deeply

wind cut and polished where they are overlain by basal fine sand (eolian?) of the Illinoian drift. In other places, some of the crystalline boulders are much decomposed. The direction of movement of Kansan ice is deduced from very tenuous evidence as having been almost due south. There is no evidence as to the maximum extent of the Kansan ice sheet.

#### ILLINOIAN DRIFT

The patchy Kansan till is overlain by a widespread and varied sequence of sediments that are thought to be Illinoian in age. The Illinoian drift is divided into a lower unit of sorted, stratified sediments overlain by till, believed to be of early Illinoian age, and an upper till that may represent late Illinoian Glaciation. In the central and northern part of Gay Head Cliff and in several pits in the interior of the island the basal Illinoian drift consists of fine-grained light-gray laminated sand that grades up into crossbedded, somewhat glauconitic, uniform fine to medium sand and finally up into a somewhat quartzose gravel. In the southern part of Gay Head Cliff and in Lamberts Cove, the basal Illinoian consists of glauconitic sand and quartzose gravel that somewhat resemble the Aftonian sequence of Wequobsque Cliff. In the southern part of Gay Head Cliff, in Squibnocket Cliff, and in the cliff of Nomans Land (fig. 1), the basal Illinoian is brown to gray clay and silt overlain by fine to medium sand. There is no evidence of weathering of any of these basal deposits beneath Illinoian till.

These sorted, basal sediments are unfossiliferous (except for fossils that were obviously reworked from Miocene beds) and for the most part are probably non-marine. The glauconite is probably reworked from older greensand. Indeed, in texture and type of bedding and crossbedding, some of the deposits resemble outwash sand and gravel, and eolian sand. The thick clay-sand sequence may be marine and quite comparable to the clay-sand sequence at the base of the Wisconsin drift, which is thought to be a marine deposit made up of rock flour and sand derived from the advancing ice sheet. Because of these reasons and the absence of a pre-till weathering profile it seems more reasonable to consider these sediments as Illinoian rather than Yarmouth in age.

The early Illinoian till is best exposed in cliffs at Squibnocket Point and in the cliffs on the south shore of Nomans Land, 3½ miles to the south. It also is found at the north end of Lamberts Cove and in pits in the interior of the western part of the island. It is an exceedingly compact well-graded till, eroding into "badland" forms. In places it is strikingly stratified. The color is slightly mauve to pinkish gray. More than 60

feet of till is present in the cliffs of Nomans Land and Squibnocket. This very compact stratified till was called the Montauk Till Member of the Manhasset Formation in Long Island by Fuller (1914), and the name Montauk was extended to Martha's Vineyard and Block Island by Woodworth and Wigglesworth (1934).

Unlike the Kansan and Nebraskan tills but in common with all later tills, the pebbles, cobbles, and boulders of the early Illinoian till are predominantly of crystalline rock. Much of the deep pre-Pleistocene regolith had been removed from the New England crystalline terrane by the two earlier ice sheets, and by Illinoian time a large expanse of unweathered rock lay exposed for the glacial ice to quarry. From rock types in the till the direction of movement of the early Illinoian ice is thought to have been toward the east-southeast. The thick till exposed at Squibnocket Point and Nomans Land probably represents parts of the terminal moraine, and the limits of the ice are inferred to have been a deep lobe, the edge of which trended southwest from Lamber's Cove through Nomans Land, curving northward to the west to include Block Island, where this till is also well exposed (Kaye, 1960, fig. 51). The bathymetry of open waters between the islands gives evidence of this lobate ice margin. Hydrographic charts and recent surveys show that a broad ridge marked here and there by boulder concentrations follows this alignment.

The late Illinoian till can be seen in only a few small exposures in the eastern part of Wequobsque Cliff. The former widespread presence of this till, however, is deduced from the marked structural effects that the ice sheet had on all older deposits and from the widespread occurrence of a lag concentration of large boulders of a characteristic type that were carried by the ice and that may have once been part of a till sheet. Where exposed in Wequobsque Cliff, the till is medium to dark gray and has an abundance of cobbles and boulders. Two rather distinctive rock types are found in the clasts: a coarsely porphyritic granite containing large pink to red microcline phenocrysts, and a dark-gray diorite. Boulders of these rocks, commonly of very large size, litter the surface of much of western Martha's Vineyard. Their greatest concentration is in areas of pronounced structural imbrication, and they are particularly abundant in the hilly western section of the island. These hills are the remains of a great pushed, or imbricated, terminal moraine of the late Illinoian ice. The intervening valleys are erosional, cut by streams in Sangamon time. The lobate outline of the late Illinoian terminal moraine is suggested by the change in strike of the thrust sheet produced by it.

It is also shown by the topographic axis of the western part of the island. The southernmost point reached by this lobe was just north of Squibnocket.

No deposits of Sangamon age have been recognized. Sangamon time was, however, a time of considerable erosion and profound weathering. Deep oxidation developed during this interval is found on Sangamon erosion surfaces in all the cliffs.

#### EARLY WISCONSIN DRIFT

The earliest Wisconsin deposit is thick gray clay overlain by sand. The sequence very much resembles the clay and sand of the early Illinoian drift and probably formed under similar conditions. The early Wisconsin clay and sand crop out in the high central and western part of Wequobsque Cliff where they have been repeated by a series of thrust faults, and in the cliffs on the north side of the island where they were pushed up from Vineyard Sound against the north flank of the eroded Illinoian moraine by early Wisconsin ice. In Wequobsque Cliff the lower 10 feet of the clay is varved, grading up into an unfossiliferous medium-gray massive clay. Pollen studies of this clay indicate a fairly mild climate at the outset of deposition, becoming colder as clay was deposited toward the top of this zone. The sediment probably represents a proglacial deposit formed by rock flour coming from the distant early Wisconsin ice. As the ice advanced, crustal subsidence caused by ice loading produced a relative rise of sea level. This changed the estuarine or lacustrine depositional environment (varved clay) to a marine environment (massive clay). The overlying uniform sand is in effect a deltaic continuation of the same deposition and marked the approach of the ice front. In western Wequobsque Cliff the sand grades up into gravelly outwash, which in turn is overlain by compact early Wisconsin till.

The morainic deposits of the early Wisconsin ice range from a well-graded till containing some interstratified thin lenticular sand and gravel, on the west, to a stratified medium to coarse sand containing minor amounts of gravel in the eastern part of the island. In the central part of the island the two types of deposits tend to grade into each other. In the westernmost part of the island the cobbles and boulders in the till consist of an unusually wide variety of rock types and include many that are recognized as coming from distant outcrops to the northwest, in Massachusetts and Rhode Island. The erratics in the eastern part of the island lack the diversity of type and the distinctive and sometimes traceable rocks that are found in the till to the west. This is very probably due to differences in the direction of ice movement as suggested by the bilobate configuration of the ice front (fig. 1).

The broad triangular outwash plain making up the central section of Martha's Vineyard is a product of the early Wisconsin glaciation. The plain was fed mainly by the eastern lobe of the ice, although some sediment was contributed by the western lobe where small tongues of ice broke through the north ridge of the eroded Illinoian moraine (fig. 1).

### MIDDLE WISCONSIN GLACIATION

Martha's Vineyard was probably free of ice during the middle Wisconsin. It was during part of this interval that the large moraine of the Elizabeth Islands, only 4 miles to the northwest, was formed. Some oxidation of earlier deposits and the development of podsol soil took place on Martha's Vineyard during the interval between early Wisconsin glaciation and the maximum advance of middle Wisconsin ice. Later, when the ice front stood at the Elizabeth Islands moraine, solifluction and other frost action occurred on Martha's Vineyard. Large soil involutions, ice-wedge structures, and deeply cut and polished ventifacts are found on the early Wisconsin moraine, outwash plain, and the uplands. Even the previously developed podsol soil was involuted. Solifluction carried surface material down-slope; characteristic deposits of iron-stained solifluction debris can be seen rimming the lower flanks of hills in many sea cliffs.

### LATE WISCONSIN DRIFT?

The presence of late Wisconsin drift on Martha's Vineyard, dating from about 13,000–14,000 years B.P., is inferred from several lines of evidence. A radiocarbon date of  $15,300 \pm 800$  years B.P. (W-1187, Washington laboratory, U.S. Geological Survey) was obtained from leaves of tundra plants embedded in clay in Zacks Cliff, a low sea cliff about midway between Squibnocket Point and Gay Head. The clay overlies middle Wisconsin solifluction gravel and compact early Wisconsin till. The clay is overlain by foreset bedded sand. The outlines of the body of water in which this material was deposited are no longer evident and probably were removed by erosion. At two places the clay and sand are overlain by till, or a till-like deposit (cobbles, gravel, in a silty sand matrix). Inland from here, low roadcuts show similar till (?) interbedded with sand.

About 2 miles southeast of Zacks Cliff, about 10 feet of postglacial peat and organic sediment is exposed in the upper part of the sea cliff at Squibnocket (Kaye, 1962; Ogden, 1963). The lower 2 feet of this

deposit contains fossils of tundra plants, and pollen studies indicate that a tundra flora existed when the earliest sediments were deposited here. A radiocarbon date of  $12,700 \pm 300$  years B.P. (W-710, Washington laboratory, U.S. Geological Survey, Rubin and Alexander, 1960) was obtained from a very thin sample at the base of the section resting on early Illinoian till.

The two Martha's Vineyard dates viewed in isolation do not in themselves provide a very strong basis for deducing the presence of an ice sheet of intermediate age. However, such an interpretation is given strong support by the fact that no basal material from post-glacial organic sediments in eastern Massachusetts and Rhode Island has yielded a date older than that at Squibnocket. The deposition of sediment in depressions seems to have begun sometime after 13,000 years B.P. In the Boston area the earliest date obtained is 12,170 years B.P. (Kaye and Barghoorn, 1964); on Block Island, 12,090 years B.P. (Kaye, 1960). All of these are thin samples collected in open exposures. In Boston a date of 14,000 years B.P. was obtained from shells in marine clay, but these clays have been preconsolidated to considerable depth, and it is believed that this is the result of overriding by an ice sheet, presumably the same glacial advance that reached Martha's Vineyard.

Another line of evidence for glaciation that was approximately contemporaneous with the Port Huron ice advance of the Great Lakes area (Flint, 1963) is that the middle Wisconsin solifluction deposits of eastern Wequobsque Cliff are faulted and the entire surface has been planed smooth, removing the upthrown scraps of the faults. The faulting may be the result of ice shove, as are so many of the structures exposed in the cliffs, and the smoothly truncated surface may have been caused by glacial erosion. Other examples of surface planation have been noted in the cliffs. An interesting one is in the western part of Wequobsque Cliff where an undrained depression has been entirely removed and only the well-developed gley zone that formed beneath it is preserved.

### REFERENCES

- Dall, W. H., 1894, Notes on the Miocene and Pliocene of Gay Head, Martha's Vineyard, Massachusetts, and on the "land phosphate" of the Ashley River district, South Carolina: Am. Jour. Sci., 3d ser., v. 48, p. 296–301.
- Flint, R. F., 1947, Glacial geology and the Pleistocene Epoch: New York, John Wiley and Sons, Inc., 589 p.
- , 1963, Status of the Pleistocene Wisconsin stage in central North America: Science, v. 139, p. 402–404.
- Fuller, M. L., 1914, The geology of Long Island, New York: U.S. Geol. Survey Prof. Paper 82, 231 p.

- Kaye, C. A., 1960, Surficial geology of the Kingston quadrangle, Rhode Island: U.S. Geol. Survey Bull. 1071-I, p. 341-396.
- , 1962, Early postglacial beavers in southeastern New England: Science, v. 138, p. 906-907.
- Kaye, C. A., and Barghoorn, E. S., 1964, Late Quaternary sea-level change and crustal rise in Boston, Massachusetts, with notes on the autocompaction of peat: Geol. Soc. America Bull., v. 75, p. 63-80.
- Ogden, J. G., III, 1963, The Squibnocket cliff peat: radiocarbon dates and pollen stratigraphy: Am. Jour. Sci., v. 261, p. 344-353.
- Raup, D. M., and Lawrence, D. R., 1963, Paleontology of Pleistocene mollusks from Martha's Vineyard, Massachusetts: Jour. Paleontology, v. 37, p. 472-485.
- Rubin, Meyer, and Alexander, C., 1960, U.S. Geological Survey Radiocarbon dates V: Am. Jour. Sci. Radiocarbon Supplement, v. 2, p. 129-185.
- Woodworth, J. B., and Wigglesworth, Edward, 1934, Geography and geology of the region including Cape Cod, the Elizabeth Islands, Nantucket, Martha's Vineyard, No Mans Land and Block Island: Harvard Univ. Museum Comparative Zoology Mem. 52, 322 p., 38 pl.

X

## ILLINOIAN AND EARLY WISCONSIN MORAINES OF MARTHA'S VINEYARD, MASSACHUSETTS

By CLIFFORD A. KAYE, Boston, Mass.

*Abstract.*—Three well-defined morainic systems are present on Martha's Vineyard. Remnants of an early Illinoian moraine occur at the southernmost point of the island and on Nomans Land, a nearby island. Hydrographic surveys show a deeply lobate submarine continuation to the west. The hills and valleys of western Martha's Vineyard are the eroded remains of a very large moraine pushed up by late Illinoian ice. Early Wisconsin ice was partly stopped by this moraine in the western part of Martha's Vineyard but overrode it in the eastern part. The entire eastern half of the island consists of the early Wisconsin moraine and its outwash plain.

Six drifts, very probably representing Nebraskan, Kansan, two Illinoian, and two Wisconsin Glaciations are found on Martha's Vineyard. The two earliest drifts, the Nebraskan and Kansan, and the late Wisconsin do not give evidence of the maximum extent of their respective ice sheets, and it is very likely that the ice terminated well south of the island. However, study of the two Illinoian and the early Wisconsin drifts, and their respective topographic characteristics, indicates that the drifts are terminal moraines. By some curious coincidence, therefore, the terminal moraines of three successive continental glaciations appear to have crossed what is now western Martha's Vineyard (fig. 1).

### EARLY ILLINOIAN MORaine

The oldest moraine is probably early Illinoian in age. It is made up mainly of exceedingly compact mauve to pinkish-gray till that is commonly strikingly stratified. The topography is low and hummocky with many shallow swampy depressions. The depressions, however, may be partly the result of erosion by late Wisconsin ice, which seems to have occupied the area but which left only a very thin and fragmentary drift cover. On Martha's Vineyard the early Illinoian moraine as such is restricted to Squibnocket Point (fig. 1), the southernmost tip of the island. In the interior of the western part of Martha's Vineyard, pinkish compact early Illinoian till is found within the moraine of the succeeding

late Illinoian ice sheet where it had been faulted up, along with earlier deposits, in an imbricated series of thrusts.

The same type of thick till and similar terrane features as at Squibnocket are found on Nomans Land, a small island  $3\frac{1}{2}$  miles south-southwest of Squibnocket. Hydrographic charts show a low, interrupted submarine ridge of broadly lobate form connecting Nomans Land and Block Island, lying about 40 miles to the west, where similar very compact stratified till crops out with considerable thickness in the cliffs. The same type of very compact stratified till also occurs in eastern Long Island, where it was called the Montauk Till Member of the Manhasset Formation by Fuller (1914). The probable ice margin of the early Illinoian ice in the Martha's Vineyard area is shown on figure 1.

### LATE ILLINOIAN MORaine

The high-standing, hilly western section of Martha's Vineyard is the terminal moraine of late Illinoian ice. Northeast of Menemsha the moraine has been much eroded, both by stream action and by landsliding. Two rather deep northeast-trending valleys and a number of tributary valleys and gullies have been cut into it, producing a pleasant hill-and-dale topography with a relief of up to 175 feet. To the west the moraine is interrupted by a low sag occupied by two large ponds between Menemsha and Squibnocket Point; farther west the moraine occurs in the high land near Gay Head.

The interior of the moraine is well exposed in Gay Head Cliff, the high sea cliff at the western tip of Martha's Vineyard. Here the moraine is seen to consist of Late Cretaceous, Miocene, and pre-late Illinoian Pleistocene deposits, broken by a great number of faults and, at several places, distorted into complex folds. These structures continue below sea level, and there is no evidence of how thick the morainic complex is here. A detailed study of the structure exposed in

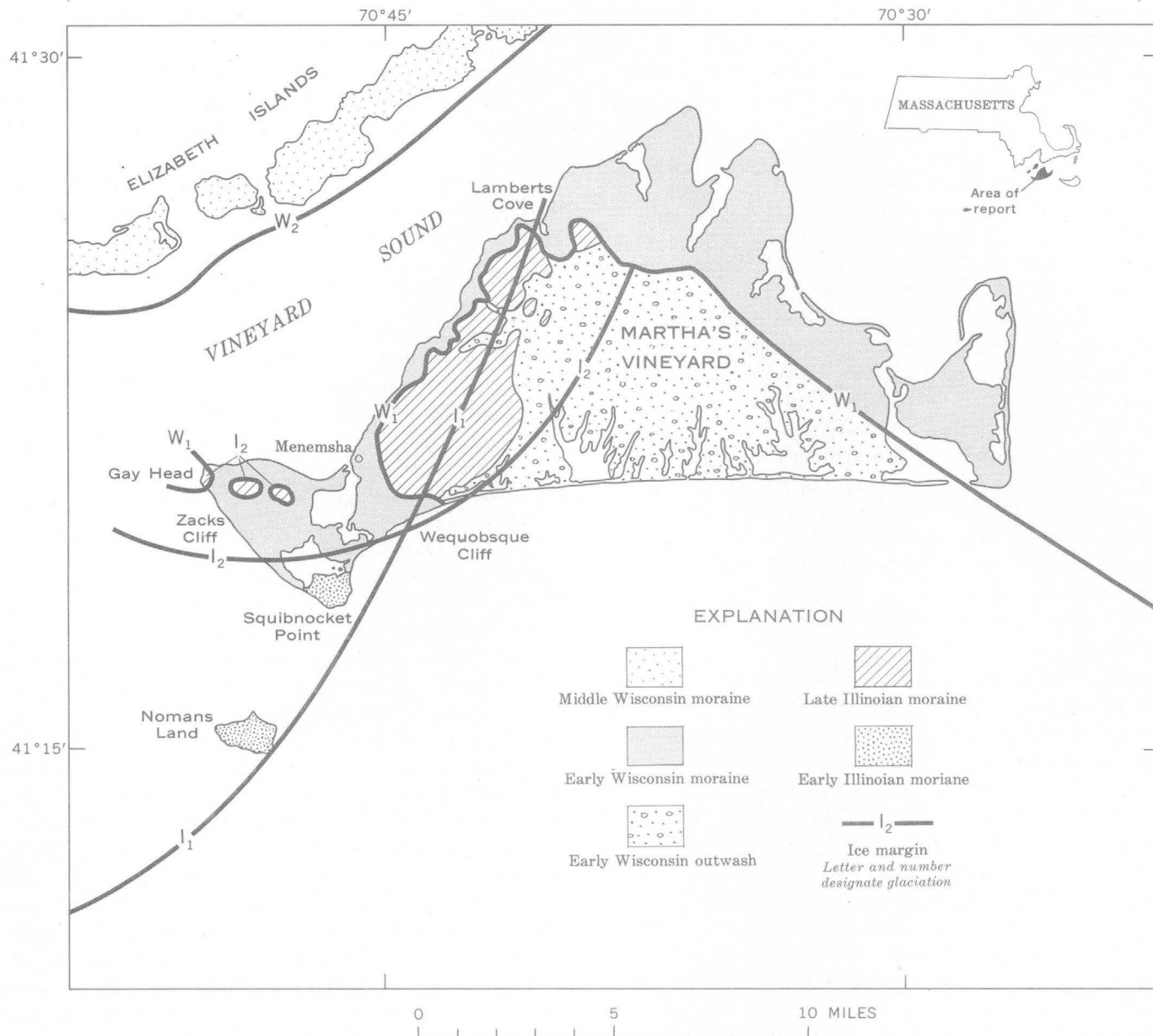


FIGURE 1.—Map of Martha's Vineyard and surrounding islands, showing inferred ice margins and moraines of early Illinoian ( $I_1$ ), late Illinoian ( $I_2$ ), early Wisconsin ( $W_1$ ), and middle Wisconsin ( $W_2$ ) ice sheets.

the cliff shows that the moraine is mainly made up of imbricated thrust sheets pushed from the north. Distortions of the thrust plates—presumably formed as they piled up in front of the ice—created secondary fault structures and large-scale rumpling. The impression conveyed by Gay Head, that the structure is an imbrication of thrust plates moved from the north, is confirmed by detailed mapping and study of exposures in the hilly section of the moraine northeast of Menemsha. Here the same imbrication of thrust plates, with individual plates attaining thicknesses of 100 feet or

more, can be seen. Upper Cretaceous deposits are repeatedly thrust over Pleistocene.

The major thrust sheets in Gay Head Cliff strike nearly east. East of Menemsha, the strike is northeast; the shift in orientation reflects the lobate form of the moraine. A study of aerial photographs shows that the eroded moraine northeast of Menemsha is marked by a series of low parallel ridges. From exposures in some of these ridges, one can see that they parallel the strike of the thrust sheets and are, in fact, small erosional cuestas produced by the outcrops of more resist-

ant beds (mostly of early Illinoian till) within the thrust sheets. They therefore are useful in outlining the deformational structure of the moraine and they nicely indicate the form of the ice lobe that produced the deformation.

Over most of this moraine late Illinoian till is absent. At many places, however, there is an impressive concentration of boulders. Many of these are of a characteristic coarsely porphyritic granite with pink to red euhedral phenocrysts of microcline, 2 inches or more in length, that is not found in older drifts. These boulders are thought to have been transported by the late Illinoian ice and, in part, may represent a lag concentration left after whatever late Illinoian till that may have been deposited on or in the moraine had been removed by interglacial erosion.

The late Illinoian ice was not unique in producing thrust or push structures. All the glaciations appear to have deformed to varying degrees the preexisting sediments. In Gay Head and other cliffs, there is a problem of distinguishing the deformation produced by the several ice sheets. It is clear, however, that the late Illinoian ice produced the most important deformation.

The mechanism responsible for the imbricated moraine was probably the shearing off of broad flat fragments of the ground surface lying in front of the ice and the piling up of these plates as the ice moved forward. Plates were successively added at the base, rather than the top of the pack, and the moraine in effect was built from the base upwards. Something of the sort can be seen if one pushes his hand horizontally against the surface of a sandy beach on which there is a thin crust of salt-cemented sand. The essential condition is that the surface plates have greater rigidity and strength than the substrata along which they shear. Perhaps, therefore, the ground in front of the ice was frozen and the thrust plates may therefore largely represent the permafrost zone existing at the time, and the thickness of each thrust sheet may measure the thickness of the carapace of frozen ground. The stripping and bulldozing effect was probably facilitated by the existence of weak clayey beds beneath the permafrost. Moreover, the piling from the base upwards may have been aided by a thawed surface (the "active zone") on the frozen ground. This would have reduced frictional resistance to the movement of the heavy morainic pile as it was pushed out over the ground surface.

The late Illinoian moraine appears to have had a deep sag in the area now occupied by ponds between Menemsha and Squibnocket Point. Elements of the moraine are now lacking in this lowland, a fact that cannot be entirely explained by erosion by the early

Wisconsin ice known to have passed through here. More likely the absence of the moraine is a result of a low point in the pre-late Illinoian surface.

The lack of porphyry boulders and of characteristic deformational structures in the Squibnocket area suggests that the southern margin of the late Illinoian moraine probably passed immediately north of here. With this as a point of control, the lobate southern margin of the moraine has been drawn (fig. 1).

#### EARLY WISCONSIN MORAINES

The next ice sheet to have reached Martha's Vineyard was probably early Wisconsin in age. The moraine of this ice probably correlates with the Ronkonkoma moraine of Long Island (Fuller, 1914). Many of the physiographic features produced by this ice are still evident on Martha's Vineyard and can be best appreciated on aerial photographs. In the western part of Martha's Vineyard, the ice was stopped by the late Illinoian moraine. Northeast of Menemsha the ice lapped up against the north flank of the northernmost of the three erosional ridges, generally reaching no higher than the present 150-foot contour. Till deposited by this ice rarely exceeds 25 feet in thickness, and the ice left little in the way of an actual moraine.

One effect of the glaciation was the rumpling and thrusting up of the early Wisconsin proglacial deposits into ridges. These consisted of thick marine clay overlain by sand that had been deposited in Vineyard Sound, in the Menemsha sag, off the south coast, and in fact, in all low-lying places. Besides the resulting push ridges and thin till, another topographic effect of the glaciation was the erosion of the late Illinoian moraine and the removal of many of its more delicate features. For example, the thrust ridges were destroyed, and today we can see many of these ridges truncated at the margin of the early Wisconsin moraine.

The strip occupied by the early Wisconsin moraine along the northwest coast of the island is narrow, averaging about half a mile in width. However, where low cols or small transverse valleys had cut across the crest of the northern ridge of the late Illinoian moraine, the ice front was able to project south for short distances into the erosional valley beyond. The largest of these projecting tongues of ice was south of Lamberts Cove, where a bulbous lobe of ice reached about a mile south of the main front.

West of the main late Illinoian moraine the ice pushed through the Menemsha sag and then spread east and west. The ice also flowed south through Vineyard Sound, around the highlands of Gay Head, joining the ice pushing through the Menemsha sag. The highest

land near Gay Head rose above the ice as low nunataks. Today three patches of high ground, including the higher part of Gay Head Cliff and the land immediately behind it, give evidence of having been ice free. The early Wisconsin ice may have reached as far south as Nomans Land. Thin drift that may be early or late Wisconsin in age caps all but the highest ground of this small island.

In the eastern part of Martha's Vineyard the early Wisconsin ice was able to push south across the entire width of the late Illinoian moraine and to form a very broad lobe. The entire eastern half of Martha's Vineyard is the product of this lobe, as is most of Nantucket Island to the east. On Martha's Vineyard the moraine of this lobe is a belt of low hummocky ground, about 2 miles wide, that follows the northeastern shore. From many good exposures in cliffs it is clear that much of the moraine is made up of horizontally stratified sand

with some interbedded gravel. This material is not noticeably different from the sand and gravel in the outwash plain that spreads from the foot of the moraine to the south shore of the island. The morainic sand may represent a superglacial, headward continuation of the outwash plain. However, the moraine stands higher than the outwash plain. This relationship is difficult to explain in terms of the topographic inversion to be expected in superglacial deposits (Kaye, 1960, p. 358). The manner in which the early Wisconsin moraine in eastern Martha's Vineyard was built is therefore a question that merits further study.

#### REFERENCES

- Fuller, M. L., 1914, The geology of Long Island, New York: U.S. Geol. Survey Prof. Paper 82, 231 p.  
Kaye, C. A., 1960, Surficial geology of the Kingston quadrangle, Rhode Island: U.S. Geol. Survey Bull. 1071-I, p. 341-396.



## GLACIAL GEOLOGY OF THE MOUNTAIN IRON-VIRGINIA-EVELETH AREA, MESABI IRON RANGE, MINNESOTA

By R. D. COTTER and J. E. ROGERS,  
St. Paul, Minn., Alexandria, La.

*Work done in cooperation with  
the Minnesota Department of Iron Range Resources and Rehabilitation*

**Abstract.**—The surficial clayey till in the vicinity of Mountain Iron, Virginia, and Eveleth is of post-Cary age. In the southern part of the area studied, this till is overlain by deposits of glacial Lake Upham, and throughout the area it is underlain successively by stratified drift and bouldery till, both of Cary age, and by remnants of older tills.

Unconsolidated deposits related to 3, or possibly 4, Pleistocene glaciations have been recognized in the Mountain Iron-Virginia-Eveleth area in St. Louis County, Minn. The area described here is roughly square and is bordered on the north and northeast by the Laurentian divide; it extends about 9 miles both westward and southward from Virginia. The glacial deposits occupy a southwest-trending structural trough in rocks of Precambrian age.

The Precambrian bedrock consists of granite, graywacke, greenstone, slate, schist, and gneiss, and an overlying sequence of metamorphosed sedimentary rocks that consist, in ascending order, of the Pokegama Quartzite, the Biwabik Iron-Formation, and the Virginia Slate. The Biwabik is exposed in a 2-mile-wide belt south of the older bedrock. South of this the entire area is underlain by the Virginia Slate. These rocks were deeply weathered before the first Pleistocene glacier passed over the area.

### GLACIAL STRATIGRAPHY

The surface deposits are shown on figure 1. Most of the area is mantled with reddish-brown clayey till, but to the south, silt and sand of glacial Lake Upham overlie the till. A wave-cut beach at an altitude of 1,370 feet marks the contact between the till and the lake deposits, except in the southeast where it is obscured by eolian deposits.

In the report area, 7 types of till are differentiated on the basis of color, texture, or lithology; 3 types (1, 2, and 3 in the accompanying table) have not previously been described. Two bouldery types (3 and 4) prob-

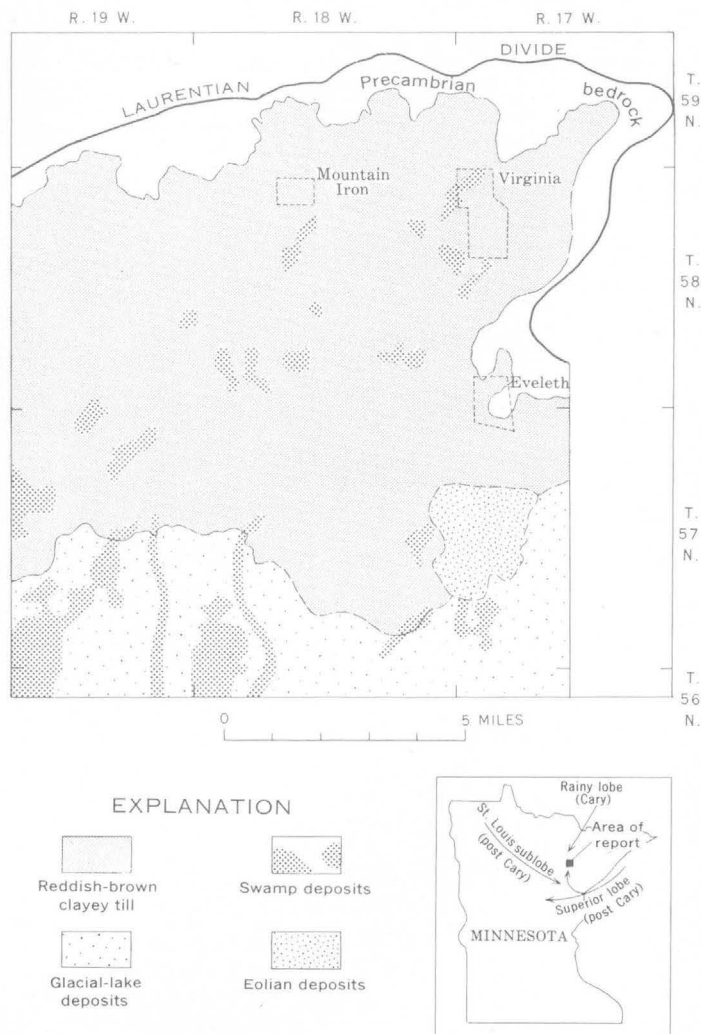


FIGURE 1.—Surficial geology of the Mountain Iron-Virginia-Eveleth area, St. Louis County, Minn.

ably represent a single interval of deposition, and 3 clayey types (6, 7, and 8) another interval.

The stratigraphic relations of the several tills are shown on figure 2 and in the accompanying table.

*Stratigraphy of glacial deposits in the Mountain Iron-Virginia-Eveleth area, Minnesota*

[Numbers in parentheses keyed to text discussion]

Age	Type of deposit	Distinguishing characteristics	Known thickness (feet)	Known distribution within Mountain Iron-Virginia-Eveleth area
Post-Cary <sup>1</sup>	(10) Eolian	Very well sorted, fine-grained sand and silt; probably derived largely from glacial lake beds; contains numerous wind-faceted pebbles.	0-5	Surficial (fig. 1). Deposits are probably more extensive than shown.
		Finely laminated, well-sorted, fine-grained sand, silt, and clay. Surface very flat.	0-26	Surficial (fig. 1).
	Till	Clayey, silty; contains a few pebbles of local origin.	0-26	Surficial (fig. 1). In subsurface beneath the lake deposits.
			0-61	In subsurface; discontinuous bodies within the areal extent of reddish-brown clayey till.
		(6) Greenish gray; contains pebbles of limestone and shale; also occurs as lenses in units 7 and 8.	0-28	In subsurface; a few lenses are within the reddish-brown and brownish-gray clayey till.
	(5) Stratified drift	Clay, silt, sand, and gravel; bedded, sorted; rock types are of local origin.	0-129	In subsurface; underlies reddish-brown clayey till, except within about 1 mile of its north and east limits.
Cary	(4) Till	Gray to buff, bouldery, sandy; contains numerous coarse fragments of local origin.	0-95	In subsurface beneath lake deposits and reddish-brown clayey till, except where removed by stream channeling.
		Orange, bouldery, sandy; contains coarse fragments of local granite, slate, and iron-formation. Color is from hematitic silt.	0-25	In subsurface; scattered lenses within a few miles of the Laurentian divide.
Pre-Cary	(2) Till and outwash	Chocolate brown, silty and sandy; contains fragments of volcanic rock, weathered igneous and metamorphic rock, calcareous concretions, limestone, and banded agate.	0-32	In subsurface; scattered lenses within a few miles of the Laurentian divide.
		Black; consists largely of decomposed slate and a few pebbles of fresh slate.	0-8	In subsurface; scattered lenses in central and southern part of the area, overlying the Virginia Slate.

<sup>1</sup> Age in doubt; see Wright (1956, p. 19-23) and Zumberge and Wright (1956, p. 65-80).

The oldest Pleistocene unit identified is a black till (1) as much as 8 feet thick, resting on the Virginia Slate. Samples, which were obtained only from test holes, contained pebbles of fresh slate in a matrix of decomposed slate.

In open-pit iron mines the oldest exposed glacial deposit consists of remnants of a chocolate-brown silty and sandy till and associated outwash (2). This till contains fragments of volcanic rock, calcareous concretions, limestone, banded agate, and weathered local igneous and metamorphic rock.

Locally, an orange, bouldery, sandy till (3) overlies the chocolate-brown till in the iron mines. The coarse fraction is composed of fragments derived from local bedrock. More than 50 percent of the fragments are granite, and the remainder are slate, metamorphic rock,

and Biwabik Iron-Formation. The orange color is due to included fragments of red hematitic silt.

Stratigraphically above the orange till, but resting on the Virginia Slate in much of the area, is a gray to buff, bouldery, sandy till (4). The lithology of this till is similar to the orange till. Stratified drift (5) generally overlies this gray bouldery till. It consists of clay, silt, sand, and gravel that is lithologically similar to these size fractions in the underlying gray bouldery till. The pitted topography of the central and west-central part of the area reflects the highly irregular upper surface of the stratified drift.

A series of three clayey, silty tills overlie the bouldery tills and associated stratified drift. The lowest of these three is a greenish-gray clayey till (6) which occurs also within and between overlying reddish-brown and

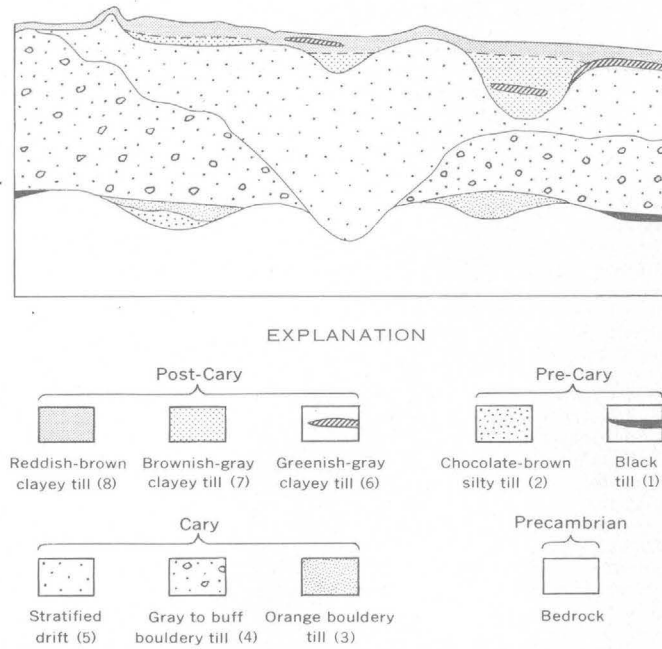


FIGURE 2.—Diagrammatic cross section of glacial till and stratified drift in the Mountain Iron-Virginia-Eveleth area, St. Louis County, Minn.

brownish-gray clayey tills. In addition to local rock types, the greenish-gray till contains numerous limestone and shale pebbles.

Locally resting on the greenish-gray till is a brownish-gray, clayey, silty till (7) containing few pebbles, most of which are of local rock, but a few of which are of volcanic rock and banded agate. It is discontinuous throughout the area, but commonly forms the lower part of thick sections of the clayey tills.

The uppermost till (8), exposed at the surface in the north and central parts of the area, is reddish brown, clayey, and silty. Contained rock types are the same as in the underlying brownish-gray till. The color break between these two tills is sharply defined, but otherwise they are the same.

#### GLACIAL HISTORY

The observed sequence of tills permits some additions to the current interpretation of the glacial history of the area.

The earliest Pleistocene glaciers to cross the area reworked the weathered slate surface and deposited the black till (unit 1 in table). A later glaciation deposited the chocolate-brown till (2). Volcanic rock fragments and agate in the chocolate-brown till indicate that the ice moved into the area from the Lake Superior Basin.

According to Wright (1956, p. 10, 11), the Rainy lobe advanced through the area from the northeast during the Cary Substage of Wisconsin time. It

crossed the Laurentian divide and deposited the gray bouldery till (4). The authors believe that the orange bouldery till (3) is a part of this same till sheet, the orange color being caused by inclusion of fragments of altered Biwabik Iron-Formation. Because the gray bouldery till (4) rests on bedrock in most of the area, the glacier must have incorporated most of the older glacial deposits.

After the ice front of the Rainy Lobe wasted to a position north of the Laurentian divide, melt water poured through notches in the divide and cut channels into or through the gray bouldery till. Stratified drift (5) was deposited around residual ice blocks, which later melted, resulting in the present pitted topography.

Wright (1956, p. 20) suggested that the Superior lobe of Post-Cary<sup>1</sup> age advanced southwestward out of the Lake Superior Basin, encountered the St. Louis sublobe of the Des Moines Lobe advancing southeastward, and split into two segments. One segment presumably was diverted northward to the Mesabi Range, where it deposited a till that is referred to in the present article as reddish-brown clayey till (8).

The authors' current view is that the reddish-brown (8) and brownish-gray (7) clayey tills are different facies of one unit deposited by the Superior lobe and that oxidation accounts for the reddish-brown color. The color difference might alternatively be explained if the brownish-gray till (7) represents an advanced stage of Post-Cary ice that is less red because of the incorporation of gray glacial lake deposits. However, the lack of any significant deposition separating the two units and the presence of brownish-gray till (7) only where the till fills depressions in the surface of the stratified drift supports the former hypothesis.

The greenish-gray clayey till (6) probably was derived from the St. Louis sublobe. Abundant limestone and shale pebbles indicate a source area to the northwest. Because this till is not continuous in the subsurface, it is postulated that the St. Louis sublobe did not actually advance into the Mountain Iron-Virginia-Eveleth area, and that the lenses of greenish-gray till represent materials carried into the area by the Superior lobe from the confluence of Superior and St. Louis ice.

#### REFERENCES

- Wright, H. E., Jr., 1956, Sequence of glaciation in eastern Minnesota, in Geological Society America Guidebook, 1956 Annual Meeting, Minneapolis, Minn.: p. 1-24.
- Zumberge, J. H., and Wright, H. E., Jr., 1956, The Cary-Mankato-Valders problem, in Geological Society America Guidebook, 1956 Annual Meeting, Minneapolis, Minn.: p. 65-81.

<sup>1</sup> Age in doubt; see Wright (1956, p. 19-23) and Zumberge and Wright (1956, p. 65-80).



## RECENT RETREAT OF THE TETON GLACIER, GRAND TETON NATIONAL PARK, WYOMING

By JOHN C. REED, JR., Denver, Colo.

**Abstract**—Comparison of a plane-table map of the Teton Glacier made in 1963 with a map prepared from aerial photographs taken in 1954, and with older maps and photographs, indicates that the rate of retreat of the terminus has decreased, and that the thickness of the upper part of the glacier has increased since 1954. These observations suggest that the terminus of the glacier may begin to advance within the next few years.

The Teton Glacier is one of about a dozen small alpine glaciers cradled in shady east- or north-facing cirques among the high peaks of the Teton Range in Grand Teton National Park, Wyo. The glacier, which occupies a spectacular east-facing cirque between the east ridge of the Grand Teton and Mount Owen, has been well described by Fryxell (1933a, 1933b, 1935). The glacier is apparently nourished in large part by avalanches from the encircling cliffs, some of which are more than 3,000 feet high.

Because of its scenic setting and relatively easy access, the Teton Glacier is one of the most frequently visited and photographed glaciers in Grand Teton National Park, but it has received little systematic study. In addition to the studies by Fryxell (1933a, 1933b, 1935), brief surveys of the glacier were made by Carl E. Jepson in 1949 and 1950, and by M. T. Millett in 1960. Reports of these studies were not published, but are available in the Grand Teton National Park library.

In August 1963, the writer made a plane-table survey of the lower part of the Teton Glacier, with the assistance of R. Alan Mebane, Assistant Park Naturalist, David D. Steller, and A. C. Chidester. The map has been placed on open file by the U.S. Geological Survey, and stable base copies at the original scale (1 inch=200 feet) are available for examination at park headquarters and at the U.S. Geological Survey offices in Denver, Colo. In addition, a contour map of the glacier has been prepared with a Kelsh plotter, from 1954 high-altitude aerial photographs. The two maps are combined on figure 1. The position of the terminus in 1950 is taken from Jepson's map; the 1929 terminus

is sketched from a photograph (Fryxell, 1935, fig. 5) and Fryxell's description. Photographs taken by W. O. Owen in 1898 indicate that at that time the ice had already retreated 10 to 20 feet from the crest of the terminal moraine, but the photographs were taken from a considerable distance at a time when the glacier and moraine were snow covered, so that the position of the terminus could not be sketched accurately on the map. Millett's report does not include a map showing the terminus in 1960, but his photographs indicate that it was at virtually the same position as in 1963. Profiles (fig. 1) sketched from the map show thinning and retreat of the terminus.

The general character and condition of the glacier at the time of the 1963 survey are shown in the photographs (fig. 2, 3, and 4), negatives of which are on file in the field-records file of the U.S. Geological Survey, Denver, Colo.

The location and marking of the control points shown on figure 1 are given in table 1. In addition, iron pipes were driven into the ice along a line extending across the glacier through control points *E* and *F* for use in any future studies of movement and ablation. The location and altitude of points on this line are given in table 2.

The map and profiles (fig. 1) show that the terminus of the glacier has retreated markedly since 1929. The approximate volume of ice lost since 1929 from the glacier below the line of profile *Y-Y'* of figure 1 has been calculated from the 1954 and 1963 contours and from approximate contours reconstructed on the basis of the positions of the ice margin in 1950 and 1929. These data (fig. 5) show that the rate of loss of ice between 1954 and 1963 was much less than between 1929 and 1954. Profile *X-X'* (fig. 1) shows that the upper part of the glacier was thicker in 1963 than in 1954. The decreasing rate of loss of ice from the lower part of the glacier and the thickening of the upper part may result in an advance of the terminus within the next few years.

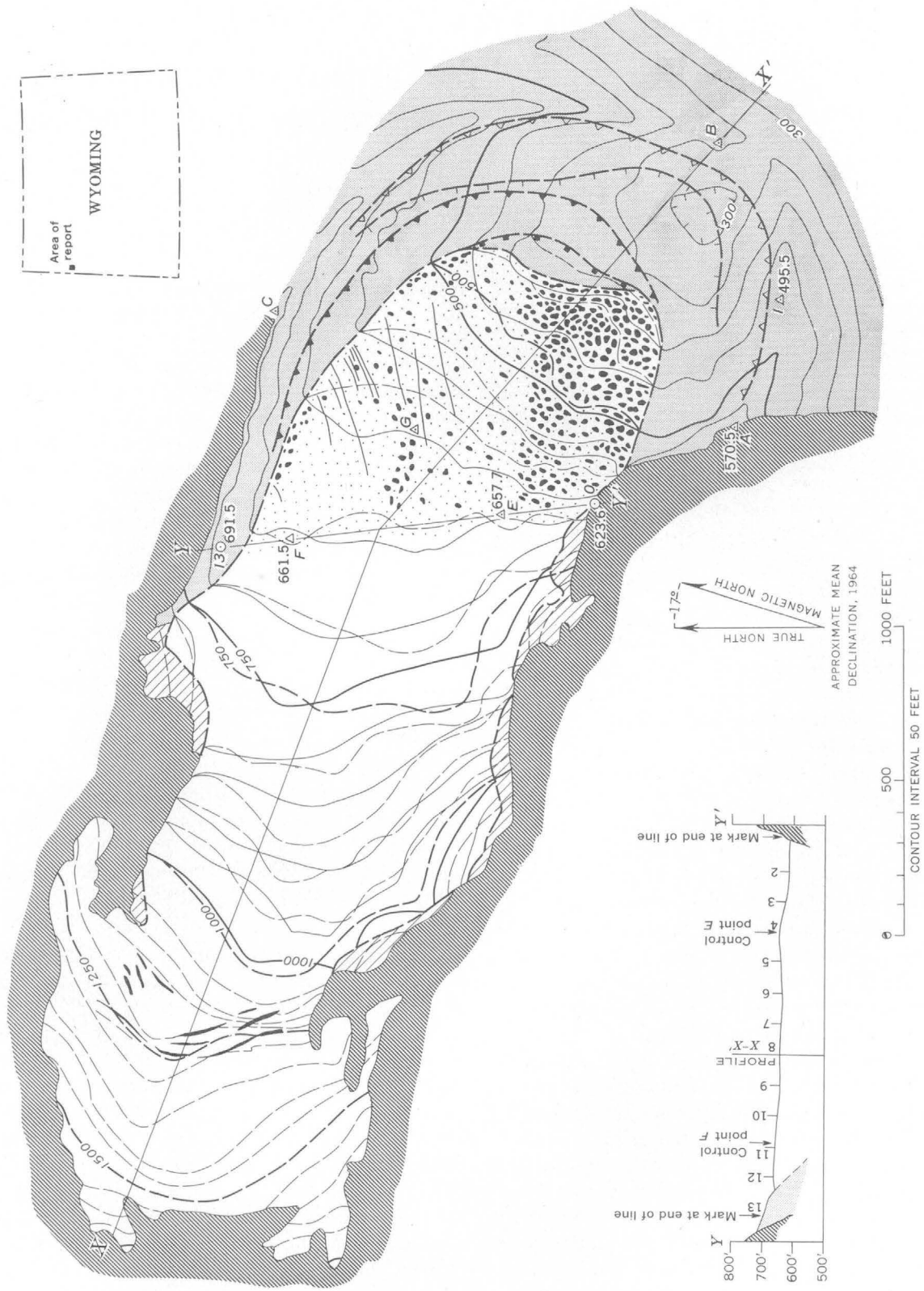


FIGURE 1

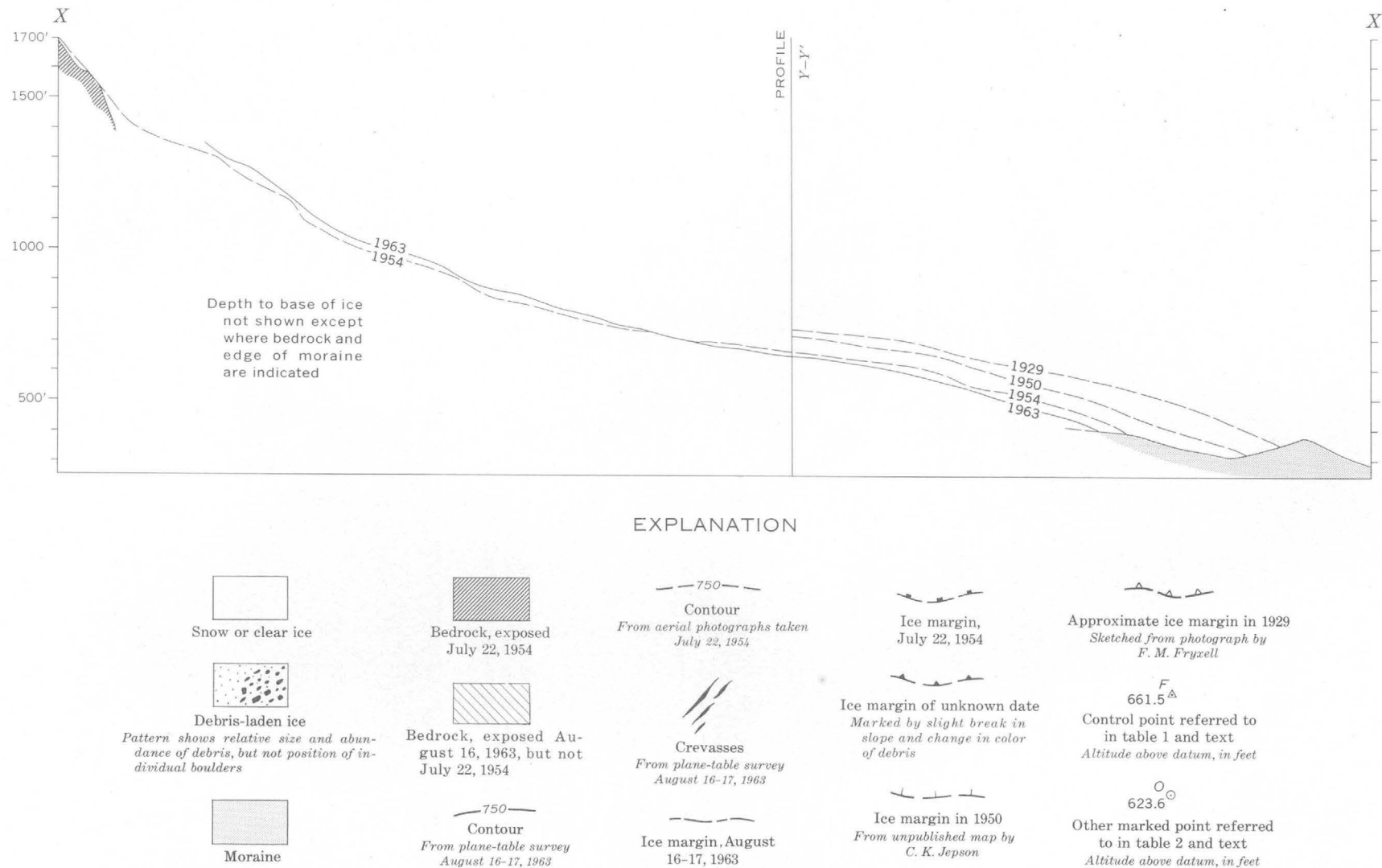


FIGURE 1.—Map of the Teton Glacier, showing former positions of terminus and profiles of the glacier. Outline of lower glacier from plane-table survey of August 16 and 17, 1963; outline of upper part of glacier from Army Map Service high-altitude aerial photographs taken July 22, 1954. Approximate profiles in 1929 and 1950 projected from ice margins shown on map. Numbered ticks along profile Y-Y' show position of iron pipes set during 1963 survey. All altitudes above arbitrary datum; add 9,780 feet to convert to approximate altitude above mean sea level.



FIGURE 2.—Photographic panorama of the lower part of the Teton Glacier from point A (fig. 1), August 17, 1963. Position of point C is indicated. Approximate ice margin in 1929 sketched from photograph by Fryxell (1935); approximate ice margin in 1950 sketched from photograph by C. E. Jepson. Photographs by M. T. Millett indicate that ice margin in 1960 was virtually the same as in 1963. Photographs by R. Alan Mebane, National Park Service. Distance from camera to point C is about 1,540 feet.

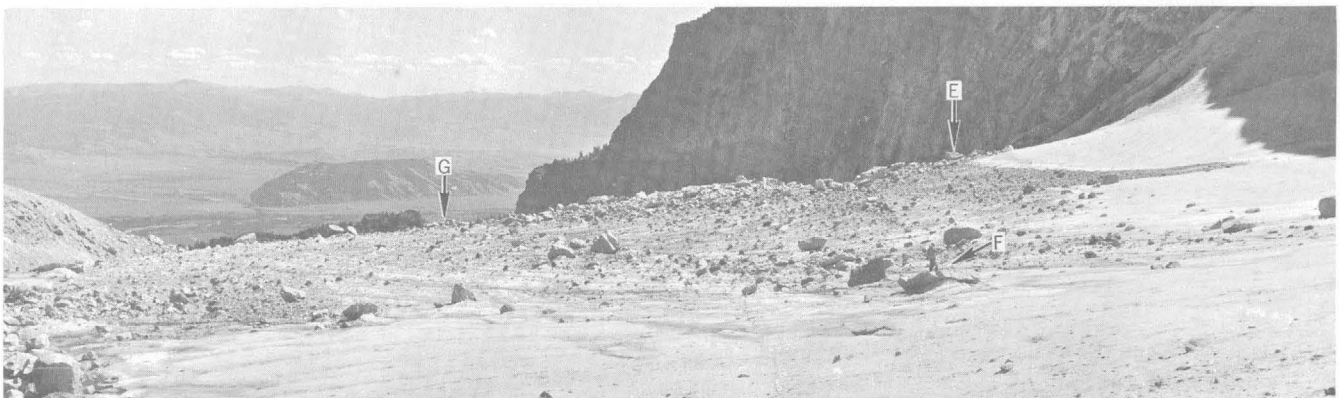


FIGURE 3.—Photographic panorama of the middle segment of the Teton Glacier from the mark (13, fig. 1) at the north end of the line of iron pipes set during the 1963 survey. Positions of control points E, F, and G (fig. 1) are indicated. Photographs by R. Alan Mebane, National Park Service, August 17, 1963. Distance from camera to point E is about 925 feet.

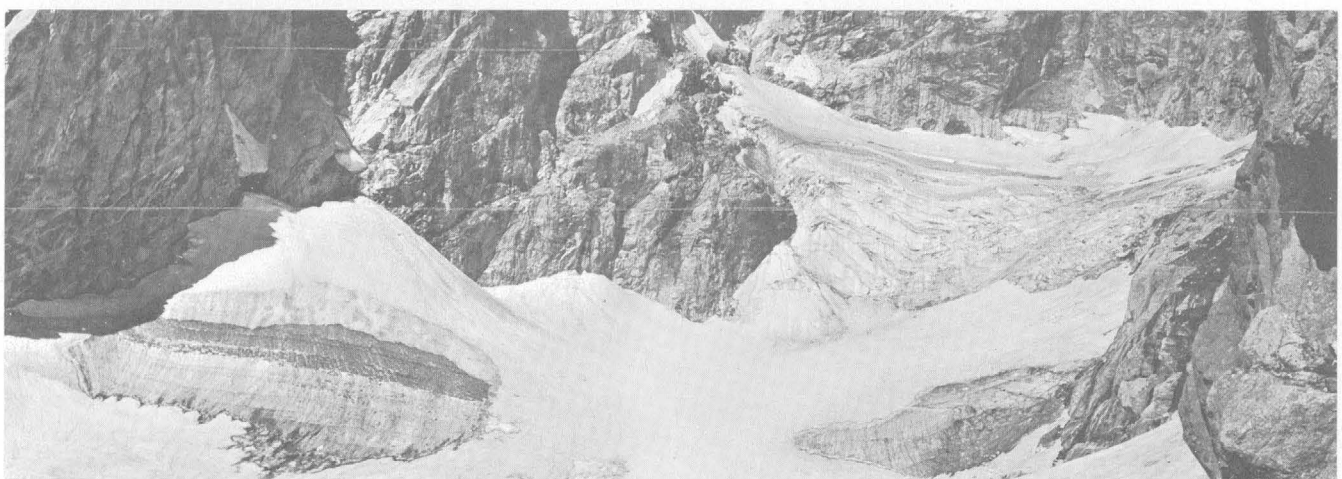


FIGURE 4.—Photographic panorama of the upper part of the Teton Glacier from point C (fig. 1). Photographs by R. Alan Mebane, National Park Service, August 17, 1963. Distance across narrowest part of ice fall is about 700 feet.

TABLE 1.—Description of control points  
[Location of control points shown on figure 1]

Control point	Altitude above datum <sup>1</sup>	Location and markings	Remarks
A-----	570.5	Brass tablet set in bedrock at south end of terminal moraine; marked with silver paint by Millett in 1960.	Point A of Jepson's 1949 and 1950 surveys marked by steel pin in rock about 5 ft southeast.
B-----	About 365.	Triangle and "B" in silver paint on boulder in terminal moraine about 150 feet north of low point; marked by Millett in 1960.	Point C of Jepson's 1949 survey.
C-----	About 730.	Brass tablet set in bedrock at north end of terminal moraine; marked with silver paint by Millett in 1960.	Point B of Jepson's 1949 survey marked by steel pin in rock about 5 ft northwest.
D-----		Not marked.	
E-----	657.7	Mark and letter "E" in red paint in several places on erratic boulder; marked in 1963.	
F-----	661.5	Mark and letter "F" in red paint in several places on erratic boulder; marked in 1963.	
G-----	About 612.	Mark and letter "G" in red paint in several places on erratic boulder; marked in 1963.	
I-----	495.5	Temporary marker on top of prominent knoll on terminal moraine about 500 feet southwest of low point.	Datum for 1963 survey.

<sup>1</sup> Instrument altitude at point I assumed 500.0 feet. Vertical-angle observations to bench marks in Jackson Hole indicate ground altitude at point I is 10,275 ± 5 feet.

## REFERENCES

- Fryxell, Fritiof, 1933a, The formation of glacial tables: *Jour. Geology*, v. 41, p. 642-646.  
 ——— 1933b, The migration of superglacial boulders: *Jour. Geology*, v. 41, p. 737-747.  
 ——— 1935, Glaciers of the Grand Teton National Park, Wyoming: *Jour. Geology*, v. 43, p. 381-397.

TABLE 2.—Location and altitude of other marked points, on line across glacier through control points E and F  
[Location of other marked points shown on figure 1]

Other marked point	Distance from mark on south wall (feet)	Mark	Altitude above datum (feet)	Remarks
0-----	0	Red paint "X" on bedrock.	623.6	
1-----	29	Iron pipe 18 in. long driven 12 in. into ice, projecting end painted red.	614.2	Ice surface.
2-----	117	do	617.8	Ice surface.
3-----	215	do	629.6	Do.
4 (control point E).	310	Red paint mark on erratic boulder.	657.7	Top of boulder 5 ft above ice surface.
5-----	410	Iron pipe as at 1	645.4	Ice surface.
6-----	510	do	639.2	Do.
7-----	610	do	646.8	Do.
8-----	710	do	649.7	Do.
9-----	810	do	647.4	Do.
10-----	910	do	650.8	Do.
Control point F.	1,000	Red paint mark on erratic boulder.	661.5	Top of boulder 2 ft above ice surface.
11-----	1,010	Iron pipe as at 1	660.0	Ice surface.
12-----	1,110	do	661.8	Do.
North edge of glacier.	None	None	663.4	Do.
13-----	1,233	Red paint "X" on boulder in lateral moraine.	691.5	

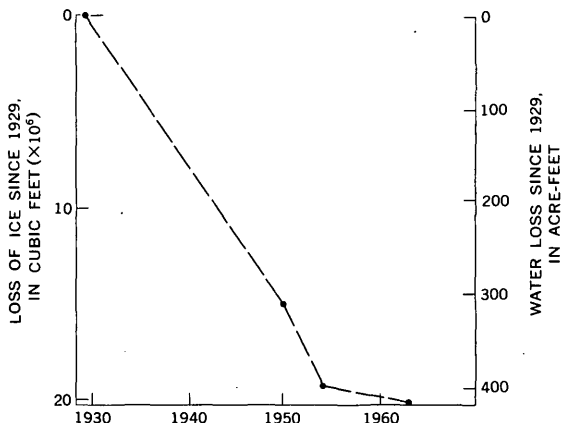


FIGURE 5.—Graph showing approximate ablation loss since 1929 from the Teton Glacier below profile Y-Y' of figure 1. Calculation of water equivalent based on assumed density of ice of 0.9 grams per cubic centimeter.

**A SIMPLE OXYGEN SHEATH FOR FLAME PHOTOMETRY**

By IRVING MAY, J. I. DINNIN, and FRED ROSENBAUM, Washington, D.C.

**Abstract.**—A simple brass oxygen sheath is described for use with an atomizer burner for a flame photometer. Its use imparts increased flame stability and gives enhanced emissions comparable to those reported by other investigators. The unit is in routine use for determining sodium and potassium content, with natural gas in place of hydrogen as the fuel.

A sheathed atomizer burner for flame photometry possesses several advantages over the standard burner. In a sheathed burner the flame is enclosed by a flow of gas, usually oxygen, resulting in a steadier, more stable flame. Emission intensities are increased severalfold by the oxygen sheath, so that narrower slits can be used and resolution can thereby be improved. For a few elements there is also increased emission relative to background, resulting in increased sensitivity. The oxygen sheath also makes it possible to burn hydrocarbon gases such as natural gas and propane in the hydrogen atomizer burner.

A sheath based on a design by Gilbert (1961; Beckman Instruments, Inc., 1962) is now available commercially but must be ordered fitted to a particular burner. A simpler sheath which can be fitted by a Teflon gasket over a Beckman-type atomizer burner has been described by Rain and others (1961) of the Oak Ridge National Laboratory.

The sheath described here is similar in design to the Oak Ridge unit. No special fitting is required, and it can be slipped onto any Beckman atomizer burner. The conical head of the burner acts to stop and center the sheath, and a rubber o-ring seals the bottom of the chamber. The sheath may be left in place regardless of whether or not it is being used. It can also be removed readily for cleaning or adjusting the atomizer burner.

Construction details for the sheath are given in figure 1. The unit is machined from a 1-inch length of  $\frac{7}{8}$ -inch round bar stock of brass. An  $1\frac{1}{32}$ -inch hole is drilled through the piece and then bored to a 0.3675-

inch diameter. Two other concentric holes are then bored, one with a diameter of  $2\frac{1}{32}$  inch and depth of  $2\frac{3}{32}$  inch and the other with a diameter of  $1\frac{1}{16}$  inch and a depth of  $\frac{1}{2}$  inch. The outside diameter of the piece is then turned to  $1\frac{3}{16}$  inch. The work is then reversed in the lathe and faced off until the length is  $1\frac{5}{16}$  inch. The groove for the o-ring is cut with a relief tool to fit a  $\frac{3}{8}$ -inch-ID o-ring. The brass tubing for the hose connection,  $\frac{3}{16}$ -inch-OD and 0.120-inch-ID, is turned down at one end to  $1\frac{1}{64}$ -inch and pressed into an  $1\frac{1}{64}$  (0.171)-inch hole cut in the side of the shield. The tubing is then silver soldered into place. A  $\frac{7}{32}$ -inch hole is drilled in the center of a brass disc,  $1\frac{1}{16}$ -inch in diameter and  $\frac{1}{16}$ -inch thick. Sixteen holes ( $\frac{1}{16}$ -inch diameter) are drilled uniformly spaced on a circle  $\frac{1}{4}$ -inch from the center. The disc is pressed into the  $1\frac{1}{16}$ -inch hole until it seats on the shoulder.

The operation of the oxygen-sheathed burner with a Beckman DU flame photometer was tested with solutions of potassium, lithium, rubidium, cesium, magnesium, calcium, barium, and manganese. Oxygen pressure for the burner was 15 pounds per square inch, hydrogen was 4 psi, and the oxygen flow in the sheath was 2 cubic feet per hour. Enhanced sensitivities were obtained with calcium, lithium, manganese, and barium as follows:

Element	Wavelength ( $m\mu$ )	Enhancement factor
Calcium-----	422	2
Lithium-----	671	2
Manganese-----	403	3
Barium-----	455	5

Although the barium line at  $455 m\mu$  is not the most sensitive line for this element, it is nevertheless a useful line because there is less interference here than in the more sensitive spectral region.

The sheathed hydrogen burner with natural gas as fuel is now being used in the Washington laboratory of the Analytical Laboratory Branch of the Geological Survey for routine sodium and potassium determinations on rocks. Piped natural gas is of course more

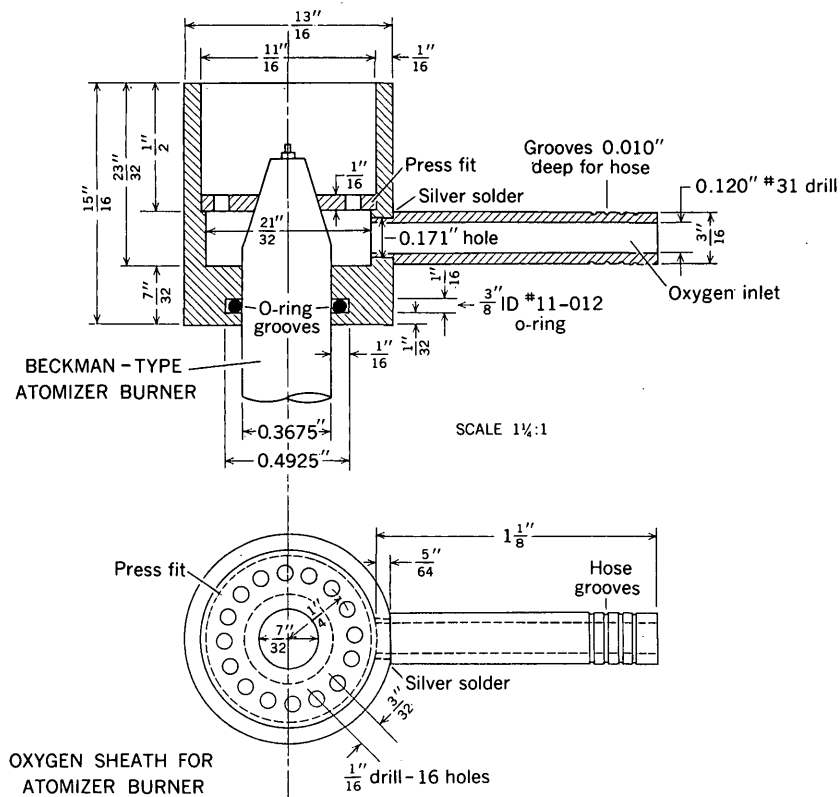


FIGURE 1.—Working drawing of oxygen sheath for an atomizer burner.

convenient and cheaper than cylinder hydrogen. Oxygen consumption is also decreased as the burner oxygen pressure is 5 psi rather than 10–15 psi normally used with hydrogen. The sheath flow is low, approximately 4 cubic feet per hour. The natural gas need not be controlled with a regulator; the gas valve is merely adjusted to give a flame of optimum height.

With natural gas there is a small decrease in sensitivity compared to that of the hydrogen flame, about 25 percent for sodium and 15 percent for potassium. This represents no problem as there is sensitivity to spare for this application. The flame is stable and the reproduc-

bility of measurements is comparable to that with the hydrogen-oxygen flame.

Oxygen-sheathed burners possess enough advantages to justify their adoption as a standard accessory to a flame photometer using the atomizer burner.

#### REFERENCES

- Beckman Instruments, Inc., 1962, Sheathed atomizer burner: Fullerton, Calif., Bull. 3063.
- Gilbert, P. T., Jr., 1961, New horizons in flame spectrophotometry: Beckman Instruments, Inc., Analyzer, v. 2, no. 4, p. 3.
- Rains, T. C., Ferguson, Marion, and Zittel, H. E., 1961, Annual Report: Oak Ridge Natl. Lab., p. 44.

## DETERMINATION OF IODINE IN VEGETATION

By MARGARET CUTHBERT and F. N. WARD, Denver, Colo.

*Abstract.*—A method for determination of iodine in vegetation is described wherein small samples of dry vegetation are oxidized quickly in an oxygen flask and the combustion products collected in dilute alkali. The dissolved iodide is then measured by its catalytic effect on the reduction of ceric ion by arsenious ion in acid solution. As little as 1 ppm iodide in a 0.1-g sample of finely ground plant can be determined by this procedure. The speed of sample oxidation and the small sample size needed are the chief advantages over other procedures.

The determination of small amounts of iodine in vegetation is of importance in establishing the range of iodine content of various species of plants grown in different geologic environments. Prior to its determination the iodine must be converted to a soluble form amenable to measurement; the conversion or dissolution of vegetation samples without loss of iodine can be lengthy and tedious.

In the published methods for determining iodine in plant material, algae included, sample dissolution is accomplished by dry ignition after treatment of the sample with potassium carbonate to prevent loss of iodine (Brühlmann, 1959). In a similar manner Gustun (1959) used a potassium hydroxide treatment instead of the carbonate prior to ignition of foods. Dissolution of plant material is also accomplished by wet oxidation with hot chromic acid (Leipert, 1933) or with a hot mixture of nitric, sulfuric, and perchloric acids (Pauwels and Van Wesemael, 1962).

After sample dissolution the amount of iodine is measured by the color produced in a chloroform extract (Brühlmann, 1959) or by the catalytic effect of iodide on the rate of reduction of cerium(IV) by arsenious acid, a reaction that was noted by Lang (1926) and developed by Sandell and Kolthoff (1937). This reduction is a first-order reaction, and several techniques are used to relate the iodide concentration to the rate of the reaction. In some procedures the reaction is stopped after a fixed time by the addition of

silver ion (C. G. Mitchell, oral communication, 1963) and the extent of reaction is determined by an instrumental measurement of the decrease in color of the cerium(IV). In other procedures (Rogina and Du-bravčič, 1953) the reaction is stopped by the addition of iron(II), and the amount of cerium(IV) remaining in the solution is determined indirectly by allowing the iron(III) formed to react with thiocyanate and measuring the color intensity of the iron thiocyanate.

Determination of the iodine by the catalytic reaction described above is relatively simple and rapid; however, sample dissolution can be rather involved, especially with plant material. It occurred to the authors that dry vegetation could be oxidized quickly in an oxygen flask such as is used to oxidize relatively pure organic compounds prior to other halogen determinations (Schöniger, 1955) and that the iodine in the combustion products could be measured by the same catalytic reaction discussed above. The iodine in the combustion products is assumed to be either an iodide or some form such as the element or the iodate that is readily reduced to iodide by the arsenious acid.

Ions which interfere in the reaction include chloride, bromide, citrate, mercury, silver, and osmium (Chaney, 1950). Chloride did not interfere in this method in concentrations up to 10,000 parts chloride to 1 part iodide. Bromide did not interfere in concentrations up to 1,000 parts bromide to 1 part iodide. Citrate would likely be oxidized during the ignition.

Waxy films which form on the inside of the combustion flask during ignition caused erratic results. These films are probably caused by incomplete oxidation of the more resistant waxes, and their accumulation with successive ignitions could conceivably result in a cumulative error. Fortunately, the film is easily removed between runs by a chromic acid rinse.

The procedure described below is suitable for determining as little as 1 part per million iodine starting with a 0.1-g sample of finely ground plant material.

### REAGENTS

All solutions are prepared with demineralized water and reagent-grade chemicals unless otherwise indicated.

Arsenious acid: 0.3*N* H<sub>3</sub>AsO<sub>3</sub> (reducing agent). Add 14.8 grams of As<sub>2</sub>O<sub>3</sub> to about 500 milliliters of demineralized water in a 1000-ml beaker. Next, add slowly 28 ml of concentrated (96 percent) H<sub>2</sub>SO<sub>4</sub>, and warm the mixture until the As<sub>2</sub>O<sub>3</sub> is dissolved. Cool, transfer to a 1-liter volumetric flask, and dilute to mark with demineralized water. Add a small piece of metallic arsenic to stabilize the solution.

Ceric sulfate: 0.1*N* Ce(HSO<sub>4</sub>)<sub>2</sub> (oxidizing agent). Prepare in a 600-ml beaker by dissolving 52.8 g of anhydrous Ce(HSO<sub>4</sub>)<sub>2</sub> in 5*N* H<sub>2</sub>SO<sub>4</sub>. Warm the mixture and stir occasionally, until a clear solution is obtained (approximately 1 hour). Dilute to 1.0 liter with 5*N* H<sub>2</sub>SO<sub>4</sub>.

Iodide standard, 200 ppm. Dissolve 0.262 g of potassium iodide in 1 liter of water.

Silver nitrate reagent, 0.01 percent W/V. Dissolve 0.01 g of the salt in 100 ml water. Store in dark bottle.

Sodium hydroxide, 1*N*. Dissolve 40 g of pellets in 1 liter water.

Sulfuric acid, concentrated.

### EQUIPMENT

In addition to ordinary laboratory equipment such as pipets and volumetric flasks, the following items are necessary:

Schöniger combustion flask, 1-liter size, with ignition basket and firing apparatus.

Spectrophotometer, Beckman Model B.

Pyrex test tubes, 25×150-mm size (fit directly in spectrophotometer).

Sieve, stainless steel, 50 mesh.

### PROCEDURE

Weigh 0.1 g of minus 50-mesh plant material and roll up in a filter paper cut for use in the Schöniger apparatus. Attach the paper to the ignition basket. Add 5 ml of 1*N* NaOH to the Schöniger flask, flush the flask with oxygen for about 20 seconds, and place the ignition basket in the flask. Place the flask with basket in the firing apparatus and ignite. Wash the NaOH solution around the sides of the flask and slosh NaOH over the basket. Let the apparatus stand for 15–20 minutes while the vapor is absorbed in the alkali.

Transfer contents of the flask to a 25×150-mm test tube. Rinse flask with three 5-ml portions of demineralized water and add these portions to the test tube. If aliquots are used in order to extend the range upward, pipet the appropriate volume from Schöniger flask to test tube. Make up the volume of the aliquot to 5 ml with 1*N* NaOH. Neutralize contents of test tube (litmus) with 5–6 drops of concentrated sulfuric acid and bubble nitrogen through the solution for 2 minutes

to remove carbon dioxide. Add 1 ml 0.3*N* arsenious acid, 0.5 ml concentrated sulfuric acid, and make volume up to 30 ml in the tube with demineralized water.

Place the tube in a water bath at 30°C ±1.0° for about 20 minutes. Then add, with stirring, 1 ml 0.1*N* ceric sulfate (also at 30°C), and after exactly 10 minutes, add, with stirring, 2 drops 0.01-percent silver nitrate. Within 1 minute measure the percent transmittance at 450 mμ with a spectrophotometer.

The standard curve is prepared by placing increasing amounts of standard iodide solution on a filter paper as follows: 0.1 microgram on first filter paper, 0.2 μg on second filter paper and so on including 0.8 μg on last filter paper. The filter papers are ignited successively in the ignition apparatus and the products are taken through the remaining steps of the procedure. The transmittance is plotted against the iodide concentration and calculations of iodide content are made as follows:

$$\frac{\text{volume in ml}}{\text{aliquot in ml}} \times \frac{\text{micrograms I}^{-1} \text{ from curve}}{\text{sample weight in grams}} = \text{I}^{-1} \text{ in ppm}$$

Prepare a new standard curve for each batch of reagents.

### RESULTS

The possible loss of iodine during the ignition was tested by adding known amounts of iodine to the 1*N* NaOH and taking these dilute alkaline solutions through the remainder of the procedure and finally comparing the results with those obtained as in the preparation of standard curve. The comparison data are shown in table 1. Slight losses occur during the ignition as shown above, but they do not exceed 10 percent and in fact have little influence on the results obtained with plant samples because they are processed by the same procedure used in making the standard curve.

TABLE 1.—Recovery of added iodine

Sample No.	Iodine content (μg)	Absorbance (ml/μg cm)	
		No ignition	After ignition
1-----	0	0.89	-----
2-----	.2	.66	0.71
3-----	.4	.48	.54
4-----	.6	.33	.39
5-----	.8	.20	.17

Iodine recoveries were also tested by adding calculated amounts in the form of different organic iodides to filter paper and igniting the latter in the oxygen flask. Iodine in the combustion products was measured as in the proposed procedure, with the results shown in table 2.

TABLE 2.—*Recovery of added iodides*

Sample No.	Compound used as source of iodine	Number of determinations	Iodine added (ppm)	Iodine found (ppm)	
				Range	Mean
1	Diiodomethane <sup>1</sup>	2	3	2-3	2
2	Diiodomethane <sup>1</sup>	3	31	20-40	30
3	Triiodomethane	6	10	7-15	12
4	Triiodomethane	3	21	20-26	22
5	Iodobenzene	8	23	13-25	22

<sup>1</sup> Stabilized with copper wire.

Plant samples containing known amounts of iodine are scarce, and the lack of such materials increases the difficulty of testing the proposed procedure adequately. However, one technique which is perhaps a better test of precision than of accuracy involves the analysis of mixtures containing different proportions of previously analyzed plant materials. Accordingly, mixtures

TABLE 3.—*Determination of iodine in plant mixtures*

Sample No.	Composition of mixture	Calculated iodine content (ppm)	Iodine found by method described in this article (ppm)
1	HTS-8, 25 mg	260	230
	HTS-6, 25 mg		
2	HTS-8, 13 mg	260	210
	HTS-6, 13 mg		
3	HTS-8, 15 mg	230	240
	HTS-6, 10 mg		
4	HTS-8, 10 mg	330	310
	HTS-6, 20 mg		
5	HTS-6, 50 mg	230	195
	62-868, 50 mg		

were prepared using 3 samples, HTS-6, HTS-8, and 62-868, containing respectively 450, 80, and 2 ppm of iodine. These mixtures were analyzed by the proposed procedure; the results are given in table 3. The application of such technique may be risky due to heterogeneity of the samples and nonuniformity of mixing; but in spite of these hazards, the results are surprisingly good. They confirm the usefulness of the proposed procedure for determining traces of iodine in air-dried plant material.

## REFERENCES

- Brühlmann, R., 1959, Determination of iodine in algae and other plant materials: *Mitt. Lebensm. u. Hyg.*, v. 50, p. 4-7.  
 Chaney, A. L., 1950, Instrumental improvements for microdetermination of protein-bound iodine in blood: *Anal. Chemistry*, v. 22, p. 939.  
 Gustun, M. I., 1959, Determination of small quantities of iodine content in soils, foods, animal bodies, and drinking water: *Voprosy Pitaniya*, v. 18, p. 80-82.  
 Lang, R., 1926, Catalysis of the reaction between arsenious acid and permanganic acid and its application in analytical chemistry: *Z. anorg. allgem. Chem.*, v. 152, p. 197-206.  
 Leipert, T., 1933, Determination of minute amounts of iodine in organic matter: *Biochem. Z.*, v. 261, p. 436-443.  
 Pauwels, G. W., Borst, F. H., and Wesemael, J. Ch. Van, 1962, A new routine method for determination of iodine in plant materials: *Anal. Chim. Acta*, v. 26, p. 532-540.  
 Rogina, B., and Dubravčić, M., 1953, Microdetermination of iodides by arresting catalytic reduction of ceric ions: *Analyst*, v. 78, p. 594.  
 Sandell, E. B., and Kolthoff, I. M., 1937, Microdetermination of iodine by a catalytic method: *Mikrochim. Acta*, v. 1, p. 9-25.  
 Schöniger, W., 1955, Rapid microanalytical determination of halogen in organic compounds: *Mikrochim. Acta*, p. 123-129.



## JUDGING THE ANALYTICAL ABILITY OF ROCK ANALYSTS BY CHI-SQUARED

By FRANCIS J. FLANAGAN, Washington, D.C.

*Abstract.* The ability of an analyst can be assessed objectively by summing squared standardized normal deviates that are distributed as  $\chi^2$ . For a well-analyzed rock like G-1, the differences between the oxide contents by an analyst and the published means are divided by the accepted standard deviation to obtain these standardized deviates.

Supervisors of geochemical laboratories must occasionally evaluate the ability of rock analysts. The usual method is to compare, oxide by oxide, the analysis by a novice, for example, with the analysis of the same material by a competent analyst. The latter undoubtedly acquired his reputation for competence by a similar procedure. Under the assumption that each analysis totals reasonably close to 100 percent, the geochemist makes a series of subjective judgments of whether the oxide determinations by the novice are sufficiently close to those by the competent analyst. He then makes a summary subjective judgment by concluding that the results by the novice are in excellent, good, fair, or poor agreement with those by the competent analyst.

The publication of the original analysis of G-1 and W-1 (Fairbairn and others, 1951) showed a sad state of affairs in rock analysis, but improvements have been noted in subsequent compilations (Stevens and others, 1960; Fleischer and Stevens, 1962). Stevens and others (1960, p. 41) note that a major accomplishment of these investigations is to show the individual analysts how their results compare with data by others, but each analyst will undoubtedly make a subjective evaluation of his ability as will readers not directly concerned with the analyses.

Although subjective judgments have some value, an objective assessment of ability would be more valuable. With the large number of analyses of G-1 and W-1 available, the means and standard deviations for all analyses reported by Stevens and others (1960, tables 3 and 4) can be assumed to be the population means and standard deviations for each oxide. Other than

the analyses reported by Fleischer and Stevens (1962) and Ingamells and Suhr (1963), there are only a few other analyses available, and since all the data are in close agreement with the published means the effect on the assumed parameters will not be noticeable. Nevertheless, the assumed parameters used in the accompanying table represent only about 90 percent of the population of known chemical analyses of G-1, and the computed value of  $\chi^2$  should be considered as a good approximation rather than as an exact value.

Since the major obstacle in judging an analysis is that of making judgments of agreement on a dozen or more pairs of oxides and then in some unspecified manner summing these subjective judgments to arrive at a final conclusion of ability, a mathematical process that converts the differences between each pair of oxides to a common base would be more efficient. The easiest method of treating these differences is to convert them to standardized normal deviates. Each standardized normal deviate, obtained for each oxide by dividing the difference between the analyst's value and the published mean by the respective standard deviation, can then be squared. The  $n$  squared standardized normal deviates can then be summed and such sums are distributed as  $\chi^2$  (Bennett and Franklin, 1954, p. 96) with  $n$  degrees of freedom.

The technique of summing these squared standardized normal deviates has the added advantage of versatility as it can be used for any number of comparisons. It is useful, for example, when each of a number of analysts does not report the same number of oxides; in such cases a comparison among a number of analysts may be made by using those determinations common to all. The analytical ability tested is overall competence, consisting at least of the manipulative skill of the analyst and of his ability to choose an analytical method of proven accuracy and precision. In the example cited, namely results on G-1, methods of analysis have not accompanied much of the analytical data submitted in the last few years, and it is therefore impossible to remove the effects of questionable procedures. It is

of course possible that a single analyst may have submitted the perfect analysis and yet have his individual determinations differ from the calculated averages. Until much more data are available, however, we must assume that these averages are the best estimates of the true values.

The accompanying table shows an example of the calculation of  $\chi^2$  using the data of analyst 47 (Stevens and others, 1960, p. 12) for G-1 and the means and standard deviations for G-1 for all analyses (Stevens and others, 1960, table 3). The computed value, 2.70, should be compared to a fractile of the  $\chi^2$  distribution for 14 degrees of freedom for which, for example at the 95-percent probability level, the value of 23.7 is given in tables. The computed value is very much less than the table value and it may be inferred that the data by analyst 47 are not significantly different at the specified probability level from the mean values given for G-1.

Computation of  $\chi^2$ 

	1 Analyst 47 (Stevens and others, 1960) (weight percent)	2 Mean (Stevens and others, 1960, table 3, all analyses, p. 31) (weight percent)	3 (1-2)	4 Standard deviation (Stevens and others, 1960, table 3, all analyses, p. 31)	5 (3/4)	6 (5 <sup>2</sup> )
SiO <sub>2</sub> ---	72.45	72.35	+0.10	0.48	0.21	0.0441
Al <sub>2</sub> O <sub>3</sub> ---	14.18	14.32	-0.14	.37	-.38	.1444
Fe <sub>2</sub> O <sub>3</sub> ---	.75	.95	-.20	.30	-.66	.4356
FeO---	.98	.99	-.01	.11	-.09	.0081
MgO <sup>1</sup> ---	.35	.40	-.05	.13	-.38	.1444
CaO <sup>2</sup> ---	1.36	1.40	-.04	.12	-.33	.1089
Na <sub>2</sub> O---	3.28	3.31	-.03	.23	-.13	.0169
K <sub>2</sub> O <sup>3</sup> ---	5.54	5.42	+.12	.39	.31	.0961
H <sub>2</sub> O---	.03	.06	-.03	.05	-.60	.3600
H <sub>2</sub> O+---	.26	.36	-.10	.18	-.56	.3136
TiO <sub>2</sub> ---	.26	.26	0	.04	-----	-----
P <sub>2</sub> O <sub>5</sub> ---	.09	.10	-.01	.06	-.17	.0289
MnO---	.02	.03	-.01	.01	-1.00	1.000
CO <sub>2</sub> ---	.08	.08	0	.01	-----	-----
$\chi^2 \cong \Sigma = 2.7010$						

<sup>1</sup> Plus 0.63 BaO.<sup>2</sup> Plus SrO.<sup>3</sup> Plus Rb<sub>2</sub>O.

It can be noted in the table that the data reported by the analyst for TiO<sub>2</sub> and CO<sub>2</sub> are identical to the means of all data and that there are no squared standardized

normal deviates to contribute to the summation for  $\chi^2$ . If analyst 47 had not reported these two oxides, a standardized deviate could not have been computed for them and the summation would have been identical to that shown in the table. However, had these determinations not been reported, one would refer to tables of  $\chi^2$  at the 95-percent probability level for 12 rather than 14 degrees of freedom for which a value of 21.0 is given.

The deviations of the data by analyst 47 from the means of G-1 are not excessively large, and the use of  $\chi^2$  merely confirms the geochemist's subjective judgment that the analysis is not too bad. Conversely, the rejection of a poor analysis because of very large deviations can be made subjectively, and almost exclusively, with a knowledge of the sources of error in rock analysis (Stevens and others, 1960, p. 9), but the summed squared standardized deviates can be used if an objective rejection is desired.

With the improvements in rock analysis that can be noted in the last two compilations of the data for G-1 and W-1 it seems unlikely that any future analysis of these rocks will be rejected at the 95-percent level as unsuitable by the technique outlined. However, those who wish to make a more rigorous test of analytical ability can choose a lower percentage probability level at which ability may be tested.

Although the example above concerns rock analysis and the data of G-1, the technique is applicable in many fields in which data for a well-analyzed standard are available.

#### REFERENCES

- Bennett, C. A., and Franklin, N. L., 1954, Statistical analysis in chemistry and the chemical industry; New York, John Wiley and Sons, Inc., 724 p.
- Fairbairn, H. W., and others, 1951, A cooperative investigation of precision and accuracy in chemical, spectrochemical, and modal analysis of silicate rocks: U.S. Geol. Survey Bull. 980, 71 p.
- Fleischer, Michael, and Stevens, R. E., 1962, Summary of new data on rock samples G-1 and W-1: Geochim. et Cosmochim. Acta, v. 26, p. 525-543.
- Ingamells, C. O., and Suhr, N. H., 1963, Chemical and spectrochemical analysis of standard silicate samples: Geochim. et Cosmochim. Acta, v. 27, p. 897-910.
- Stevens, R. E., and others, 1960, Second report on a cooperative investigation of the composition of two silicate rocks: U.S. Geol. Survey Bull. 1113, 126 p.



## ULTRASONIC DISPERSION OF SAMPLES OF SEDIMENTARY DEPOSITS

By R. P. MOSTON and A. I. JOHNSON, Denver, Colo.

**Abstract.**—Particle-size analyses of samples disaggregated by ultrasonic energy indicate a lower percentage of silt-size particles and a higher percentage of clay-size particles than when the standard disaggregation method is used. Use of ultrasonic energy apparently facilitates dispersion of samples of fine-textured sedimentary deposits being prepared for particle-size analysis.

As one phase of research on land subsidence in California (Inter-Agency Committee on Land Subsidence in the San Joaquin Valley, 1958; Poland and Green, 1962), approximately 500 core samples of sedimentary deposits were taken from depths as great as 2,000 feet in the San Joaquin and Santa Clara Valleys. Particle-size analyses of these samples were made in the Hydrologic Laboratory of the U.S. Geological Survey, Denver, Colo. Because the accuracy of a particle-size analysis depends largely on the effectiveness of the method used to separate the sample into its primary particles, the authors made several tests to determine whether use of ultrasonic energy would result in more complete disaggregation than the standard method of dispersion. This article presents some of the results of this comparative testing.

Sound waves audible to humans have frequencies within the range of about 20 to 20,000 cycles per second; sound waves of higher frequency are termed ultrasonic. The use of ultrasonic energy for the testing and processing of a wide variety of materials has invaded virtually every phase of science and industry. Ultrasonic cleaning of delicate mechanical parts has become widespread, and it is ultrasonic cleaning equipment that was adapted for use in this study.

Ultrasonic cleaning equipment suitable for use in dispersion of fine-textured sediment samples consists of two main units: an electronic signal generator, and a primary-fluid container to which is attached one or more acoustic transducers. The sample to be dispersed is mixed with water in a glass or metal beaker (secondary-fluid container) that then is placed inside the

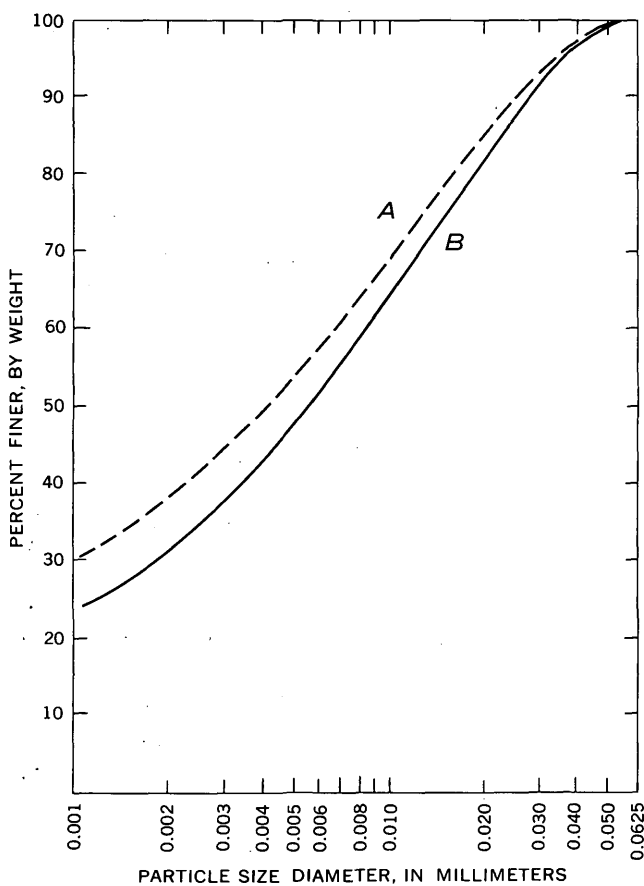
primary-fluid container. The remaining space in the primary-fluid container is filled with water, which is the most efficient medium for transmission of ultrasonic energy.

The standard procedure in preparing samples for particle-size analysis (American Society for Testing Materials, 1958) consists of (1) mechanical disaggregation, (2) soaking for at least 18 hours in distilled water after addition of a chemical deflocculating agent, and (3) agitation by shaking or stirring. The standard mechanical disaggregation reduces the aggregates of fine particles to a size that will pass through a sieve with 0.5-mm openings. A mortar and rubber-covered pestle are used.

To compare the results of the ultrasonic method of dispersion with those of the standard method, particle-size analyses were made on duplicate samples prepared by the conventional procedure of mechanical disaggregation and by ultrasonic dispersion. Mechanical disaggregation with the mortar and pestle was used to prepare duplicate splits of a number of samples to pass a sieve with 0.5-mm openings. To provide a sample with even smaller aggregates than normally is obtained by the standard procedure of mechanical disaggregation, the first split of a sample was further disaggregated to pass through a sieve with 0.0625-mm openings. Following the usual soaking, deflocculating, and agitating procedure, the ASTM standard method for particle-size analysis was then used to determine the particle-size distribution.

The second split of the sample was treated by ultrasonic agitation. The 50-gram sample was placed in a 400-milliliter beaker containing 190 ml of water and 10 ml of a solution of the chemical deflocculant, sodium hexametaphosphate (density 1.098 g per ml at 20°C), and was agitated with a stirring rod. The long soaking period required in the standard method was eliminated. The beaker was placed in the primary-fluid container of the ultrasonic cleaning equipment and was subjected to

ultrasonic agitation for a period of 15 minutes. Following the ultrasonic agitation, the particle-size distribution of the sample was determined by the standard method for particle-size analysis.



	Clay sizes (<0.004 mm)	Silt sizes (0.004-0.0625 mm)
A	49.4	50.6
B	43.5	56.5

FIGURE 1.—Particle-size distribution curves for a silty clay dispersed by (A) ultrasonic separation, and (B) mechanical separation.

The analytical results, as shown by the curves on figure 1, indicate that the sample disaggregated by ultrasonic energy contained a smaller percentage of silt-size particles and a greater percentage of clay-size particles than the sample disaggregated by the standard procedure.

It should be noted that the two curves on figure 1 diverge in the silt size range (0.004–0.0625 mm) but are almost parallel in the clay size range (<0.004 mm), indicating that the ultrasonic agitation caused breakdown of silt-size aggregates that were not broken down by the standard procedure.

The authors have observed aggregates of silt- and clay-size particles that were retained on a U.S. No. 230 screen (opening 0.062 mm) following the hydrometer test when the standard method of disaggregation was used. No such aggregates were retained on the No. 230 screen when splits of these samples were disaggregated by ultrasonic agitation.

Particle-size analyses of several samples that were agitated ultrasonically for different lengths of time showed that the degree of disaggregation was not increased significantly by extending the period of agitation beyond 15 minutes.

Dispersion by purely mechanical means and chemical deflocculation, even when the sample is disaggregated to pass through a sieve having 0.0625-mm openings, does not appear to be as complete as dispersion by ultrasonic energy (fig. 1). The clay-size fraction of samples that had been dispersed by ultrasonic energy was as much as 20 percent greater than that of samples dispersed by the standard procedure.

#### REFERENCES

- American Society for Testing Materials, 1958, Standard method of mechanical analysis of soils: Am. Soc. Testing Materials, Procedures for Testing Soils, p. 88–93.
- Inter-Agency Committee on Land Subsidence in the San Joaquin Valley, 1958, Progress report, land-subsidence investigations in the San Joaquin Valley, Calif., through 1957: Sacramento, Calif., 160 p., 45 pls.
- Poland, J. F., and Green, J. H., 1962, Subsidence in the Santa Clara Valley, Calif., a progress report: U.S. Geol. Survey Water-Supply Paper 1619-C, 16 p.



## TRITIUM CONTENT AS AN INDICATOR OF AGE AND MOVEMENT OF GROUND WATER IN THE ROSWELL BASIN, NEW MEXICO

By H. O. REEDER, Albuquerque, N. Mex.

*Work done in cooperation with the State Engineer of New Mexico  
and the New Mexico Institute of Mining and Technology*

**Abstract.**—The concentrations of tritium in ground-water samples collected in 1959-61 show that all samples of water from the Roswell basin were in part less than 35 years old. Some of the water has moved 5 to 15 miles in less than 5 years, indicating much faster ground-water movement than previously regarded as likely.

The Roswell basin, one of the richest farming and industrial areas in southeastern New Mexico, lies within the Pecos River valley. Ground water is obtained from two distinctly different aquifers: the "main" aquifer in rocks of Permian age (principally the San Andres Limestone but also the Artesia Group and Yeso Formation); and the overlying valley fill of Quaternary age. Thick beds of limestone and dolomite in the main aquifer contain solution conduits. As the conduits are not restricted to certain beds but are irregularly distributed both vertically and laterally, closely spaced wells may be drilled into conduits that are interconnected only indirectly or by circuitous routes. The main aquifer is recharged in its intake area directly by infiltrating precipitation, by infiltration of streamflow, and by flood runoff that collects in depressions, or topographic basins, underlain by porous rocks. The eastern boundary of the intake area is 5 to 15 miles west of the Pecos River. The valley-fill aquifer is recharged by infiltration of precipitation and irrigation water applied to crops, by leakage from artesian wells tapping the main aquifer, and by natural upward percolation from the main aquifer.

The water in the main aquifer is under little or no artesian pressure in the intake area but is under progressively greater artesian pressure eastward from the

intake area. The artesian pressure in local areas near the Pecos River is sufficient to raise water in tightly cased wells to as much as 60 feet above the land surface in winter when pumping is minimal. At present, water in the main aquifer is discharged principally by wells and by upward movement into the valley fill. Water in the shallow aquifer is unconfined and is discharged by seepage along the Pecos River and tributary streams and by pumping from wells.

Although ground-water studies have been in progress almost continuously since 1925, the complex hydrology of the Roswell basin still is not completely understood. A program was started in 1959 to explore the possibility of utilizing tritium, the radioisotope of hydrogen, as a tool in determining the age of water in various parts of the main aquifer in the Roswell basin. The study does not include artificial injection of tritium into the water but makes use of tritium already present in the water. The study was made in cooperation with the State Engineer of New Mexico; water samples were analyzed for tritium by the New Mexico Institute of Mining and Technology.

Detonation of the first large hydrogen bomb in March 1954 and other hydrogen bomb tests between 1954 and October 1961 released large quantities of tritium to the atmosphere. Recharge to ground water from precipitation following the tests contained above-normal amounts of tritium. These releases of tritium provided age-dated sources of water from which the time of recharge can be computed. The content of natural pre-bomb tritium in the atmosphere over North America ranged from 1.16 T.U. (tritium units; 1 T.U. is equivalent to 1 atom of tritium in  $10^{18}$  atoms of hydrogen)

to as much as 66.0 T.U. but averaged (weighted) about 5.2 to 8.8 T.U. in the interior of the United States, on the basis of analyses of precipitation at Chicago, Ill., and in the Mississippi Basin (Kaufman and Libby, 1954, and von Buttlar and Libby, 1955). More than 9 T.U. probably indicates the presence of some post-bomb water.

The results of tritium analyses differ from one laboratory to another because of variations in technique and equipment. Analyses of a few identical samples showed that (1) analyses by the New Mexico Institute of Mining and Technology laboratory in Socorro indicate from 1.2 to a little more than 3 times the values determined by the U.S. Geological Survey laboratory in Washington, D.C., and (2) the analyses of neither laboratory are likely to be directly proportional to the values from the early work cited above. These differences do not necessarily affect the interpretation if the analyses of only one laboratory are used in a study.

Although the analyses by neither the U.S. Geological Survey nor the New Mexico Institute of Mining and Technology can be compared directly with the analyses reported by Kaufman and Libby (1954) and von Buttlar and Libby (1955), the analyses by the New Mexico Institute of Mining and Technology laboratory showing more than 9 T.U. are assumed here to indicate the presence of some postbomb water. Although this assumption may not be wholly valid, the error probably is small and the use of a more precise value would not appreciably affect the interpretations presented in this article. Ground water containing 1 to 9 T.U. in 1959, when most of the samples were collected, is considered to be largely—but probably not exclusively—water recharged before detonation of the first large hydrogen bomb in 1954 but not earlier than about 1924. The basis for the 1924 date is the fact that 35 years is required for the half-life of tritium to result in decay from a concentration of 7 T.U. (the median of the weighted averages of prebomb water) to about 1 T.U.

Ground-water samples analyzed include 44 collected from January through May 1959, 1 collected in October 1960, and 15 collected from April through July 1961. Samples in the latter group are mostly repeat collections from sites previously sampled. Most of the samples were collected from wells or springs yielding water from the main aquifer, but four were from wells in the valley-fill aquifer. All those from wells were obtained while the wells were being pumped. Also, 1 sample of rainwater and 5 samples of surface water were analyzed (see fig. 1.).

The ground-water samples analyzed to date for this project are too few and too widely spaced areally, in time of collection, and in depth from which obtained

for a detailed appraisal to be made. However, tentative conclusions reached on the basis of the available data are presented in the following paragraphs.

All the samples of ground water from the Roswell basin contained at least some water that has been in the ground less than 35 years, on the basis of the above assumptions as to age. Samples from 38 sites contained some water that entered the ground since 1954, samples from 2 sites contained little or no water that entered the ground after 1954 (contained 9 T.U. or less), and samples from 5 sites sampled more than once contained, at different times, water recharged both after and before 1954.

The distribution of high values for tritium content in water from the main aquifer indicates wide differences in the rate of water movement. Because water in the main aquifer moves principally through open solution channels, a high rate of withdrawal from a well can cause rapid transport of water from rather long distances through the system of solution channels tapped by the well. Water movement in systems of solution channels not subject to large withdrawals probably is small by comparison. Therefore, recharge high in tritium may, before decay to low levels of concentration, travel relatively long or short distances in different systems of solution channels, depending on the rate of water movement in response to withdrawals. Areas having wells of large yield (Fiedler and Nye, 1933, p. 133–134 and pl. 41) are shown on figure 1 for comparison with the tritium values.

A slight difference in tritium content with depth was noted in a well in the NE $\frac{1}{4}$ NE $\frac{1}{4}$ SE $\frac{1}{4}$  sec. 8, T. 11 S., R. 25 E., about 5 miles east of Roswell. This well consists of two separate strings of casing which are perforated at different intervals of depth. Samples collected on the same day from depths of about 480 feet and 600 to 800 feet show higher tritium content at the shallower depth in January 1959 (19 T.U. as opposed to 14 T.U. from the deeper zone) and also in April 1961 (22 T.U. from the shallower zone and 15 T.U. from the deeper zone). Other differences in tritium content from well to well may possibly be due to differences in the depths sampled.

The high tritium content of several samples collected from wells near the Pecos River suggests that ground water moves much faster than has been generally believed. Some of the water apparently has moved from the intake area eastward 5 to 15 miles in less than 5 years, and perhaps even in as little as 2 to 3 years. Although the data are not sufficiently complete to compute the traveltimes more accurately, they demonstrate rapid circulation of water in the cavernous San Andres Limestone.

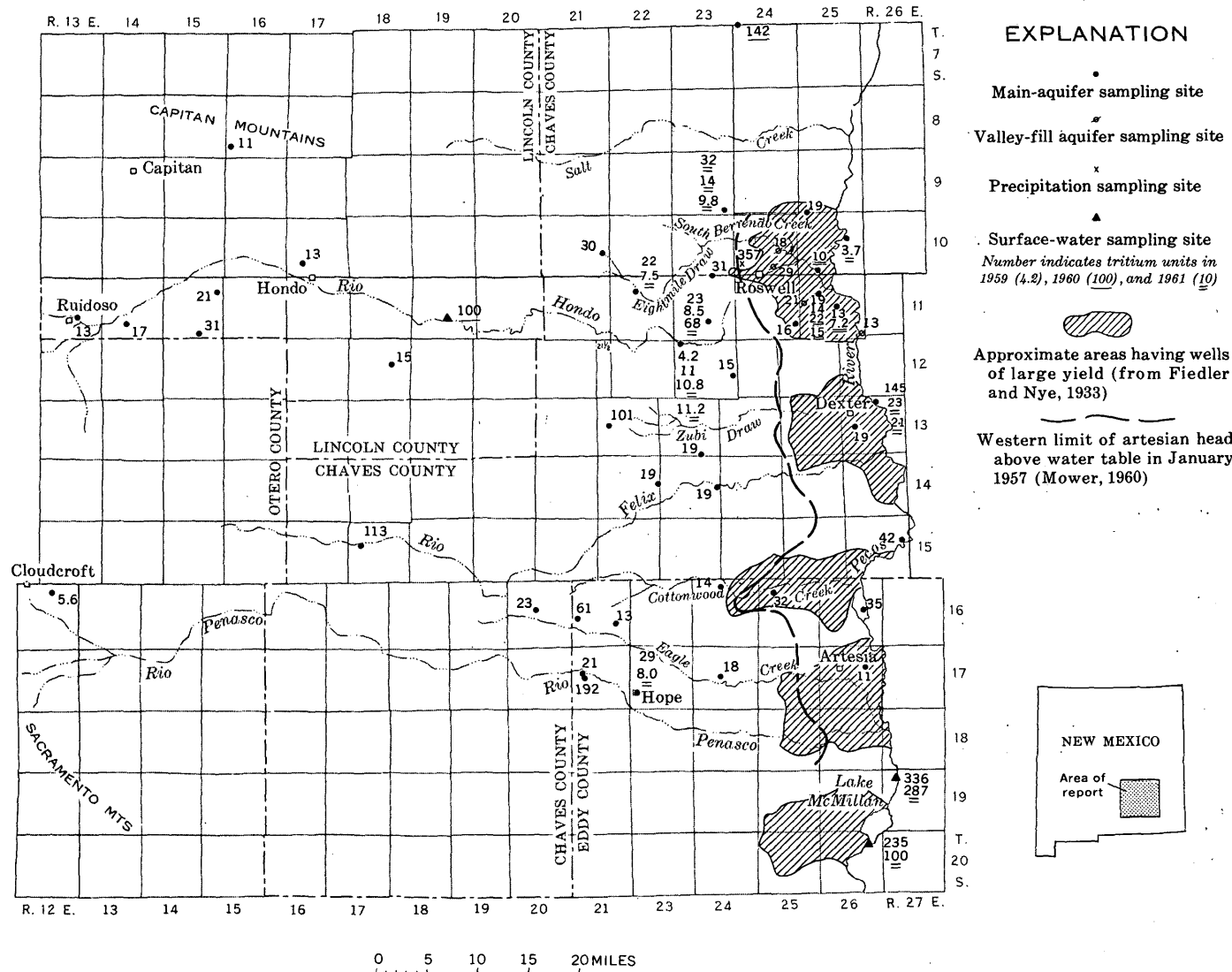


FIGURE 1.—Map showing sampling sites and tritium content of water samples.

#### REFERENCES

- Buttlar, Haro von and Libby, W. F., 1955, Natural distribution of cosmic-ray produced tritium II: Jour. Inorganic Nuclear Chemistry, v. 1, no. 1, p. 75-91.  
 Fiedler, A. G., and Nye, S. S., 1933, Geology and ground-water resources of the Roswell artesian basin, New Mexico: U.S. Geol. Survey Water-Supply Paper 639, 372 p., 46 pls.  
 Kaufman, Sheldon, and Libby, W. F., 1954, The natural distribution of tritium: Phys. Rev., v. 93, no. 6, p. 1337-1344.  
 Mower, R. W., 1960, Pumpage in the Roswell basin, Chaves and Eddy Counties, New Mexico: U.S. Geol. Survey open-file report, 88 p., 21 figs.



## RELATION OF SURFACE-WATER HYDROLOGY TO THE PRINCIPAL ARTESIAN AQUIFER IN FLORIDA AND SOUTHEASTERN GEORGIA

By V. T. STRINGFIELD, Washington, D.C.

*Abstract.*—The main source of some of the largest limestone springs in the world and of some streams in Florida and Georgia is discharge from the principal artesian limestone aquifer where it is at or near the surface on two major geologic structures in Florida and in the belt of outcrops in Georgia. During flood stage, water from some of the larger streams may enter the aquifer, but recharge is chiefly in interstream areas.

The principal artesian aquifer in Florida and southeastern Georgia is one of the most extensive and productive artesian systems in the United States. The aquifer underlies all the drainage basins in Florida, southeastern Georgia, and adjacent parts of Alabama and South Carolina. In some parts of the region, the surface streams are connected hydrologically with the aquifer, but in other areas they are completely unconnected. In recharge areas, the water level in the principal aquifer may represent the water table, but in other areas, there is a separate water-table aquifer wherein the water table may be above or below the piezometric surface of the artesian water.

The purpose of this article is to outline briefly some of the relations of the water in the limestone to the surface-water hydrology, including the coincidence and lack of coincidence between surface drainage and ground-water flow.

The principal artesian aquifer consists chiefly of limestone of Tertiary age as much as 1,000 feet thick. In Florida, it is known as the Floridan aquifer and is the source of some of the largest limestone springs known in the world (Ferguson and others, 1947). It yields water to thousands of wells and is the source of most large industrial, irrigation, and municipal supplies. The aquifer includes as many as seven geologic formations, ranging in age from middle Eocene to middle Miocene. In Florida the basal unit of the

aquifer is the Lake City Limestone of middle Eocene age. In Georgia also, limestone of middle Eocene age is the basal unit. Limestone in the lower part of the Hawthorn Formation of Miocene age forms the top of the aquifer in a large part of the area.

The principal aquifer is at or near the land surface in a belt extending northeast from western Florida and southeastern Alabama across Georgia into South Carolina (fig. 1). In general, it dips toward the Atlantic and Gulf coasts except where the dip is interrupted by geologic structures, such as the Ocala uplift in north-central Florida, and the Chattahoochee anticline in west Florida and southwest Georgia. The aquifer is as much as 150 feet above sea level on the Ocala uplift and 175 feet on the Chattahoochee anticline. It dips in all directions from the Ocala uplift. Its depth below sea level along the Atlantic coast is about 200 to 250 feet at Savannah and 500 feet in northeastern Florida and southeastern Georgia. It is only about 100 feet below sea level along much of the Atlantic coast in northern Florida. In south Florida, the principal aquifer is as much as 1,000 feet below sea level. The aquifer is at or near the surface along the west coast of Florida from Tampa Bay north to the panhandle, and in the western part of the panhandle it dips to more than 1,000 feet below sea level.

Precipitation can infiltrate to the aquifer where the aquifer is exposed at the land surface or covered only with permeable materials. In addition to these recharge areas, water enters the aquifer where sinkholes extend from the ground surface through relatively impervious beds of the Hawthorn Formation to the underlying principal aquifer. Lakes with no surface outlet in the upland regions of Florida and in the Valdosta area of southern Georgia occupy many of these sinks (fig. 1). Some of the sinks are more than 200 feet deep, and a few of these are free from sediment and are occu-

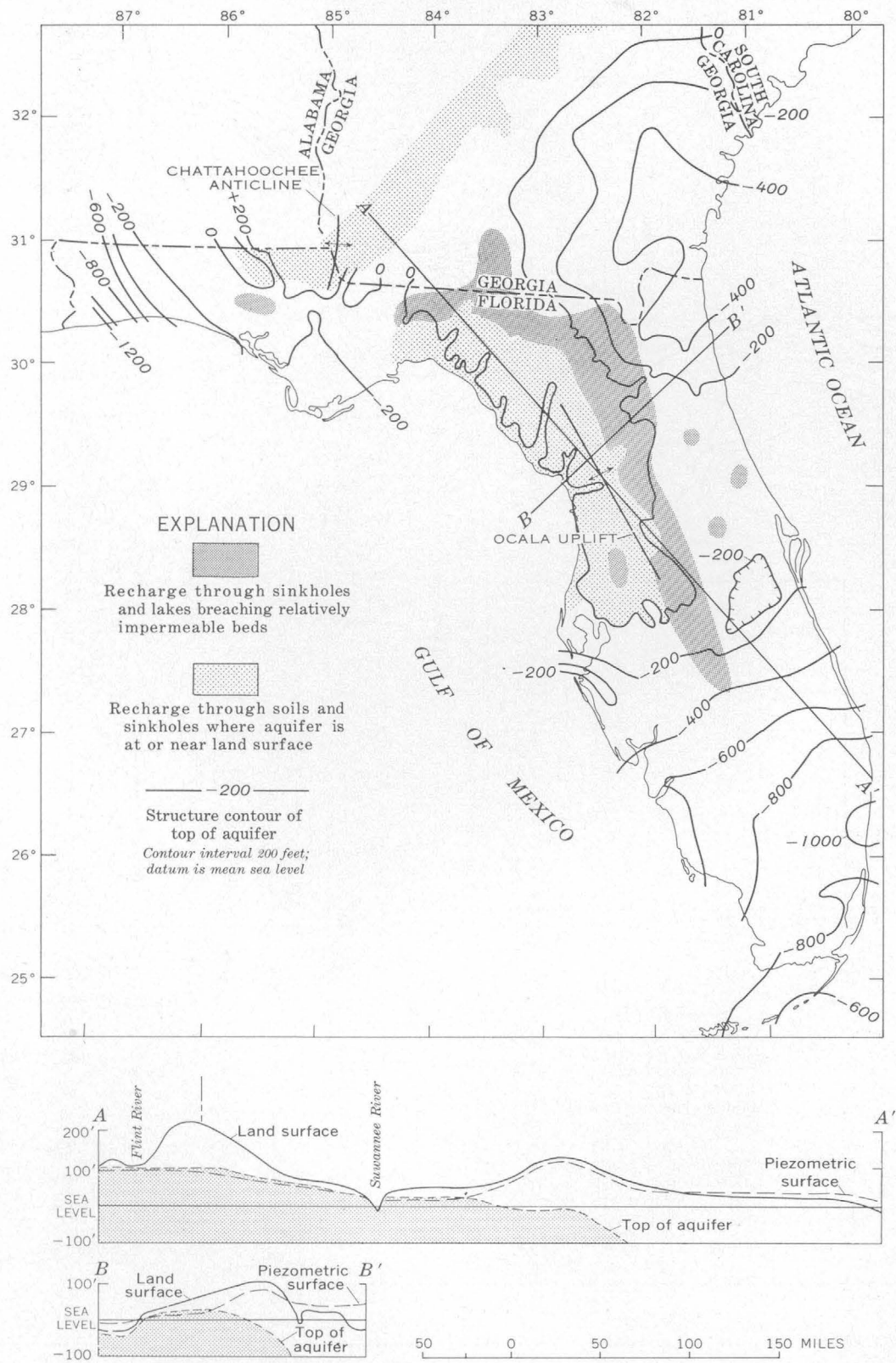


FIGURE 1.—Map showing geologic structure of top of principal artesian aquifer in Florida and southeastern Georgia, and location of recharge areas. Florida portion after Vernon (1955); Georgia portion after Warren (1944).

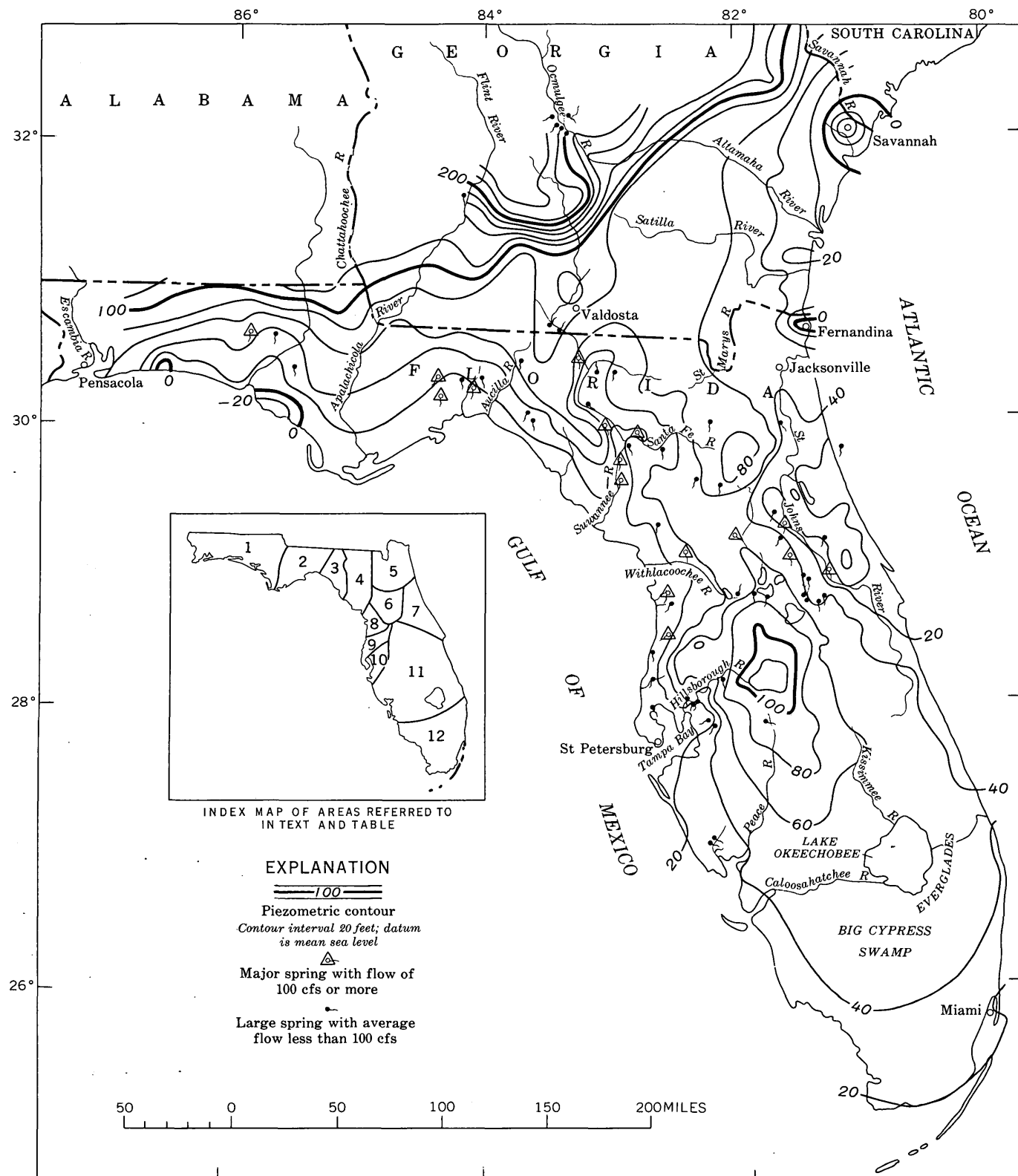


FIGURE 2.—Configuration of the piezometric surface of the principal artesian aquifer in Florida and southeastern Georgia as of 1960. In part after Healy (1962), Stewart and Counts (1958), and Stewart and Croft (1960).

pied by lakes and springs (Ferguson and others, 1947). Many of these sinkholes are now almost completely filled with permeable sand through which water moves downward to the aquifer.

The altitude of the land surface and the sinkholes compared to the water level or artesian head in the aquifer determines whether the sink is a place of recharge or discharge. Recharge occurs where the water level in the sink, or of the lake which occupies the sink, is higher than the water level or artesian head in the aquifer. Where the head in the aquifer is higher than the land surface at the sink, an artesian spring flows from the sink. This is the explanation of nearly all the large springs of Florida and Georgia.

Water enters the aquifer in recharge areas and moves down the hydraulic gradient to points of discharge at lower elevations. Natural discharge of the principal aquifers occurs through springs and at places where the aquifer is exposed in surface streams and in the ocean, and by upward leakage into the overlying formations. The location of the major streams and springs is shown in figure 2. The average flow of each of 17 of the largest springs is more than 100 cubic feet per second. Discharge occurs to the ocean where the artesian head at the submarine outcrop is greater than the pressure of sea water. There are many submarine springs in the Gulf of Mexico west of areas 8 and 9 (fig. 2), and a large spring is known to discharge in the Atlantic east of area 7.

Some recharge may occur through relatively im-

pervious beds of the Hawthorn Formation where the head in the artesian aquifer is less than that of the Hawthorn. However, such recharge is not revealed on maps of the pressure surface of the artesian water.

#### RELATION OF SURFACE DRAINAGE TO RECHARGE AND DISCHARGE

A map (fig. 2) representing the piezometric surface of the water in the artesian aquifer shows the height, in feet, to which water would rise in tightly cased water wells penetrating the aquifer as of 1960. Except in a few areas of large withdrawal of water, the major features of this map are virtually the same as those shown on earlier maps and described by Stringfield, (1936, 1950) and by Warren (1944), indicating that there is no detectable net change in the artesian head in areas unaffected by heavy withdrawal by pumping or natural flow from wells. Earliest available records indicate that in coastal Georgia, as of 1885, movement of water in the principal aquifer was northeast toward a submarine discharge area northeast of Savannah (Stringfield and others, 1941). These maps of the piezometric surface indicate the general areas of recharge and discharge and the directions of lateral movement of the water. Ground water moves down the hydraulic gradient at right angles to the contours. In general, recharge is in the relatively high areas of the piezometric surface, and discharge is in the low areas; in some areas, both discharge and recharge occur. Some of these features are given in the accompanying table.

*Relations of piezometric surface to surface hydrology*

Area <sup>1</sup>	Recharge	Discharge	Surface drainage
Georgia—outcrop of aquifer in belt extending from southeastern Alabama, northeastward across Georgia into South Carolina.	Piezometric surface ranges from 250 feet to about 100 feet above sea level. Recharge occurs in interstream areas.	Discharge to streams where piezometric surface is higher than stream level, as on the Flint, Ocmulgee, and Savannah Rivers.	Rivers such as the Savannah, Ogeechee, and Ocmulgee cross the outcrop belt of the aquifer. The Flint River cuts deep into the aquifer in southwestern Georgia (Wait, 1963).
Withlacoochee Valley and Valdosta area in southern Georgia.	Piezometric surface is as much as 100 feet above sea level in Valdosta area where recharge occurs through sinkholes and drainage wells.	Discharge along the Withlacoochee River.	Surface drainage is into lakes, sinkholes, and drainage wells in the lake region in Valdosta area.
Southeastern Georgia-----	Little or no recharge because the aquifer is overlain by as much as 500 feet of the Hawthorn Formation. Recharge through sinkholes may occur in the Okefenokee Swamp.	Artesian water in the limestone moves east and northeast. Original piezometric surface indicated submarine discharge northeast of Savannah.	Surface streams not related to the aquifer; drainage is sluggish.
West Florida, area 1-----	Aquifer is recharged where it is near the surface in northern part of the area and adjacent parts of Alabama.	Some discharge to streams in the eastern part of the area. Water in the aquifer moves generally south. One spring has an average discharge of more than 100 cfs.	Aquifer is too deep to be related to surface streams in the western part of the area.

*Relations of piezometric surface to surface hydrology—Continued*

Area <sup>1</sup>	Recharge	Discharge	Surface drainage
Area 2-----	Recharge through lakes and sinkholes. The aquifer is near the land surface in the southern part of the area.	A broad valley in the piezometric surface is caused by underground flow to the Gulf of Mexico and to springs. Wakulla Spring and two other springs each have an average discharge of more than 100 cfs.	Much of the drainage is underground in limestone. Some of it reappears at the surface, forming Wakulla Spring, Wakulla River, and other streams.
Area 3-----	Recharge occurs in the inter-stream area.	Discharge occurs to the Suwannee and Aucilla Rivers.	Poor surface drainage in inter-stream areas.
Area 4-----	Recharge occurs in interstream areas. During flood stages the Suwannee and Santa Fe Rivers lose water to the aquifer.	Large discharge occurs chiefly as springs and directly into the Suwannee and Santa Fe Rivers and forms large valleys in the piezometric surface. Five springs have average discharge of more than 100 cfs.	The Suwannee and Santa Fe Rivers cut into the aquifer (Clark and others, 1962).
Area 5-----	Recharge through sinkholes in the southwestern part causes the piezometric surface to stand as much as 80 feet above sea level. A recent description of part of this area is given by Clark and others (1963).	Water moves laterally in all directions from recharge area. Part moves into the Santa Fe River drainage basin.	In upland lake region, drainage is into sinkholes and lakes. Aquifer is too deep to affect the St. Johns River and other streams.
Area 6-----	Aquifer at or near the surface. Large recharge from precipitation.	Although there is large local recharge and artesian water moves into area from north and south, discharge through Silver Springs and Rainbow Springs, averaging 1,507 cfs, causes a saddle in the piezometric surface.	Water from Silver Springs flows to the east and that from Rainbow Springs flows to the west. In most of area, there are no surface streams.
Area 7-----	Recharge is through sinkholes in the upland lake regions east of the St. Johns River.	Piezometric surface is only a few feet above sea level in part of the St. Johns valley where there is large discharge of artesian water to the river. There is submarine discharge in the Atlantic Ocean.	The St. Johns River, a tidal stream, flows northward through area in which its channel is cut into deposits overlying the aquifer. In that part of the valley, each of four springs has an average discharge of more than 100 cfs.
Areas 8, 9, and 10-----	Aquifer is at or near the surface in most of the area and is recharged by precipitation. In the upland lake region, where the piezometric surface is as much as 80 feet above sea level, recharge is through sinkholes.	Large discharge through springs, many of which are in the Gulf of Mexico. Artesian water constitutes a large part of the flow of the Withlacoochee and Hillsborough Rivers and other streams.	Largest streams are the Withlacoochee and Hillsborough Rivers. Drainage is poor in the upper courses of the streams where the piezometric surface is near the land surface. Two of the springs each have an average discharge of more than 100 cfs.
Area 11-----	Recharge through sinkholes and lakes in the lake region in the central part of the area causes the piezometric surface to be more than 100 feet above sea level.	Lateral movement of water is in all directions from recharge areas in the upland lake region.	In the lake region surface drainage is into lakes and sinkholes. Surface streams are not related to the aquifer except in the northern, northeastern, and northwestern parts, where some artesian water discharges directly into streams.
Area 12-----	No detectable recharge to the aquifer. Piezometric surface is above the land surface.	No detectable discharge to surface streams. Discharge offshore may occur where the artesian pressure at submarine outcrop exceeds ocean pressure.	Surface drainage not related to aquifer.

<sup>1</sup> In Florida, areas are numbered as shown on index map, figure 2.

### SUMMARY AND CONCLUSIONS

The flow of some of the largest limestone springs known in the world and some of the principal streams of Florida is discharge from the artesian aquifer. Each of 17 of the largest of these springs has an average flow of more than 100 cfs. The surface hydrology is closely related to the recharge and discharge of the aquifer under the following conditions, as indicated by patterns on figure 1: (1) Where the streams cross the belts of outcrop of the aquifer, water from nearby recharge areas discharges into the streams. (2) Where the Hawthorn Formation has been removed by solution and erosion in the Flint River valley in Georgia and in a large region in north-central and north Florida (bordering the Gulf of Mexico from west Florida to Tampa Bay) the major streams occupy channels cut into the aquifer, and water discharges from the aquifer into the stream. In east-central Florida, a large area of artesian discharge occurs where the St. Johns River cuts through deposits overlying the aquifer. The large limestone springs in Florida and Georgia occur in the areas where the Hawthorn has been removed and the principal artesian aquifer is at or near the surface. (3) Where sinkholes in the lake region extend from the land surface through the Hawthorn to the aquifer, local recharge occurs. In some of these areas there are no surface streams, indicating that all drainage is subsurface.

Surface-water hydrology is unrelated to the aquifer where the aquifer is far below the land surface, as in southeastern Georgia and northeastern, southern, and western Florida. In these areas, representing more than half of the extent of the aquifer, local recharge is not sufficient to be recognized on the piezometric surface of the principal aquifer.

In the discharge areas, the chemical quality of the artesian water affects the quality of the surface water. In the recharge areas, the surface water affects the quality and temperature of the artesian water. Discharge of water from the aquifer to streams and springs has increased the permeability of the aquifer and caused more rapid circulation. This circulation has accelerated the removal of salt water that entered the aquifer in some areas when the sea stood higher in Pleistocene time than at the present.

The surface drainage has a dendritic pattern characterized by many tributaries where the streams are inde-

pendent of the aquifer, except on coastal Pleistocene terraces where the drainage pattern is influenced by the topography left by the sea. In areas where recharge or discharge of the aquifer is sufficient to cause anomalies on the piezometric surface, as in the Suwannee and Santa Fe basins in Florida, the streams have few tributaries.

In studies of the water resources and planning for their development in this region, the relation between the artesian system and the surface hydrology should be recognized and understood to determine whether the surface and subsurface hydrology should be considered separately or be treated as a unit.

### REFERENCES

- Clark, W. E., Musgrove, R. H., Menke, C. G., and Cagle, J. W., Jr., 1962, Interim report on the water resources of Alachua, Bradford, Clay, and Union Counties, Florida: Florida Geol. Survey Inf. Circ. 36.
- 1963, Hydrology of Brooklyn Lake near Keystone Heights, Florida: Florida Geol. Survey Rept. Inv. 33.
- Ferguson, G. E., Lingram, C. W., Love, S. K., and Vernon, R. O., 1947, Springs of Florida: Florida Geol. Survey Bull. 31.
- Healy, H. G., 1962, Piezometric surface and areas of artesian flow of the Floridan aquifer in Florida, July 6-17, 1961: Florida Geol. Survey map ser., No. 4.
- Stewart, J. W., and Counts, H. B., 1958, Decline of artesian pressures in the coastal plain of Georgia, northeastern Florida and southeastern South Carolina: Georgia Geol. Survey Mineral Newsletter, v. 11, No. 1.
- Stewart, J. W., and Croft, M. A., 1960, Ground-water withdrawals and decline of artesian pressures in the coastal counties of Georgia: Georgia Geol. Survey Mineral Newsletter, v. 13, No. 2.
- Stringfield, V. T., 1936, Artesian water in the Florida peninsula: U.S. Geol. Survey Water-Supply Paper 773-C, p. 115-195.
- 1950, Ground-water geology in the southeastern States, in Proceedings of symposium on mineral resources of the southeastern States: Knoxville, Tenn., Univ. Tennessee Press.
- Stringfield, V. T., Warren, M. A., and Cooper, H. H., Jr., 1941, Artesian water in the coastal area of Georgia and northeastern Florida: Econ. Geology, v. 37, No. 7, p. 699-711.
- Vernon, R. O., 1955, Safe and adequate and you drink it: Florida Eng. and Indus. Exept. Sta. Bull. 72.
- Wait, R. L., 1963, Geology and ground-water resources of Dougherty County, Georgia: U.S. Geol. Survey Water-Supply Paper 1539-P.
- Warren, M. A., 1944, Artesian water in southeastern Georgia, with special reference to the coastal area: Georgia Geol. Survey Bull. 49.



## CONTAMINATION OF GROUND WATER BY DETERGENTS IN A SUBURBAN ENVIRONMENT—SOUTH FARMINGDALE AREA, LONG ISLAND, NEW YORK

By N. M. PERLMUTTER, MAXIM LIEBER,<sup>1</sup> and H. L. FRAUENTHAL,<sup>2</sup>  
Mineola, N.Y.; Hempstead, N.Y.

*Work done in cooperation with the Nassau County Department of Health  
and the Nassau County Department of Public Works*

**Abstract.**—Water in the upper 20 feet of the water-table aquifer, composed of glacial-outwash deposits, is contaminated by ABS (alkylbenzenesulfonate) in concentrations generally between 1 and 5 ppm but locally as high as 32 ppm. Most of the water in the remainder of the aquifer contains less than 1 ppm and does not foam. Effluent from hundreds of randomly distributed cesspools is the source of contamination.

Large-scale suburban development of Long Island since World War II has brought not only the pleasures of suburban living to many former city dwellers but also, in some areas, the problem of foaming and bad-tasting ground water. Foaming is caused by ABS, a surface-active organic compound which constitutes about 30 to 40 percent of the ingredients in common household detergents. The ABS, along with associated contaminants such as chloride, phosphate, nitrate, nitrite, bacteria, and possibly viruses in domestic wastes, has entered the shallow water-table aquifer by seepage of effluent from thousands of cesspools. Substitution of detergents for soap has increased markedly during the past 15 years, and in places where detergent in water supplies has resulted in deterioration of quality, users have become more acutely aware of the recirculation of wastes in the ground water. ABS in water generally is regarded as more of an appearance or taste problem than a menace to health, as ABS by itself is not considered to be toxic in concentrations commonly found in ground water. Nevertheless, the presence of

ABS may indicate the occurrence, possibly in harmful concentrations, of other contaminants from cesspool wastes. Hence, the U.S. Public Health Service (1962) recommends that the concentration of ABS in water to be used for drinking or cooking should not exceed 0.5 parts per million.

Contamination by detergents is particularly widespread in unsewered parts of southern Nassau and Suffolk Counties. What is the extent of the contamination? How deep has it penetrated and in what concentrations? Are public supply wells in danger of contamination? These and related questions have been the subject of much speculation. Consequently, during the past few years investigations have been made individually and cooperatively in parts of Nassau and Suffolk Counties by State and County agencies and the U.S. Geological Survey to find answers to some of these questions (New York State, 1963, p. 69–90). Of the current investigations, some deal with contamination in the immediate vicinity of a single cesspool or well field, whereas others are of wider areal scope. This article is a summary of the results of an areal investigation in east-central Nassau County (figs. 1 and 2).

Appreciation is expressed to Commissioner Eugene F. Gibbons of the Nassau County Department of Public Works and to Dr. Joseph H. Kinnaman, Commissioner of the Nassau County Department of Health, for their enthusiastic support of the investigation. We also thank all the Nassau County and U.S. Geological Survey personnel who assisted in the field and laboratory work.

<sup>1</sup> Assistant Director, in charge of Sanitation Laboratories, Division of Laboratories and Research, Nassau County Department of Health.

<sup>2</sup> Hydraulic Engineer, Division of Sanitation and Water Supply, Nassau County Department of Public Works.

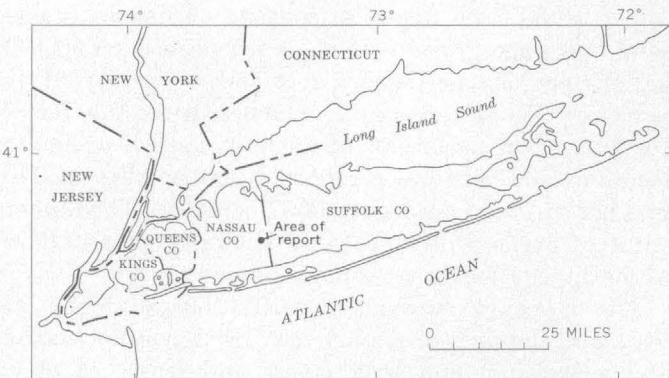


FIGURE 1.—Map of Long Island, N.Y., showing location of the South Farmingdale area.

During an investigation in 1962 of contamination of ground water by plating wastes in the South Farmingdale area (Perlmutter and others, 1963), samples of water at various depths in test wells were analyzed for ABS as well as for the principal contaminants in the plating wastes. This area is well suited for a study of ABS contamination because it is unsewered and the wastes from about 250 small homes are disposed of by means of individual cesspools or septic tanks.

The area investigated by test drilling is about 4,000 feet long and about 400 to 1,400 feet wide. The land surface is a gently rolling plain that slopes southward from about 70 to about 40 feet above sea level. Surface



FIGURE 2.—Aerial photograph of South Farmingdale area, showing water-table contours (heavier lines), in feet, and location of hydrogeochemical sections (lighter lines). Arrows indicate direction of ground-water flow. Datum is mean sea level.

drainage consists of several narrow, shallow tributary streams which form the headwaters of Massapequa Creek (fig. 2). Scattered catch basins and storm-drainage trunk lines carry runoff from paved areas to nearby Massapequa Creek.

### METHODS OF INVESTIGATION

In 1962, the Nassau County Department of Public Works installed about 90 test wells along selected streets and in the vicinity of Massapequa Creek (figs. 2, 3, and 4). Nearly all the wells were constructed with 1½-inch casing and a 3-foot drive point. Water samples were collected by means of a pitcher pump at 5-foot intervals during the driving of the wells. The samples were analyzed for ABS in the laboratory of the Nassau County Department of Health, generally 1 day after collection.

The concentration of ABS was determined by a tentative method (American Health Association, 1960, p. 246-248), using methylene blue dye, chloroform extraction, and colorimetric comparison of the extract with standard solutions. Although certain organic and inorganic compounds are known to interfere with the determination of ABS by the methylene blue method, the writers have considered this fact as well as the overall chemical quality of the ground water and have concluded that determinations of ABS as low as 0.1 ppm are significant in the report area. Hence, the lower limit of contamination shown by the shading in figures 3 and 4 is indicated by the depth at which the concentration of ABS was approximately 0.1 ppm. Because of the limitations of the data the position of the zero isopleth of ABS could not be determined accurately. It is estimated, however, to be less than 20 feet below the lower limit of the shaded area shown on the sections.

Water-level measurements made in selected wells were referenced to mean sea level to determine the shape and altitude of the water table and the direction of ground-water movement (fig. 2).

### GEOLOGIC AND HYDROLOGIC CONTROLS

The water-bearing units of chief interest in the South Farmingdale area are an upper unit of glacial outwash of late Pleistocene age and an underlying unit of sand and clay of Late Cretaceous age (fig. 3).

The upper Pleistocene deposits consist of beds of brown fine to coarse sand and gravel and some scattered thin lenses of silt, and have an average thickness of about 80 feet. Two core samples of the outwash deposits were tested for hydraulic properties by the Hydrologic Laboratory of the U.S. Geological Survey in Denver, Colo. One sample, typical of most of the

upper Pleistocene deposits, consists of fine to coarse sand and some gravel. It has a permeability of 1,600 gallons per day per square foot and a porosity of 33 percent. The other sample, which represents a facies common in the lower part of the unit, consists of fine to medium sand, and has a reported permeability of 440 gpd per sq ft and a porosity of 37 percent. The higher value of permeability probably is more representative of the upper Pleistocene deposits as a unit.

The Upper Cretaceous deposits consist chiefly of lenticular deposits of nonmarine gray fine sand, clayey and silty sand, and thin layers and lenses of clay. These deposits have relatively low permeability. As there is no evidence that water in the Cretaceous deposits is contaminated by ABS, they are not described further in this article.

Water in the upper Pleistocene deposits is under water-table, or unconfined, conditions. It is derived mainly by subsurface inflow from the area north of South Farmingdale but also by downward percolation of precipitation (such recharge averages about 1 million gallons per day per square mile), effluent from cesspools, and possibly some leakage from water mains and storm sewers. The water table ranges from about 15 feet below the land surface in the northern part of the area to less than a few inches at and near Massapequa Creek in the southern part (figs. 3 and 4). Contours of the water table (fig. 2) show that most of the water is moving southerly toward Massapequa Creek. The upstream bending of the contours in the vicinity of Massapequa Creek indicates that part of the ground water is discharged into the stream. The arrows on section A-A' (fig. 3) show that the ground water is moving nearly horizontally, except for local downward components at shallow depths beneath the recharge basins and cesspools (not shown) and upward components beneath Massapequa Creek.

Ground water is discharged from the area by subsurface outflow, by lateral and upward seepage into Massapequa Creek, by discharge from a small number of lawn-sprinkling wells, and to a lesser extent, by direct evaporation from the water table and transpiration of plants whose roots tap the water table. By substituting in Darcy's law an average hydraulic gradient of about 12 feet per mile, laboratory determinations of permeability of 440 and 1,600 gpd per sq ft and a porosity of 33 percent, an average lateral ground-water velocity of about 0.5 to 1.5 feet per day is calculated for the upper Pleistocene deposits. On the basis of the overall lithology of the deposits, the average velocity is estimated to be about 1 foot per day under natural conditions. In the vicinity of pumped wells the rate of movement is somewhat greater.

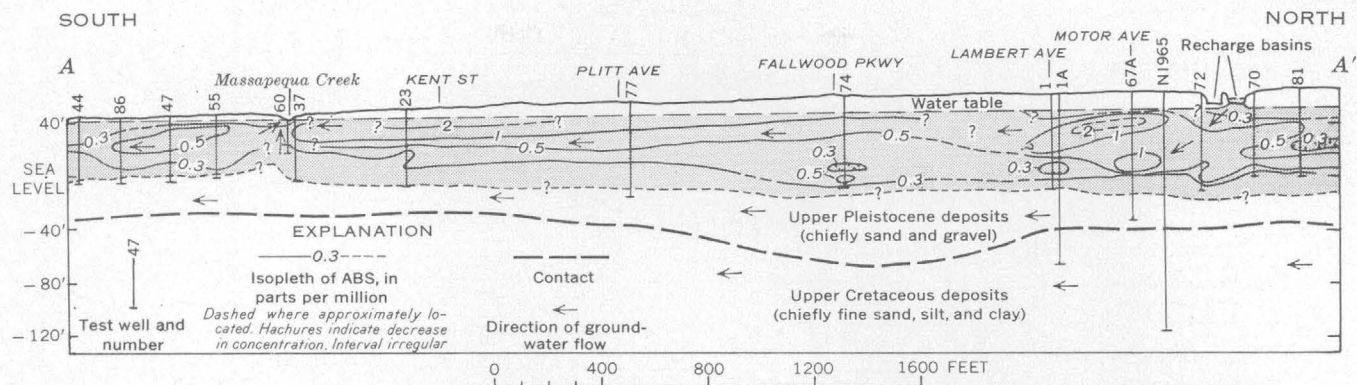


FIGURE 3.—Hydrogeochemical section parallel to the direction of ground-water flow, showing isopleths (lines of equal concentration) of ABS in 1962. Contaminated water is shaded; lower limit shown at about 0.1 ppm of ABS.

#### CONCENTRATION AND MOVEMENT OF ABS

The distribution of ABS in the ground water is the resultant of the coalescence of several hundred randomly distributed slugs of cesspool waste that have infiltrated to the zone of saturation. The slugs differ in volume and in concentration of ABS, and while moving downgradient they commingle and are diluted mainly by recharge from precipitation and by mixing with less contaminated ground-water underflow. The concentration of ABS in cesspools may be as high as 60 ppm, and the highest concentrations in the ground water generally are found within a distance of about 40 feet downgradient from a source cesspool and less than 20 feet below the water table. The pattern of distribution of ABS is shown by the isopleths (lines of equal concentration) in the section parallel to the direction of ground-water flow (fig. 3) and in the sections oblique to the direction of ground-water flow (fig. 4).

In evaluating the isopleths it is important to note that the first water sampled in most of the wells ranged from about 3 to 18 feet below the water table, so that water containing higher concentrations of ABS than those illustrated doubtless is in the upper few feet of the zone of saturation in some places. Determinations of ABS ranged from less than 0.02 to about 32 ppm. The depth of detectable contamination ranged from the water table to about 60 feet below. Although the ABS is distributed throughout the upper two-thirds of the saturated part of the upper Pleistocene deposits, at most depths the concentration is less than 1 ppm and would not be detected by the user. However, in a few places, such as the middepth intervals in well 67 on Motor Avenue (*B-B'*, fig. 4) and in wells 1 and 2 on Lambert Avenue (*C-C'*, fig. 4) the concentrations ranged from about 1 to 5 ppm. This local center of relatively high concentration of ABS may be due to wastes from an industrial park north of Motor Avenue,

from commercial buildings on Motor Avenue, or from both sources. The downward sag in the isopleths of relatively high concentration at the extremities of section *B-B'* (fig. 4) results from these areas being occupied by facilities such as parking lots and buildings which do not contribute cesspool effluent to the underlying water table.

An unusually high concentration of ABS, about 32 ppm, in water collected from a depth of about 6.5 feet below the water table in test well 28 (section *F-F'*, fig. 4), suggests that the well penetrates the center of a slug of wastes from a nearby cesspool. Except for anomalous patterns of contamination in the immediate vicinity of individual disposal systems, the zonation shown in sections *D-D'* to *F-F'* (fig. 4) is probably typical of the general pattern of contamination beneath most unsewered residential areas in southern Nassau and Suffolk Counties.

A few analyses of the contaminated water show a range in chloride content of 8 to 30 ppm, whereas the natural chloride content in the area is about 5 ppm. Similarly, the observed range in nitrate as  $\text{NO}_3$  is 10 to 22 ppm in contaminated water, whereas the natural content is commonly less than 5 ppm. Concentrations of ABS, chloride, and nitrate higher than those reported above probably characterize the ground water immediately adjacent to cesspools.

The bulk of the highly contaminated ground water flows at shallow depths toward the headwaters of Massapequa Creek and is discharged as surface water. Water at greater depths, containing moderate to low concentrations of ABS, moves downgradient as underflow and discharges eventually in the lower reaches of Massapequa Creek. Although the ABS content of Massapequa Creek in April 1963 decreased from about 1 ppm near the headwaters to about 0.6 ppm near the mouth of the stream (south of the report area), the actual load of ABS increased from about 0.5 pound per

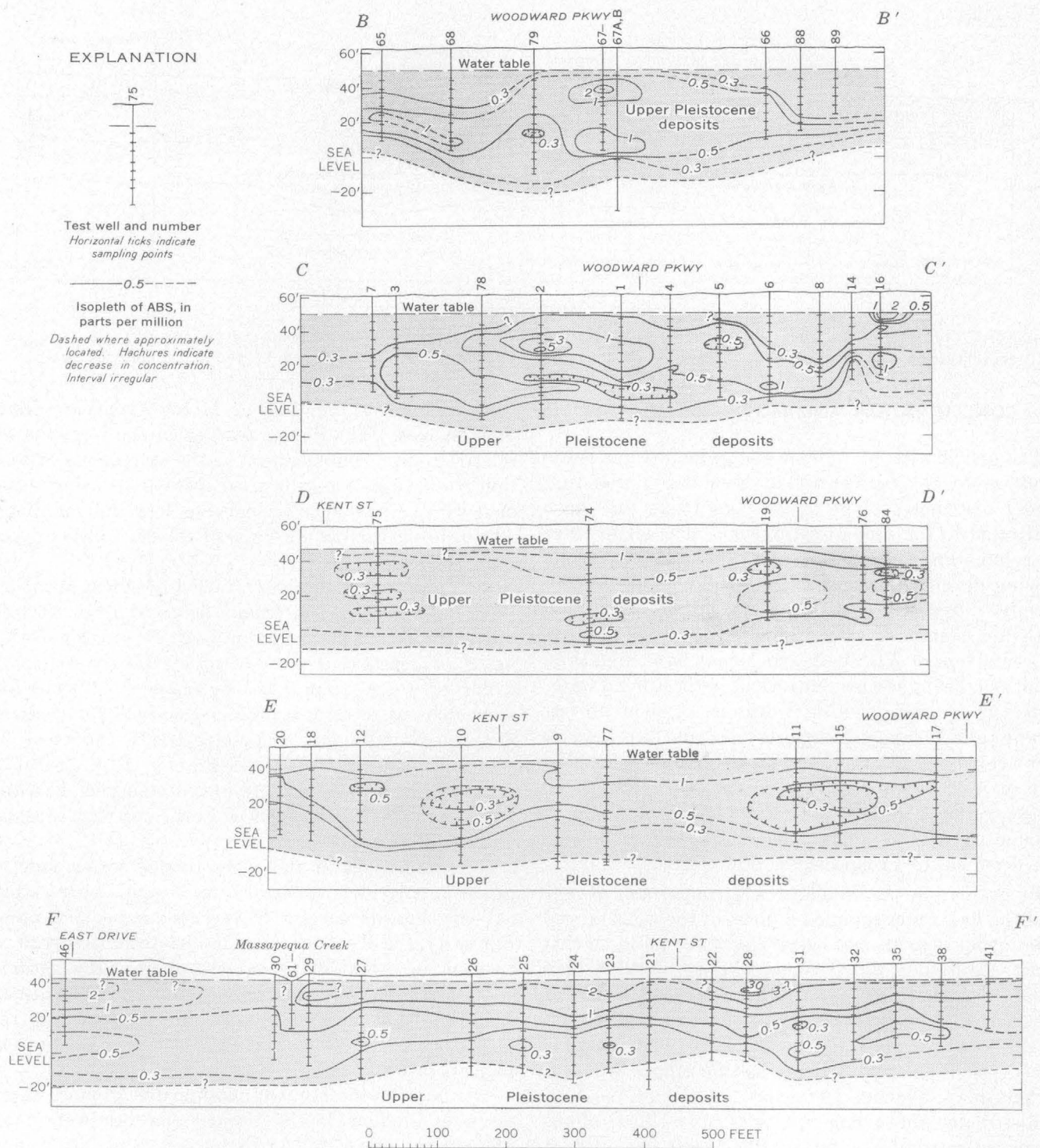


FIGURE 4.—Hydrogeochemical sections oblique to the direction of ground-water flow, showing isopleths (lines of equal concentration) of ABS in 1962. Contaminated water is shaded; lower limit shown at about 0.1 ppm of ABS.

day near the headwaters to about 25 pounds per day near the mouth, due to the pickup of contaminated ground water by the stream.

#### POTENTIAL THREAT OF CONTAMINATION OF WATER IN THE CRETACEOUS DEPOSITS

Because the contaminated water in the South Farmingdale area is moving mostly laterally, it is unlikely under present conditions that significant amounts of ABS, if any, have moved down from the upper Pleistocene deposits into the Cretaceous deposits, which are the source of water for most public-supply wells. No public-supply wells are in the immediate area of investigation, but analyses of water from nearby public-supply wells, which range in depth from about 150 to 600 feet, show no indication of ABS to date.

In the vicinity of the main ground-water divide, north of the report area, ground water has a natural downward gradient which favors slow contamination of the Cretaceous deposits by downward leakage, but evidence of this has not been reported. Near the north and south shores of Nassau County, water in the deep aquifers generally moves upward to discharge areas at the shore or offshore. This natural flow pattern inhibits downward leakage of cesspool waste in the south shore areas. In some parts of Nassau County, however, particularly in the southern half, heavy and continuous pumping of public-supply wells screened in the Cretaceous deposits could disturb the natural flow pattern described above and create local and, eventually, extensive areas of downward gradient between the upper Pleistocene deposits and the Cretaceous deposits, which would induce some downward movement of contaminated water. Such movement would be extremely slow where, as is generally the case, thick beds of relatively low permeability separate the water-bearing zones, and the hydraulic gradients developed by pumping are low.

Although, under present hydraulic conditions, pumping is unlikely to cause extensive downward movement of contaminated water into the Cretaceous deposits for many tens of years, additional studies should be made to locate and to monitor those areas where unusual geo-hydrologic conditions could result in contamination sooner than anticipated. Parts of the deep aquifers may be contaminated locally through breaks in well casings or inadequate grouting of the annular space around casings of wells drilled by the rotary method.

Regulatory agencies should be constantly alert to this subtle method of contamination so that it does not become a serious problem.

Further studies of hydraulic gradients and variation in vertical permeability of the Cretaceous deposits as well as the adsorptive and ion-exchange capacities of Cretaceous silts and clays are required before more quantitative predictions can be made of the rate of movement of ABS and associated contaminants into the deeper water-bearing zones in Nassau County. Even if more degradable detergents are produced in the near future, the problem of contamination by other cesspool wastes will not be eliminated. Therefore, most investigators agree that a public-sewer system is the only practical remedy. Southwestern Nassau County is sewered already and, within the next 20 years, the South Farmingdale area and most of the remainder of the county probably will be sewered also.

As cesspools are eliminated, ABS already in the ground water generally will be diluted gradually by recharge from precipitation, underflow, dispersion, and diffusion. On the other hand, the ABS concentration may increase temporarily in some places after sewerage, as slugs of contaminated water move downgradient through uncontaminated or less contaminated areas to points of natural discharge. The time required for the removal of the bulk of the ABS from the water by natural discharge from the upper Pleistocene deposits may be several tens of years. However, in most places, dilution of the contaminated water below the lower limit of foaming, about 1 ppm, should take place within a few years after sewerage, as the highest concentrations are generally found a short distance below the water table where recharge from precipitation is most effective as a dilutant.

#### REFERENCES

- American Public Health Association, 1960, Standard methods for the examination of water and waste water: New York, Am. Public Health Assoc., Inc., 11th ed., 626 p.
- New York State, 1963, Progress report of the Temporary State Commission on Water Resources Planning: Legislative Doc. (1963) No. 40, 210 p.
- Perlmutter, N. M., Lieber, Maxim, and Frauenthal, H. L., 1963, Movement of waterborne cadmium and hexavalent chromium wastes in South Farmingdale, Nassau County, Long Island, N.Y.: Art. 105 in U.S. Geol. Survey Prof. Paper 475-C, p. C179-C184.
- U.S. Public Health Service, 1962, Drinking water standards: U.S. Public Health Service Pub. 956, p. 22-25; also in Federal Register, Mar. 6, p. 2152-2155.



## RELATION OF CHEMICAL QUALITY OF WATER TO RECHARGE TO THE JORDAN SANDSTONE IN THE MINNEAPOLIS-ST. PAUL AREA, MINNESOTA

By MARION L. MADERAK, Lincoln, Nebr.

*Work done in cooperation with the  
Division of Waters, Minnesota Department of Conservation*

**Abstract.**—Maps that show areal variations in concentration of dissolved solids can be used to detect possible recharge areas and direction of ground-water movement. For the Jordan Sandstone in the Minneapolis-St. Paul area, the anomalous areas of low concentration of dissolved solids coincide with the recharge areas indicated by the highest elevations on a piezometric map.

Lines of equal dissolved-solids concentration of ground water from the Jordan Sandstone of Cambrian age in the Minneapolis-St. Paul area, Minnesota, agree closely with patterns of ground-water movement as deduced from water-level contour maps. Recharge to the Jordan is indicated by high head and low dissolved-solids concentration of the ground water; migration of water is toward areas of low head and high dissolved-solids concentration.

Alluvial and glacial deposits of Quaternary age, ranging from clay to boulders, are the youngest deposits in the area (fig. 1). Limestone, dolomite, shale, siltstone, and sandstone of Ordovician age and shale, siltstone, and sandstone of Cambrian and Precambrian age form the bedrock. Crystalline basement rocks underlie sedimentary rocks of Precambrian age. The consolidated sedimentary rocks have been folded into a broad basin, slightly elongated northeast-southwest and centered several miles north of the confluence of the Minnesota and Mississippi Rivers. The approximate extent of the structural basin is indicated in figure 2 by the lines showing the eastern and western limits of the Jordan Sandstone.

Small yields of water can be obtained from almost all rocks in the basin, but large yields of water sufficient for municipal and industrial supplies generally are available only from the glacial drift, St. Peter Sand-

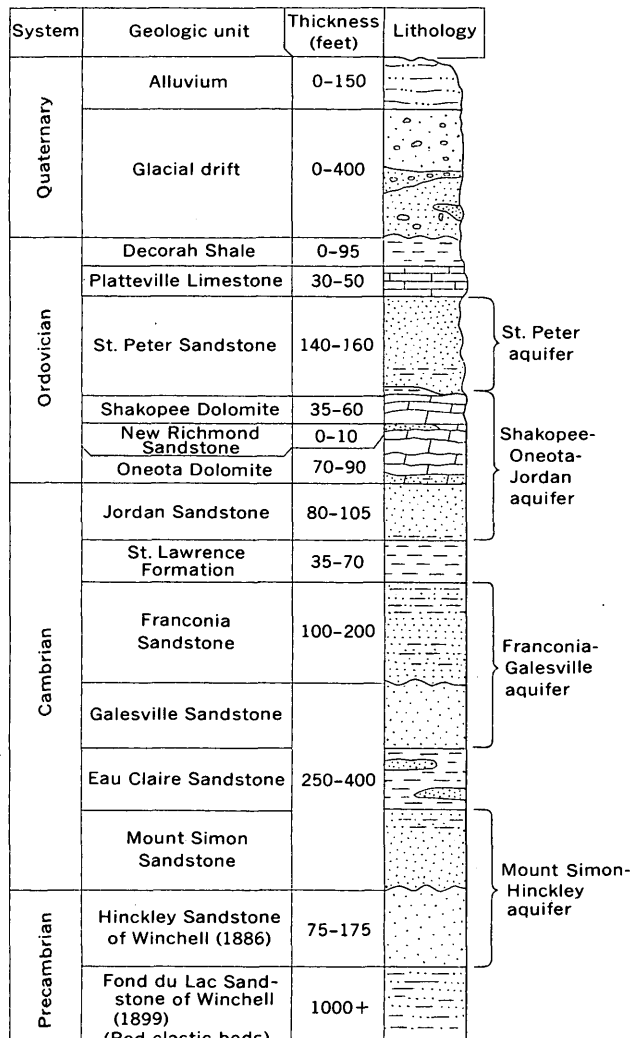


FIGURE 1.—Sedimentary sequence in the Minneapolis-St. Paul area.

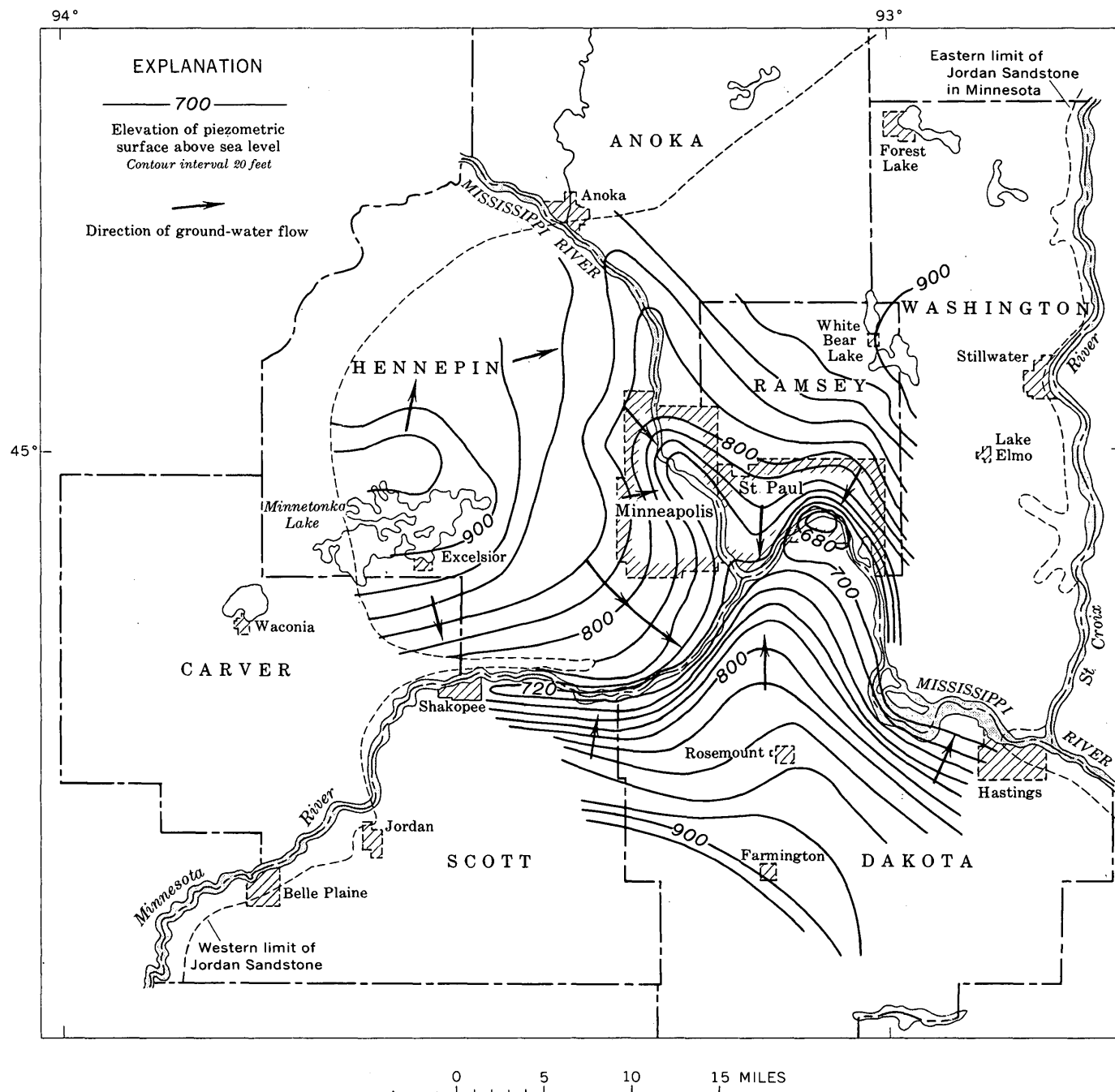
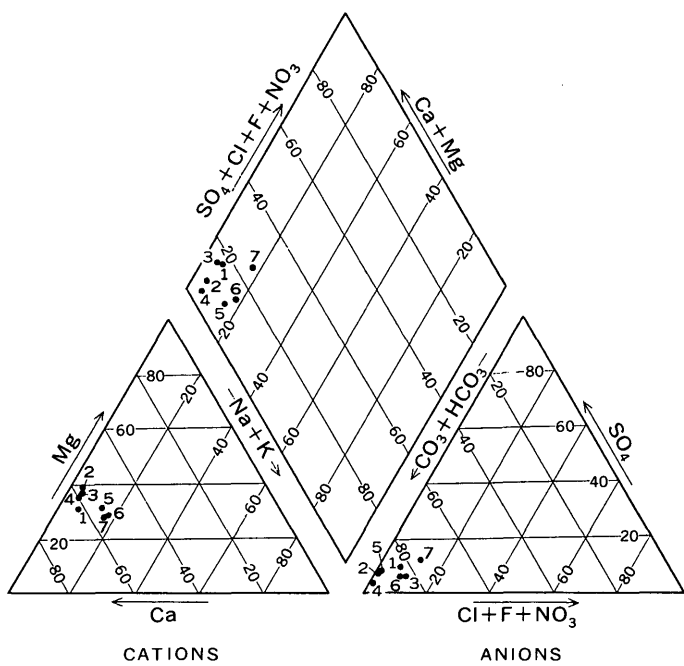


FIGURE 2.—Map of the piezometric surface of water in the Jordan Sandstone (after Liesch, 1961).

stone, Shakopee Dolomite, Oneota Dolomite, Jordan Sandstone, Franconia Sandstone, Galesville Sandstone, Mount Simon Sandstone, and Hinckley Sandstone of Winchell (1886). Because the Jordan Sandstone underlies most of the basin, has a uniform thickness, lies at fairly shallow depths, yields the large amounts of water necessary for industrial and municipal demands, and contains water of fairly good quality, it is the most

commonly used source. The Jordan is a loosely cemented fine- to coarse-grained white sandstone that dips about 20 feet per mile toward the center of the basin. Exposure of the sandstone to an oxidizing atmosphere changes the Jordan from white to yellow.

Immediately underlying the glacial drift in much of the area are the St. Peter, Shakopee, Oneota, and Jordan aquifers. The Shakopee, Oneota, and Jordan



No. on diagram	No. of wells or sources of surface water sampled	Average dissolved solids (ppm)	Geologic unit
<b>Ground water</b>			
1-----	43	384	Glacial drift.
2-----	8	360	St. Peter Sandstone.
3-----	7	360	Shakopee and Oneota Dolomites.
4-----	23	266	Jordan Sandstone.
5-----	12	356	Franconia and Galesville Sandstones.
6-----	9	309	Mount Simon Sandstone and Hinckley Sandstone of Winchell (1886).
<b>Surface water</b>			
7-----	9 (8 lakes and 1 stream).	205	

FIGURE 3.—Average chemical character of water from principal sources in the Minneapolis-St. Paul area, in percentage of total equivalents per million.

are hydraulically connected and have, therefore, been regarded as a single aquifer. According to Liesch (1961) water in the central part of the basin (downtown Minneapolis-St. Paul area) can move directly from the St. Peter through the dolomite section to the Jordan Sandstone. The New Richmond Sandstone of Ordovician age is thin and yields little water to wells. Except in the central part of the basin and in recharge areas, the Oneota Dolomite contains a shale or siltstone that partly restricts the downward movement of water to the Jordan. Because of the restriction of the downward movement of water, the quality of the water in the

Jordan Sandstone is slightly different from that in the overlying formations. Underlying the Jordan Sandstone is the St. Lawrence Formation, which forms the lower confining layer for the Shakopee-Oneota-Jordan aquifer.

Recharge to the aquifers overlying the St. Lawrence Formation is mostly from the glacial drift. Natural discharge is mostly from springs and seeps along the Minnesota and Mississippi Rivers. Because they are hydraulically connected, the Franconia Sandstone and underlying Galesville Sandstone are here referred to as the Franconia-Galesville aquifer, and the Mount Simon Sandstone and Hinckley Sandstone of Winchell (1886) are referred to as the Mount Simon-Hinckley aquifer.

Water from the principal sources in the Minneapolis-St. Paul area is of the calcium bicarbonate type and is similar in chemical character to water from eight representative lakes and one stream in the area (fig. 3). Of the principal sources of water, the Jordan Sandstone has the lowest average dissolved-solids content and the Mount Simon-Hinckley has the next lowest average.

The direction of ground-water flow in the Jordan is shown by a piezometric map (fig. 2). An isocon map (fig. 4) shows areal variations in the total concentration of dissolved solids in water from 23 wells that tap the Jordan Sandstone and are evenly spaced across the Minneapolis-St. Paul artesian basin. Each isocon on the map connects points of equal concentrations of dissolved solids. Except for the anomalous areas near Excelsior and White Bear Lake, the dissolved-solids concentrations indicated by the isocons tend to increase toward the west; the recharge from the glacial drift in the western part of the basin generally has a higher average dissolved-solids concentration than the recharge in the eastern part of the basin. The anomalous areas near Excelsior and White Bear Lake (fig. 4) coincide fairly well with the highest water-surface elevations (fig. 2); future investigations may show that detailed chemical-quality data can be useful in determining areas of recharge and direction of ground-water movement. The recharge moves generally from the Excelsior and White Bear Lake areas into the drift aquifers, through the St. Peter, Shakopee, and Oneota to the Jordan, and then downdip to the central part of the basin. Some recharge to the Jordan also occurs in the downtown Minneapolis-St. Paul area from the overlying St. Peter, Shakopee, and Oneota (Liesch, 1961); this recharge may account for the irregularity of the isocons in the downtown area.

Although the isocon anomalies and the recharge areas coincide for the Minneapolis-St. Paul artesian basin, some anomalous dissolved-solids concentrations may not

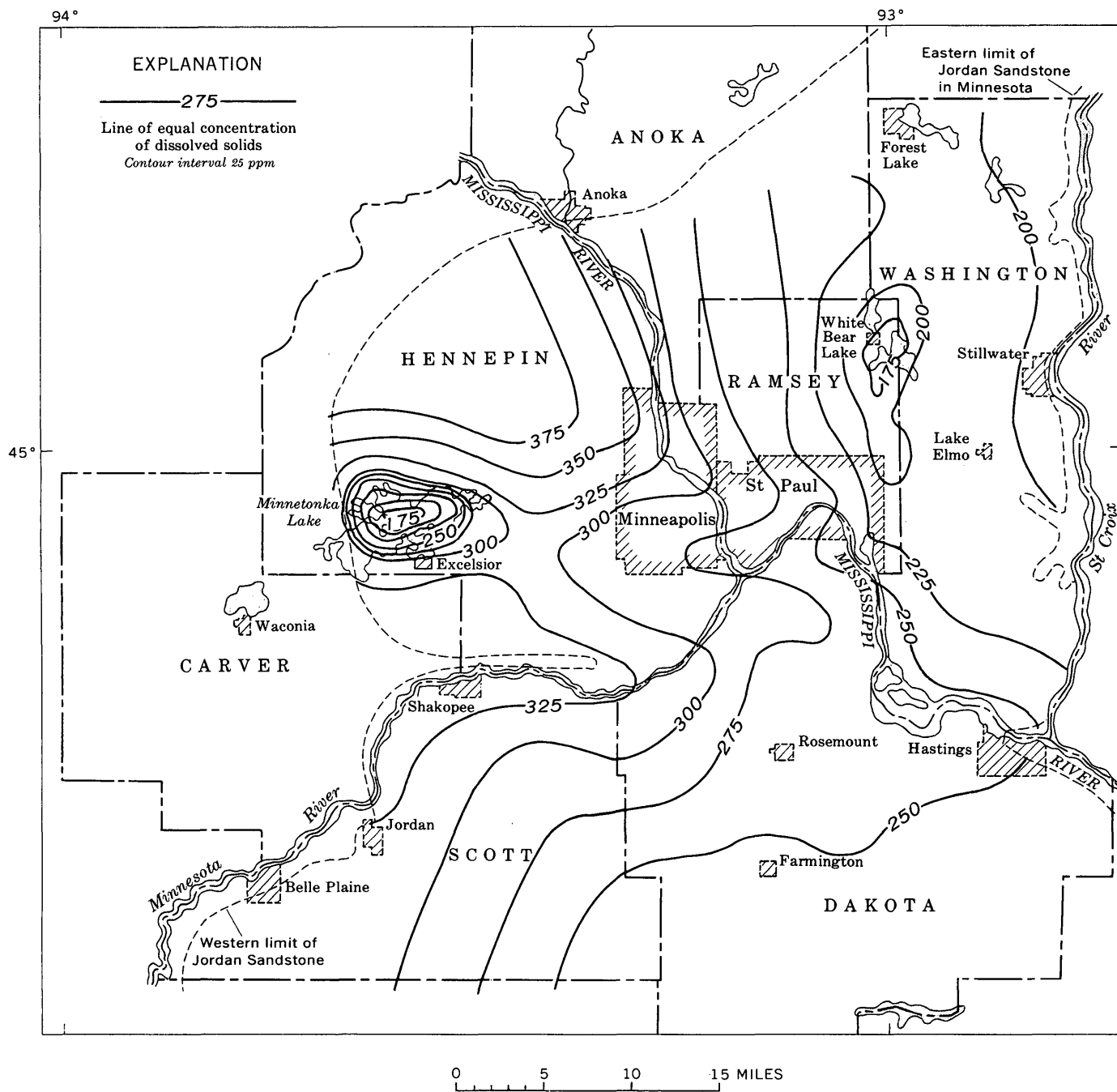


FIGURE 4.—Isocon map of dissolved solids in water from the Jordan Sandstone.

indicate recharge areas and instead may only be the result of well construction that allows water from one zone to mix with that of another. However, if piezometric information for an aquifer is scanty or unreliable, isocon maps used in conjunction with the piezometric information may be of value in locating major recharge areas and in relating changes in the dissolved solids concentration to the ground-water movement.

#### REFERENCES

- Liesch, B. A., 1961, Geohydrology of the Jordan aquifer in the Minneapolis-St. Paul area: Div. Waters, Minnesota Dept. Conserv., Tech. Paper 2.  
 Winchell, N. H., 1886, Revision of stratigraphy of the Cambrian in Minnesota: Minnesota Geol. Survey Ann. Rept. 14.  
 — 1899, Geology of St. Louis County, Minn.: Minnesota Geol. Survey final rept., v. 4, p. 502-580.



## GEOHYDROLOGY OF STORAGE OF RADIOACTIVE WASTE IN CRYSTALLINE ROCKS AT THE AEC SAVANNAH RIVER PLANT, SOUTH CAROLINA

By GEORGE E. SIPPLE, Columbia, S.C.

*Work done in cooperation with the U.S. Atomic Energy Commission*

**Abstract.**—Geologic, hydrologic, and water-quality studies indicate two distinct aquifer systems at the Savannah River Plant: one in crystalline basement rock, and the other in the overlying 900-foot sequence of sedimentary strata. A confining layer of saprolite separates the two systems, preventing significant exchange of water between them and retarding circulation within the crystalline rocks. Safe storage of radioactive wastes in sound crystalline rocks appears feasible.

A major question in appraising the feasibility of storage of partially cooled high-level radioactive waste in mined excavations deep in crystalline basement rocks at the Atomic Energy Commission Savannah River Plant is whether, in case of accidental escape of radioactive material to the basement rocks, the radioactive material would contaminate overlying aquifers and surface streams. Two basic considerations are whether the basement rocks are permeable and whether water in the basement rocks can move freely into the overlying sedimentary rocks.

Geologic and hydrologic studies reported here indicate that a laterally extensive layer of saprolite effectively separates an aquifer system in the basement rocks from aquifers in the overlying sedimentary sequence. This affords one of several substantial barriers to the migration of the waste; the presence of kaolinitic clay in the overlying Tuscaloosa Formation, with its attendant high ion-exchange capacity, represents another. Thus, at this intermediate stage of the project, storage of high-level waste in cavities in the basement appears feasible. Subsequent reports, based on information from at least 11 additional test wells and extensive hydrologic and chemical data, will indicate in a more definitive manner the possibility of using this storage medium.

The crystalline rocks in the vicinity of the Savannah River Plant consist of chlorite-hornblende schist, quartz-feldspar gneiss, hornblende gneiss, and slate of Precambrian age intruded by granite of Paleozoic age (Carboniferous?). The schistosity strikes northeast and dips 55° to 75° SE. The crystalline rocks are overlain by a succession of gently southeast-dipping unconsolidated sediments of marine, deltaic, estuarine, and continental origin of Cretaceous and younger age. The thickness and general description of the lithology and water-bearing characteristics of the individual rock units are given in the accompanying table.

In the preliminary investigation reported here, four test holes (DRB 1, 2, 3, and 4) were drilled in an area near the center of the plant property (fig. 1 and inset of fig. 2). These holes, which were more than 1,900 feet deep, encountered fresh crystalline rock at depths ranging from 895 to 970 feet. The holes were drilled by conventional rotary methods until hard crystalline rock was reached. A log was made as the hole progressed, and continuous core was taken of about 1,000 feet of the crystalline rocks at each test hole. Gamma-ray, neutron, and temperature logs and a directional survey were made of the entire section at each hole. Resistivity logs were made of several observation wells in the sediments. In addition, sonic logs were made in the crystalline-rock section of holes DRB 2, 3, and 4; caliper and microlaterologs were made in the crystalline-rock section of all four holes.

The gamma-ray logs were particularly useful for distinguishing the contact of the Tuscaloosa Formation with the saprolite at the top of the crystalline zone (fig. 2). Neutron logs provided supplemental confirmation of this identification. The sonic logs and

*Geologic units in the vicinity of the Savannah River Plant*

System	Series	Geologic unit	Thickness (feet)	Lithology and water-bearing characteristics
Quaternary	Recent	Alluvium (unnamed)	0-40	Stream-deposited clay, silt, sand, and gravel; tan to gray; underlies flood plains and bordering terraces; of minor importance as an aquifer.
	Pleistocene	Wicomico, Sunderland, Coharie(?), and Hazlehurst(?) Formations.		Alluvial and estuarine deposits of tan, orange, and red sand and sandy clay; underlie coastal terraces; yields sufficient water for domestic supply.
Tertiary	Miocene	Hawthorn Formation	0-80	Marine and colluvial deposits of sandy clay enclosing lenses of gravel and cut by clastic dikes; yields small to moderate amounts of water to wells.
	Eocene	Upper Barnwell Formation	0-90	Marine and colluvial deposits of sandy clay and crossbedded to massive fine to coarse sand; red, brown, yellow, and buff; yields sufficient water for domestic supply.
Cretaceous(?)	Upper Cretaceous(?)	McBean and Congaree Formations.	100-250	Marine deposits of fine to coarse glauconitic quartz sand interbedded with clay, sandy marl, and siliceous limestone; sand is yellow brown to mustard green, and clay and marl are green, red, yellow, and tan; yields sufficient water for moderate to large-scale industrial and municipal use. Water generally is hard and in places high in dissolved iron content.
Cretaceous	Upper Cretaceous	Ellenton Formation	10-100	Marine and estuarine deposits of medium- to dark-gray micaceous coarse sand and gravel and dark-gray to black lignitic micaceous sandy clay containing disseminated crystals of gypsum; yields moderately large to large amounts of water to wells. Water generally moderately high in sulfate and quite high in iron content.
		Tuscaloosa Formation	300-600	Marine, estuarine, deltaic, and continental deposits of micaceous quartzitic and arkosic sand and gravel interbedded with clay and kaolin; sand and gravel is tan, buff, red, and white; clay is gray, red, brown, and purple; kaolin is white; yields as much as 2,000 gpm to 8- to 12-inch gravel-packed wells. Water is soft and is low in dissolved-solids content. Average coefficient of transmissibility, about 200,000 gpd per foot.
Precambrian to Carboniferous(?)		Crystalline rocks of the Carolina slate belt and Charlotte belt.	-----	Basement rocks consisting of chlorite-hornblende schist, quartz-feldspar gneiss, hornblende gneiss, and slate of Precambrian age intruded by granite of early Paleozoic to Carboniferous(?) age; uppermost part consists of saprolite formed during long exposure to weathering. Fractures in fresh rock yield small amounts of water to wells. In outcrop areas, water in granite generally is soft and low in total dissolved-solids content, whereas water in mafic rocks generally is harder and more mineralized. In deeply buried rocks, water is very highly mineralized.

caliper logs were valuable in distinguishing fractured from unfractured crystalline rock. In most holes the zone of fractured rock extended 400 to 500 feet below the base of the saprolite layer.

Although saprolite was identified at each of the four test holes, the principal evidence for its lateral continuity and impermeable character is the marked difference in head and quality between confined water in the basement rocks and water in the Tuscaloosa Formation. Fractures are common, much more so in the upper part

of the fresh crystalline rock than at greater depths. Many of these fractures have been healed by quartz, calcite, chlorite, and zeolite, but the open fractures are interconnected and will transmit water to a well that intersects them. The crystalline rocks thus constitute a deeply buried artesian aquifer. The water is confined by a layer of saprolite, or disintegrated rock (mostly clay) which formed in a subaerial environment when the basement rocks were exposed to weathering prior to the deposition of the Tuscaloosa Formation in Late Creta-

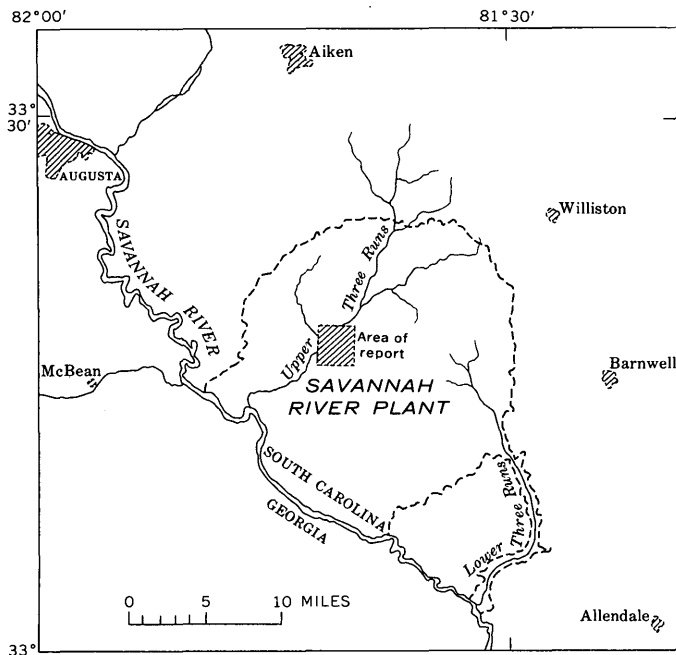


FIGURE 1.—Location of Savannah River Plant and report area.

ceous time. Presumably the saprolite was compacted and possibly somewhat altered after being buried beneath the sedimentary strata.

The piezometric surface of the water in the crystalline rocks is less than 100 feet below the land surface throughout the test area and is above the valley floor of the Upper Three Runs (fig. 2). Moreover, the head in the basement rocks is about 20 feet higher than in the Tuscaloosa throughout the test area.

The configuration of the piezometric surface in the Tuscaloosa, as shown by Siple (1957), indicates that the direction of water movement in the vicinity of the Savannah River Plant is toward the south and southwest and that discharge is effected laterally toward streams draining the outcrop area and vertically (upward) by leakage into the Savannah River in an area downstream from the outcrop.

The hydraulic gradient between the test area and the Savannah River is 4 to 5 feet per mile; permeability and porosity of the coarser beds were determined to be approximately 1,500 gallons per day per square foot and 30 percent, respectively. Substitution of these values in an expression for the Darcy law (Darcy, 1856) indicates an average velocity of water movement in the Tuscaloosa Formation in this area to be about 0.5 foot per day, or about 185 feet per year.

Chemical analyses indicate a marked difference in quality between water from the Tuscaloosa and water from the basement rocks at the test area. The specific conductance of water from the basement rocks exceeds

1,000 micromhos, while that of water from the Tuscaloosa is generally less than 100 micromhos. For example, preliminary tests indicate a conductivity of 1,250 micromhos for water from well DRB-3, whereas the water from well 35-H, screened in the Tuscaloosa Formation in the same area, has a conductivity of only 43 micromhos. The principal cation in the water from the crystalline rocks at the test area is sodium, and the principal anion is sulfate. The concentration of these constituents—and also of chloride, potassium, magnesium, and bicarbonate—is much higher than in areas where the crystalline rocks crop out or are near the surface. Water from the Tuscaloosa is typically of the sodium chloride type with low dissolved-solids content.

A plausible explanation for the occurrence of fresh water in the crystalline rocks in and near the area where they crop out and of highly mineralized water in the crystalline rocks when they are deeply buried is illustrated on figure 3. In the outcrop area the water in these rocks is unconfined because the saprolite is not continuous and, where present, it is more permeable than where deeply buried beneath thick sedimentary strata. Recharge results from the direct infiltration of precipitation, and water in the zone of saturation is free to move laterally to places where it can escape either to the land surface or into overlying sediments. Down-gradient from the "lip" of the continuous sheet of saprolite, little or no escape of water from the crystalline rocks is possible and the water in these rocks is stagnant or nearly so.

An alternate explanation to this continuity system is the possibility that the saprolite functions as a semipermeable membrane and that osmotic diffusion (by movement of Tuscaloosa water across the membrane of saprolite confining the highly concentrated rock water) might account, in whole or in part, for the greater hydrostatic pressure of water in the crystalline rock over that in the overlying sediments.

The evidence presented here lends support to a tentative conclusion that storage of high-level radioactive wastes in mined caverns within the crystalline rocks would not result in either contamination of water in the overlying sedimentary strata or in contamination of streams. Even if the water filling fractures in the upper part of the crystalline rocks were to become contaminated, the layer of saprolite would present a formidable barrier to the escape of the contaminated water into the overlying aquifers and thence to points of natural discharge or withdrawal through wells. The chemical or physical factors involved in the compatibility or suitability of the basement rock for storage of the radioactive waste are discussed in general terms by Horton (1961) and Prout (1962).

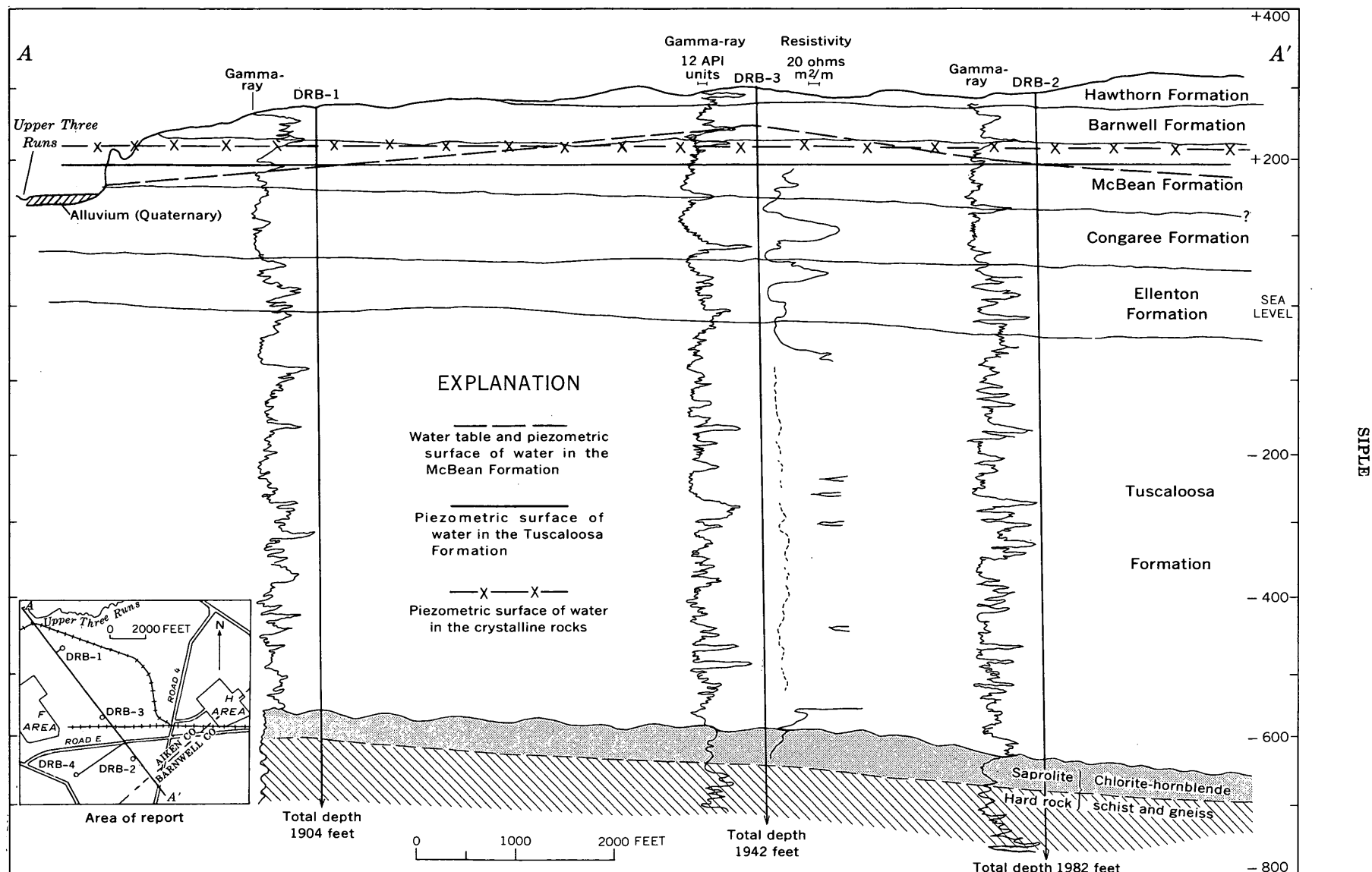


FIGURE 2.—Geologic section A-A', showing logs of test holes, and water-level profiles in the report area.

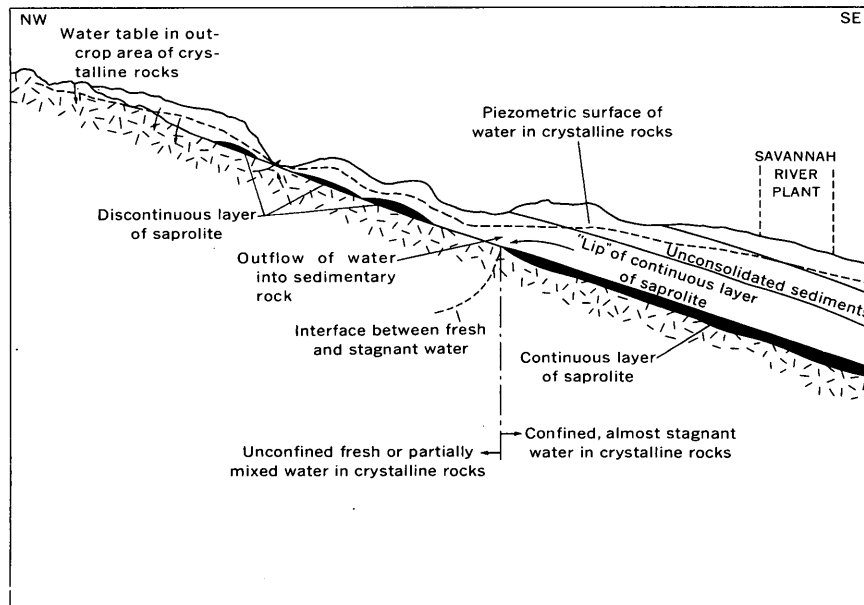


FIGURE 3.—Diagrammatic section illustrating a possible explanation for the occurrence of both fresh and salty water in the crystalline basement rocks.

#### REFERENCES

- Darcy, Henri, 1856, *Les fontaines publiques de la ville de Dijon*: Paris, Victor Dalmont, 647 p.  
 Horton, H. H., Jr., 1961, Radioactive waste management at the Savannah River Plant: DP-564, E. I. duPont de Nemours, 13 p.  
 Prout, W. G., 1962, Studies of the containment of radioactive wastes in underground mined caverns at the Savannah

River Plant: Second General Disposal of Radioactive Wastes Conference, Chalk River, Canada, Sept. 26-29, 1961, U.S. Atomic Energy Comm., Div. Tech. Inf., TID-7628, p. 380-390.

- Siple, G. E., 1957, Geology and ground water in parts of Aiken, Barnwell and Allendale Counties, South Carolina: U.S. Geol. Survey open-file report, 131 p.  
 U.S. Army, Corps of Engineers, 1952, Geologic-Engineering Investigations, Savannah River Plant.



## STREAM DISCHARGE REGRESSIONS USING PRECIPITATION

By H. C. RIGGS, Washington, D.C.

*Abstract.*—Monthly mean discharge from two pairs of basins, one pair adjacent and one pair 100 miles apart, is related by use of each of four regression models. Best results were obtained from the two models which included basin precipitation.

A common problem in hydrology—that of estimating stream discharge at times not included in the period of gaging—is commonly solved by a regression on stream discharge at a nearby site having a longer record, or by a regression on basin precipitation.

D. R. Dawdy (written communication, 1960) has pointed out that three different types of regression models are useful in estimating stream discharge and that the appropriate one for a particular problem depends on the distance between the basins producing the discharges. He postulates that for adjacent basins of small size, the difference in precipitation would be negligible and a simple regression between discharges would give results as good as those from a more sophisticated model. For basins a great distance apart the relation between discharges would be slight and best results would be expected from a regression of discharge on precipitation. For an intermediate distance between basins, multiple regressions on discharge and precipitation would give the best results.

This article suggests useful regression models and presents results of a limited empirical study that partly verify Dawdy's postulates. The majority of the discharge-precipitation relations in the literature are applied to annual mean discharge. This study is concerned with monthly mean discharge.

Monthly mean discharges of a stream for different calendar months are not homogeneous data because the discharges for individual calendar months have different means and variances. In order that the data used in this study be homogeneous and not serially correlated the data for only 1 calendar month of each year is used in each regression.

The monthly mean discharges of nearby streams for any given calendar month are quite similarly affected

by antecedent conditions. If streams are similar hydrologically, particularly with respect to base-flow characteristics, the variation of individual points from a curve of relation between concurrent discharges is largely due to differences in precipitation during the month. Therefore, inclusion of precipitation values on the two basins should improve the relation.

Precipitation can be included in the regression model in several ways. No one way is entirely satisfactory from a physical standpoint because an effect (discharge) is being related to another effect (discharge) and to the two respective causes (precipitation on each of the basins). Nevertheless, the addition of the precipitation values in some arbitrary form often results in appreciable improvement in the discharge-discharge relation. The model used in this investigation is

$$\log Q_A = \log a + b_1 \log Q_B + b_2 \log (P_A/P_B), \quad (1)$$

where  $Q_A$  and  $Q_B$  are discharges from the two basins,  $P_A$  and  $P_B$  are the respective concurrent precipitation values,  $b_1$  and  $b_2$  are regression coefficients, and  $a$  is the regression constant.

Model 1 is considered suitable for the condition in which the discharge from a nearby basin is the primary independent variable and the precipitation values of the two basins are additional but less influential variables.

As the distance between the two basins increases, it is postulated that the relation between the discharges deteriorates until the simple relation between discharge from the dependent basin and precipitation on that basin is better than the simple relation between discharges from the two basins. If the two basins are generally affected by the same storms the discharge from the independent basin may be used as a measure of the effect of antecedent conditions on the discharge-precipitation relation. One way to do this is suggested below. It is a variation of a method used by Carter and others (1949).

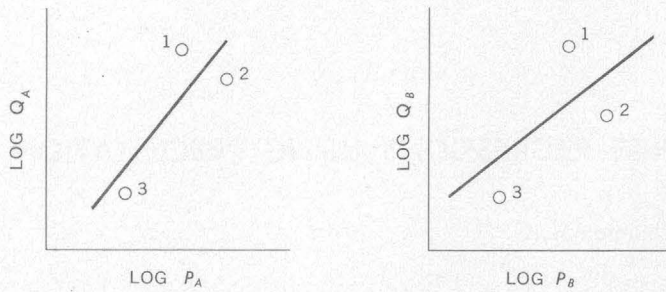


FIGURE 1.—Schematic discharge-precipitation relations for two basins affected by the same storms. Symbols:  $Q_A$  and  $Q_B$ , discharges from the two basins;  $P_A$  and  $P_B$ , respective concurrent precipitation values.

Suppose it is desired to extend the short record of March mean discharges from basin A on which long records of precipitation are available. Long records of both discharge and precipitation are also available on basin B which is at a considerable distance from basin A. If antecedent conditions similarly affect the discharges from the two basins the deviations of corresponding points from the respective discharge-precipitation relations would be in the same direction. (See figure 1.)

Under these conditions the simple discharge-precipitation relation for basin A can be improved by use of the deviations of plotted points from the discharge-precipitation relation for basin B. On figure 1, the plotting of point 1 on both relations indicates greater discharge than expected from the measured precipitation, presumably as a result of greater than average carryover from the preceding period. Points 2 and 3 indicate less than average carryover.

Deviation of a plotted point from the relation line for basin B can be expressed as  $\log(Q_B/\hat{Q}_B)$  where  $Q_B$  is the measured value and  $\hat{Q}_B$  is the value from the relation line corresponding to  $P_B$ . Then the regression model utilizing this variable would be

$$\log Q_A = \log a + b_1 \log P_A + b_2 \log(Q_B/\hat{Q}_B) \quad (2)$$

The usefulness of models 1 and 2 can be measured against the results obtained from the corresponding simple models:

$$\log Q_A = \log a + b_1 \log P_A, \text{ and} \quad (3)$$

$$\log Q_A = \log a + b_1 \log Q_B. \quad (4)$$

Empirical tests were made using each of the 4 models and data from 3 basins in the Mississippi Embayment of Tennessee. Figure 2 shows location of the basins and of the precipitation stations. Drainage areas of Wolf River at Rossville, Hatchie River at Bolivar, and North Fork Obion River near Union City are 503, 1,430, and 480 square miles, respectively. The Hatchie River and Wolf River basins are adjacent. The North Fork

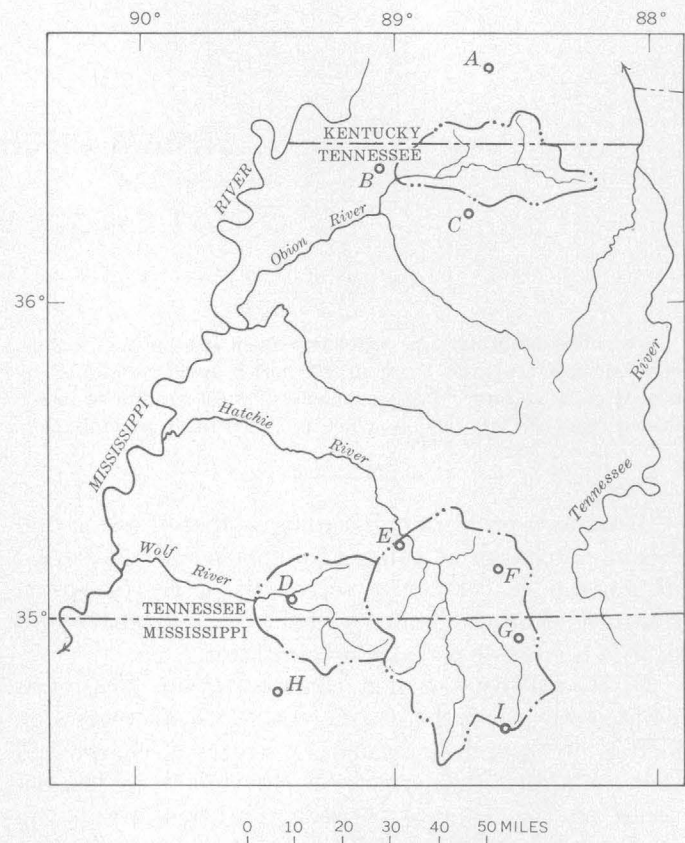


FIGURE 2.—Map of western Tennessee showing the location of the drainage basins (broken lines) and precipitation stations used in this study. Precipitation stations: A, Mayfield, Ky.; B, Union City, Tenn.; C, Dresden, Tenn.; D, Moscow, Tenn.; E, Bolivar, Tenn.; F, Selmer, Tenn.; G, Corinth, Miss.; H, Holly Springs, Miss.; and I, Boonville, Miss.

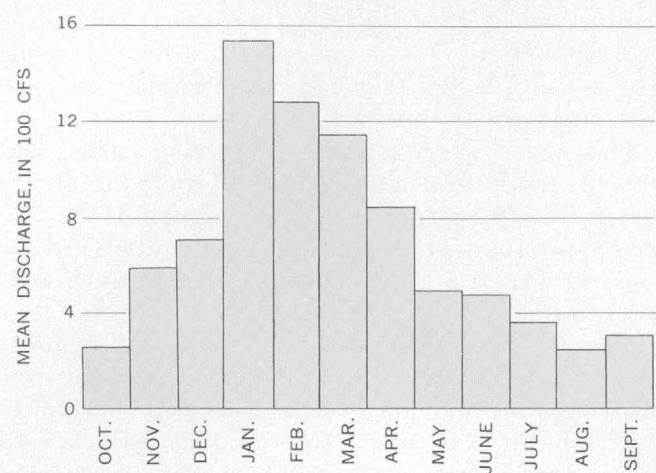


FIGURE 3.—Distribution of discharge, by months, of Wolf River at Rossville, Tenn., 1930–50.

Obion River and the Wolf River basins are 100 miles apart. The distribution of discharge by months for Wolf River at Rossville is shown on figure 3.

The discharge variables used were monthly means. Precipitation for each month was obtained by averaging precipitation measured at several stations in each basin. Precipitation on the Wolf River basin above Rossville is the mean of precipitation totals for Moscow and Bolivar, Tenn., and Holly Spring, Miss. Precipitation on the Hatchie River basin above Bolivar is the mean of precipitation totals for Bolivar and Selmer, Tenn., and Corinth, and Booneville, Miss. Precipitation on the basin of the North Fork Obion River above Union City is the mean of precipitation totals at Union City and Dresden, Tenn., and Mayfield, Ky.

The discharge of Hatchie River at Bolivar was related to precipitation and to discharge of and precipitation on the basin of Wolf River above Rossville for each of the months January, March, May, July, September, and November, using each of the four regression models. The discharge of North Fork Obion River at Union City was related to the same factors in the Wolf River basin for the same months and using the same regression models. Values of  $\hat{Q}_B$  were obtained from graphical relations between discharge and precipitation for Wolf River. Results are shown in figure 4 in terms of the standard error of estimate.

Study of figure 4 indicates the following:

(1) In general the discharge of Hatchie River can be estimated more closely from the discharge of the adjacent basin of Wolf River than from precipitation on the Hatchie River basin (model 4 shows lower standard errors than model 3 except for March).

(2) In general the discharge of North Fork Obion River can be estimated more closely from basin precipitation than from the discharge of Wolf River 100 miles away (model 3 has lower standard errors than model 4 except for January).

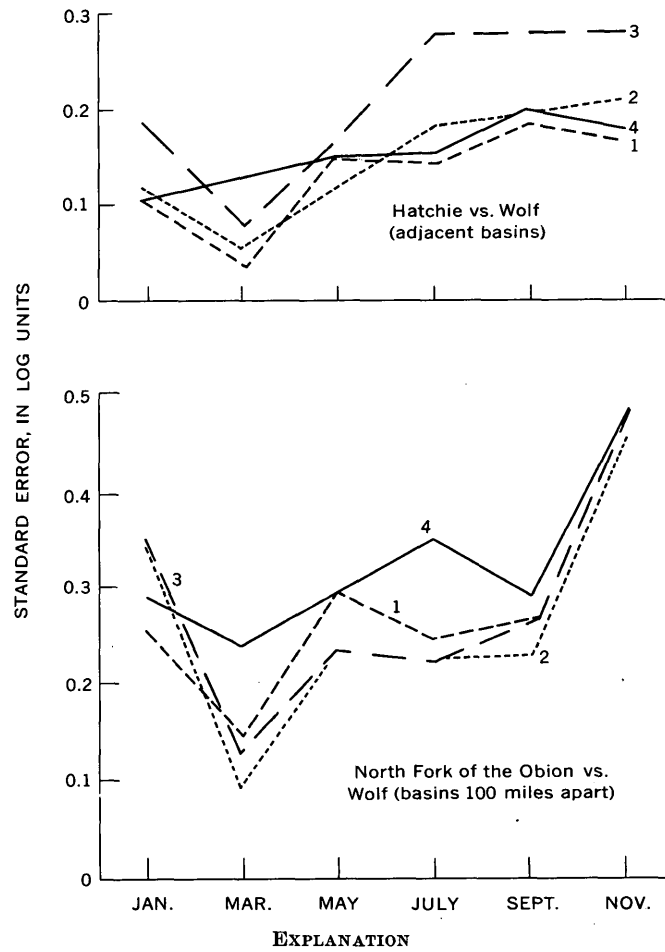
(3) Use of model 1, which includes a precipitation variable, reduces the standard error appreciably for most months with respect to model 4, both for adjacent basins and for basins 100 miles apart.

(4) Model 2, which includes an index of antecedent conditions based on discharges of another stream, provides a smaller standard error than model 3 which is the simple discharge-precipitation relation. The advantage of model 2 over model 3 is large for the adjacent basins and moderate for the basins 100 miles apart.

(5) No clear superiority of one regression model for a particular pair of stations for all months is indicated.

(6) The reliability with which monthly mean discharges can be estimated varies considerably with the calendar month.

The results of this empirical study partly verify



- EXPLANATION
1.  $\log Q_A = \log a + b_1 \log P_A + b_2 \log (P_A/P_B)$
  2.  $\log Q_A = \log a + b_1 \log P_A + b_2 \log (Q_B/\hat{Q}_B)$
  3.  $\log Q_A = \log a + b_1 \log P_A$
  4.  $\log Q_A = \log a + b_1 \log Q_B$

FIGURE 4.—Reliability of the regressions based on models 1—4.

Dawdy's postulates as to the conditions under which each of the three types of regression models are useful for estimating stream discharge. However, the inclusion of a variable describing the precipitation totals on each basin apparently will improve the discharge-discharge relation even for adjacent basins which are as large as 500 square miles. Results of this study also showed that the discharge-precipitation relation on a basin may be improved by including an index of antecedent conditions based on discharge of a stream basin 100 miles away.

#### REFERENCE

- Carter, R. W., Williams, M. R., LaMoreaux, P. E., and Hastings, W. W., 1949, Water Resources and hydrology of southeastern Alabama: Alabama Geol. Survey Spec. Rept. 20, p. 187-195.



## RELATION OF ANNUAL RUNOFF TO METEOROLOGICAL FACTORS

By MARK W. BUSBY, Topeka, Kans.

**Abstract.**—The average annual runoff at 62 selected stations throughout the conterminous United States was related to 9 meteorological factors as recorded at a U.S. Weather Bureau first-order weather station near each point of runoff study. Seven of these factors were significant at the 80-percent level or higher. On the basis of these 7 factors, the standard error of estimate of the average annual runoff is about 30 percent.

A statistical study of records from 62 stream-gaging stations and nearby first-order weather stations distributed throughout the conterminous United States indicated that, of 9 meteorological factors tested, 5 were highly significant, 2 were moderately significant, and 2 showed only slight relation to annual runoff. Lack of U.S. Weather Bureau first-order weather stations near long-record streamflow stations limited the number of stations available for study. The length of record at the 62 streamflow stations ranged from 11 years to 45 years and averaged 24 years. The size of the basins studied ranged from 8.5 square miles to 1,680 square miles and averaged 286 square miles. Streamflow records were used as defined and were not combined or adjusted to a common base period.

The meteorological records were from Weather Bureau reports entitled, "Climates of the States" (published for each State). The nine factors tested were: (1) average annual precipitation, (2) average annual temperature, (3) average snowfall, (4) average wind velocity, (5) average number of days with measurable precipitation, (6) average number of days with temperatures of 90°F or more, (7) average heating degree days,<sup>1</sup> (8) average relative humidity, and (9) percent of total possible sunshine. The factors of precipitation, temperature, and degree days were averages for the period 1921–50 as computed and published by the Weather Bureau. All other meteorological factors were averages for the full period of weather record. The

weather data were considered representative of conditions over a whole basin upstream from the nearby streamflow station. Because only annual averages are used, this assumption is probably valid.

Of the 9 factors tested, 4 were statistically significant, at higher than the 99-percent level, in relation to annual runoff. One factor was statistically significant at the 95-percent level, and 2 more factors at the 80-percent level. The 2 remaining factors had significance levels below 60 percent. The equation determined from seven factors was as follows:

$$R = 150 + 0.42P^* - 2.23T^* + 0.083S^* - 0.38W\dagger + 0.071D_p\dagger + 0.054D_t\dagger - 0.008d,$$

where

$R$ =average annual runoff, in inches,

$P$ =average annual precipitation, in inches,

$T$ =average annual temperature, in degrees F,

$S$ =average annual snowfall, in inches,

$W$ =average wind velocity, in miles per hour,

$D_p$ =average number of days with measurable precipitation,

$D_t$ =average number of days with temperature of 90° F or more, and

$d$ =average heating degree days.

\* Statistically significant at greater than 99-percent level.

† Statistically significant at greater than 80-percent level.

‡ Statistically significant at greater than 95-percent level.

The standard error of estimate from this relation was computed to be 30 percent. Of the 9 factors tested the 2 not included in the equation are average relative humidity and percent of total possible sunshine.

By eliminating the two factors that were significant at the 80-percent level, the equation changes to:

$$R = 118 + 0.39P^* - 1.73T^* + 0.088S^* + 0.059D_p\dagger - 0.007d,\dagger$$

where the terms are the same as before. The standard error of estimate from this relation was 31 percent.

The effect of precipitation on runoff is self evident. The temperature is a measure of the potential evapotranspiration, or losses in runoff. A better measure of

<sup>1</sup> The value for heating degree days is determined by subtracting the average temperature for each day from 60°F and multiplying by the number of days. When the average temperature is above 60°F, no value is computed.

this would be solar radiation, since this is the source of energy for the evapotranspiration. However, because solar radiation is measured at only about 50 Weather Bureau stations throughout the country, temperature was used instead. The snowfall affects runoff to the extent that it is an important part of total precipitation in many regions where most of the runoff is from snowmelt. The average wind velocity affects runoff as it affects the actual evapotranspiration. The average number of days with measurable precipitation, the average number of days with 90°F temperature or more, and the average heating degree days are general climatic factors describing features such as the variability of the temperature, the intensity of rainfall, and the severity of the winters.

Because runoff in inches expresses discharge as an average over the whole basin, drainage area is already in the relation. By substituting discharge and drainage area for runoff, the first equation would become:

$$Q = 150 + 0.074A + 0.42P - 2.23T + 0.0835 - 0.38W + 0.071D_p + 0.054D_t - 0.008d,$$

where

$Q$  = average annual discharge, in cubic feet per second, and

$A$  = drainage area, in square miles.

The standard error of estimate is, of course, unknown. Experience, however, has shown that discharge and drainage area are not related arithmetically, but more nearly logarithmically.

The meteorological factors will only explain part of the runoff relations. As soon as the water comes into physical contact with the land surface of the basin, the physical characteristics of the basin, such as drainage area, slope, drainage density, and geology, modify the runoff. A further study, therefore, should use annual runoff in cubic feet per second and introduce physical characteristics of the basin into the relation. Such a study might indicate which factors to consider when attempting to explain other discharge probabilities such as high or low flow.



## PHOTOGRAHMETRIC CONTOURING OF AREAS COVERED BY EVERGREEN FORESTS

By JAMES HALLIDAY, Washington, D.C.

**Abstract.**—New studies have been undertaken to establish the accuracy and elevational consistency of contouring by photogrammetric methods where dense evergreen stands of timber obscure the ground detail. By comparing compilations from several distinctive sets of aerial photographs for an area in northern Maine, the photographic conditions most conducive to accurate contouring in such areas were evaluated. Best results were obtained with a flight-height/contour-interval ratio of about 700, panchromatic film, and photography in early spring with light snow cover and no deciduous leaves. Obtaining accurate contours of the ground surface in such areas by applying corrective data to treetop contours proved unpromising.

A perennial difficulty in topographic mapping by photogrammetric methods has been the problem of compiling planimetry (the plan details) and hypsography (topographic relief) in areas of dense evergreen timber with sufficient accuracy to meet National Map Accuracy Standards. The fundamental obstacle to accurate compilation is the dense evergreen foliage canopy which obstructs a clear view of the ground in all seasons.

The latest Geological Survey research on the subject has been directed toward more exact determinations of the accuracy and consistency to be expected when contouring areas of dense evergreen forests. Also, by compiling from aerial photographs representing various combinations of flight height, film emulsion, and prevailing seasonal conditions, it was anticipated that those photographic conditions most conducive to consistently accurate contouring in dense evergreens might be determined. In a supplementary study, a determination was to be made of the consistency attained by a number of compilers when the upper surface of the evergreen canopy was contoured intentionally. This information was to be used to evaluate the desirability of further study to develop a method for contouring the ground surface beneath dense evergreens by applying corrective data to treetop contours.

A 6-square-mile area in the vicinity of Baker Lake in northern Maine was selected as typical of the evergreen-forested portions of that State. The terrain in

this locality displays many of the topographic features common to areas of continental glaciation, including numerous swamps and ponds. The moderate relief consists of medium but occasionally irregular slopes. The area selected has 100-percent timber cover, predominantly evergreen. The trees are 30 to 60 feet high. The accepted contour interval for U.S. Geological Survey quadrangle mapping for this type of terrain is 20 feet.

A test line was surveyed on the ground through the densest evergreen woods in the area. Accurate horizontal positions and elevations were obtained for more than 120 points along the line for use in evaluating the accuracy of contour compilations.

The typically short flying season and the generally poor photographic weather in northern Maine added to the difficulty of obtaining photography under the desired conditions. Nevertheless, four sets of acceptable vertical, wide-angle photographs covering the general area were obtained. The distinguishing characteristics of these coverages are given in table 1.

TABLE 1.—*Characteristics of the photographic coverages of the Baker Lake area, Maine*

Coverage	Flight height above ground (feet)	Type of film	Season	Deciduous leaves	Snow cover on ground
1-----	7,000	Panchromatic.	Late spring.	Partial----	None.
2-----	14,000	Panchromatic.	Late fall.	None-----	None.
3-----	14,000	Panchromatic.	Early spring.	None-----	Light.
4-----	14,000	Infrared.	Early spring.	None-----	Light.

### PROCEDURES

A group of 18 employees especially proficient in photogrammetric surveys was selected to produce the contour manuscripts required in this research. The selections were based on high levels of visual acuity, general ability, background, experience, and, most

important, a demonstrated competence with the Kelsh plotter, the instrument to be used in this study. The participants were furnished with identical compilation materials, including print copies (on Mylar stable bases) of the appropriate quadrangle manuscript, for which the aerotriangulation and compilation of planimetry had been completed. Also furnished were electronically dodged Kelsh diapositive plates, appropriate photographic prints annotated with the necessary pass-point and supplemental vertical control information, and lists of other pertinent basic horizontal- and vertical-control data. All information relating to the test line was purposely withheld from the participants before and during contouring operations to prevent accidental misuse of the data.

Each compiler was directed to contour the designated project area four times by using appropriate exposures from a different set of photographic coverage for each compilation. The stereomodels were oriented, adjusted in horizontal scale, positioned to provide a best fit between the pass points and the previously compiled planimetry, and leveled to a vertical datum determined

by the supplemental elevations. Each compiler was instructed to use his customary procedures for contouring the ground surface in areas of dense evergreen timber. In addition, the compilers were directed to contour the upper surface of the foliage canopy for one designated model using coverage 1 (table 1), for use in the previously mentioned supplementary study.

The ground-contour compilations were evaluated for accuracy by comparison with the test-line survey in accordance with standard Topographic Division practice. To form a basis for evaluating the consistency of the contouring of the upper canopy surface, these compilations were compared with test-line data to determine apparent tree heights at the test points. Deviations from the mean apparent tree-height values at the various test points were then used to determine the consistency of such contouring among the several stereocompilers.

## RESULTS

Table 2 lists the accuracy attained by the various compilers each time they contoured the ground surface beneath the dense evergreen trees. Results are given

TABLE 2.—Results of photogrammetric ground contouring

Compiler	Coverage 1				Coverage 2				Coverage 3				Coverage 4				Average of all tests			
	RMSE (ft)		Percent passing		RMSE (ft)		Percent passing		RMSE (ft)		Percent passing		RMSE (ft)		Percent passing		RMSE (ft)		Percent passing	
	Before shift	After shift	Before shift	After shift	Before shift	After shift	Before shift	After shift	Before shift	After shift	Before shift	After shift	Before shift	After shift	Before shift	After shift	Before shift	After shift	Before shift	After shift
1	11.6	9.7	72	76	15.3	12.3	55	66	9.3	7.3	74	85	12.6	10.2	57	67	12.2	9.9	65	74
2	10.0	7.6	73	81	10.9	8.4	67	86	8.6	6.9	79	91	7.6	5.4	83	95	9.3	7.1	76	88
3	8.9	6.8	71	84	10.6	8.4	78	80	7.0	5.2	86	94	6.5	4.7	89	92	8.3	6.3	81	88
4	9.2	7.1	78	87	14.7	12.2	58	70	7.6	5.7	93	96	7.6	5.7	88	94	9.8	7.7	79	87
5	9.1	6.3	69	92	10.7	8.0	72	76	8.3	6.4	77	88	9.6	7.5	76	88	9.4	7.1	74	86
6	7.6	5.4	80	93	10.2	8.4	77	84	6.3	4.5	90	96	8.3	6.1	80	89	8.1	6.1	82	91
7	14.3	11.7	51	63	9.4	6.9	75	87	6.8	4.8	90	92	8.6	6.8	88	93	9.8	7.6	76	84
8	8.7	6.4	88	92	14.7	12.5	46	57	5.2	3.6	97	97	6.1	4.2	94	97	8.7	6.7	81	86
9	9.4	6.6	72	91	8.4	6.2	78	87	5.4	3.4	96	97	5.8	3.9	91	96	7.3	5.0	84	93
10	25.1	21.7	29	41	20.8	17.9	40	50	6.8	4.3	89	97	8.5	5.8	79	91	15.3	12.4	59	70
11	17.7	14.7	43	57	13.5	10.1	39	65	6.2	3.8	92	96	8.0	5.1	78	92	11.4	8.4	63	78
12	17.4	13.8	42	53	14.7	11.6	48	61	7.1	4.5	89	97	8.5	6.1	79	83	11.9	9.0	65	74
13	19.7	16.0	23	35	14.7	12.1	51	65	8.9	6.1	85	90	8.5	5.8	82	90	13.0	10.0	60	70
14	11.5	8.9	68	78	14.9	12.1	49	61	9.4	6.4	81	91	10.3	7.9	71	76	11.5	8.8	67	77
15	11.1	8.8	67	87	8.2	6.0	84	94	9.2	6.7	80	93	7.8	5.0	90	94	9.1	6.6	80	92
16	8.3	6.1	74	89	6.2	4.3	91	98	5.5	3.9	95	96	6.1	4.6	93	96	6.5	4.7	88	95
17	13.2	9.3	56	80	9.4	7.0	71	87	10.0	7.0	71	79	11.7	9.2	73	80	11.1	8.1	68	82
18	7.3	5.0	81	94	6.9	4.7	87	93	6.3	3.8	91	96	6.5	4.0	90	98	6.8	4.4	87	95
Average	12.2	9.6	63	76	11.9	9.4	65	76	7.4	5.2	86	93	8.3	6.0	82	90	10.0	7.6	74	84
No. of compilers meeting vertical accuracy standards			0	5			1	3			8	15			5	12				

RMSE: root mean square error =  $\sqrt{\sum \epsilon^2 / n}$ , where

$\epsilon$  = vertical compilation error, at a point on the test-line survey, determined by comparing the elevation indicated by the ground contours with field-established elevation at that point.

n = number of test-line points involved.

Percent passing: percentage of points tested at which the vertical error does not exceed 10 feet ( $\frac{1}{2}$  contour interval).

Before shift: value before allowable horizontal shift.

After shift: value after allowable horizontal shift.

in terms of root mean square error (RMSE) in feet, also in terms of the percentage of points tested at which the vertical error did not exceed 10 feet (one-half contour interval).<sup>1</sup> The accuracy values for both presentations have been computed both with and without allowance for the horizontal shift permitted by Survey Order 160.

Table 3 shows the consistency of contouring attained when the participating compilers attempted to contour the upper surface of the foliage canopy in accordance with the requirements of the supplementary study. The standard deviation values in this table have been computed on the basis of deviations from values of mean apparent tree height at the various test points. The allowable horizontal shift was not considered in this study, primarily because the necessary basic data were not readily available.

TABLE 3.—Results of photogrammetric treetop contouring

Compiler	Number of points tested	Standard deviation (ft)	Percentage evaluation
1	24	5.8	83
2	23	11.1	52
3	26	11.4	50
4	26	6.9	88
5	26	6.6	88
6	26	5.2	96
7	26	5.1	92
8	26	5.4	92
9	26	14.8	50
10	21	4.0	100
11	21	10.6	57
12	21	5.0	95
13	21	5.4	95
14	21	5.7	95
15	21	5.3	95
16	26	5.1	100
17	26	6.1	88
18	26	6.6	92
Average values		7.0	84

$$\text{Standard deviation} = \sqrt{\sum (H_i - H_m)^2 / (n - 1)}, \text{ where}$$

$H_i$  = apparent height of trees at a point on the test-line survey determined by comparison of the elevation indicated by treetop contours with field-established ground elevation at that point.

$H_m$  = mean apparent height of trees at a point on the test-line survey determined by averaging all  $H_i$  data at that point.

$n$  = number of test-line points involved.

Percentage evaluations are given in terms of the percentage of points tested at which the deviations from the mean apparent tree height value do not exceed 10 feet (½ contour interval).

<sup>1</sup> For a map to comply with National Map Accuracy Standards, Survey Order 160 requires that "vertical accuracy, as applied to contour maps on all publication scales, shall be such that not more than 10 percent of the elevations tested shall be in error by more than one-half the contour interval. In checking elevations taken from the map, the apparent vertical error may be decreased by assuming a horizontal displacement within the permissible horizontal error for a map of that scale."

## CONCLUSIONS

The accuracy and consistency of ground contouring varied through a considerable range, depending primarily on the characteristics of the aerial photographs that were used. Of the combinations studied, the photographic conditions that appear to be most conducive to consistently accurate ground contouring in dense evergreen woods in Maine are those found in coverage 3. They include: a flight-height/contour-interval ratio (C-factor) of about 700, panchromatic film, early spring photographic season, no leaves on deciduous trees in the area, and a light snow cover on the ground. Of particular significance in this respect was the finding that a considerably lower flight height (represented in coverage 1) did not result in improved contouring accuracy or consistency for the dense evergreen-forested conditions under study. This is contrary to general photogrammetric experience.

The ground-contouring results attained with coverage 3 displayed surprisingly excellent accuracy and consistency;<sup>2</sup> however, further research is needed to find ways and means of improving this record. Studies should be aimed at providing the stereocompiler with more and better ground information, so that photographs obtained under less than the ideal conditions outlined above may be used to produce maps of standard quality. The stereocompiler would be aided by (1) more precisely photoidentified, more accurately located pass points, (2) more accurate supplemental elevations for model control, (3) additional elevations on controlling topographic features, such as tops, saddles, and drain forks, within the stereomodels, and (4) multiple photographic coverage aimed at most advantageous recording of specific types of ground detail.

Further exploration of the potentials of infrared photography and infrared electronic sensors for mapping in this type of country appears to be warranted because of the good quality of the ground contouring results attained with coverage 4,<sup>3</sup> and the recognized usefulness of infrared coverage in the detection and delineation of the more obscure hydrographic details.

The contouring of the upper surface of the evergreen canopy was remarkably consistent;<sup>4</sup> however, serious

<sup>2</sup> After the allowable horizontal shift, 15 of the 18 compilations met standard accuracy requirements, while another fell just short, at 88 percent. See table 2.

<sup>3</sup> After the allowable horizontal shift, 12 of the 18 compilations met standard accuracy requirements, while 2 more fell just short, at 89 and 88 percent. See table 2.

<sup>4</sup> In 10 of the 18 compilations the contours were within 10 feet (one-half contour interval) of the mean compiled values at 90 percent or more of the points tested. See table 3.

obstacles bar the way to successful development of ground contours by the method of applying corrective data to treetop contours. Because tree heights vary with microclimatology in different parts of the terrain and important topographic details are very often obscured by the canopy, the tree-canopy surface is at best only a generalized representation of the ground surface

beneath. Also, despite the commendable consistency of the contouring, significant differences were noted in the contour shaping in the various compilations. For these reasons, treetop contouring could not be properly transformed into an acceptable ground-contour presentation without considerable additional effort and expense.





## **SUBJECT INDEX**

[For major headings such as "Economic geology," "Geophysics," "Structural geology," see under State names or refer to table of contents]

Page	Page				
ABS, contaminant of ground water, New York.....	C170	Devonian, Maine, stratigraphy.....	C28	K	
Alaska, copper deposit, south-central part.....	117	Maine, structural geology.....	28	Kentucky, geochemistry, southern part.....	C92
laumontite, western part.....	74	Montana, stratigraphy.....	50	sedimentation, western part.....	130
Analcime, potential deposits, California.....	114	Disaggregation, sedimentary samples, ultrasonic method.....	159	Kilauea volcano, seismicity of east rift zone.....	103
Analysts, chemical, rating of ability.....	157	Discharge, stream, estimation from precipitation records.....	185		
Apache Group, Arizona, stratigraphy.....	43	Dripping Spring Quartzite, Arizona, stratigraphy.....	43	<b>L</b>	
Arizona, paleontology, Grand Canyon area.....	39			Laccoliths, Colorado, post-Paleocene.....	66
stratigraphy, Grand Canyon area.....	39			Lake deposits, Pleistocene, Kentucky-Illinois.....	130
south-central part.....	43			Laumontite, occurrence and origin, in Alaska.....	74
Artesian aquifers, Florida-Georgia, effect on surface water.....	164			Lithium, association with beryllium, in tuff.....	86
Atapulgite, in cave fill, New Mexico.....	82				
<b>B</b>					
Basement rocks, New Jersey, petrography.....	55	Earthquakes, island of Hawaii, Kilauea rift zone.....	103	<b>M</b>	
Beryllium, association with lithium in tuff, Utah.....	86	Eocene, Florida-Georgia, ground water.....	164	Magnesite-calcite-rhodochrosite system, diagram.....	84
Bolsa Quartzite, Arizona, stratigraphy.....	43	Georgia, paleontology.....	64	Maine, stratigraphy, northeastern part.....	28
<b>C</b>		stratigraphy.....	61	structural geology, northeastern part.....	28
Calcite-rhodochrosite-magnesite system, diagram.....	84	Erionite, potential deposits, California.....	114	Massachusetts; glacial geology, Martha's Vineyard.....	134, 140
California, potential zeolite deposits, Mojave Desert.....	114	Exchange rate, of montmorillonite, measurement.....	96	Maywood Formation, Montana, stratigraphy.....	50
structural geology, northwestern part.....	1			Mescal Limestone, Arizona, stratigraphy.....	43
Cambrian, Arizona, stratigraphy.....	43			Mesozoic, California, structural geology.....	1
Maine, stratigraphy.....	28			Nevada, structural geology.....	10
structural geology.....	28	Faults, strike-slip, Idaho-Montana tear, west-central Utah.....	14	<i>See also</i> Cretaceous.	
Cationic diffusion rate, of montmorillonite, measurement.....	96	Fischer assay, use in study of weathering of shale.....	19	Meteorological factors, effect on runoff.....	188
Catoctin Formation, Virginia, petrology.....	69	Fish fossils, Devonian, Montana.....	50	Michigan, glacial geology, Upper Peninsula.....	126
Cave filling, clay content.....	82	Florida, ground water, Statewide artesian aquifer.....	164	Minnesota, glacial geology, Mesabi iron range ground water, Minneapolis-St. Paul area.....	144
Cavities (tafoni), in bedrock, northern Chile.....	121	surface water, effect of artesian aquifer on Floridian aquifer, Florida-Georgia, effect on surface water.....	164	Miocene, Florida-Georgia, ground water.....	164
Channel deposits, Devonian, Montana.....	50	Foraminifera, Eocene, Georgia.....	64	Georgia, stratigraphy.....	61
Chattanooga Shale, Tennessee-Kentucky, geochemistry.....	92	Fractures, explosion-produced, structural analysis.....	100	Mississippian, Arizona, stratigraphy.....	39
Chemical quality, ground water, relation to recharge.....	176			Montana, paleontology, southwestern part.....	50
Chemists, analytical, rating of ability.....	157	Gabbro, intrusive body, Connecticut.....	22	stratigraphy, southwestern part.....	14
Chi-square method, use in rating chemists.....	157	Geochemical prospecting, metals, North Carolina.....	88	Montmorillonite, cationic diffusion and exchange rates.....	96
Chile, geomorphology, northern part.....	121	Georgia, ground water, southern part.....	164	Moraines, Illinois and Wisconsin age, Massachusetts.....	140
Clay, effect on subsidence, Texas.....	79	paleontology, eastern part.....	64	Wisconsin age, Michigan.....	126
in cave filling, New Mexico.....	82	stratigraphy, Savannah area.....	61		
Clay minerals, montmorillonitic, cationic diffusion and exchange rates.....	96	surface water, southern part.....	164		
occurrence in Pleistocene sediments, Texas.....	79	Glacial deposits. <i>See</i> Moraines.			
Clinoptilolite, potential deposits, California.....	114	Glaciers, retreat of Teton Glacier, Wyoming.....	147		
Colorado, petrology, west-central part.....	16	Greenstone, chemical composition, Virginia.....	69		
Connecticut, petrology, east-central part.....	22				
Contouring, photogrammetric, of evergreen forest areas.....	190	<b>H</b>			
Copper, abundance in alluvium, North Carolina.....	88	HARDHAT event, Nevada, study of explosion-produced fractures.....	100		
Copper deposits, ore controls, Alaska.....	117	Hawaii, geophysics, Island of Hawaii.....	103		
Corals, Mississippian, Arizona.....	39				
Cretaceous, Alaska, occurrence of laumontite, South Carolina, ground water.....	74	<b>I</b>			
	180	Idaho, structural geology, east-central part.....	14		
<b>D</b>		Illinois, sedimentation, southern part.....	130		
Detergents, contaminants of ground water, New York.....	170	Iodine, method of determination in vegetation.....	154		
		<b>J</b>			
		Jordan Sandstone, Minnesota, ground water.....	176		
		<b>O</b>			
		Oligocene, Florida-Georgia, ground water.....	164		
		Georgia, stratigraphy.....	61		
		Ordovician, Maine, stratigraphy.....	29		
		Maine, structural geology.....	29		
		Ore controls, copper deposit, Alaska.....	117		

## SUBJECT INDEX

Page		Page	
Oregon, structural geology, southwestern part.....	C1	Texas, clay mineralogy, Houston-Galveston Bay area.....	C79
Oxygen sheath, for flame photometer, new design.....	152	Thrust sheets, Mesozoic age, California and Oregon.....	1
<b>P</b>			
Paleogeography, relation of phosphorite distribution to.....	106	Topographic maps, contouring, evergreen-forest areas.....	190
Paleomagnetism, relation of phosphorite distribution to.....	106	Tritium, as indicator of age and movement of ground water.....	161
Paleozoic, California, structural geology.....	1		
South Carolina, ground water.....	180		
<i>See also</i> Cambrian, Ordovician, Silurian, Devonian, Mississippian.			
Particle-size analyses, use of ultrasonic disaggregation.....	159		
Phosphorite, paleolatitudinal and paleogeographic distribution.....	106		
Photogrammetric contouring, evergreen-forest areas.....	190		
Photometer, flame, new oxygen sheath.....	152		
Pioneer Formation, Arizona, stratigraphy.....	43		
Pleistocene, Georgia, stratigraphy.....	61		
Kentucky-Illinois, sedimentation.....	130		
Massachusetts, glacial geology.....	134, 140		
Michigan, glacial geology.....	126		
Minnesota, glacial geology.....	144		
Texas, clay mineralogy.....	79		
Precambrian, Arizona, stratigraphy.....	43		
South Carolina, ground water.....	180		
Virginia, petrography.....	69		
Precipitation records, use in estimating stream discharge.....	185		
<b>Q</b>			
Quaternary, South Carolina, ground water.....	180		
<i>See also</i> Pleistocene.			
<b>R</b>			
Radioactive waste, storage, possible effect on ground water.....	C180		
Recharge, ground water, effect on chemical quality.....	176		
Redwall Limestone, Arizona, stratigraphy.....	39		
Regression models, use in estimating stream discharge.....	185		
Rhodochrosite-magnesite-calcite system, diagram.....	84		
Runoff, relation to meteorological factors.....	188		
<b>S</b>			
Seismic studies, island of Hawaii.....	103		
Silurian, Maine, stratigraphy.....	28		
structural geology.....	28		
South Carolina, ground water, Savannah River Plant.....	180		
Stream capture, Recent, Michigan.....	126		
Streamflow, estimated from precipitation records.....	185		
relation to meteorological factors.....	188		
Subsidence, Texas, effect of clay on.....	79		
<b>T</b>			
Tafoni (cavities), in bedrock, northern Chile.....	121		
Tennessee, geochemistry, northern part.....	92		
surface water, western part.....	185		
Tertiary, California, potential zeolite deposits.....	114		
Colorado, petrology.....	66		
South Carolina, ground water.....	180		
<i>See also</i> Eocene, Oligocene, Miocene.			
<b>V</b>			
Vegetation, determination of iodine content.....	154		
Virginia, petrography, Blue Ridge area.....	69		
<b>W</b>			
Weathering, formation of tafoni, in bedrock of shale, evaluation by Fischer assay.....	121, 92		
Wyoming, glaciology, Grand Teton Park.....	147		
<b>Z</b>			
Zeolite deposits, in tuffaceous rocks, California.....	114		
Zinc, abundance in alluvium, North Carolina.....	88		

## AUTHOR INDEX

<b>B</b>	<b>Page</b>	<b>Page</b>	<b>O</b>	<b>Page</b>	
Boucot, A. J.	C28	Herrick, S. M.	C61, 64	Olive, W. W.	C130
Breger, I. A.	92	Hoare, J. M.	74		
Brown, Andrew	92	Houser, F. N.	100		
Brown, T. E.	96				
Busby, M. W.	188				
<b>C</b>		<b>I</b>		<b>P</b>	
Condon, W. H.	74	Irwin, W. P.	1	Patton, W. W., Jr.	74
Corliss, J. B.	79			Pavlides, Louis	28
Cotter, R. D.	144			Perlmutter, N. M.	170
Cuthbert, Margaret	154	Johnson, A. I.	159	Prinz, W. C.	84
<b>D</b>		<b>J</b>		<b>R</b>	
Davies, W. E.	82	Kane, M. F.	22	Reed, J. C., Jr.	69, 147
Dinnin, J. I.	152	Kaye, C. A.	134, 140	Reeder, H. O.	161
Duke, Walter	86	Koyanagi, R. Y.	103	Riggs, H. C.	185
<b>E</b>		<b>K</b>		Rogers, J. E.	144
Emerick, W. L.	100	Lieber, Maxim.	170	Rosenbaum, Fred.	152
<b>F</b>		<b>L</b>		Ruppel, E. T.	14
Finch, W. I.	130				
Flanagan, F. J.	157			<b>S</b>	
Frauenthal, H. L.	170			Sandberg, C. A.	50
<b>G</b>				Sando, W. J.	39
Gaskill, D. L.	66	McClymonds, N. E.	43	Segerstrom, Kenneth	121, 126
Godwin, L. H.	66	McCollum, M. J.	61	Shawe, D. R.	86
Gude, A. J., 3d	114	McHugh, J. B.	88	Sheldon, R. P.	106
<b>H</b>		MacKevett, E. M., Jr.	117	Shepard, W. M.	19
Halliday, James	190	McMannis, W. J.	50	Sheppard, R. A.	114
Heindl, L. A.	43	Maderak, M. L.	176	Silberling, N. J.	10
Henriquez, Hugo	121	May, Irving	152	Siple, G. E.	180
<b>N</b>		Meade, R. H.	79	Snyder, G. L.	22
		Mencher, Ely	28	Southwick, D. L.	55
		Morris, H. T.	19	Stringfield, V. T.	164
		Moston, R. P.	159	Stromquist, A. A.	88
		Mountjoy, Wayne	86	<b>W</b>	
				Wallace, R. E.	10
		Naylor, R. S.	28	Ward, F. N.	154
				White, A. M.	88
				Wolfe, E. W.	130

C197

○